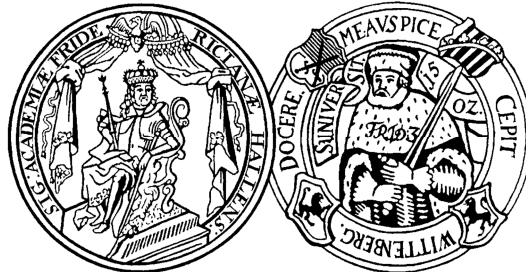


Neue Aspekte in der Regulation und in der Funktion von Aminopeptidase N (APN)/ CD13 und Ubiquitin-Carboxy-terminale Hydrolase L1 (UCHL1)



Dissertation

zur Erlangung des
Doktorgrades der Naturwissenschaften (Dr. rer. nat.)

der
Naturwissenschaftlichen Fakultät I – Biowissenschaften –
der Martin-Luther-Universität Halle-Wittenberg

vorgelegt
von Herrn Dipl.-Biochem. Jens Wulfänger
geboren am 19. März 1978 in Stendal

Gutachterin/ Gutachter:

1. Prof. Dr. Sven-Erik Behrens, Institut für Biochemie, Martin-Luther-Universität Halle (Saale)
2. Prof. Dr. Barbara Seliger, Institut für Medizinische Immunologie, Martin-Luther-Universität, Halle (Saale)
3. Prof. Dr. Dirk Reinhold, Institut für Molekulare und Klinische Immunologie, Otto-von-Guericke-Universität, Magdeburg

Verteidigung: Halle (Saale), den 01. Oktober 2014

für meine Familie und Freunde.

Und ein kleines bisschen auch für mich.

Inhaltsverzeichnis

Abbildungs- und Tabellenverzeichnis.....	I
Abkürzungsverzeichnis.....	II
1 Einleitung.....	1
1.1 Ubiquitin-Carboxy-terminale Hydrolase L1 (UCHL1)	1
1.2 Aminopeptidase N (APN)/ CD13	6
2 Ziel der Arbeit	14
3 Kurzbeschreibung der publizierten Manuskripte	16
3.1 Manuskript 1: Heterogeneous expression and functional relevance of the ubiquitin carboxyl-terminal hydrolase L1 in melanoma.....	16
3.2 Manuskript 2: Promoter methylation of aminopeptidase N/ CD13 in malignant melanoma	18
3.3 Manuskript 3: Aminopeptidase N (APN)/ CD13-dependent CXCR4 downregulation is associated with diminished cell migration, proliferation and invasion.....	20
3.4 Manuskript 4: Functional co-localization of monocytic aminopeptidase N/ CD13 with the Fc gamma receptors CD32 and CD64	22
4 Publierte Manuskripte.....	23
4.1 Manuskript 1: Heterogeneous expression and functional relevance of the ubiquitin carboxyl-terminal hydrolase L1 in melanoma.....	23
4.2 Manuskript 2: Promoter methylation of aminopeptidase N/ CD13 in malignant melanoma.	39
4.3 Manuskript 3: Aminopeptidase N (APN)/ CD13-dependent CXCR4 downregulation is associated with diminished cell migration, proliferation and invasion.....	57
4.4 Manuskript 4: Functional co-localization of monocytic aminopeptidase N/ CD13 with the Fc gamma receptors CD32 and CD64.....	70
5 Diskussion	75
5.1 UCHL1, ein interessanter Kandidat für die Generierung/ Etablierung neuer Therapieformen des malignen Melanoms.....	75
5.2 DNA-Methylierung des myeloischen Promotors als neuer epigenetischer Regulationsmechanismus der APN-Genexpression	83
5.3 Etablierung und Charakterisierung eines Modellsystems zur Funktionsanalyse der APN-Enzymaktivität	89

5.4	Deregulation der SDF-1 α / CXCR4-vermittelten Zellmigration durch APN ...	93
5.5	Interaktion von APN und Fc γ -Rezeptoren in der Phagozytose und Signaltransduktion	99
6	Zusammenfassung	102
7	Summary	104
8	Literaturverzeichnis.....	106
9	Eigenständigkeitserklärung.....	122
10	Lebenslauf	123
11	Liste von Publikationen und Präsentationen	125
12	Danksagung	128

Abbildungs- und Tabellenverzeichnis

Abbildung 1:	Molekulare und zelluläre UCHL1-Funktionen.....	6
Abbildung 2:	Genlocus, mRNA-Spezies und Proteinstrukturen von APN.....	8
Abbildung 3:	Genregulatorische Mechanismen der APN-Expression.....	11
Abbildung 4:	Multiple zelluläre Funktionen von APN.....	13
Abbildung 5:	Differentielle CpG-Methylierung des myeloischen APN-Promotors.....	86
Abbildung 6:	Mechanismus der hydrolytischen Peptidspaltung durch APN.....	91
Abbildung 7:	Multiple Funktionen der SDF-1 α / CXCR4-Achse in der Tumorbiologie.....	94
Abbildung 8:	Modell der SDF-1 α / CXCR4-Blockade durch APN-WT.....	97
Tabelle 1:	Immunhistochemische Analysen zur UCHL1-Expression in soliden Tumoren.....	3
Tabelle 2:	Immunhistochemische Analysen zur APN-Expression in soliden Tumoren.....	12

Abkürzungsverzeichnis

Akt	Proteinkinase B
AML	akute myeloische Leukämie
Ang	Angiotensin
APN	Aminopeptidase N/ CD13
AS	Aminosäure
BAX	<i>BCL2-associated X protein</i>
bFGF	basischer Fibroblasten-Wachstumsfaktor
CD33	<i>myeloid-specific sialic acid-binding receptor</i>
CDK	Cyclin-abhängige Kinase
COBRA	kombinierte Bisulfitbehandlung und Restriktionsanalyse
DAC	5'-Desoxyazacytidin
DPIV	Dipeptidylpeptidase IV/ CD26
EGF	epidermaler Wachstumsfaktor
EMT	epithelial-mesenchymale Transition
ERK	<i>extracellular signal-regulated kinase</i>
FRET	Förster-Resonanzenergietransfer
GFP	grün-fluoreszierendes Protein
HEK293	humane embryonale Nierenepithelzellen 293
HGF	hepatozellulärer Wachstumsfaktor
I κ B α	Inhibitor von NF κ B
IFN	Interferon
IL	Interleukin
JAB-1	<i>Jun-activation domain-binding protein 1</i>
MAPK	Mitogen-aktivierte Proteinkinase
MART1	<i>melanoma antigen recognized by T cells</i>
MHC	Haupthistokompatibilitätskomplex
MITF	Microphthalmie-assoziiertes Transkriptionsfaktor
MMD	Membran-Mikrodomäne (Rafts/ Caveolae)
MMP	Matrixmetalloprotease
NEP	Neutrale Endopeptidase/ CD10
NF κ B	<i>nuclear factor 'kappa-light-chain-enhancer' of activated B-cells</i>
NZK	Nierenzellkarzinom
PHLPP1	<i>PH domain and leucine rich repeat protein phosphatase 1</i>
PI $_3$ K	Phosphoinositid-3-Kinase
PTEN	<i>Phosphatase and Tensin homolog</i>
ROS	reaktive Sauerstoffspezies
SDF	<i>stromal cell-derived factor</i>
TCF/ Lef	<i>T cell-specific transcription factor/ lymphoid enhancer-binding factor</i>
TGF	transformierender Wachstumsfaktor
TMA	Gewebemikroarray
TNF	Tumornekrosefaktor
UCH	Ubiquitin-Carboxy-terminale Hydrolase
WT	wildtypische Sequenz

1 Einleitung

1.1 Ubiquitin-Carboxy-terminale Hydrolase L1 (UCHL1)

Die Ubiquitin-Carboxy-terminale Hydrolase L1 (UCHL1), auch *protein gene product 9.5* (PGP9.5) genannt, ist eine Cystein-Protease der UCH-Familie, denen auch UCHL3, UCHL5/ UCH37 und das *breast cancer type 1 susceptibility protein* BRCA1 angehören. Diese Familie ist gekennzeichnet durch eine hoch konservierte Sequenzhomologie und der deubiquitinierenden Funktion. Deswegen bilden die Proteasen eine von fünf Untergruppen der deubiquitinierenden Enzyme [1]. Der kodierende Bereich des UCHL1-Gens ist auf dem kurzen Arm des Chromosoms 4 (4p14) lokalisiert und umspannt neun Exone über einen Bereich von ca. 11,5 kb. Die Genexpression kann durch verschiedene Mechanismen reguliert werden. DNA-Methylierung der CpG-Stellen im UCHL1-Promotor ist ursächlich für eine stark verringerte Genaktivität, vorwiegend bei der Pathogenese einer Vielzahl von Tumoren [2, 3]. Der Transkriptionsstart befindet sich ca. 45 bp (Position +1) vor dem translationsinitiiierenden Startkodon [4]. Der minimal notwendige Promotorbereich befindet sich von -210 bis -129 bp [4]. Verschiedene Bindungsstellen diverser Transkriptionsfaktoren wurden identifiziert (z. B. für *nuclear factor 'kappa-light-chain-enhancer' of activated B-cells* NFκB bzw. für *signal transducers and activators of transcription* STAT) [4]. Als Aktivatoren sind der hämatopoetische Transkriptionsfaktor Pu.1 über die Bindung an einer TATA-Box sowie der β-Catenin-TCF/ Lef (*T cell-specific transcription factor/ lymphoid enhancer-binding factor*)-Komplex beschrieben [5, 6]. Interessanterweise kann UCHL1 in seiner Funktion als Hydrolase β-Catenin stabilisieren, welches als Transkriptionsfaktor wirkend, die UCHL1-Genaktivität in einem positiven Rückkopplungsmechanismus erhöht [6]. Sowohl Aktivierung von NFκB als auch oxidativer Stress beeinflussen die UCHL1-Transkription negativ [7, 8]. Auf posttranskriptioneller Ebene wird die UCHL1-Translation über eine sogenannte *long non-coding RNA* (lncRNA) positiv beeinflusst [9]. Diese *Antisense*-UCHL1-RNA-Spezies werden unter zellulärem Stress vom Zellkern in das Zytoplasma transloziert, binden an die kodierende mRNA und stabilisieren die Ausbildung von Polysomen der Proteinsynthese. In neuronalen Zellen kann die UCHL1-Expression epigenetisch durch die miR-181b posttranskriptionell reguliert werden [10]. Dabei korreliert das exprimierte Protein der Hydrolase positiv mit der miRNA-Menge. Das globulär strukturierte UCHL1-Protein besteht aus 223 Aminosäuren (AS) mit einem Molekulargewicht von ca. 25 kDa. Röntgenkristallstrukturanalysen belegen die für Hydrolasen charakteristische katalytisch aktive Triade, bestehend aus Cys90, His161 und Asp76 [11]. Ebenfalls besitzt UCHL1 eine sogenannte *crossover loop*-Struktur, die bei der Substraterkennung und bei der

Diskriminierung großer Proteinsubstrate fungiert [11]. Posttranslational kann UCHL1 ohne Einflussnahme auf die Enzymaktivität O-glykosyliert werden [12]. Monoubiquitinierungen von UCHL1 können durch strukturelle Konformationsänderungen in der Nähe des aktiven Zentrums die proteolytischen Eigenschaften blockieren [13]. Dieser Prozess ist durch Autohydrolyse reversibel. Während einer Phase des oxidativen Stresses in der Zelle kann die Protease am Tyr80 nitriert werden [14]. Die Hydrolase ist vorwiegend im Zytoplasma lokalisiert [15], kann aber gewebsspezifisch auch im Zellkern nachgewiesen werden [16, 17]. Eine Farnesylierung am C-terminalen Bereich verleiht UCHL1 hydrophobe Eigenschaften, die eine Interaktion mit den Membranen des endoplasmatischen Retikulums ermöglicht [18].

Physiologische UCHL1-Funktionen

Mit einem Anteil von ca. 2 % aller Proteine ist UCHL1 konstitutiv stark in neuronalen bzw. neuroendokrinen Geweben des zentralen und peripheren Nervensystems exprimiert [19]. Moderatere Expressionsraten sind in den Tubulusepithel-, Sammelrohr- sowie Parietalzellen der Niere, in Ovarien und in Testis beschrieben [20-23]. Die Funktion der Hydrolase in den jeweiligen Geweben ist unvollständig aufgeklärt. Es wird angenommen, dass UCHL1 die Peptidbindungen hydrolytisch am C-terminalen Glycin von kleinen Ubiquitin-Konjugaten spaltet bzw. die Deubiquitinierung von Proteinen katalysiert [19, 24]. Diese Proteolyseschritte erlauben die Generierung und Zurückgewinnung (*recycling*) von monomeren Ubiquitin-Molekülen. Deubiquitinierte Proteine sind vor der proteasomalen Degradation geschützt. Die Hydrolaseaktivität ist bei UCHL1 gegenüber den anderen UCH-Mitgliedern signifikant geringer [25]. Die reversible kovalente Bindung von Monoubiquitin an die Protease trägt zu dessen Stabilisierung bei [13]. Mit der Dimerisierungs- und ATP-unabhängigen Ligaseaktivität verknüpft UCHL1 Proteinsubstrate kovalent über K63-Bindungen [26]. Im Gegensatz zur K48-Quervernetzung von Ubiquitin, die Proteine zur proteasomalen Degradation markiert, werden K63-Ubiquitin-ligierte Proteine davor geschützt. Es wird angenommen, dass UCHL1 mit seinen bivalenten Enzymaktivitäten eine wichtige Rolle in der Aufrechterhaltung der zellulären Homöostase durch die Regulation des Proteinhaushaltes einnimmt und folglich in diversen Zellprozessen (z. B. Zellzyklus, Apoptose, Differenzierung und Signaltransduktion) involviert ist [25]. Während der Differenzierung renaler Tubuli und bei der Zellzyklusregulation von parietalen epithelialen Zellen der Bowman'schen Kapsel ist UCHL1 entscheidend an der Ausbildung der Nieren-Anatomie beteiligt [20]. Im akrosomalen Bereich von Spermatozoon lokalisiert, scheint es bei der Penetration der Oozyte während des Befruchtungsvorgangs mitzuhelfen [27]. UCHL1-

Negativität bei der Oogenese ist mit einer schlechteren Eizellreifung assoziiert [28]. In Beta-Zellen des Pankreas exprimiert, fungiert die Hydrolase bei der Insulinsekretion und der Glukosetoleranz sowie als antiapoptotisches Protein unter lipotoxischen Stressbedingungen [29]. Jedoch sind die exakten physiologischen Funktionen und die zu Grunde liegenden molekularen Mechanismen unvollständig aufgeklärt. Eine gewebsspezifische UCHL1-Funktion wird von unserer Arbeitsgruppe postuliert. Vor allem *in vitro*- bzw. *in vivo*-Beweise für die Ligasefunktion und von UCHL1-prozessierten Interaktionspartnern fehlen.

UCHL1 in der Tumorgenese und potentielle molekulare Mechanismen

Je nach Entität sind für UCHL1 sowohl tumorsupprimierende als auch –fördernde Eigenschaften belegt [30]. Während eine heraufregulierte Expression mit meist schlechterer Prognose und Überlebensraten beispielsweise für Burkitt-Lymphome, nicht-kleinzellige Lungentumore, Neuroblastome sowie für Pankreas- und medulläre Schilddrüsenkarzinome einhergeht [5, 31-34], ist UCHL1 im Nasopharynx-, Ovarial- und Leberkarzinom sowie beim Prostatakrebs und den diffusen Magentumoren meist vermindert exprimiert [3, 35-39]. Tabelle 1 fasst weitere Resultate verschiedener immunhistochemischer Analysen zur UCHL1-Expression in Tumoren zusammen.

Tabelle 1: Immunhistochemische Analysen zur UCHL1-Expression in soliden Tumoren.

Entität	UCHL1-Expression		Antikörper	Referenz
	gesundes Gewebe ¹	Tumor ²		
Brust	negativ	25/234	polyklonal	[40]
Kolon	schwach positiv	33/74	polyklonal	[41]
		31/65	polyklonal	[42]
Lunge	negativ	47/140	NCL-PGP9.5	[43]
Gallenblase	negativ	15/27	polyklonal	[44]
Prostata	positiv	71/139	NCC-F2711	[36]
Nebenschilddrüse	negativ	19/127	polyklonal	[45]

¹ gesunde Gewebszellen meist negativ mit Ausnahme UCHL1-positiver neuronaler Zellen in den Geweben

² Anzahl der UCHL1-positiven Tumore im Verhältnis zur Gesamtzahl der analysierten Tumorproben (oft keine separaten Angaben zur Häufigkeit der UCHL1-Expression in histologischen Subtypen bzw. Metastasen)

Arbeiten unserer eigenen Arbeitsgruppe können eine vom Tumortyp und -stadium abhängige UCHL1-Expression beim Nierenzellkarzinom (NZK) charakterisieren [2, 46]. Während die meisten Primärtumore im Vergleich zum korrespondierenden gesunden Nierenzellepithel verringerte Proteinmengen aufweisen, sind nach Metastasierung dieser Tumore gesteigerte UCHL1-Konzentrationen exprimiert. Dieses bivalente progressionsabhängige Expressionsmuster der Hydrolase ist ebenfalls für das kolorektale Karzinom belegt [37, 42]. Der bisher am besten charakterisierte genregulatorische Mechanismus in der Expressionskontrolle von UCHL1 während der Tumorentstehung ist die epigenetische Genstilllegung mittels Promotor-DNA-Methylierung. So ist ein erhöhter CpG-Methylierungsgrad mit dem UCHL1-Verlust beim Prostata-, Ovarial- und Leberkarzinom sowie beim NZK assoziiert [2, 36-39].

Diverse Transfektionsstudien bekräftigen das gewebspezifische onkogene bzw. supprimierende Potential der Hydrolase [47]. Die genauen zellulären und molekularen Funktionen sind jedoch unvollständig charakterisiert. Es wird angenommen, dass UCHL1 mit seinen bifunktionellen Enzymaktivitäten den Proteinhaushalt in der Zelle durch ubiquitinabhängige Stabilisierung bzw. Degradation der Polypeptidketten beeinflusst. Dies ist ursächlich für eine deregulierte Expression von Transkriptionsfaktoren, Onkogenen, Tumorsuppressoren und von Proteinen, die u. a. den Zellzyklus, die Apoptose, die Signaltransduktion, die Migration und Invasion propagieren [47].

β -Catenin ist sowohl an der Zelladhäsion in Kombination mit Cadherinen als auch an der Signaltransduktion des Wnt-Signalweges beteiligt. In humanen embryonalen Nierenepithelzellen (HEK293) verringert UCHL1 den Polyubiquitinierungsgrad von β -Catenin und verhindert somit dessen proteasomalen Abbau [6]. Angereichertes β -Catenin ist im nukleären Komplex mit TCF/ Lef an der Transkription überlebenswichtiger und antiapoptotischer Proteine (z. B. c-Myc, c-Jun und Survivin) involviert. Der epithelial-mesenchymale Transition (EMT)-fördernde Effekt von UCHL1 im Prostatakarzinom durch verstärkte Synthese von Matrixmetalloproteasen (MMP) und Vimentin bei gleichzeitiger Herunterregulation von E-Cadherin könnte ebenfalls über das Wechselspiel der Hydrolase mit β -Catenin vermittelt werden [48].

Durch verschiedene Arbeitsgruppen ist eine Modulation von verschiedenen Zellzyklusregulatoren durch UCHL1 beschrieben. So beschleunigt beispielsweise die Interaktion der Hydrolase mit dem *Jun-activation domain-binding protein 1* (JAB-1) den nukleären Export des Zellzyklusinhibitors p27, wodurch dieses Protein der proteasomalen Degradation zugänglich gemacht wird [16]. p27 kann durch Inhibition des Komplexes aus einem Cyclin (CCN) mit einer Cyclin-abhängigen Kinase (CDK) das zelluläre Wachstum hemmen [49]. Aufgrund der starken Herunterregulation in einer Vielzahl von

verschiedenen Tumorarten und aufgrund der klinischen Relevanz ist p27 ein interessantes Kandidatenprotein für die Generierung neuer Krebstherapieformen [49]. Der stabilisierende Effekt von UCHL1 auf das Tumorsuppressorprotein p53 und dessen konsekutive Akkumulation im Zellkern sind mit einer Arretierung des Zellzyklus in der G1/S-Phase und einer höheren Apoptoserate assoziiert [50-52]. In verschiedenen transformierten Zelllinien ist eine Kolokalisation der Hydrolase mit Mikrotubuli während der Mitose gezeigt worden [17]. Dadurch kann die Ausbildung des Spindelapparates inhibiert und der Zellzyklus blockiert werden.

Der Transkriptionsfaktor NF κ B reguliert eine Vielzahl zellulärer Prozesse. So ist er an der Aktivierung von proinflammatorischen und proapoptotischen Genen bei der Immunantwort bzw. dem programmierten Zelltod nach diversen exogenen Stimuli involviert. I κ B α ist der zelluläre Inhibitor von NF κ B, indem er durch Bindung die nukleäre Translokation verhindert. Zytoplasmatischer NF κ B wird über Polyubiquitinierung proteasomal abgebaut. UCHL1 kann I κ B α stabilisieren und somit die transkriptionelle Aktivität von NF κ B negativ beeinflussen [52, 53]. In nicht-kleinzelligen Lungentumorzellen korreliert UCHL1 positiv mit dem Aktivierungszustand der Phosphoinositid-3-Kinase (PI $_3$ K)/ Proteinkinase B (Akt)- bzw. des Mitogen-aktivierte Proteinkinasen (MAPK)-Signalweges [54]. Da Hyperaktivierung beider Signalwege einen entscheidenden Prozess für die Tumorprogression darstellt, wird der Hydrolase eine tumorfördernde Funktion in dieser Entität zugeschrieben. Für Lymphome ist ebenfalls eine UCHL1-abhängige Akt-Aktivierung mit erhöhtem Invasionsverhalten beschrieben [55]. Ein erklärender molekularer Prozess ist eine destabilisierende Wirkung der Hydrolase auf die *PH domain and leucine rich repeat protein phosphatase 1* (PHLPP1), ein zellulärer Akt-Inhibitor, durch einen bisher unbekanntem Regulationsmechanismus [55]. Eine deregulierte Akt-Aktivierung bewirkt eine erhöhte Polyubiquitinierung und folglich die proteasomale Degradation von p53 und ist ursächlich für das onkogene Potential des Signalweges [56]. Somit konkurrieren die beiden UCHL1-vermittelten Prozesse der erhöhten Akt-Phosphorylierung und der stabilisierenden Wirkung auf p53 miteinander und belegen die Komplexität der zellulären Veränderungen. Weiterhin kann UCHL1 die Internalisierung der Rezeptor-Tyrosinkinase c-Met nach Bindung des hepatozellulären Wachstumsfaktors (HGF) sowohl durch Deubiquitinierung als auch durch Ausbildung von Aktin-Stressfasern beeinträchtigen und somit mit dem PI $_3$ K/ Akt- bzw. dem MAPK-Signalweg interferieren [57]. Aufgrund der anomalen Aktivierung von c-Met in Tumoren werden momentan diverse Inhibitoren (z. B. Cabozantinib) im Rahmen klinischer Studien zur Behandlung von diversen Krebserkrankungen eingesetzt [58]. Somit wäre ein besseres Verständnis der UCHL1-vermittelten molekularen Prozesse auf die c-Met-Regulation im

Hinblick auf tumorrelevante Prozesse und dem Therapieansprechen von besonderem Interesse.

Abbildung 1 zeigt eine Zusammenfassung an Proteinen, die das kanzerogene Potential der Tumorzellen im Zusammenspiel mit UCHL1 beeinträchtigen können.

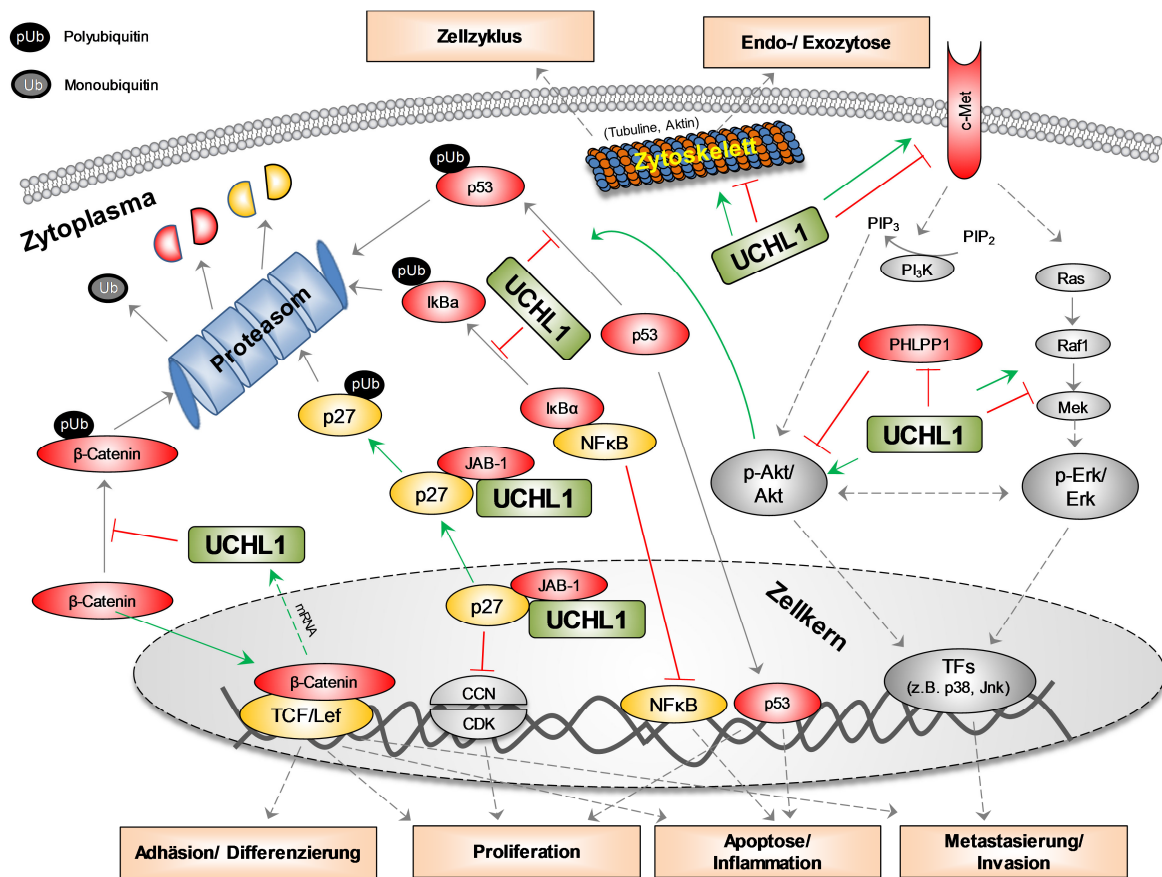


Abbildung 1: Molekulare und zelluläre UCHL1-Funktionen.

Zusammenfassende Darstellung der UCHL1-vermittelten Funktionen auf zelluläre Vorgänge. (grüner Pfeil: positive Regulation; rote Linie: inhibierende Wirkung; PIP – Phosphatidylinositolphosphate)

1.2 Aminopeptidase N (APN)/ CD13

Aminopeptidase N (APN)/ CD13, auch Alanyl- oder mikrosomale Aminopeptidase genannt, gehört zur Peptidasen-Familie M1/ Gluzincine (EC.3.4.11.2). Das Gen ist auf dem langen Arm des Chromosoms 15 (q25-q26) lokalisiert und überspannt 20 Exone mit ca. 35 kb. Die Expression wird gewebspezifisch durch zwei verschiedene hintereinander angeordnete Promotorbereiche reguliert, die etwa 8 kb voneinander entfernt sind (Abbildung 2, [59]). Der epitheliale, proximal zum translationsinitiiierenden Startkodon

befindliche Promotor weist den klassischen Aufbau einer transkriptionsregulierenden TATA-Box auf und ist vor allem in Epithelzellen des Gastrointestinaltraktes und der Niere sowie in Hepatozyten und Endothelzellen aktiv [59-63]. Genregulative Transkriptionsfaktoren sind der *hepatocyte nuclear factor 1* (HNF-1) und SP1 [64]. Der GC-reiche myeloische Promotor besitzt Bindemotive für die Transkriptionsfaktoren der Myb- und Ets-Familie und reguliert die differentielle APN-Expression während des Differenzierungsprozesses hämatopoetischer Zellen und in Fibroblasten [59, 65-67]. Zwischen beiden Promotoren ist eine ca. 300 bp lange *Enhancer*-Region lokalisiert, die über sogenannte *Loop*-Strukturen die transkriptionelle Genaktivität beider regulatorischen Genombereiche verstärkt [63]. Die jeweiligen mRNA-Spezies unterscheiden sich nur um ca. 170 bp Länge in der 5'-untranslatierten Region, kodieren aber das gleiche Protein (Abbildung 2). APN ist ein aus 967 AS bestehendes Transmembranprotein des Typs 2. Dem intrazellulären N-Terminus (7 AS ohne initiales Methionin) folgen eine einfach-durchspannende α -helikale Transmembrandomäne (24 AS) und die große Ektodomäne mit dem katalytisch aktiven Zentrum (Abbildung 2). Membrannah befindet sich eine ca. 40 AS-lange Serin-Threonin-reiche Stielregion, die O-glykosidisch modifiziert werden kann, ohne jedoch die Enzymaktivität bzw. die Oberflächenexpression der Peptidase zu beeinträchtigen [68]. Monomerische APN hat ein Molekulargewicht von ca. 150 kDa, wobei ungefähr ein Drittel der Gesamtmasse auf Zuckermodifikationen der 10 N-Glykosylierungsstellen zurückzuführen ist. Auf der Zelloberfläche ist APN meist als nicht-kovalent gebundenes Homodimer exprimiert [69, 70]. Als zinkabhängige Metalloprotease besitzt die Aminopeptidase das charakteristische Bindungsmotiv HELAH [71, 72]. Weiterhin dient das Glutaminsäure-Motiv GAMEN der Polarisierung des gebundenen Peptidsubstrates [73, 74]. Im Jahre 2012 konnten Wong *et al.* erstmalig hochauflösend die Röntgenkristallstruktur des APN-Dimers im Komplex mit dem Substrat Angiotensin (Ang) IV bzw. mit den aminopeptidasenspezifischen Inhibitoren Bestatin bzw. Amastatin darstellen [75].

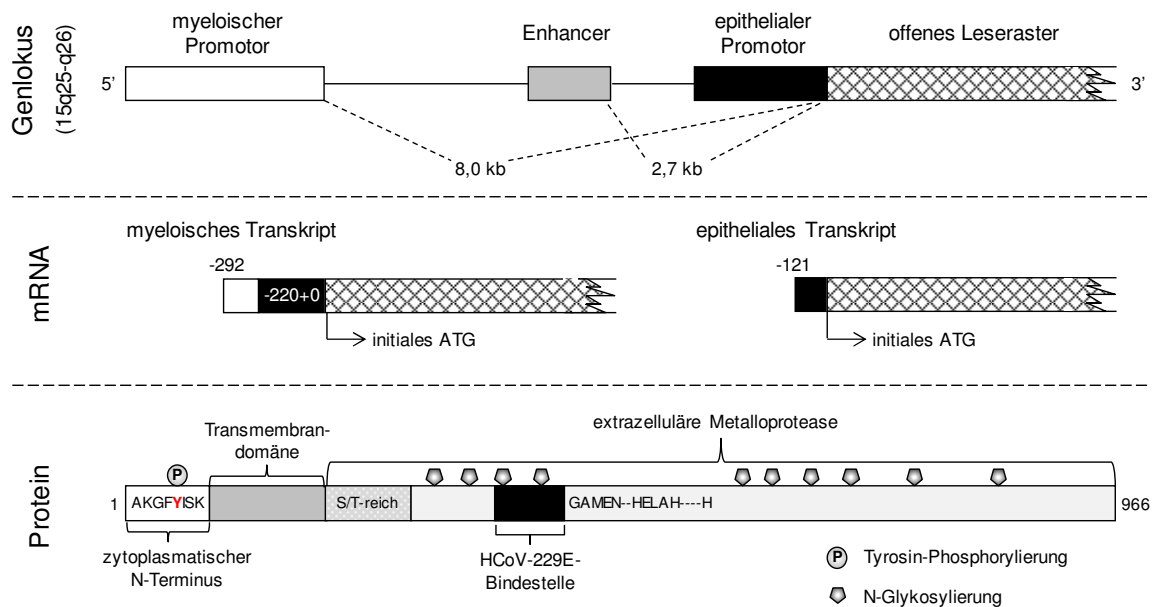


Abbildung 2: Genlokus, mRNA-Spezies und Proteinstrukturen von APN.

Schematische Darstellung des APN-Gens mit der Anordnung der beiden Promotoren und dem dazwischen kodierten Enhancer (modifiziert nach [59]), der verschiedenen APN-Transkripte mit unterschiedlicher 5'-untranslatierter Region, aber gleichem offenes Leseraster und den Strukturkomponenten des APN-Proteins (basierend auf <http://www.uniprot.org/uniprot/P15144>)

Physiologische APN-Funktionen

APN ist ubiquitär auf der Oberfläche einer Vielzahl von Zelltypen des hämatopoetischen und nicht-hämatopoetischen Systems exprimiert. Dabei übt APN je nach Gewebe entweder digestive oder regulative Funktionen aus. Digestiv fungiert die Aminopeptidase vorwiegend in den epithelialen Bürstensaummembranen der Darmmukosa und den proximalen Tubuli der Niere, indem sie zur besseren Resorption kleine Oligopeptide in monomere AS, zu einem geringeren Teil auch in Di- und Tripeptide degradiert. Dabei spaltet APN bevorzugt neutrale AS N-terminal von Oligopeptiden mit folgender Präferenz: Ala>Phe>Tyr>Leu>Arg>Thr>Trp>Lys>Ser>Asp>His>Val. Peptide mit hochmolekularen Proteinmodifikationen bzw. mit einem Prolin an zweiter Stelle der Primärsequenz sowie große Proteine können nicht prozessiert werden [76]. Renale APN reguliert durch Spaltung von Ang III zu Ang IV nicht nur die Salzresorption in die Gefäße, sondern auch den arteriellen Blutdruck [77, 78]. Auf neuronalen synaptischen Membranen kontrolliert APN die lokale Bioverfügbarkeit von Endorphinen bzw. Enkephalinen (Leu- oder Met-Enkephalin) sowie von den Neuropeptiden Neurokinin A und Bradykinin (zusammengefasst in [79]). Dadurch kann das analgetische Schmerzempfinden beeinflusst werden. In vaskulären Endothelzellen der Nabelschnur und der Aorta fungiert

APN vorwiegend bei der Formation und Morphogenese von Kapillaren [80, 81]. Lösliche APN kann unter anderem im Serum, im Urin und in bronchoalveolaren sowie synovialen Flüssigkeiten nachgewiesen werden [82-85]. Deren Funktion ist bisher unvollständig aufgeklärt.

Im hämatopoetischen System ist APN vorwiegend in Monozyten, Makrophagen, Granulozyten sowie in dendritischen Zellen und deren entsprechenden Progenitorzellen exprimiert [86, 87]. APN gilt als diagnostischer Typisierungsmarker vorwiegend für die myeloische Zellpopulation und für Stammzellen [88, 89]. Die Stärke der APN-Expression ist vom Differenzierungsgrad abhängig. Die genauen biologischen APN-Funktionen und die molekularen Zusammenhänge während der Zellreifung sind jedoch unvollständig charakterisiert. Möglicherweise trägt APN entscheidend in der homotypischen Aggregation von Monozyten bei, die eine wichtige Voraussetzung zur Zellaktivierung und -reifung dieser Zellen darstellt [90]. Die enzymatische Aktivität ist in die Degradation chemotaktischer Proteine (z. B. Chemokin CXCL11) zur Anlockung immunmodulatorischer Zellen involviert [91]. Das APN-vermittelte katalytische Prozessieren von antigenen Peptiden, die an der Bindungsfurche der Haupthistokompatibilitätskomplex (MHC)-Moleküle Klasse II gebunden sind, bewirkt ein verändertes Potential zur zellulären Erkennung durch T-Lymphozyten [92]. Weiterhin reguliert APN negativ die Tumornekrosefaktor (TNF) α -induzierte Apoptose in humanen Neutrophilen, die eine zentrale Rolle beim Abklingprozess von Entzündungsreaktionen spielt [93].

Die APN-Genexpression kann durch diverse exogene Faktoren moduliert werden. Beispielsweise ist APN bei Entzündungsprozessen durch proinflammatorische Zytokine wie Interferon (IFN)- γ und Interleukin (IL)-4 in Monozyten/ Makrophagen heraufreguliert [94, 95]. Neben weiteren Zytokinen (z. B. IL-6, epidermaler Wachstumsfaktor EGF bzw. basischer Fibroblasten-Wachstumsfaktor bFGF) wird die transkriptionelle Aktivität u. a. durch oxidativen zellulären Stress verändert [96-99]. Unsere Arbeitsgruppe konnte zeigen, dass die Aminopeptidase durch die Zytokine IL-4 und dem transformierenden Wachstumsfaktor (TGF)- β in Monozyten verstärkt, durch IL-10 jedoch verringert exprimiert ist (Abbildung 3, [100, 101]). In tubulären Nierenepithelzellen ist APN neben IL-4 durch IFN, TNF α , IL-1 bzw. IL-13 heraufreguliert [102, 103]. In konstitutiv negativen peripheren Blutlymphozyten ist die Expression durch Zell-Zell-Kontakt mit diversen APN-positiven Zellen transkriptionell induziert. So besitzen B- und T-Lymphozyten nach Kontakt mit fibroblastenähnlichen Synoviozyten, endothelialen bzw. epithelialen Zellen und Monozyten/ Makrophagen APN-Antigene und Alanin-Substrat-spaltende Enzymaktivitäten auf ihrer Zelloberfläche [104-107]. Wir postulieren, dass

induzierte APN nicht nur bei der Inaktivierung von inflammatorischen Mediatoren fungiert, sondern auch in der Zelladhäsion, in der lymphozytären Migration oder an der Antigenpräsentation durch *peptide trimming* involviert ist.

Pathophysiologische APN-Funktionen

APN spielt eine bedeutende Rolle bei pathophysiologischen Prozessen. T-Zellen der Gelenkflüssigkeit bei Patienten mit rheumatoider Arthritis haben im Vergleich zu denen gesunder Spender ebenso erhöhte APN-Konzentrationen wie periphere Blutmonozyten/Makrophagen von Patienten mit schwerem Trauma bzw. nach Operation am offenen Herzen (Abbildung 3, [108, 109]). In trachealen Epithelien dient die Aminopeptidase unabhängig von der Enzymaktivität als Eintrittsstelle für diverse Coronaviren und ist somit involviert in Infektionserkrankungen der oberen Luftwege [110, 111]. Humane Zytomegalieviren benutzen ebenfalls APN als zelluläre Eintrittsstelle [112]. Die Internalisierung erfolgt jeweilig meist durch sogenannte Membran-Mikrodomänen (MMD), auch Rafts oder Caveolae genannt [113]. Diese speziellen Membranbereiche auf der Zelloberfläche sind Zusammenlagerungen diverser membranständiger Struktur- (z. B. Flotilline, Caveoline) bzw. Rezeptorproteine (z. B. G-Proteine, Glycosylphosphatidylinositol-verankerte Proteine) mit im Vergleich zu anderen Membranbereichen erhöhten Konzentrationen an Cholesterol und Sphingolipiden. MMD fungieren in der Trans-, Endo- bzw. Exozytose, in Signaltransduktionsvorgängen sowie in der Rezeptorinternalisierung und steuern dabei diverse immunologische (u. a. B- und T-Zellantwort) sowie zelluläre Prozesse (z. B. Motilität, Sezernierung, exogene Stimulation, Stressantwort). Eine Assoziation von APN in MMD ist in Monozyten, in Epithelzellen des Dünndarms, in Endothelzellen und Fibroblasten belegt [81, 113-117]. Unsere eigene Arbeitsgruppe postuliert, dass APN in Synergie mit anderen Peptidasen wie Neutrale Endopeptidase (NEP)/ CD10 oder Dipeptidylpeptidase IV (DPIV)/ CD26 sogenannte peptidasereiche *Hot spots* in MMD bildet, die diverse zelluläre Prozesse im Zusammenspiel vermitteln [116]. Weiterhin ist APN in der Absorption von endo- und exogenem Cholesterol involviert [115].

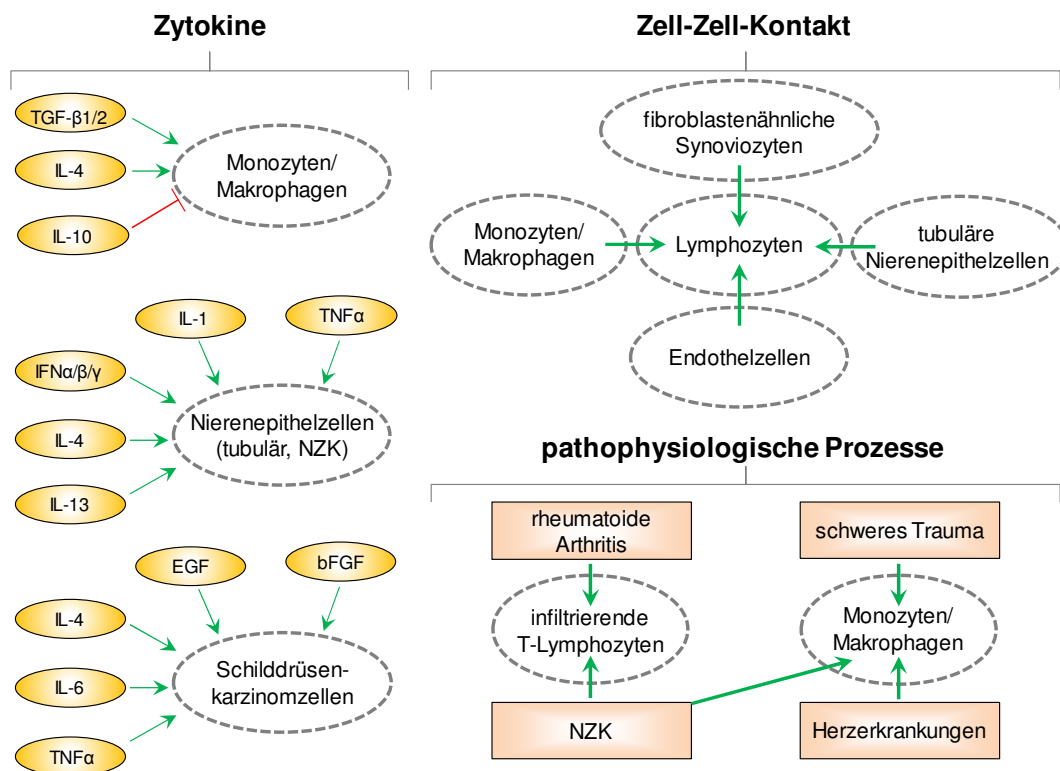


Abbildung 3: Genregulatorische Mechanismen der APN-Expression.

(grüner Pfeil: erhöhte APN-Expression, rote Linie: Verminderung)

In bösartigen hämatopoetischen Erkrankungen wird APN routinemäßig als Indikator für myelomonozytäre Zellen, z. B. bei akuten myeloischen Leukämien (AML), eingesetzt [118, 119]. Die Expression ist bei der malignen Transformation dieser Zellen abnormal erhöht. Antiproliferative Effekte sowie blockierte Differenzierungsvorgänge durch aminopeptidasenspezifische Inhibitoren sind Belege für eine funktionelle Expression von APN in den Leukozyten [120-122]. Verschiedene Sequenzaberrationen tragen dabei zur tumorrelevanten Ausprägung bei [123-125]. In soliden Tumoren ist APN im Vergleich zu den korrespondierenden gesunden Geweben oft dereguliert (Tabelle 2). Die Regulationsrichtung ist dabei stark von der jeweiligen Tumorentität abhängig. Eine erhöhte APN-Expression im Vergleich zum gesunden Gewebe bzw. zu APN-negativen Tumoren ist mit schlechteren Prognosen für Tumore des Pankreas und der Lunge sowie bei Kopf-Hals-Plattenepithelkarzinomen assoziiert [126-129]. Weiterhin konnte belegt werden, dass in undifferenzierten vergleichend zu differenzierten Schilddrüsenkarzinomen bzw. zum gesunden Struma-Gewebe mehr APN-Protein nachweisbar ist [127]. Im Kolonkarzinom korreliert die APN-Expression mit dem Tumorstadium [130]. Das krankheitsfreie bzw. das Gesamtüberleben der Patienten ist bei APN-Positivität im kanzerogenen Gewebe signifikant geringer. Patienten mit APN-negativen Metastasen überleben länger. Hohe Konzentrationen von löslicher APN in Patientenserum beim Bronchialkarzinom sind mit schlechter Prognose für die erkrankten Personen

assoziiert [131]. Prostatakarzinom-Patienten mit verringerten APN-Konzentrationen haben bessere Überlebensraten als die mit APN-positiven Tumoren [132]. Eine verminderte APN-Expression im Vergleich zu entsprechenden gesunden Geweben ist u. a. beim NZK und beim malignen Meningeom nachweisbar [133]. Beim NZK ist APN in ca. 30 % aller klarzelligen bzw. chromophilen Tumore, jedoch nicht in chromophoben Formen exprimiert [134]. Der Prozentsatz an APN-Positivität ist bei tumorinfiltrierenden T-Lymphozyten des NZK im Vergleich zu denen gesunder Patienten stark erhöht [135]. Die APN-Expression kann durch verschiedene Zytokine moduliert werden (Abbildung 3). In NZK-Zellen führen u. a. IL-1, IL-4 und IL-13 [102, 103], in Schilddrüsenkarzinomzellen z. B. EGF, bFGF oder IL-6 zu einer vermehrten Oberflächenexpression der Aminopeptidase [127]. Tabelle 2 fasst die Ergebnisse verschiedener immunhistochemischer Analysen zur Untersuchung der APN-Expression in gesunden bzw. tumoralen Gewebe zusammen.

Tabelle 2: Immunhistochemische Analysen zur APN-Expression in soliden Tumoren.

Entität	APN-Expression		Antikörper	Referenz ³
	gesundes Gewebe ¹	Tumor ²		
Ösophagus	negativ	35/65	38C12	[136]
Magen	negativ	84/121	?	[137]
Pankreas	positiv	25/50	MH8-11	[126]
	positiv	20/53	WM-15	[138]
Kolon	positiv	67/114	MH8-11	[130]
Leber	positiv	51/53	38C12	[139]
Brust	nur in Adipozyten	50/135	38C12	[140]
Lunge	negativ	68/194	MH8-11	[129]
Prostata	positiv	9/33	F23	[141]
	positiv	132/331	38C12	[132]

¹ Aufgrund häufig fehlender Analysen/ Aussagen in den jeweiligen Studien wurden Informationen zur APN-Expression im gesunden Gewebe ausschließlich aus der Datenbank <http://www.proteinatlas.org/ENSG00000166825/tissue> verwendet.

² Anzahl der APN-positiven Tumore im Verhältnis zur Gesamtzahl der analysierten Tumorproben (oft keine separaten Angaben zur Häufigkeit der APN-Expression in histologischen Subtypen bzw. Metastasen)

³ nur Studien mit einer größeren Anzahl an analysierten Tumorproben aufgelistet

Durch den Einsatz verschiedener aminopeptidasenspezifischer Inhibitoren bzw. in Transfektionsstudien der Genüberexpression/ -stilllegung konnten multiple tumorrelevante Funktionen für APN charakterisiert werden. Adhäsive, migratorische und invasive Veränderungen werden durch hydrolytische Spaltung von extrazellulären Matrixproteinen (z. B. Kollagene des Typs I bzw. IV) vermittelt [97, 142-146]. Weiterhin ist ein verändertes Ansprechen sowohl gegenüber dem Chemotherapeutikum Cisplatin im Ovarialkarzinom als auch gegenüber einer Strahlentherapie bei zervikalen Tumoren nachgewiesen worden [147, 148]. Ein genereller genregulatorischer Mechanismus der differentiellen APN-Expression sowie eine allgemeine tumorentitätsunabhängige APN-Funktion sind bisher nicht charakterisiert worden.

Aufgrund der unterschiedlichen Aufgaben und aufgrund vieler unbekannter struktureller und funktioneller Komponenten wird APN auch als *moonlighting ectoenzyme* bezeichnet [79]. Abbildung 4 fasst schematisch APN-vermittelte zelluläre Prozesse zusammen.

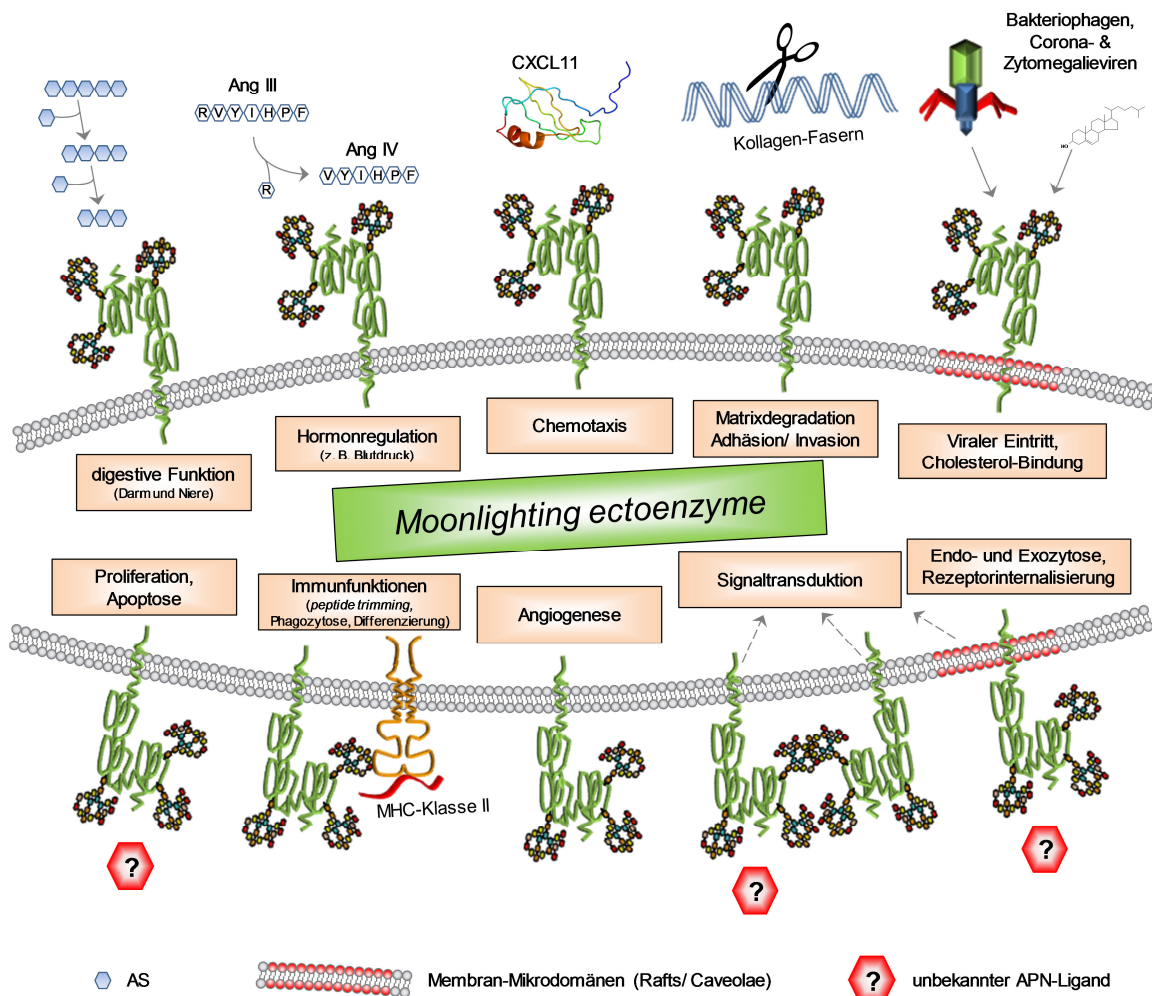


Abbildung 4: Multiple zelluläre Funktionen von APN.

2 Ziel der Arbeit

Unter der Anleitung von Prof. Dr. Jürgen Langner bzw. seit 2003 von Prof. Dr. Barbara Seliger beschäftigt sich das Institut für Medizinische Immunologie der Martin-Luther-Universität Halle-Wittenberg mit der Identifizierung und Charakterisierung potentieller Biomarker, die für neue Therapieformen zur zielgerichteten Behandlung vor allem des malignen Melanoms und des NZK angewendet werden könnten. Dabei werden diverse Hochdurchsatzverfahren (*RNA-Microarray*, Proteom-basierende Analysen, Mutations-/ Polymorphismus-Bestimmung mittels hochauflösender Schmelzpunktanalyse) eingesetzt, die molekulare Aberrationen nachweisen und ihre Auswirkungen auf zellbiologische bzw. tumorrelevante Prozesse belegen. Neben immunologischen Fragestellungen stehen unter anderem Expressions- und Funktionsanalysen diverser zytosolischer und transmembraner Peptidasen sowie Ubiquitin-editierender Enzyme im Fokus der Institutsforschung.

Die Expression von APN/ CD13 und UCHL1 ist oft in Tumorgewebe im Vergleich zum korrespondierenden Normalgewebe dereguliert. Weiterhin gibt es konträre Interpretationen, ob die jeweiligen hydrolytischen Enzymaktivitäten in die Tumorgenese involviert sind. Aufgrund unzureichender Informationen in der wissenschaftlichen Literatur wurden in der vorliegenden Arbeit folgende Fragestellungen bearbeitet:

- 1) Ist die Expression von APN und UCHL1 im Melanom im Vergleich zu Melanozyten bzw. zu gutartigen Nävi dereguliert? Sind diese Veränderungen mit klinisch-pathologischen Parametern assoziiert?
- 2) Welche genregulatorischen Mechanismen können die Veränderungen der möglichen differentiellen Genexpression erklären?
- 3) Welche zellbiologischen Konsequenzen hat eine deregulierte Expression von APN und UCHL1?
- 4) Haben die jeweiligen Enzymaktivitäten Einfluss auf zelluläre Funktionen?
- 5) Welche molekularen Ursachen können die möglichen APN- bzw. UCHL1-vermittelten Veränderungen begründen?

Analysen zur enzymatischen APN-Aktivität in tumorbiologischen Prozessen lieferten oft konträre Ergebnisse. Weiterhin war unklar, wie APN signaltransduzierende Prozesse in der Zelle vermittelt. Zur besseren molekularen Charakterisierung sollten als zweiter Schwerpunkt dieser Arbeit verschiedene APN-Mutanten des aktiven Zentrums generiert und in einem Transfektionsmodell von HEK293-Zellen zell- und molekularbiologisch

analysiert werden. Weiterhin sollten mittels diverser zellbasierender Kollaborationsstudien neue Interaktionspartner von APN in Monozyten bzw. in myeloischen Leukämiezellen identifiziert werden, die in Assoziation mit der Aminopeptidase signaltransduzierende Vorgänge vermitteln könnten.

3 Kurzbildschreibung der publizierten Manuskripte

3.1 Manuskript 1: Heterogeneous expression and functional relevance of the ubiquitin carboxyl-terminal hydrolase L1 in melanoma

Jens Wulfänger, Katharina Biehl, Anja Tetzner, Peter Wild, Kristian Ikenberg, Stephanie Meyer, Barbara Seliger.

International Journal of Cancer (2013), 133(11):2522-32.

Das Manuskript fasst die Ergebnisse der UCHL1-Expressionsanalysen in Gewebemikroarrays (TMA), Kurzzeitkulturen bzw. etablierten Zelllinien von Melanomen und die *in vitro*-Funktionsuntersuchungen der Hydrolase zusammen. In Melanozyten stark exprimiert, konnte UCHL1 in keinem der 50 Nävi, in 24 von 331 Melanomläsionen sowie in ca. 10 % der Kurzzeitkulturen bzw. der Melanomzelllinien nachgewiesen werden. Diese Expressionsreprimierung korrelierte mit einem verstärkten CpG-Methylierungsgrad des UCHL1-Promotors in den UCHL1-negativen Zelllinien im Vergleich zu den UCHL1-positiven Melanozyten und Melanomzellen. Demethylierungsexperimente mit 5'-Desoxyazacytidin (DAC) konnten die UCHL1-Expression zumindest partiell rekonstituieren. Unter Verwendung von diversen Transfektionsmodellen der Genüberexpression bzw. -stilllegung konnte eine proliferationsfördernde Funktion der Hydrolase auf die Zellen durch die positive Modulation des MAPK-Signalweges bestimmt werden. Diese Effekte waren von der Hydrolaseaktivität abhängig, da die defiziente UCHL1-Variante C90S sich wie die Kontrollzelllinien verhielt. Weiterhin wurde gezeigt, dass UCHL1 über eine veränderte Aktivierung des PI₃K/ Akt-Signalweges die Sensitivität der Zellen gegenüber reaktiven Sauerstoffspezies (ROS) am Beispiel von Wasserstoffperoxid modifiziert. Dieser Effekt war abhängig von der exprimierten UCHL1-Menge in dem entsprechenden Zellmodell.

Beiträge der Autoren

Jens Wulfänger hat das Manuskript zusammen mit Barbara Seliger konzipiert und geschrieben sowie folgende Experimente durchgeführt: Zellkultur und -behandlung (DAC, ROS) sowie Proliferationsanalysen (XTT, Weichagartest), Expressions- und epigenetische Untersuchungen (PCR, kombinierte Bisulfitbehandlung und Restriktionsanalyse (COBRA), Bisulfit-Sequenzierung), statistische Auswertung.

Katharina Biehl hat bei der Generierung der diversen UCHL1-Transfektionssysteme und deren Analyse mitgewirkt. Weiterhin bewerkstelligte sie die Immunblotuntersuchungen.

Anja Tetzner hat die ortsgerichtete Mutagenese von C90S und die Demethylierungsanalyse mittels HRM durchgeführt.

Peter Wild, Kristian Ikenberg, Stephanie Meyer haben die verwendeten TMA etabliert und die immunhistochemischen Analysen der UCHL1-Expression, deren statistische Auswertung und die Korrelation mit klinischen Parametern durchgeführt.

Barbara Seliger hat das Projekt vorgeschlagen, war an der Projektkonzeption und dem Schreiben des Manuskripts beteiligt.

Unterschrift Prof. Dr. Barbara Seliger

3.2 **Manuskript 2: Promoter methylation of aminopeptidase N/ CD13 in malignant melanoma**

Jens Wulfänger, Heike Schneider, Peter Wild, Kristian Ikenberg, Monica Rodolfo, Licia Rivoltini, Stephanie Meyer, Dagmar Riemann, Barbara Seliger

Carcinogenesis (2012), 33(4):781-790.

Das Manuskript beschreibt erstmalig die epigenetische Regulation der APN-Expression durch die Promotor-DNA-Methylierung im Melanom. Unter Verwendung von TMA, Kurzzeitkulturen bzw. etablierten Zelllinien konnte eine heterogene Expression von APN nachgewiesen werden. Da hohe myeloische Transkriptmengen bestimmt wurden, ist von einem aktiven myeloischen Promotor des APN-Gens auszugehen. *In silico* wurde erstmalig eine CpG-Methylierungsstelle in diesem Promotorbereich identifiziert und sowohl *in vitro* als auch *in vivo* charakterisiert. Der Verlust der APN-Expression in Melanomzellen war direkt mit einem hohen Grad an CpG-Methylierung assoziiert. Mittels des demethylierenden Agens DAC wurden myeloische Transkripte und APN-Protein sowohl zeit- als auch konzentrationsabhängig in den Melanomzelllinien induziert. Weiterhin zeigten die Zytokine TGF- β 1 und IL-4, jedoch nicht bFGF, IL-6 und EGF einen additiven induktiven Effekt nach DAC-Behandlung. Die APN-Expression war invers korrelierend mit der von melanozytären Markern wie Microphthalmie-assoziiierter Transkriptionsfaktor (MITF), Tyrosinase und *melanoma antigen recognized by T cells* (MART1). Zellbiologisch fungierte APN in Melanomzellen migrationsfördernd, hatte jedoch keinen Einfluss auf die Zellproliferation bzw. das verankerungsunabhängige Wachstum. Nach APN-Induktion durch DAC konnte eine Aminopeptidase-abhängige Migrationssteigerung in den behandelten Zellen nachgewiesen werden. In TMA wurde APN-Protein vorwiegend in primären Melanomläsionen detektiert, während in Nävi und Metastasen kaum APN nachweisbar war. Die Korrelation mit klinisch-pathologischen Parametern der Patienten zeigte, dass APN in der untersuchten Kohorte keine klinische Signifikanz hat.

Beiträge der Autoren

Jens Wulfänger hat das Manuskript zusammen mit Barbara Seliger konzipiert und geschrieben und folgende Experimente geplant, durchgeführt und interpretiert: *In silico-*

Identifizierung der CpG-Insel, Expressionsuntersuchungen (PCR, Durchflusszytometrie), epigenetische Untersuchungen (COBRA, Bisulfit-Sequenzierung), Zellbehandlung (DAC, Zytokine, APN-Inhibitoren) und anschließende Analyse der APN-Induktion (PCR, Durchflusszytometrie), der Migration (Transwell-Tests) und der Proliferation (XTT).

Heike Schneider generierte die stabil transfizierte Zelllinie WM-1862 und führte die Migrationsanalysen und Proliferationsstudien der Melanomzelllinien durch.

Peter Wild, Kristian Ikenberg, Stephanie Meyer etablierten die verwendeten TMA und führten die immunhistochemischen Analysen der APN-Expression, die anschließende Korrelation mit den entsprechenden klinischen Parametern sowie deren statistische Auswertungen durch.

Monica Rodolfo, Licia Rivoltini stellten die genomische DNA und RNA von Suspensionen bzw. Kurzkulturen der Melanome sowie deren klinikrelevanten und pathologischen Parametern zur Verfügung.

Dagmar Riemann wirkte bei der Generierung stabil transfizierter Zelllinien mittels Fluoreszenz-aktivierten Zellsortierens mit. Ebenfalls half sie beim Planen des Manuskripts, der Diskussion und beim Korrekturlesen.

Barbara Seliger war an der Idee, an der Konzeption und am Schreiben des Manuskripts beteiligt.

Unterschrift Prof. Dr. Barbara Seliger

3.3 Manuskript 3: Aminopeptidase N (APN)/ CD13-dependent CXCR4 downregulation is associated with diminished cell migration, proliferation and invasion

Jens Wulfaenger, Susanna Niedling, Dagmar Riemann, Barbara Seliger

Molecular Membrane Biology (2008), 25(1):72-82.

In diesem Manuskript wird die Funktion der APN-Enzymaktivität in einem HEK293-Transfektionsmodell der APN-Überexpression beschrieben. Mittels ortsgerichteter Mutagenese wurden diverse Basensubstitutionen in den Kodonen des HELAH- bzw. GAMEN-Motivs eingeführt und stabil exprimierende Transfektanten generiert. Jegliche Mutation führte zu einem kompletten Verlust der APN-Enzymaktivität. Die Oberflächenexpression der Aminopeptidase war jedoch nicht beeinträchtigt. Die Expression von aktiver wildtypischer APN auf der Zelloberfläche von HEK293-Zellen führte sowohl zu einer verringerten Proliferation (Verdopplungszeiten und verankerungsunabhängiges Wachstum) als auch zu reduzierten Migrationsraten gegenüber Kollagen. Weiterhin konnte gezeigt werden, dass aktive APN nicht nur zu einer verminderten Expression des Chemokinrezeptors CXCR4 auf mRNA- und Proteinebene in den Zellen führte, sondern auch die chemotaktische Migration zum entsprechenden Liganden, dem *stromal cell-derived factor* (SDF)-1 α , negativ beeinflusste. Da in allen Experimenten die inaktive E388G-Variante ein vergleichbares Verhalten wie die parentalen bzw. Vektorkontrollzellen zeigte, konnte zusammenfassend festgestellt werden, dass die APN-Enzymaktivität ursächlich für die veränderten Zellcharakteristika und für die verschlechterte SDF-1 α -vermittelte Chemotaxis der CXCR4-positiven Zellen war.

Beiträge der Autoren

Jens Wulfänger hat das Manuskript zusammen mit Dagmar Riemann und Barbara Seliger geplant und geschrieben und folgende Experimente durchgeführt: ortsgerichtete Mutagenese von E388G, Generierung des HEK293-Transfektionssystems, Bestimmung der Enzymaktivitäten und der enzymatischen Parameter, Proliferationsuntersuchungen, Migrationsanalysen, Expression der Chemokinrezeptoren, Chemotaxis
Susanna Niedling generierte im Rahmen ihrer Diplomarbeit die Mehrzahl der verwendeten Plasmide.

Dagmar Riemann wirkte bei der Generierung stabil transfizierter Zelllinien mittels Fluoreszenz-aktivierten Zellsortierens mit. Ebenfalls half sie beim Planen und Schreiben des Manuskripts.

Barbara Seliger war an der Konzeption und am Schreiben des Manuskripts beteiligt.

Unterschrift Prof. Dr. Barbara Seliger

3.4 **Manuskript 4: Functional co-localization of monocytic aminopeptidase N/ CD13 with the Fc gamma receptors CD32 and CD64**

Dagmar Riemann, Anatolij Tcherkes, Gert H. Hansen, **Jens Wulfaenger**, Tanja Blosz, E. Michael Danielsen

Biochemical and Biophysical Research Communications (2005), 331(4):1408-1412.

Aufgrund weniger Informationen über die funktionelle Relevanz von APN in Monozyten wurden in diesem Manuskript putative Interaktionspartner der Aminopeptidase untersucht und identifiziert. Der Schwerpunkt der Untersuchungen lag dabei auf der Komplexbildung mit diversen Fc γ -Rezeptoren. Unter Verwendung der konfokalen Laser-Scanning-Mikroskopie, der Elektronenmikroskopie mit Nano-Goldpartikeln und des Förster-Resonanzenergietransfers (FRET) in der Durchflusszytometrie konnte erstmalig eine starke Kolokalisation von APN mit dem Fc γ -Rezeptor II/ CD32 bzw. mit dem Fc γ -Rezeptor I/ CD64 nicht nur in der monozytären Leukämiezelllinie THP-1, sondern auch in humanen peripheren Blutmonozyten nachgewiesen werden. Dagegen wurde keine Interaktion mit dem *myeloid-specific sialic acid-binding receptor* CD33 detektiert. Daher könnte das Zusammenspiel von APN mit den Fc γ -Rezeptoren einen funktionellen Signaltransduktionskomplex in Monozyten darstellen.

Beiträge der Autoren

Dagmar Riemann hat das Manuskript konzipiert und geschrieben sowie zusammen mit Anatolij Tcherkes die FRET-Untersuchungen sowie die immunologischen Fluoreszenzfärbungen durchgeführt.

Gert H. Hansen und E. Michael Danielsen führten die Kolokalisationsstudien mittels Rasterelektronenmikroskopie unter Verwendung von Nano-Goldpartikeln durch.

Jens Wulfänger generierte die Abbildungen der konfokalen Laser-Scanning-Mikroskopie und half zusammen mit Tanja Blosz beim Schreiben des Manuskripts sowie beim Korrekturlesen.

4 Publizierte Manuskripte

4.1 Manuskript 1: Heterogeneous expression and functional relevance of the ubiquitin carboxyl-terminal hydrolase L1 in melanoma.



Heterogeneous expression and functional relevance of the ubiquitin carboxyl-terminal hydrolase L1 in melanoma

Jens Wulfänger¹, Katharina Biehl¹, Anja Tetzner¹, Peter Wild², Kristian Ikenberg², Stefanie Meyer³ and Barbara Seliger¹

¹Martin Luther University Halle-Wittenberg, Institute of Medical Immunology, 06112 Halle (Saale), Germany

²University Hospital Zuerich, Institute of Pathology, CH-8091 Zuerich, Switzerland

³University Hospital Regensburg, Clinic for Dermatology, 93053 Regensburg, Germany

The expression of ubiquitin carboxyl-terminal hydrolase 1 (UCHL1) is deregulated in human cancer cells with tumor inhibiting or promoting functions. Due to less knowledge on the role of UCHL1 in melanoma progression, the expression pattern and function of UCHL1 as well as the deregulated signaling pathways were characterized. A large number of melanoma cell lines, tissue microarrays of melanoma lesions and control tissues were analyzed for UCHL1 expression using PCR, Western blot and/or immunohistochemistry. The analysis revealed that melanocyte cultures, 24 of 331 melanoma lesions, two of 18 short-term cultures and two of 19 melanoma cell lines tested, respectively, heterogeneously expressed UCHL1. The low frequency of UCHL1 expression in melanoma cells was due to gene silencing by promoter DNA hypermethylation. Using different transfection models an enzyme activity-dependent growth promoting function of UCHL1 *via* the activation of the mitogen-activated protein kinase signaling pathway was found in melanoma cells. Under oxygen stress a dose-dependent effect of UCHL1 was detected, which was mediated by a dynamic modification of the PI3K-Akt signaling. Thus, the aberrant UCHL1 expression in melanoma cells is linked to dynamic changes in growth properties and signal transduction cascades suggesting that UCHL1 provides a novel marker and/or therapeutic target at least for a subset of melanoma patients.

Ubiquitination plays a key role in the post-translational modification of proteins and regulates in combination with phosphorylation and other post-translational alterations a number of cellular processes such as differentiation, proliferation, apoptosis and neoplastic transformation. The ubiquitination of proteins is controlled by so called deubiquitinating enzymes (DUB), which revert the binding between ubiquitin (ub) and their substrates,¹ protect proteins from proteasomal degradation and recycle ub-molecules of poly-ub chains. The DUB family is categorized into five different groups: (i) the ubiquitin carboxyl-terminal hydrolases (UCH), (ii) the ubiquitin-specific proteases (USP), (iii) the ovarian tumor proteases, (iv) the protein domain proteases of the Machado-Josef-disease and (v) the Jab1/MPN domain associated metalloproteinases.²

The UCH family member UCHL1, also known as PGP9.5, GAD or PARK5, is a cysteine protease with a molecular weight of approximately 25 kDa. Next to its hydrolase activity UCHL1 also possesses ligase activity,^{3,4} thereby the protein repertoire is multivalent regulated by its involvement in the cellular protein degradation and stabilization processes as well as in the homeostasis of the ub balance. Although UCHL1 is mainly expressed in neuronal and neuroendocrine tissues and represents about 2% of the total protein content of the brain,³ it is also found in the tubule epithelium of the kidney,^{5,6} in ovary⁷ as well as in testis.⁸ In neurodegenerative diseases such as Alzheimer's (AD) or Parkinson's disease (PD), an altered expression of UCHL1 could be indicated^{9,10} suggesting that protein imbalance by aberrant UCHL1 may

Key words: UCHL1, ubiquitination, melanoma, biomarker

Abbreviations: AD: Alzheimer's disease; COBRA: combined bisulfite restriction analysis; Ctrl: control; DAC: 5-aza-2'-desoxycytidine; DUB: deubiquitinating enzymes; Erk: extracellular signal-regulated kinase; GAPDH: glyceraldehyde-3-phosphate dehydrogenase; HPR1: hypoxanthine-guanine phosphoribosyltransferase; HRP: horseradish peroxidase; IHC: immunohistochemistry; MAPK: mitogen-activated protein kinase; med: medium; MJD: Machado-Josef-disease; PCR: Polymerase chain reaction; PD: Parkinson's disease; PI3K: phosphatidylinoside 3-kinases; PPIA: peptidylprolyl isomerase; RCC: renal cell carcinoma; ROS: reactive oxygen species; shCtrl: scramble-shRNA; shUCHL1: UCHL1-specific shRNA; TMA: tissue microarray; TNF: tumor necrosis factor; ub: ubiquitin; UCH: ubiquitin carboxyl-terminal hydrolase; USP: ubiquitin-specific proteases; wt: wild type; XTT: tetrazolium salt

Additional Supporting Information may be found in the online version of this article.

Grant sponsor: Mildred Scheel Foundation; **Grant number:** BS, FKZ 108529, SM, FKZ 108134

DOI: 10.1002/ijc.28278

History: Received 12 Nov 2012; Accepted 2 May 2013; Online 17 May 2013

Correspondence to: Prof. Dr. Barbara Seliger, Martin Luther University Halle-Wittenberg, Institute of Medical Immunology, Magdeburger Str. 2, 06112 Halle, Germany, Tel.: +49-0-345-557-4054, Fax: +49-0-345-557-4055, E-mail: barbara.seliger@uk-halle.de

What's new?

The ubiquitin-specific hydrolase L1 (UCHL1) is an enzyme that protects ubiquitinated proteins from degradation and recycles ubiquitin moieties. UCHL1 is mainly expressed in the brain but has been associated with different tumors outside the brain. Here, the authors analyzed the expression pattern of UCHL1 in melanoma cell lines and primary tumors. They report a wide-spread loss or reduced expression of UCHL1 in melanoma cells, which was directly correlated with promoter DNA hypermethylation. The subset of melanoma cells, which still expressed UCHL1, showed altered growth properties and tolerances against reactive oxygen species as compared to UCHL1-negative cells. The authors propose that UCHL1 may function as a new diagnostic biomarker or therapeutic target for the treatment of UCHL1-positive melanomas.

be an important issue in both diseases. Despite mutations and protein modifications of UCHL1 have been detected in neurodegenerative tissues,^{10–14} their functional role and their *in vivo* relevance are controversially discussed.^{4,12} UCHL1 downmodulates the beta-site amyloid precursor protein (APP) cleaving enzyme-1 mediated processing of the amyloid β protein¹⁵ suggesting that UCHL1 may be an interesting target structure for the AD drug development.

Due to the differential expression pattern of UCHL1 in various tumor entities, this protease might represent a novel therapeutic structure for the treatment of patients with cancer. While UCHL1 expression is downregulated in *e.g.* lymphatic leukemia,¹⁶ mammary carcinoma and colon carcinoma compared to control tissue,^{17,18} it is upregulated in neuroblastoma,¹⁹ pancreatic²⁰ as well as prostate carcinoma.²¹ These differences are often mediated by an altered DNA methylation status of the UCHL1 promoter. Thus, cytosine-phosphate-guanine (CpG) hypermethylation was correlated with a loss or diminished expression of the hydrolase in a wide variety of tumor cells.^{22,23} In *in vitro* transfection studies, the cancer-inhibiting or -progressing function of UCHL1 dependent on the tumor entity could be demonstrated. In addition, in renal cell carcinoma (RCC) UCHL1 overexpression correlated with an enhanced proliferative capacity and an invasive and metastatic behavior.²⁴ However, UCHL1 restricted the growth and migration properties of malignant colon and mammary carcinoma cells.²⁵ Based on these data a tumor-specific and disease-dependent dynamic regulation of UCHL1 is postulated, but the underlying molecular mechanisms controlled by UCHL1 expression are unknown. Little information exists about UCHL1 expression in melanoma. Recently, a frequent DNA methylation of the UCHL1 promoter has been described.²⁶ However, the role of UCHL1 in the pathogenesis of this disease is unclear. Therefore, the aim of this study was to analyze the expression, regulation, function and clinical relevance of UCHL1 in melanoma cells.

Materials and Methods**Cell lines and cell treatment**

The human melanoma cell lines were obtained from EST-DAB²⁷ or were kindly provided by Soldano Ferrone (Hillman Cancer Research Institute, Pittsburgh, PA) and have been authenticated. UCHL1-overexpressing or gene silenced

melanoma cells were generated by transfection using the Lipofectamine 2000 reagent (Invitrogen, Carlsbad, CA) as previously described.²⁸ All cell lines and transfectants were cultured in RPMI1640 medium supplemented with 10% fetal calf serum (FCS), 2 mM L-glutamine, 10 mM HEPES and respective antibiotics. Short-term melanoma cultures of single cell tumor suspensions (termed T1–18) were grown under standard conditions as previously reported.²⁹ Normal human epidermal melanocytes (NHEMs; PromoCell, Heidelberg, Germany) were derived from normal skin of different donors and cultivated in melanocyte medium MGM-3 (Gibco, Eggenstein, Germany) under a humidified atmosphere of 5% CO₂ at 37°C.

For demethylation studies, melanoma cell lines were treated daily with fresh medium containing different concentrations (0–10 μ M) of 5-aza-2'-desoxycytidine (DAC; Sigma, St. Louis, MO) for the time points indicated. For cell treatment with hydrogen peroxide, 24 hr post-seeding cell culture medium was exchanged to serum-reduced (0.5% FCS) medium containing the indicated hydrogen peroxide concentration ranging from 0 to 75 μ M for additional 24 hr. The influence of UCHL1 on melanoma growth *via* the mitogen-activated protein kinase (MAPK) signal transduction was analyzed by adding 10 μ M U0126 inhibitor (Sigma, St. Louis, MO) to the cells for one day.

UCHL1 overexpression and silencing

The full-length sequence of the human wild type UCHL1 (wtUCHL1) was isolated from total cellular RNA of HEK293 cells using the UCHL1-specific primers 5'-ATAAAGCTTACCATGCAGCTCAAGCCGATGGAGATCAAC-3' (forward) and 5'-TACCGCGGTTAGGCTGCCTTGCAGAGAGCA-3' (reverse). The cDNA was cloned into the *Hind*III and *Sac*II restriction sites of a cytomegalovirus (CMV)-based mammalian expression vector. The enzymatic inactive form C90S was generated with the polymerase chain reaction (PCR)-based QuikChange XL site-directed Mutagenesis Kit (Stratagene, La Jolla, CA) according to the instruction manual. For gene silencing, the GeneClip U1 Hairpin Cloning System (Promega, Madison, WI) and the UCHL1-targeting sequence GGGTAGATGACAAGGTGAATT were used. Oligonucleotides were designed, annealed and ligated into the

vector backbone according to the manufacturer's protocol. The integrity of all vectors was confirmed by DNA sequencing.

qPCR analysis

RNA from short-term melanoma cultures and from melanoma cell lines was prepared and reverse transcribed into cDNA as recently described.²⁸ qPCR was performed on a Rotor-Gene 6000 system (Corbett Research, Sydney, Australia) employing the Platinum SYBR Green qPCR SuperMix-UDG (Invitrogen, Carlsbad, CA) and the respective primers (Supporting Information Table 1). The mRNA levels were normalized to the expression of the three reference genes glyceraldehyde-3-phosphate dehydrogenase (GAPDH), peptidylprolyl isomerase (PPIA) as well as hypoxanthine-guanine phosphoribosyltransferase (HPRT). Data were analyzed with the comparative quantitation mode of the Rotor-Gene 6000 software version 1.7. Results are presented as relative expression level to the indicated control of at least three independent experiments.

Immunoblot analysis

Protein quantification studies were performed as previously described.²⁸ Briefly, 50 µg total protein/lane were separated in sodium dodecyl sulfate polyacrylamide gel electrophoresis (SDS-PAGE), transferred to nitrocellulose membrane and immunoblotted with the indicated primary antibodies (Supporting Information Table 2). Equal protein loading was determined using an anti-GAPDH antibody (Cell Signaling, Danvers, MA). After incubation with appropriate horseradish peroxidase (HRP)-conjugated secondary antibodies, protein bands were visualized using a chemiluminescence-based system. The expression levels were densitometrically quantified using the AIDA software program (Raytest, Straubenhardt, Germany). Results are expressed as mean ± SD of at least four independent experiments.

Immunohistochemistry of tissue microarrays

To investigate UCHL1 expression in melanoma lesions, tissue microarrays (TMAs) consisting of 364 primary malignant melanoma lesions, 39 metastases and 62 benign nevi were used. The generation of paraffin-embedded sections, the clinicopathological characteristics and the protocol of TMA stainings are summarized in the work by Wulfänger *et al.*²⁸ For immunohistochemistry, the TMA blocks were freshly cut (3 µm) and mounted on super frost slides (Menzel Glaeser, Braunschweig, Germany). After deparaffinization and rehydration of tissues, the TMAs were incubated with the UCHL1-specific primary antibody (clone 13C4/I3C4, Abcam, Cambridge, UK) overnight at 4°C followed by immunostaining with the UltraView Universal HRP Detection Kit (Ventana Medical Systems, Tucson, AZ). Slides were counterstained with hematoxylin, dehydrated and mounted. The surgical pathologists (K.I. and P.W.) performed a blinded evaluation of the stained slides with a classification of negative or positive UCHL1 expression, respectively.

Positive immunoreactivity was defined if at least a faint staining could be observed.

Combined bisulfite restriction analysis

Combined bisulfite restriction analysis (COBRA) was performed as previously described.²² Briefly, genomic DNA was isolated and bisulfite converted according to the manufacturer's protocols. After nested PCR amplification (primer listed in Supporting Information Table 1) products were digested with the different restriction enzymes *Bst*UI, *Taq*²I and *Hpy*188I (New England BioLabs, Frankfurt, Germany) recognizing CpG specific sequences. After separation of cleaved products on 3% agarose gels, the degree of cleavage to the corresponding uncleaved control and consequently the methylation status was categorized into different groups as representatively shown in Supporting Information Figure 1A.

Soft agar cloning and growth curve analysis

The anchorage-independent growth of melanoma cells was analyzed as previously described with one modification.²⁸ After staining and digitalizing of viable cells, colonies were further quantified using the analysis software Proteomweaver (Version 4.0, Bio-Rad, Hemel Hempstead, UK).

For analysis of the proliferation rate, the tetrazolium salt (XTT)-based colorimetric Cell Proliferation Kit II (Roche Applied Science, Mannheim, Germany) was used. Briefly, 5×10^5 cells were seeded in triplicates in the cavities of a 96-well culture plate. After 48 hr cell growth was monitored by incubation with the XTT-labeling mixture for 4 hr followed by a spectrophotometric measurement at a wavelength of 490 nm. Results are expressed either as absorbance or as relative growth to the indicated control of at least three independent experiments.

Results

UCHL1 expression in melanoma cells

Due to the little knowledge about the expression of UCHL1 in melanoma cells, a melanoma-specific TMA containing 331 informative melanoma lesions and 50 benign nevi was stained with an anti-UCHL1-specific mAb as described.²⁴ Twenty-four of 331 melanoma lesions were defined as positive with an at least weak cytoplasmic staining (Fig. 1a), but with no preference to any melanoma subtype (data not shown). In contrast, none of the 50 benign nevi showed a positive immunoreactivity (Fig. 1a). Using short-term cultures as well as melanoma cell lines the heterogenic UCHL1 expression in tumor cells was confirmed. Two of 18 short-term cultures (Fig. 1b) and about 11% of all melanoma cell lines (Fig. 1c) showed abundant UCHL1 mRNA amounts which correlated with the protein expression in the cell lines, respectively (Fig. 1c). Analysis of melanocytes revealed the highest UCHL1 mRNA amounts as representatively shown for two melanocyte cultures (Fig. 1c). Thus, a suppression of UCHL1 expression in the early phases of melanoma progression is postulated.

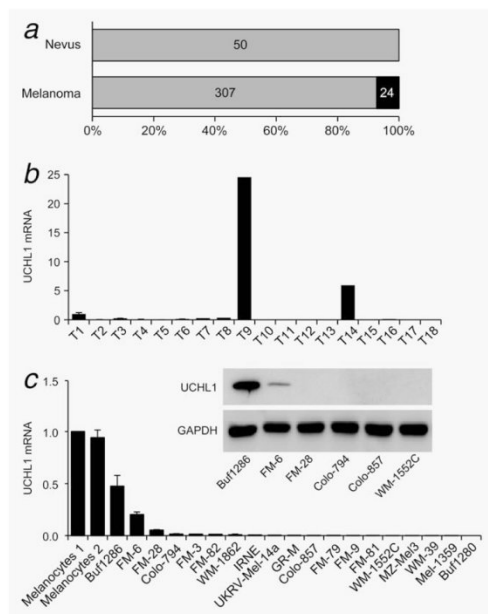


Figure 1. Induced UCHL1 expression in melanoma cells. (a) Cumulative bar charts including the number of cases with negative (gray bars) and cytoplasmic UCHL1 immunoreactivity (black bars) in nevi and melanoma are shown. (b) UCHL1 mRNA expression in short-term melanoma cultures. qPCR analysis were performed as described in the Materials and Methods section. Relative mRNA levels normalized to probe T1 (set to 1) are presented. (c) Decreased UCHL1 expression in melanoma cell lines. UCHL1 mRNA amounts of three biological duplicates of 19 melanoma cell lines were normalized to the expression of the melanocyte sample 1 (set to 1). A representative immunoblot of UCHL1 protein in melanoma cells is shown.

Impaired UCHL1 expression by DNA methylation of its promoter

To analyze whether epigenetic hypermethylation could be a crucial regulatory mechanism of deficient UCHL1 expression, the DNA methylation status of the corresponding promoter was analyzed in several melanoma cells using COBRA. Hypermethylation of the UCHL1 promoter DNA observed by cleavage of PCR products was associated with low or marginal mRNA expression in short-term cultures as well as in established cell lines (Figs. 2a and 2b). In contrast, high UCHL1 transcript amounts correlated with a low or lack of methylation of the UCHL1 promoter DNA in both melanoma cells as well as in melanocytes, which was also confirmed by direct bisulfite sequencing (data not shown). Treatment of melanoma cell lines with the DNA base analogue DAC induced UCHL1 transcription in several negative melanoma cell lines (Fig. 2c), whereas DAC affected no or marginal the mRNA levels of UCHL1-positive cells. The induction by DAC was dose- and time-dependent. Already 0.5 μM DAC was sufficient for an

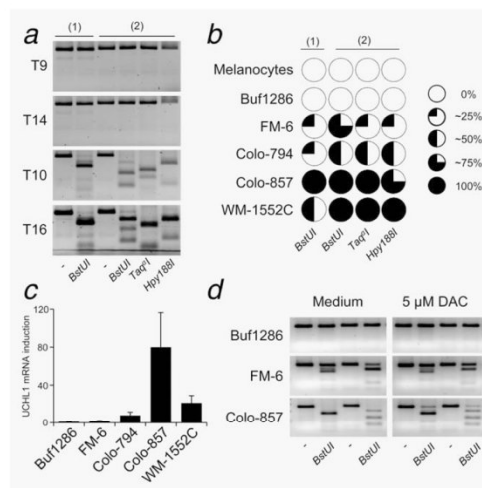


Figure 2. Epigenetic controlled UCHL1 expression in human melanoma cells. (a) Distinct promoter DNA methylation pattern in short-term melanoma cultures. COBRA was performed as described in Materials and Methods. (b) Different methylation status of UCHL1 promoter DNA. Results of COBRA using different restriction enzymes with percentage classification of DNA methylation pattern are summarized. (c) UCHL1 mRNA induction by DAC. Melanoma cells were treated with 5 μM DAC daily for a period of four days prior to mRNA isolation and qPCR analysis. Results are expressed as x-fold mRNA induction relative to untreated cells of at least three independent experiments. (d) Representative COBRA of untreated and DAC treated melanoma cells.

upregulation with highest UCHL1 mRNA levels upon incubation with 5 μM DAC for 96 hr (Supporting Information Fig. 1B). Interestingly, the UCHL1 protein expression was found only partially affected by DAC treatment. DAC further enhanced protein level in constitutive positive FM-6 cells (Supporting Information Fig. 1C), whereas in UCHL1-negative melanoma cells no re-expression of protein was detectable after DAC treatment. Analyzing DAC-treated cells with COBRA only a partial demethylation of the UCHL1 promoter was observed as shown for Colo-857 (Fig. 2d). Using an established high resolution melt curve analysis (HRM) differences in the guanine-cytosine (GC) content of bisulfite-treated genomic DNA in tested cell lines was observed. Furthermore, a decreased number of CpG sites by DAC treatment reflected in a lower melting point was confirmed in Colo-857 and FM-6 cells (Supporting Information Fig. 1D). Consequently, a high grade of promoter DNA methylation is responsible for lack of UCHL1 protein in melanoma cells.

Proliferation-promoting function of UCHL1 in melanoma cells

To investigate growth-promoting properties of an UCHL1 expression in melanoma cells, the proliferative capacity of the UCHL1-positive cell lines Buf1286 and FM-6 was compared

Carcinogenesis

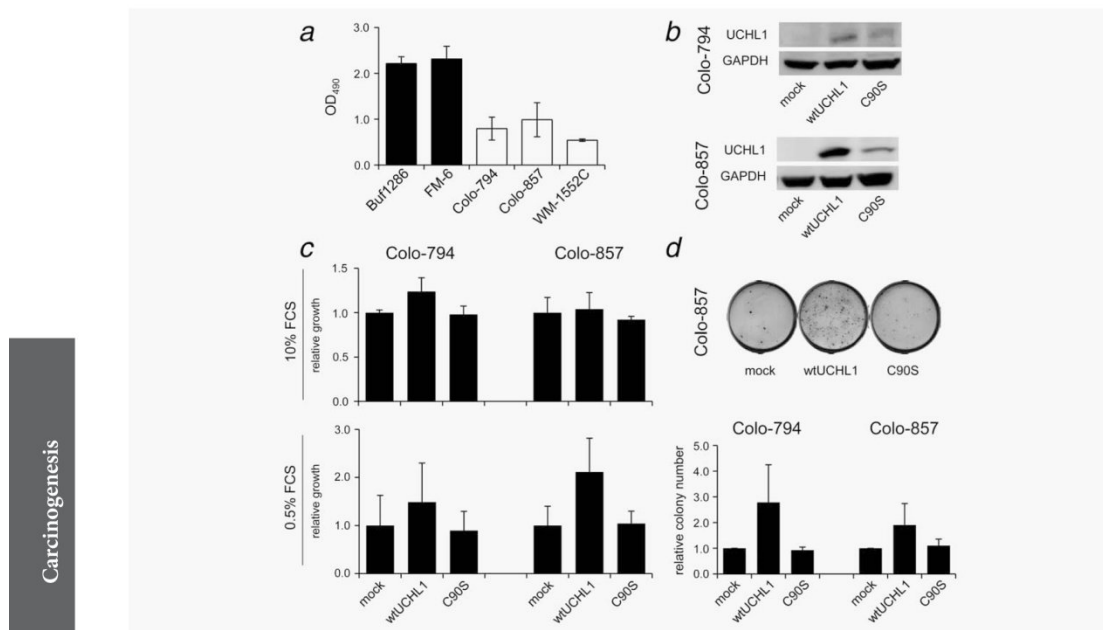


Figure 3. UCHL1 overexpression increases melanoma growth properties. (a) Different proliferation rates of UCHL1-positive (black bars) compared to UCHL1-negative melanoma cell lines (white bars). Growth of cells was analyzed with XTT under cell culture conditions as described in Materials and Methods. Values represent the average of three independent experiments. (b) UCHL1 overexpression in melanoma cells. Representative immunoblots of stable transfectants are presented. (c) Increased proliferation in wtUCHL1-, but not in C90S-transfectants. Cell growth with serum (10% FCS) as well as under serum-starved culture conditions (0.5% FCS) was determined using a XTT-based assay. Growth rates of melanoma transfectants in relation to mock control of at least three independent experiments are displayed. (d) wtUCHL1-mediated upregulation of anchorage-independent cell growth. Representative colony formation assays as well as relative colony numbers of three independent experiments are shown.

to three negative cell lines using a XTT-based assay. Both the cell lines, Buf1286 and FM-6, grew approximately two-fold faster than Colo-794, WM-1552C and Colo-857 cells (Fig. 3a). To specify the involvement of the hydrolase in growth properties, several UCHL1 transfection systems of melanoma cells were established, in which the hydrolase was either overexpressed or gene silenced. UCHL1 expression into the UCHL1-negative melanoma cell lines Colo-794 and Colo-857 (Fig. 3b) increased cell proliferation compared to the corresponding mock controls. These effects differed in extent and dependent on the culture conditions. Using 10% FCS in the medium, only Colo-794 wtUCHL1 overexpressing cells showed a higher proliferation rate, whereas under serum starvation by FCS depletion (0.5%) an enhanced proliferation rate was observed for wtUCHL1 overexpressing cells both in Colo-794 and in Colo-857 (Fig. 3c). Furthermore, wtUCHL1 transfectants were able to form colonies in soft agar to a higher extent than the corresponding mock controls (Fig. 3d).

Vice versa, an approximately 50% gene silencing in Buf1286 melanoma cells using UCHL1-specific shRNA (Fig. 4a) resulted in a decreased proliferative capacity of cells under

normal culture conditions and upon serum starvation (Fig. 4b) as well as in soft agar (Fig. 4c) compared to corresponding shRNA control cells (shCtrl). After wtUCHL1 overexpression in Colo-794 cells as well as after gene silencing in Buf1286, an altered polyubiquitination status of proteins was observed by immunoblot analyses of protein extracts (Supporting Information Fig. 2). Thereby, the grade of polyubiquitinated proteins correlated inversely to the levels of wtUCHL1 expression. Thus, results showed a functional relevance of UCHL1 expression on melanoma cell growth in the transfection models. Furthermore, the inactive UCHL1-variant C90S³⁰ displayed no significant differences in growth properties compared to mock controls, suggesting that the growth-stimulating capacity of wtUCHL1 was dependent on the enzyme activity.

Modification of the mitogen-activated protein kinase signaling pathway by UCHL1

Several abnormalities in the MAPK signal transduction cascade are associated with the initiation and progression of melanoma.³¹ To establish a link between UCHL1 expression and MAPK activation, the phosphorylation status of the

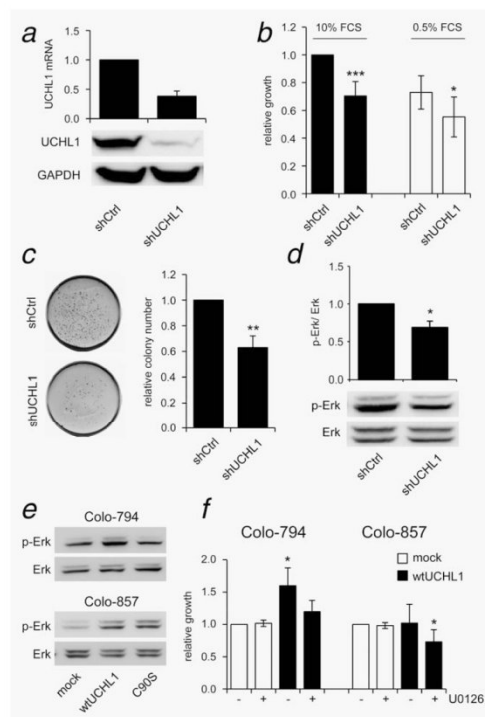


Figure 4. UCHL1-mediated cell proliferation control via the MAPK pathway. (a) Gene silencing by shUCHL1 in Buf1286 cells. Downmodulation was controlled by qPCR and immunoblotting. (b) Decreased cell growth after shUCHL1 transfection. Cell growth was determined by the XTT assay. Values represent growth rates relative to shCtrl under normal (black bars, *** $p < 0.001$) and serum-starved conditions (0.5% FCS; white bars, * $p < 0.05$) of at least three independent experiments. (c) Reduced formation of soft agar colonies in shUCHL1 transfectants compared to shCtrl. Colony forming assay was performed as described in Materials and Methods. Representative colony staining and relative numbers of two independent experiments are displayed (** $p < 0.01$). (d) Decreased MAPK activation after UCHL1 silencing. Representative immunoblots of p-Erk and Erk are presented (* $p < 0.05$). (e) Increased MAPK activation in wtUCHL1 transfectants. (f) Growth inhibition of wtUCHL1 transfectants by the MAPK-specific inhibitor U0126 cells were incubated in the presence or absence of 10 μ M U0126 during the proliferation assay. Results are expressed as x-fold growth of wtUCHL1 transfectants (black bars) in relation to the mock control (white bars). (* $p < 0.05$).

extracellular signal-regulated kinase (Erk)1 and Erk2 (p-Erk) was determined in the different transfection models. While the total amounts of Erk proteins were not affected, UCHL1 gene silencing in Buf1286 resulted in a strong decrease of p-Erk compared to the corresponding shCtrl (Fig. 4d). In wtUCHL1 transfectants of both Colo-794 and Colo-857 cells a higher level of Erk activation was found (Fig. 4e) suggesting a synergistic positive regulation of the MAPK pathway by UCHL1. The

influence of the different phosphorylation status of Erk1 and Erk2 on the melanoma growth was confirmed by the treatment of melanoma cells with the MEK1/2 specific inhibitor U0126 (Fig. 4f). The proliferation-promoting effects of UCHL1 were strongly inhibited by U0126 in Colo-794 and Colo-857 cells. In contrast, the corresponding mock control demonstrated no significant differences in growth properties after treatment.

Distinct UCHL1-dependent response to H₂O₂-induced inhibition of cell viability

Increased sensitivity to reactive oxygen species (ROS) could contribute to an increased efficacy of therapeutic strategies in patients with malignant melanoma.³² To investigate whether UCHL1 could influence the tolerance of melanoma cells to ROS and whether it could therefore represent a therapeutic target of selected melanoma patients, various UCHL1-positive and UCHL1-negative model systems were treated with increasing concentrations of H₂O₂ (0–75 μ M). The constitutive UCHL1-expressing melanoma cells Buf1286 and FM-6 showed a significant higher tolerance to H₂O₂ compared to UCHL1-negative cells (Fig. 5a). In contrast, the wtUCHL1 transfectants of both Colo-794 and Colo-857 cells altered sensitivities to the ROS treatment to a different extent. While UCHL1 expression sensitized Colo-794 cells to H₂O₂, Colo-857 cells were increasingly resistant (Fig. 5b). These opposite effects might be due of the different UCHL1 expression levels in the respective cell lines. Extended studies using additional melanoma transfection models showed that high expressed UCHL1 levels in Buf1280, FM-82 and Colo-857 correlated with an increased H₂O₂ tolerance compared to mock controls, whereas low UCHL1 amounts expressed in WM-1552C, IRNE and Colo-794 cells caused reduced cell viabilities under the same conditions (Fig. 5c). This phenomenon was confirmed with cell clones of shUCHL1-transfected Buf1286 showing different levels of UCHL1 gene silencing. The H₂O₂ resistance was highest in Buf1286 cell clones expressing median UCHL1 levels, whereas lower or higher UCHL1 expression in these cells resulted in an increased sensitivity to ROS (Fig. 5d). Using 10 μ M H₂O₂ a significant increase of cell viability was observed in relation to untreated cells, which represents a stimulatory growth effect during oxidative stress mediated by an unknown UCHL1-dependent mechanism. Analysis of different UCHL1-positive FM-6 cell clones with variable UCHL1 expression levels demonstrated a correlation of the UCHL1 amounts with the UCHL1 promoter DNA methylation status (Supporting Information Fig. 3A) as well as with the cell viability after ROS treatment which further supported a UCHL1 concentration-dependent resistance or sensitivity in all analyzed melanoma model systems (Supporting Information Fig. 3B).

Altered Akt activation by UCHL1

In addition to MAPK, the phosphoinositol-3-kinase (PI3K)-Akt signaling pathway is involved in the development of melanoma.³¹ Thus, the expression and activation of Akt were

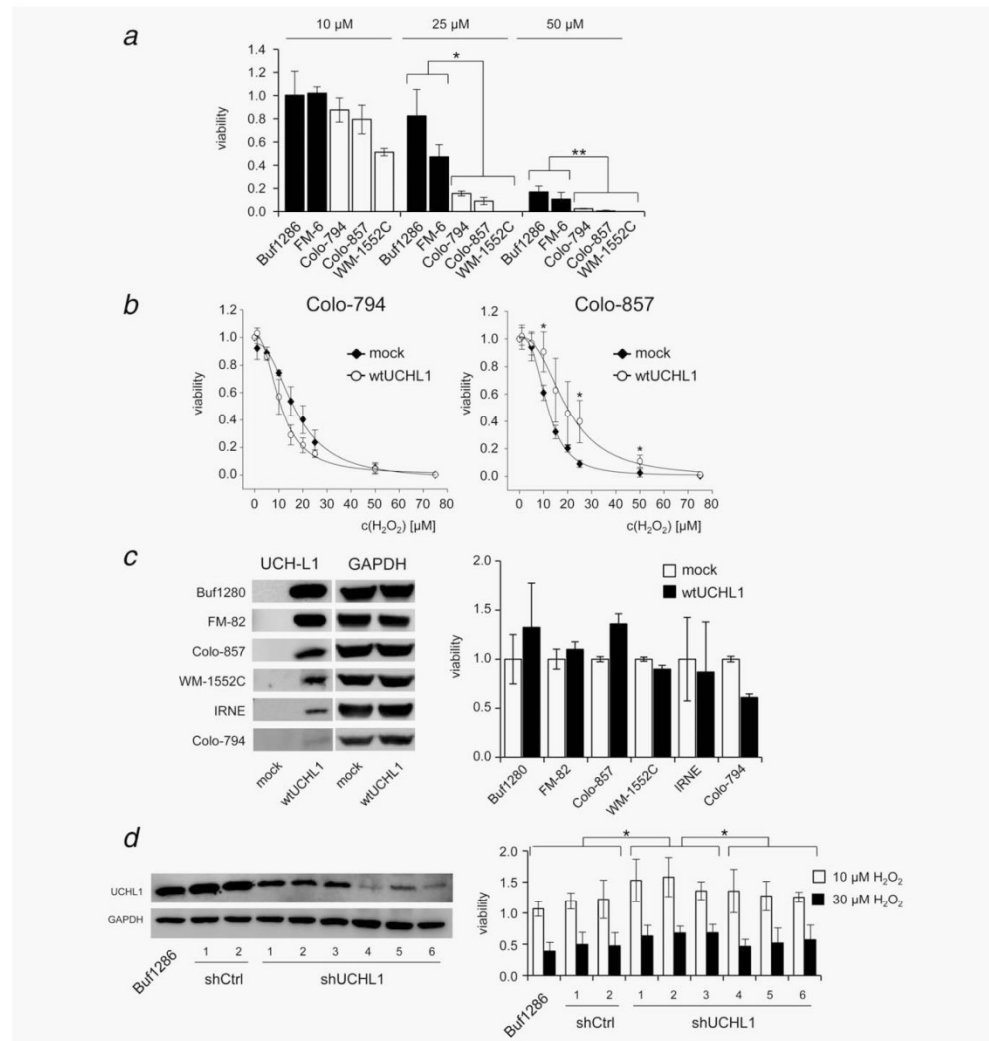


Figure 5. Distinct sensitivities of UCHL1-expressing cells to hydrogen peroxide. (a) Higher resistance against H₂O₂ by UCHL1 expression. After 24 hr seeding, cells were incubated with different H₂O₂ concentration for additional 24 hr. Then, cell viability of UCHL1-positive (black) and UCHL1-negative melanoma cells (white bars) was measured using XTT and normalized to the viability of untreated cells (set to 1; **p* < 0.05; ***p* < 0.01). Results are expressed as averaged values of at least three independent experiments. (b) Distinct H₂O₂ sensitivity of different UCHL1 transfectants. The data demonstrates viabilities of two wtUCHL1-overexpressing cells in comparison to mock controls obtained from three independent experiments (**p* < 0.05). (c) UCHL1 dose-dependent sensitivity to hydrogen peroxide. Representative immunoblots and cell viability after 24 hr exposure to 10 μM H₂O₂ of wtUCHL1^{low} and wtUCHL1^{high} transfectants as well as corresponding mock controls are displayed. (d) UCHL1 knock down causes altered sensitivities of Buf1286 melanoma cells with highest resistance to the indicated H₂O₂ concentrations in transfectants with median UCHL1 levels compared to mock controls and cell clones with very strong UCHL1 silencing (**p* < 0.05).

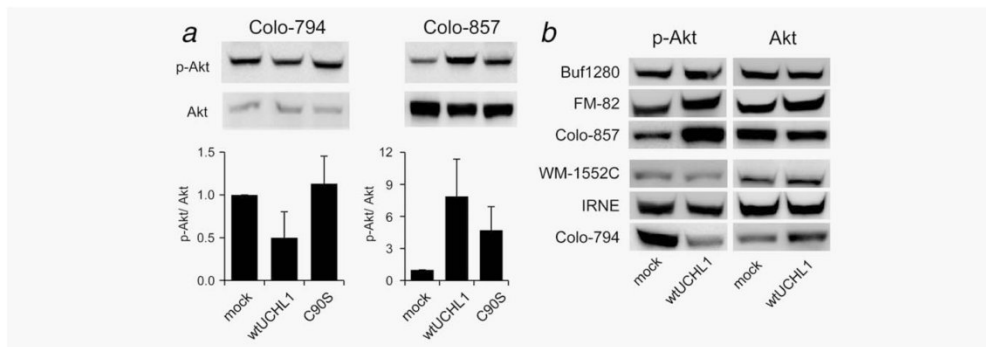


Figure 6. UCHL1-mediated alterations of the PI3K-Akt signaling pathway. (a) Different impact of wtUCHL1 expression on the Akt phosphorylation status. Representative immunoblots as well as the average of AIDA quantification of at least three independent experiments are shown. Results of the UCHL1-specific transfectants are expressed in relation to the corresponding vector controls. (b) Dose-dependent influence of UCHL1 expression on Akt activation. Immunoblot analyses of six melanoma cell lines overexpressing distinct levels of UCHL1 and the corresponding control cells are presented.

monitored in the present study. A distinct regulation of the Akt phosphorylation status was found in two wtUCHL1 transfection models. Whereas weak UCHL1-positive Colo-794 transfectants showed decreased p-Akt levels, an increased Akt activation was detected in UCHL1 strong expressing Colo-857 cells compared to the corresponding vector controls (Fig. 6a). In contrast, the inactive C90S variant lacked or only marginally influenced the p-Akt levels suggesting that the hydrolytic activity was involved in Akt signaling. The UCHL1-mediated, dose-dependent regulation of p-Akt was further confirmed using wtUCHL1 transfectants of six different melanoma cell lines with various expression levels. Strong positivity correlated with an activation of Akt, while weak expression had opposite effects (Fig. 6b). Thus, UCHL1 has an impact on the activation status of the PI3K-Akt in a dose-dependent manner.

Discussion

Due to its differential gene expression and various molecular and cellular functions, UCHL1 represents an interesting target for the design of novel molecular-targeted cancer treatment strategies and T cell-based immunotherapy of many tumor types.³³ The current work supports its implementation as a therapeutic target for melanoma since (i) UCHL1 expression is altered in the early phases of the melanoma progression process and is still expressed in at least a subset of melanoma cells and (ii) UCHL1 enhances the proliferation of tumor cells by modulating important cellular signaling pathways. Furthermore, UCHL1 modulates the sensitivity of cells to ROS by an altered Akt signaling.

Epigenetically controlled heterogeneous expression of UCHL1 in melanoma cells

UCHL1 is heterogeneously expressed in different tumor entities. Compared to corresponding normal tissue UCHL1 is downregulated in lymphatic leukemia,¹⁶ ovarian as well as colon carcinoma,¹⁸ while in neuroblastoma,¹⁹ prostate²¹ and

pancreatic²⁰ cancer it is upregulated. In addition, heterogeneous UCHL1 levels have been described for the RCC.²⁴ High UCHL1 amounts were detected in normal kidney epithelium and RCC metastases. In contrast, a lack or decreased UCHL1 expression was found in primary RCC leading to the hypothesis of a dynamic UCHL1 regulation depending on the tumor type, stage and grade. The expression and functions of UCHL1 in melanoma is poorly understood. Therefore, the present study analyzed the frequency of UCHL1 expression in melanoma lesions and melanoma cell lines as well as its role in the biology of this disease. Using TMAs containing a large series of tumor lesions significant UCHL1 amounts were found in approximately 7.2% of melanoma specimen, which was independent of the tumor subtype (data not shown). This frequency was confirmed for short-term melanoma cultures as well as in approximately 11% of melanoma cell lines. In melanocyte cultures, a strong UCHL1 positivity was found, which is in accordance with two independent studies demonstrating an UCHL1 expression in melanocytes, but a decreased frequency in melanoma cell lines using DNA micro array-based profilings.^{26,34} Since all of the 50 informative cases of benign nevi analyzed lack UCHL1, our data suggest that gene silencing of the hydrolase already occurs at an early step in the melanoma development. The lack or low level of UCHL1 mRNA and/or protein in the melanoma cells were directly correlated with the methylation status of the UCHL1 DNA promoter. This confirms a recent report showing a hypermethylation of the UCHL1 promoter in melanoma lesions as well as in cell lines at high frequency using a high-throughput technology for DNA methylation analyses.²⁶ Furthermore, in other solid tumors, such as renal cell, prostate, breast and colorectal carcinoma an epigenetic regulation of UCHL1 by CpG promoter methylation was described, which appears to be the major cause of its deficient expression in malignancies.^{18,22,35,36} Treatment of melanoma cells

with DAC at least partially restored the UCHL1 expression. Thus, DAC treatment caused a twofold increase of UCHL1 transcription in FM-6 cells to an 80-fold induction in Colo-857 cells. However, the mRNA induction was only prominent in FM-6 cells that increased UCHL1 protein amounts that could be detected. This discrepancy might be explained by the detection limit of commercial antibodies raised against UCHL1 and the high density of CpG methylation in the UCHL1-negative cell lines. COBRA or HRM analyses revealed that DAC treatment only partially caused a demethylation of the UCHL1 promoter DNA in UCHL1-negative cells. Changes in the DNA methylation status could be only detected in proliferating cells, but DAC exerts a strong anti-proliferative activity on melanoma cell lines.²⁸ Furthermore, other unknown regulatory mechanisms like histone acetylation, transcriptional repressors or specific micro-RNA cannot be excluded to be involved in the control of the UCHL1 expression which could counteract with the demethylation of the promoter DNA.

Growth promoting UCHL1 functions

To analyze the effect of UCHL1 on the growth properties of melanoma cells, several *in vitro* transfection models were established. The overexpression of UCHL1 in UCHL1-negative cells influenced cell proliferation and anchorage-independent growth, but not the migration potential as well as the wound healing processes (data not shown). Vice versa, gene silencing of UCHL1 affected growth properties. Thus, UCHL1 function was dependent on the enzyme activity and resulted in an altered cellular content of ubiquitinated proteins. In contrast, the inactive variant C90S exhibited neither significant difference in proliferation nor in the amount of polyubiquitinated proteins compared to the corresponding vector controls. These results agree with transfection studies of RCC cells as well as of a gene silencing model of human embryonic kidney cells describing growth promoting properties of UCHL1.^{24,37} However, it is remarkable that UCHL1 exerts growth-suppressive function in a variety of other tumor entities, in particular in colon,¹⁸ breast³⁶ and hepatocellular carcinomas.¹⁷ This could be mediated by a G₀/G₁ cell cycle arrest due to p53 stabilization.³⁶

Different impact of UCHL1 on cellular signal transduction pathways

The MAPK and PI3K-Akt signaling pathways are often activated in cancer cells like melanoma promoting development, tumor growth and metastasis,³¹ which was associated with several sequence aberrations in single components of these cascades.³⁸ For example, B-Raf is mutated (V600E substitution) in approximately 60% of all melanoma lesions leading to a constitutively active MAPK pathway.³⁹ In the current study, the growth-promoting functions of UCHL1 are mediated by activation of the MAPK cascade in melanoma cells. Since the inactive C90S mutant did not significantly affect p-Erk levels, the catalytic domain appears to be essential for

correct signal transduction. Furthermore, treatment of melanoma cells with the selective MEK1/2 inhibitor U0126 could completely abrogate these effects. Until now, few facts about the UCHL1-mediated MAPK regulation exists. UCHL1 inhibit the TNF- α -induced proliferation of vascular smooth muscle cells *via* suppressing Erk activation.⁴⁰ UCHL1 knock down in HEK293 cells caused an alteration in MAPK signaling after binding of the hepatocyte growth factor (HGF) ligand to its receptor tyrosine kinase hepatocyte growth factor receptor (MET).⁴¹ Through the interaction with the α 2-adrenergic receptor UCHL1 also diminished the agonist-mediated stimulation of MAPK signaling in a transfection model of epithelial cells.⁴²

In the literature, neuroprotective effects of UCHL1 in particular of the S18Y polymorphism was described recently.^{43,44} In this context, several ROS-mediated post-translational modifications of UCHL1, such as carbonyl groups or tyrosine nitration were identified.^{45,46} A recent study has identified UCHL1 as an apoptosis-evasion protein⁴⁷ suggesting that silencing of UCHL1 caused an increased sensitivity to apoptosis and thus might enhance therapeutic efficacy of drugs. Therefore, in addition to its enzymatic activities a detoxification function of UCHL1 is postulated. To investigate this hypothesis in melanoma cells, several UCHL1 model systems were treated with different concentrations of hydrogen peroxide followed by quantification of the cell viability. The constitutive UCHL1 expressing melanoma cells Bufl286 and FM-6 showed a significant higher tolerance to H₂O₂ compared to UCHL1-negative cells. In contrast, UCHL1 expression in Colo-794 sensitized cells to ROS, while Colo-857 cells exhibited a higher resistance. Extended studies by the integration of a panel of different cell systems confirmed that UCHL1 affects the sensitivity of melanoma cells to ROS, but the expressed amounts of the hydrolase influenced the regulation mechanism. Strong expression was predominantly associated with less sensitivity, low amounts with a higher susceptibility to ROS compared to the corresponding mock controls. However, the cellular regulatory processes of UCHL1 during oxidative stress in detail are unknown. One explanation could be the interference of UCHL1 with the PI3K-Akt pathway. Strong overexpression of the hydrolase directly correlated with an Akt activation and ROS tolerance, whereas low levels caused decreased p-Akt amounts and a higher sensitivity of melanoma cells to ROS. These data suggest that the UCHL1-mediated control on the PI3K-Akt signal pathway is more complex and occurs in a dose-dependent manner. The bivalent enzyme UCHL1 primarily functions as a hydrolase in melanoma cells cleaving polyubiquitin chains of multiple proteins (see also Supporting Information Fig. 2). Increased UCHL1 expression causes a higher grade of protein deubiquitination, which could lead to many cellular consequences such as imbalances of pro- and anti-apoptotic proteins or variances in the expression of tumor suppressor and/or of oncogenes. In addition, a variable genetic background of the transfected melanoma cell lines analyzed might also affect the

regulation. Although all transfected cell lines analyzed share a BRAF-V600E mutation, Colo-857 cells additionally harbor a genomic Jak2 deletion leading to low major histocompatibility complex (MHC) class I expression on the cell surface and a resistance to interferon (IFN)- γ stimulation.⁴⁸ Furthermore, it is assumed that the expression and mutation status of different tumor suppressor proteins, such as p53 and the phosphatase phosphatase and tension homolog (PTEN), known regulators of the PI3K-Akt signal cascades are different in the cancer biopsies and/or cell lines analyzed resulting in the distinct Akt regulation.⁴⁹ A direct association and regulation of UCHL1 by p53 has been demonstrated in breast, prostate and nasopharyngeal carcinoma demonstrating an UCHL1-mediated induction of cell cycle arrest or inhibition of cell growth by stabilization of the p53 protein.^{35,36,50} Furthermore, the tumor entity investigated could be another reason for different Akt regulation mediated by the hydrolase. In prostate cancer as well as in breast carcinoma, UCHL1 overexpression leads to a decreased activation of the Akt

signaling pathway,^{25,35} whereas in lymphoma development UCHL1 stimulates Akt signaling by increasing the p-Akt levels.⁵¹

In summary, a dose-dependent involvement of UCHL1 in different molecular processes of the progression of a subset of melanoma cells, such as the regulation of growth properties, the induction of ROS tolerance and altered signal transduction has been demonstrated suggesting that UCHL1 might serve as a therapeutic target for the subset of UCHL1-positive melanoma.

Acknowledgements

Authors would like to thank Sylvi Magdeburg and Nicole Ott for excellent secretarial work. Special thanks to Graham Pawelec (University of Tuebingen) for providing the ESTDAB melanoma cell lines and Markus Meissner (University Hospital, Clinic of Dermatology Frankfurt/M., Germany) as well as Anja Bosserhoff (University Hospital Regensburg, Institute of Pathology, Regensburg, Germany) for providing with melanocytes. Furthermore, they would like to thank Uta-Dorothee Immel (Martin Luther University Halle-Wittenberg, Department of Legal Medicine, Halle (Saale)) for authentication of the melanoma cell lines used.

References

- D'Andrea A, Pellman D. Deubiquitinating enzymes: a new class of biological regulators. *Crit Rev Biochem Mol Biol* 1998;3:337–52.
- Nijman SM, Luna-Vargas MP, Velds A, et al. Genomic and functional inventory of deubiquitinating enzymes. *Cell* 2005;123:773–86.
- Wilkinson KD, Lee KM, Deshpande S, et al. The neuron-specific protein PGP 9.5 is a ubiquitin carboxyl-terminal hydrolase. *Science* 1989;246:670–3.
- Liu Y, Fallon L, Lashuel HA, et al. The UCH-L1 gene encodes two opposing enzymatic activities that affect α -Synuclein degradation and Parkinson's disease susceptibility. *Cell* 2002;111:209–18.
- Shirato I, Asanuma K, Takeda Y, et al. Protein gene product 9.5 is selectively localized in parietal epithelial cells of Bowman's capsule in the rat kidney. *J Am Soc Nephrol* 2000;11:2381–6.
- Diomed-Camassei F, Ravà L, Lerut E, et al. Protein gene product 9.5 and ubiquitin are expressed in metabolically active epithelial cells of normal and pathologic human kidney. *Nephrol Dial Transplant* 2005;20:2714–19.
- Sehiguchi S, Kwon J, Yoshida E, et al. Localization of ubiquitin C-terminal hydrolase L1 in mouse ova and its function in the plasma membrane to block polyspermy. *Am J Pathol* 2006;169:1722–9.
- Kopylow K, Kirchhoff C, Jezek D, et al. Screening for biomarkers of spermatogonia within the human testis: a whole genome approach. *Hum Reprod* 2010;25:1104–12.
- Gong B, Leznik E. The role of ubiquitin C-terminal hydrolase L1 in neurodegenerative disorders. *Drug News Perspect* 2007;20:365–70.
- Choi J, Levey AI, Weintraub ST, et al. Oxidative modifications and down-regulation of Ubiquitin carboxyl-terminal hydrolase L1 associated with idiopathic Parkinson's and Alzheimer's diseases. *J Biol Chem* 2004;279:13256–64.
- Leroy E, Boyer R, Auburger G, et al. The ubiquitin pathway in Parkinson's disease. *Nature* 1998;395:451–2.
- Carmine Belin A, Galter D. S18Y, UCH-L1 and Parkinson's Disease. *Eur Neurol* 2009;3:41–4.
- Carmine Belin A, Westerlund M, Bergman O, et al. S18Y in ubiquitin carboxyl-terminal hydrolase L1 (UCH-L1) associated with decreased risk of Parkinson's disease in Sweden. *Parkinsonism Relat Disord* 2007;13:295–8.
- Wang L, Guo JF, Nie LL, et al. Case-control study of the UCH-L1 S18Y variant in sporadic Parkinson's disease in the Chinese population. *J Clin Neurosci* 2011;18:541–4.
- Zhang M, Deng Y, Luo Y, et al. Control of BACE1 degradation and APP processing by ubiquitin carboxyl-terminal hydrolase L1. *J Neurochem* 2012;120:1129–38.
- Mohammad RM, Maki A, Pettit GR, et al. Bryostatin 1 induces ubiquitin COOH-terminal hydrolase in acute lymphoblastic leukemia cells. *Enzyme Protein* 1996;49:262–72.
- Yu J, Tao Q, Cheung KF, et al. Epigenetic identification of ubiquitin carboxyl-terminal hydrolase L1 as a functional tumor suppressor and biomarker for hepatocellular carcinoma and other digestive tumors. *Hepatology* 2008;48:508–18.
- Okochi-Takada E, Nakazawa K, Wakabayashi M, et al. Silencing of the UCHL1 gene in human colorectal and ovarian cancers. *Int J Cancer* 2006;119:1338–44.
- Yanagisawa TY, Sasahara Y, Fujie H, et al. Detection of the PGP9.5 and tyrosine hydroxylase mRNAs for minimal residual neuroblastoma cells in bone marrow and peripheral blood. *Tohoku J Exp Med* 1998;184:229–40.
- Tezel E, Hibi K, Nagasaka T, et al. PGP9.5 as a prognostic factor in pancreatic cancer. *Clin Cancer Res* 2000;6:4764–7.
- Jang MJ, Baek SH, Kim JH. UCH-L1 promotes cancer metastasis in prostate cancer cells through EMT induction. *Cancer Lett* 2011;302:128–35.
- Seliger B, Handke D, Schabel E, et al. Epigenetic control of the ubiquitin carboxyl terminal hydrolase 1 in renal cell carcinoma. *J Transl Med* 2009;7:90.
- Tokumaru Y, Yamashita K, Kim MS, et al. The role of PGP9.5 as a tumor suppressor gene in human cancer. *Int J Cancer* 2008;123:753–9.
- Seliger B, Fedorushchenko A, Brenner W, et al. Ubiquitin COOH-terminal hydrolase 1: a biomarker of renal cell carcinoma associated with enhanced tumor cell proliferation and migration. *Clin Cancer Res* 2007;13:27–37.
- Wang WJ, Li QQ, Xu JD, et al. Over-expression of ubiquitin carboxyl terminal hydrolase-L1 induces apoptosis in breast cancer cells. *Int J Oncol* 2008;33:1037–45.
- Bonazzi VF, Nancarrow DJ, Stark MS, et al. Cross-platform array screening identifies COL1A2, THBS1, TNFRSF10D and UCHL1 as genes frequently silenced by methylation in melanoma. *PLoS One* 2011;6:e26121.
- Pawelec G, Marsh SG. ESTDAB: a collection of immunologically characterised melanoma cell lines and searchable databank. *Cancer Immunol Immunother* 2006;55:623–27.
- Wulfänger J, Schneider H, Wild P, et al. Promoter methylation of aminopeptidase N/CD13 in malignant melanoma. *Carcinogenesis* 2012;33:781–90.
- Daniotti M, Oggionni M, Ranzani T, et al. BRAF alterations are associated with complex mutational profiles in malignant melanoma. *Oncogene* 2004;23:5968–77.
- Rolén U, Freda E, Xie J, et al. The ubiquitin C-terminal hydrolase UCH-L1 regulates B-cell proliferation and integrin activation. *J Cell Mol Med* 2009;13:1666–78.
- Meier F, Schitteck B, Busch S, et al. The RAS/RAF/MEK/ERK and PI3K/AKT signaling pathways present molecular targets for the effective treatment of advanced melanoma. *Front Biosci* 2005;10:2986–3001.
- Sander CS, Chang H, Hamm F, et al. Role of oxidative stress and the antioxidant network in cutaneous carcinogenesis. *Int J Dermatol* 2004;43:326–35.
- Seliger B, Dressler SP, Massa C, et al. Identification and characterization of human leukocyte antigen class I ligands in renal cell carcinoma cells. *Proteomics* 2011;11:2528–41.
- Hoek K, Rimm DL, Williams KR, et al. Expression profiling reveals novel pathways in

- the transformation of melanocytes to melanomas. *Cancer Res* 2004;64:5270–82.
35. Ummanni R, Jost E, Braig M, et al. Ubiquitin carboxyl-terminal hydrolase 1 (UCHL1) is a potential tumour suppressor in prostate cancer and is frequently silenced by promoter methylation. *Mol Cancer* 2011;10:129.
 36. Xiang T, Li L, Yin X, et al. The ubiquitin peptidase UCHL1 induces G0/G1 cell cycle arrest and apoptosis through stabilizing p53 and is frequently silenced in breast cancer. *PLoS One* 2012;7:e29783.
 37. Bheda A, Shackelford J, Pagano JS. Expression and functional studies of ubiquitin C-terminal hydrolase L1 regulated genes. *PLoS One* 2009;4:e6764.
 38. Flaherty KT, Hodi FS, Bastian BC. Mutation-driven drug development in melanoma. *Curr Opin Oncol* 2010;22:178–83.
 39. Lee JH, Choi JW, Kim YS. Frequencies of BRAF and NRAS mutations are different in histological types and sites of origin of cutaneous melanoma: a meta-analysis. *Br J Dermatol* 2011; 164:776–84.
 40. Ichikawa T, Li J, Dong X, et al. Ubiquitin carboxyl terminal hydrolase L1 negatively regulates TNFalpha-mediated vascular smooth muscle cell proliferation via suppressing ERK activation. *Biochem Biophys Res Commun* 2010; 391:852–6.
 41. Bassères E, Coppotelli G, Pfirrmann T, et al. The ubiquitin C-terminal hydrolase UCH-L1 promotes bacterial invasion by altering the dynamics of the actin cytoskeleton. *Cell Microbiol* 2010;12: 1622–33.
 42. Weber B, Schaper C, Wang Y, et al. Interaction of the ubiquitin carboxyl terminal esterase L1 with alpha(2)-adrenergic receptors inhibits agonist-mediated p44/42 MAP kinase activation. *Cell Signal* 2009;21:1513–21.
 43. Kyratzi E, Pavlaki M, Stefanis L. The S18Y polymorphic variant of UCH-L1 confers an anti-oxidant function to neuronal cells. *Hum Mol Genet* 2008;17:2160–71.
 44. Xilouri M, Kyratzi E, Pitychoutis PM, et al. Selective neuroprotective effects of the S18Y polymorphic variant of UCH-L1 in the dopaminergic system. *Hum Mol Genet* 2012;21: 874–89.
 45. Kabuta T, Setsuie R, Mitsui T, et al. Aberrant molecular properties shared by familial Parkinson's disease-associated mutant UCH-L1 and carbonyl-modified UCH-L1. *Hum Mol Genet* 2008;17:1482–96.
 46. Guingab-Cagmat JD, Stevens SM, Jr, Ratliff MV, et al. Identification of tyrosine nitration in UCH-L1 and GAPDH. *Electrophoresis* 2011;32:1692–1705.
 47. Hsieh SY, Hsu CY, He JR, et al. Identifying apoptosis-evasion proteins/pathways in human hepatoma cells via induction of cellular hormesis by UV irradiation. *J Proteome Res* 2009;8:3977–86.
 48. Respa A, Bukur J, Ferrone S, et al. Association of IFN-gamma signal transduction defects with impaired HLA class I antigen processing in melanoma cell lines. *Clin Cancer Res* 2011;17: 2668–78.
 49. Mayo LD, Donner DB. The PTEN, Mdm2, p53 tumor suppressor-oncoprotein network. *Trends Biochem Sci* 2002;27:462–7.
 50. Li L, Tao Q, Jin H, et al. The tumor suppressor UCHL1 forms a complex with p53/MDM2/ARF to promote p53 signaling and is frequently silenced in nasopharyngeal carcinoma. *Mol Cancer* 2011;10:129.
 51. Hussain S, Foreman O, Perkins SL, et al. The deubiquitinase UCH-L1 is an oncogene that drives the development of lymphoma in vivo by deregulating PHLPP1 and Akt signaling. *Leukemia* 2010;24:1641–55.

Supplementary Table 1

Primer sequences.

Gene	RefGene	Primer sequence		Annealing	Product size [bp]
		Sense	Antisense		
A) qPCR					
Akt	NM_001014431	GTACTCTTTCCAGACCCACGAC	GCCCGAAGTCTGTGATCTTAAT		242
Erk1	NM_002746	GCTACACGCAGTTGCAGTACAT	TCAGGTCCTGCACAATGTAGAC		252
Erk2	NM_002745	CATGGTGTGCTCTGCTTATGAT	CCCTCTGAGGATCTGGTAGAGA		298
GAPDH	NM_002046	GGACTCATGACCACAGTCCAT	AGGTCCACCACACTGACACGTT		218
HPRT	NM_000194	GCTGGATTACATCAAAGCACTG	CTGACCAAGGAAAGCAAAGTCT	60 °C	219
PPIA	NM_021130	CCATCTATGGGAGAAATTTGA	CAGTCAGCAATGGTGATCTTCT		254
UCHL1	NM_004181	GGATTTGAGGATGGATCAGTTC	CCATCCACGTTGTTAAACAGAA		192
UCHL3	NM_006002	GATCCTGAACCTTAGCATGG	AGGTATCTGGCTCGTTCTTCAG		302
UCHL5	NM_015984	ACTCCCAGCTTGACACGATATT	TCTGGCGAAACTGTTGTGTAAT		224
B) COBRA					
	1. PCR	GAGTTTTAGAGTAATTGGGATGGTAAA	CCACTCACTTTATTCAACATCTAAAAACA		538
UCHL1	2. PCR	GGTTTTGTTTTGTTTTTTTGTATAGGTT	AAAAACAATACAAAAAAAAAACAAAACC	56 °C	265
	2. PCR	GGTAAAAGGATGGGTTTTTAGAAATTT	AACCTATACAAAAAAAAAACAAAACC		250

Supplementary Table 2

Primary antibodies used.

Protein	RefGene	Code	Company
Akt		9272	Cell Signaling (Danvers, MA)
p-Akt	P31749	9271	Cell Signaling
Erk	P28482/	9102	Cell Signaling
p-Erk (E-4)	Q54QB1	sc-7383	Santa Cruz Biotechnology (Santa Cruz, CA)
Ubiquitin (Ubi-1)	P62988	MAB1510	Millipore (Billerica, MA)
UCHL1	P09936	BML-PG9500	Enzo Life Sciences (Lörrach, Germany)

Supplementary Material and Methods

High resolution melt curve analysis (HRM)

Genomic DNA of DAC-treated or untreated cells were isolated and bisulfite-converted as described in the corresponding Material and Methods section of this paper. After amplification of the UCHL1 promoter using the outer primer set, the PCR products were diluted 1:50 with water. 2 μ l of this prepared DNA were subjected to HRM analysis using the EpiTect HRM PCR Kit and the Rotor-Gene Q systems (both obtained from Qiagen, Hilden, D) according to the manufacturer's protocol. Results were integrated with the corresponding software. The graph represents the median of three independent experiments.

Supplementary Figures

Supplementary Figure 1 Increased UCHL1 expression after DAC treatment.

(A) Representative COBRA using *Bst*UI restriction with percentage classification of DNA methylation pattern was shown. (B) UCHL1-negative Colo-857 cells were treated either with different DAC concentrations each of four days or with 5 μ M DAC for different time points indicated. Results are expressed as x-fold mRNA induction in relation to medium control of three independent experiments. (C) Increased protein levels in DAC-treated FM-6 cells. Representative immunoblots of three independent experiments are shown. (D) High resolution melt curve analysis. Bisulfite-converted genomic DNA of three melanoma cell line with distinct UCHL1 expression was subjected to qPCR followed by a HRM on a Rotor-Gene 6000-system. DNA of DAC-treated cells were integrated in this studies, respectively.

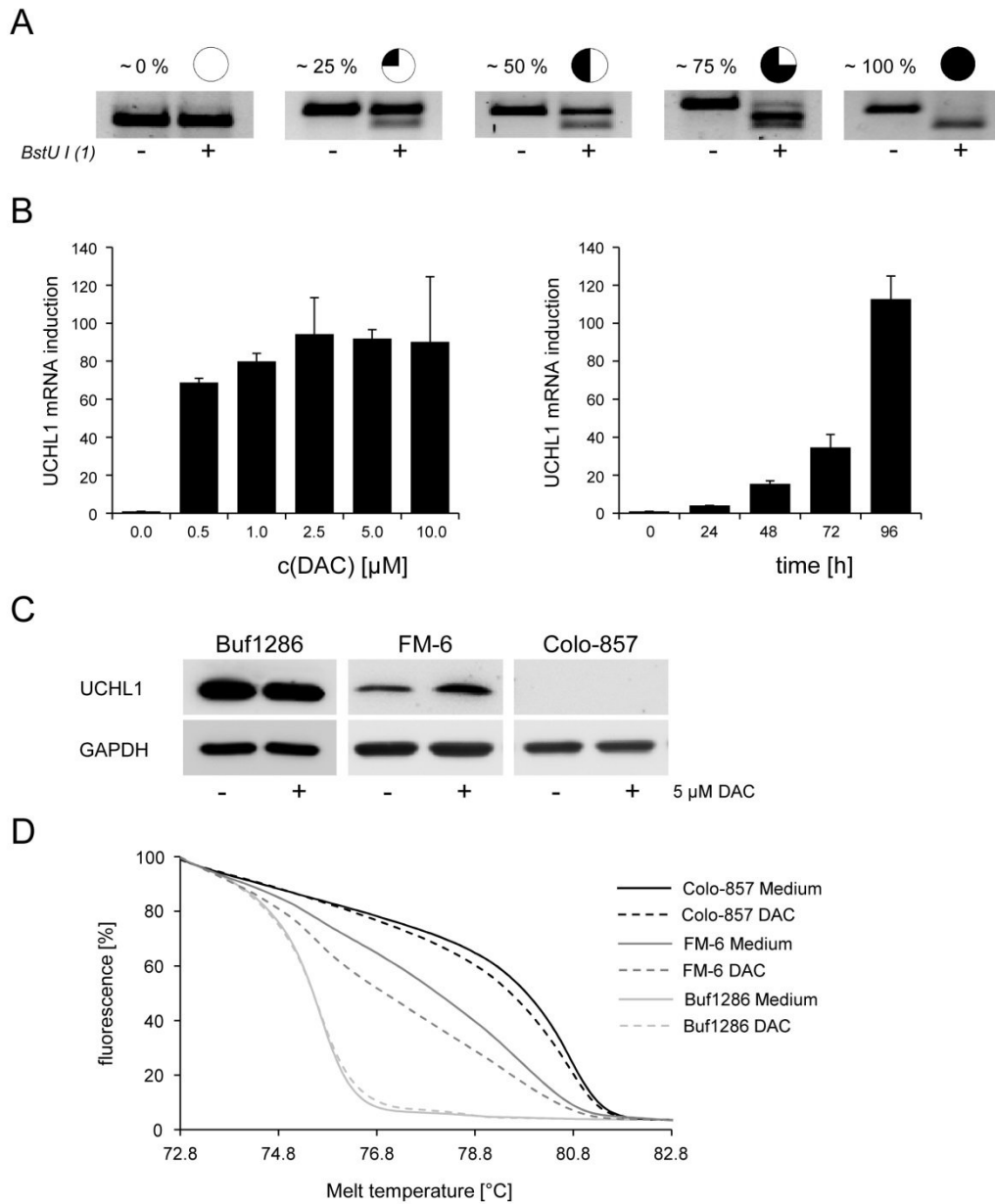
Supplementary Figure 2 UCHL1-mediated alterations of the polyubiquitination grade of proteins.

(A) Representative immunoblots using the ubiquitin-specific antibody Ubi-1 and (B) corresponding AIDA quantification of at least four independent experiments are presented.

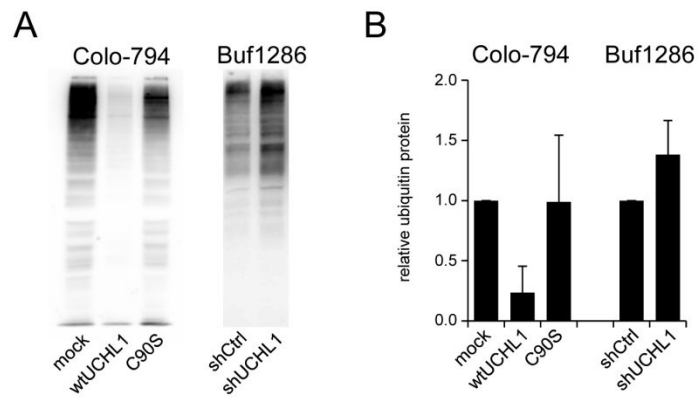
Supplementary Figure 3 Distinct resistance of parental FM-6 clones.

(A) Single cell clones of the FM-6 parental cell line were isolated and mRNA quantification and COBRA were performed as described in the Material and Methods section. (B) FM-6 clones were treated with 25 μ M H₂O₂ for 24 h before cell viabilities were measured using XTT. Results represent the x-fold viability to untreated cells of three independent experiments (* $P < 0.05$, ** $P < 0.01$).

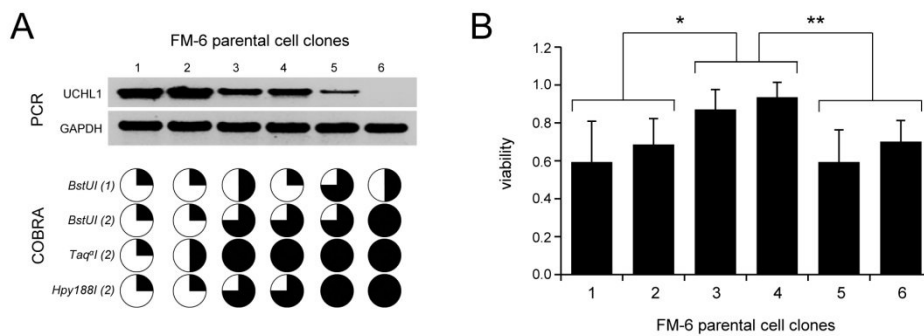
Supplementary Figure 1



Supplementary Figure 2



Supplementary Figure 3



4.2 Manuskript 2: Promoter methylation of aminopeptidase N/ CD13 in malignant melanoma.

Carcinogenesis vol.33 no.4 pp.781–790, 2012
doi:10.1093/carcin/bgs091
Advance Access publication February 3, 2012

Promoter methylation of aminopeptidase N/CD13 in malignant melanoma

Jens Wulfänger, Heike Schneider, Peter Wild¹,
Kristian Ikenberg¹, Monica Rodolfo², Licia Rivoltini²,
Stefanie Meyer³, Dagmar Riemann and Barbara Seliger*

Institute of Medical Immunology, Martin-Luther-University Halle-Wittenberg, 06112 Halle (Saale), Germany, ¹Institute of Surgical Pathology, University Hospital Zuerich, CH-8091 Zuerich, Switzerland, ²Department of Experimental Oncology, Istituto Nazionale Tumori, 20133 Milano, Italy and ³Department of Dermatology, University Hospital Regensburg, 93053 Regensburg, Germany

*To whom correspondence should be addressed. Tel. +49 (0) 345 557 4054; Fax: +49 (0) 345 557 4055; Email: Barbara.Seliger@medizin.uni-halle.de

Aminopeptidase N (APN)/CD13 as ubiquitously expressed membrane peptidase exerts important functions in diverse cellular processes, such as proliferation, migration and differentiation. Previously, a role of APN in the invasiveness of melanoma cells has been demonstrated, but the underlying molecular mechanisms controlling APN expression are not understood. The present study demonstrates that lack of APN expression in primary and established melanoma cells was directly associated with a high-grade DNA methylation status of the myeloid APN promoter. Demethylation by 5-aza-2'-deoxycytidine not only induced constitutive and cytokine-regulated APN protein expression but also resulted in an increased APN-dependent migration of melanoma cells. Furthermore, its heterogeneous expression was inversely correlated to the expression of melanocytic marker proteins in established as well as in short-term cultured human melanoma cells. Staining of tissue microarrays generated from a large series of melanoma samples and control tissues demonstrated a higher APN expression in primary melanoma lesions when compared with nevi and metastases, which was neither associated with clinicopathological parameters nor with the patients' outcome. Thus, the heterogeneous APN expression pattern in melanoma cells is epigenetically controlled and directly associated with an altered migration capacity but not of clinical significance in our study group.

Introduction

The zinc-dependent membrane alanyl-aminopeptidase [aminopeptidase N (APN)/CD13] exhibits ectopeptidase activity by hydrolyzing oligopeptides with a preference to neutral amino acids. APN expression is widely distributed and has been found on different epithelial and endothelial cells, haematopoietic cells and also on tumours of distinct origin (1). APN expression is controlled at the transcriptional level by two distinct promoters and an enhancer region between both DNA sequences. The epithelial or proximal promoter is arranged directly upstream from the start codon and is predominantly active in epithelial of the intestine, liver and kidneys as well as in endothelial cells, whereas the myeloid promoter is located about 8 kb upstream of the ATG initiation codon and is active in myeloid haematopoietic cells and fibroblasts (2,3).

Concerning its physiological function, APN is involved in various cellular processes, including the modulation of immune responses, inflammation, cell cycle control, cell differentiation and motility,

Abbreviations: APN, aminopeptidase N; bFGF, basic fibroblast growth factor; COBRA, combined bisulfite restriction analysis; DAC, 5-aza-2'-deoxycytidine; EGF, epidermal growth factor; IL, interleukin; mAb, monoclonal antibody; mRNA, messenger RNA; RFS, recurrence-free survival; RT-PCR, reverse transcription-PCR; TGF, transforming growth factor; TMA, tissue microarray.

angiogenesis as well as cellular attachment (reviewed in ref. 4,5). In addition, APN plays an important role in tumour biology, which is mainly attributed to the regulation of the local homeostasis of peptide hormone and growth factor activation (6), thereby controlling cell proliferation, angiogenesis as well as promoting the metastatic progression of tumours (5). APN expression levels are high in thyroid, lung cancer as well as in head and neck squamous cell carcinoma, which is associated with increased malignant behaviour and reduced overall survival rates (7–9). In contrast, a reduced APN expression pattern was found in a number of tumour types, including high-grade meningiomas, renal and prostate carcinoma (10–14).

Regarding APN in melanoma progression, Elder *et al.* (15) first described the expression of the 452 antigen later identified as APN in melanoma cells but not in melanocytes. Employing microbial aminopeptidase inhibitors as well as blocking antibodies, APN was characterized to exhibit important functions in invasion, extracellular matrix degradation and angiogenic processes during melanoma progression (16–19). Furthermore, APN-transfected melanoma cells demonstrated an enhanced migratory capacity, an increased degradation of type IV collagen as well as a higher frequency in the generation of lung metastases in nude mice when compared with APN-negative control cells (20).

So far, the molecular mechanisms of altered APN expression and the clinical relevance of its expression in melanoma have not yet been elucidated in detail. In this study, we show for the first time that APN expression is regulated by differential CpG methylation of its myeloid DNA promoter not only in melanoma cell lines but also in different melanoma lesions.

Materials and methods

Cell lines and tissues

The human melanoma cell lines were obtained from ESTDAB (<http://www.ebi.ac.uk/ipd/estdab/>) and were kindly provided by Graham Pawelec (University of Tübingen, Germany). APN-overexpressing melanoma cells were generated by transfection similar as described previously (21). THP-1 and Jurkat cells were purchased from DSMZ (Braunschweig, Germany). All cell lines were cultured in RPMI 1640 medium supplemented with 10% fetal bovine serum, 2 mM L-glutamine, 10 mM N-2-hydroxyethylpiperazine-N'-2-ethanesulfonic acid and respective antibiotics. Fresh tumour cell suspensions were obtained from surgical specimens by mechanical/enzymatic digestion and stored in liquid nitrogen until use (termed T1–13). Short-term melanoma cultures of single-cell suspensions (termed C1–18) were grown under standard conditions as described previously (22). The study was approved by the Institutional Ethics Committee and assigned and conducted according to the Helsinki Declaration.

Treatment of cells

For demethylation studies, cell lines were treated every day in fresh medium with different concentrations (0–10 μ M) of 5-aza-2'-deoxycytidine (DAC; Sigma, St Louis, MO) for the time-points indicated. For investigating APN regulation by cytokines, recombinant cytokines were supplemented on days 3 and 4 of DAC treatment with the following concentrations: 100 ng/ml basic fibroblast growth factor (bFGF; Cell Signaling, Danvers, MA), 10 ng/ml transforming growth factor β 1 (TGF- β 1; R&D Systems, Minneapolis, MN), 100 U/ml interleukin (IL)-4 (eBioscience, San Diego, CA), 100 U/ml IL-6 (Pan Biotech, Aidenbach, Germany) as well as 50 ng/ml epidermal growth factor (EGF; Cell Concepts, Umkirch, Germany). Blocking of APN enzyme activity was performed by treating the cells with 100 μ g/ml of the APN-specific antibody WM15 (BD Biosciences, Heidelberg, Germany) as well as with 200 μ M of the microbial aminopeptidase inhibitors bestatin or actinonin (both purchased from Sigma), respectively.

Silencing of APN expression

A total of 1×10^5 melanoma cells were seeded into six-well plates, 1 day later transfected with small interfering RNA targeting APN (NM_001150, CCACACUGGUCAAUGAGGUGACAA) as well as with unspecific non-silencing control small interfering RNA (Invitrogen, Karlsruhe, Germany) using the Lipofectamine 2000 reagent (Invitrogen) according to manufacturer's instructions. After 2 days, transfection was repeated, cells were incubated for

J. Wulfänger *et al.*

additional 48 h in complete RPMI 1640 medium and then harvested for RNA and protein analysis.

PCR analysis

RNAs from short-term melanoma cultures were isolated by using the mirVana miR isolation kit (Ambion, Austin, TX). Total cellular RNA of melanoma cells were isolated and reverse transcribed into complementary DNA as recently described (21). End-point reverse transcription-PCR (RT-PCR) was performed with *Taq* DNA polymerase (Invitrogen) and respective primers (Supplementary Table 1 is available at *Carcinogenesis* Online) using standard protocols. Real-time quantitative RT-PCR was performed and evaluated on a Rotor-Gene 6000 system (Corbett Research, Sydney, Australia) employing the Platinum SYBR Green qPCR SuperMix-UDG (Invitrogen). Messenger RNA (mRNA) levels were normalized to that of peptidylprolyl isomerase A. All quantitative RT-PCR analyses were performed using RNA from at least three independent experiments.

Flow cytometry

In total, 5×10^5 cells were stained with the phycoerythrin-conjugated APN-specific monoclonal antibody (mAb) Leu-M7 and with the appropriate mouse IgG1 phycoerythrin control (both purchased from BD Biosciences) at room temperature in the dark for 20 min. After fixation with 2% (wt/vol) paraformaldehyde for 10 min and two washing steps, fluorescence intensity was determined on a FACS can flow cytometer using the CellQuest software (BD Biosciences). The results are presented in histograms of a representative staining with mean fluorescence intensity values of at least three independent experiments. For cytokine stimulation experiments, the isotype-corrected mean fluorescence intensity values of stimulated cells were divided with the values of untreated cells. Data represent average of at least three independent experiments.

Western blot analysis

Protein expression studies were performed as described previously (21). Briefly, 50 µg total protein per lane were separated in 8% sodium dodecyl sulphate-polyacrylamide gel electrophoresis, transferred to nitrocellulose membrane and immunoblotted with anti-green fluorescent protein pAb or anti-APN mAb (both purchased from Santa Cruz Biotechnology, Santa Cruz, CA). Equal protein loading was determined using an anti-β-actin mAb (Abcam, Cambridge, UK). After incubation with appropriate horseradish peroxidase-conjugated secondary antibodies, protein bands were detected using a chemiluminescence-based system.

Analysis of the methylation status

The existence and number of CpG oligonucleotides in the myeloid APN promoter was determined and further mapped by MethPrimer (23). Bisulfite-specific primers (Supplementary Table 1 is available at *Carcinogenesis* Online) flanking 52 CpG sites in the myeloid APN promoter 600 bp upstream of the transcription start were designed. Genomic DNA from established melanoma cell lines was isolated using the QIAamp DNA Mini Kit, from short-term melanoma cultures as well as suspension of melanoma lesions using the DNeasy Blood and tissue Kit (both obtained from Qiagen, Hilden, Germany). Two micrograms of genomic DNA were subjected to bisulfite modification with the EpiTect Bisulfite Kit (Qiagen) according to the manufacturer's protocol. After nested PCR amplification, the methylation status of the myeloid APN promoter was analysed by combined bisulfite restriction analysis (COBRA) as well as DNA sequencing. For COBRA, 50 ng of the resulting amplification products were digested with the restriction enzymes BsrBI, BstUI, *Taq*I, RsaI or Hpy188I recognizing CG sequences (New England BioLabs, Frankfurt, Germany) prior to separation on 3% agarose gels. For bisulfite genomic sequencing, the nested PCR products were gel-purified and either directly subjected to sequence analysis by a commercially available service provider or cloned into the pCR2.1-Topo vector using the TOPO TA Cloning Kit (Invitrogen). From 10 randomly selected bacterial colonies, DNA was purified using QIAprep Spin Miniprep Kit (Qiagen) and then sequenced.

Soft agar cloning and growth curve analysis

The anchorage-independent growth of melanoma cells was determined by plating 3×10^4 cells in 0.3% soft agar on top of a 0.5% agar base layer, both prepared with 20% fetal bovine serum-supplemented RPMI 1640 medium. The soft agar culture plates were cultivated in a humidified CO₂ incubator for 3 weeks. Vital cells were staining with iodo-nitrotriazoliumchloride overnight and soft agar colonies were digitalized.

For analysis of the proliferation rate, 2×10^4 cells were seeded into six-well plates and incubated at 37°C and 5% CO₂. The cell number was determined in duplicates every day over a period of 5 days. The doubling time was calculated using the standard formula. The data are represented as the mean of at least three independent experiments.

Migration assay

The migration of APN-negative versus APN-expressing melanoma cell lines was analysed as recently described (21). Briefly, 2.5×10^5 cells were seeded in

the transwell insert and 10 µg/ml collagen type I (BD Biosciences) as chemo-attractant were added to the lower chamber. Cells were allowed to migrate for 22 h at 37°C in the absence or presence of APN inhibitors. Migrated cells were quantified using the Cell-Titer-Glo Luminescent Cell Viability Assay (Promega, Madison, WI) according to the manufacturer's protocol. Results are presented as percentage of migrated cells in relation to the total cell number used in the assay.

Tissue microarray

Tissue microarrays (TMAs) generated as described previously (24) were obtained from the archives of the Department of Dermatology, University of Regensburg, Regensburg, Germany. TMAs contained a total of 465 formalin-fixed, non-selected, consecutive paraffin-embedded human tissues from patients with benign melanocytic nevi, malignant melanoma and metastases.

One tissue core per specimen with a diameter of 0.6 mm was punched out of the donor block and transferred to the recipient block. In patients with multiple subsequent neoplasms, only initial and unifocal malignant melanomas were included. Haematoxylin and eosin-stained slides of all tumours were evaluated by two dermatopathologists (P.W. and K.I.). Clinical follow-up data provided by the Central Tumor Registry, Regensburg, Germany were available for all patients with primary malignant melanoma. In the group of patients with primary melanoma, the patients' age ranged from 22 to 94 years (median 61 years). The median follow-up for all patients with malignant melanoma was 51 months (range 0–186 months). Median follow-up time of censored patients was 52 months (range 1–186 months). A total of 12.9% of patients died of melanoma disease during follow-up after a median time of 26 months (range 0–154 months).

Immunohistochemistry

Paraffin-embedded preparations of tissues from patients with benign melanocytic nevi, primary melanoma and melanoma metastases were screened for APN protein expression by immunohistochemistry. The TMA blocks were freshly cut (3 µm) and mounted on superfrost slides (Menzel-Glaeser, Braunschweig, Germany). In brief, tissues were deparaffinised, rehydrated and subsequently incubated with primary antibody overnight at 4°C. Immunohistochemistry was conducted with the Ventana Benchmark automated staining system (Ventana Medical Systems, Tucson, AZ) using Ventana reagents for the entire procedure. The following primary antibodies were used: anti-APN mAb (clone 38C12, dilution 1:100; Novocastra Laboratories Ltd., Newcastle upon Tyne, UK) and anti-Ki-67 mAb (clone MIB-1, dilution 1:100; Dako, Hamburg, Germany). The primary mAbs were detected with the ultraView Universal Alkaline Phosphatase Red Detection Kit (Ventana Medical Systems). Slides were counterstained with haematoxylin, dehydrated and mounted.

A surgical pathologist (K.I.) performed a blinded evaluation of the stained slides. Samples were grouped into negative and positive APN expression, respectively. Positive immunoreactivity was defined if at least faint staining could be observed. The Ki-67 proliferation rate was defined as percentage of positive nuclei as recently described (25). High Ki-67 labelling index was defined if at least 5% of the tumour cells were positive. Causes of non-interpretable results included either lack of tumour tissue or presence of necrosis or crush artefacts.

Statistical analysis of TMA data

Contingency table analysis, two-sided chi-square and Fisher's exact tests were used to study the statistical association between clinico-pathological and immunohistochemical parameters of the TMA. Retrospective overall survival and recurrence-free survival (RFS) were defined as clinical end-points. Survival curves comparing patients with or without any of the factors were calculated using the Kaplan-Meier method, with significance evaluated by two-sided log-rank statistics. For the analysis of RFS, patients were censored at the time of their last tumour-free clinical follow-up appointment. RFS data were only available for 226 patients (62%) with a median follow-up time of 18 months (range 1–142 months). For analysis of overall survival, patients were censored at the time of their last clinical follow-up appointment or at their date of death not related to the tumour. *P* values <0.05 were considered significant. Statistical analyses were completed using SPSS version 17.0 (SPSS, Chicago, IL). In case of multiple statistical tests, the Bonferroni-Holm method was used. The University of Regensburg institutional review board granted approval for the project. Concerning other experimental results, the data are expressed as mean ± standard error of the mean. Statistical analyses were calculated by student's test.

Results

Characterization of APN-expressing melanoma cell lines

Melanoma progression from benign melanocytes to malignant tumour is a multi-phase process accompanied with many cellular and

molecular changes, e.g. down-regulated expression of melanocytic marker, epithelial to mesenchymal transition, cadherin-switch and differential cytokine secretion (reviewed in ref. 26,27). To characterize the cell lines used in this study, the APN mRNA of melanocyte samples and 17 different melanoma cell lines was first quantified using quantitative RT-PCR and compared with the protein expression data obtained with flow cytometry (Figure 1A). Despite detectable APN transcription in all cell lines, only seven melanoma lines with high mRNA levels exhibited a directly correlated APN protein surface expression (APN⁺). The other melanoma cell lines lacked APN protein as exemplarily shown for the APN-negative cell line WM-1862. APN protein positivity was correlated with a down-regulated expression of melanocytic markers, such as gp100, MART-1, S100B and tyrosinase (Figure 1B; Supplementary Table 2 is available at *Carcinogenesis* Online). Furthermore, decreased mRNA amounts of the microphthalmia-associated transcription factor, which is involved in the regulation of these markers, were determined in APN⁺ compared with APN-negative melanoma cell lines (Figure 1B; Supplementary Figure 1A is available at *Carcinogenesis* Online).

Former *in vitro* transfection or inhibitor studies demonstrated that APN expression is accompanied with a more aggressive behaviour of melanoma cells in comparison with APN-negative controls (19,20,28). In order to clarify the APN function in our system, the growth and migration properties of APN-negative cells were compared with those of APN⁺ melanoma cell lines. Since the doubling time and the number of soft agar colonies of APN-negative and APN⁺ melanoma cell lines were comparable, APN expression did neither affect the *in vitro* proliferation nor the anchorage-independent growth of melanoma cells (Supplementary Figure 1B is available at *Carcinogenesis* Online). In contrast, APN⁺ melanoma cells exhibited an increased migration capacity to collagen using the transwell system varying from 30 to 60% compared with ~12% in APN-negative melanoma cells (Figure 1C). This increase could be blocked by the aminopeptidase inhibitors bestatin and actinonin or by APN-specific small interfering RNA, whereas APN overexpression into APN-negative WM-1862 cells resulted in an enhanced motility when compared with parental cells and vector controls (Figure 1D) confirming the functional role of APN in melanoma migration.

DNA methylation of the myeloid APN promoter

Differential gene expression of various proteases is described to be accompanied with the development and progression of cutaneous malignant melanoma (reviewed in ref. 29), which is often shown to be associated with epigenetic changes. To the best of our knowledge, using a bioinformatic program we have identified for the first time a putative CpG island in the myeloid APN promoter, which consists of 123 CpG sites within a 1.3 kb DNA sequence (Figure 2A). By the way using this program, no CpG islands could be found in the epithelial promoter as well as in the transcriptional enhancer region of APN (Supplementary Figure 2A is available at *Carcinogenesis* Online).

Using two different primer sets discriminating myeloid mRNA from total APN mRNA amounts in end-point PCR analysis, high mRNA levels were generated from the myeloid promoter in APN⁺ but not in APN-negative cells (Figure 2B). To investigate whether DNA hypermethylation of the myeloid promoter could be involved in the regulation of APN expression, bisulfite-treated DNA of APN-negative and APN⁺ melanoma cells was subjected to PCR with primers amplifying a 412 bp long sequence containing 32 CpG sites directly located upstream of the transcription start of the myeloid APN promoter. Applying bisulfite sequencing, heterogeneous promoter DNA methylation was observed in the different cell lines. APN⁺ melanoma cells exhibited a significantly reduced methylation status in comparison with APN-negative melanoma cells ($P < 0.001$). Whereas in APN⁺ cells the frequency of methylated CpG sites at position 1–15 varied between 0 and 40.6%, APN-negative cells exhibited a total methylation at the same positions (Figure 2C). In addition, the overall methylation frequency was increased to 54.7–92.2% with a distribution over all 32 CpG oligonucleotides analysed (Supplementary Table 2 is available at *Carcinogenesis* Online). These

sequencing data were confirmed by COBRA for all melanoma cell lines and melanocytes on several CpG oligonucleotides (Figure 2D; Supplementary Figure 2B is available at *Carcinogenesis* Online). The human leukaemic monocytic cell line THP-1 exhibiting an APN expression comparable with WM-1552C served as a control and completely lacked CpG methylation. In contrast, in the human APN-negative T cell line Jurkat a high number of methylated CpG sites was found in the myeloid APN promoter, indicating that the extent of APN promoter DNA methylation was associated with lack of APN protein expression independent of the cell type analysed.

Demethylation induces APN expression and function

Both APN-negative as well as APN⁺ melanoma cell lines were treated with various concentrations of the demethylating reagent DAC for various time-points before APN expression studies were performed. Whereas DAC had no effect on APN⁺ GR-M cells, enhanced APN mRNA levels varying from 6.4- to 67.3-fold (Supplementary Table 2 is available at *Carcinogenesis* Online) as well as an increased transcriptional activity of the myeloid promoter were detected in APN-negative melanoma cell lines upon this treatment (Figure 3A). These were accompanied by an induction of APN surface expression as representatively demonstrated for four APN-negative melanoma cell lines (Figure 3B). The DAC-mediated changes of APN mRNA and protein levels were time- and dose-dependent (see Supplementary Figure 3, available at *Carcinogenesis* Online). Prolonged cultivation of cells in medium without DAC for 4 days further increased APN surface expression of APN-negative melanoma cells (Figure 3B). DAC treatment also caused a decreased proliferation rate of all melanoma cell lines analysed independent of the APN expression status (Figure 3C). In contrast, restored APN expression in APN-negative melanoma cells was associated with increased migration rates, which could be blocked to ~50% using the APN-specific antibody WM15 suggesting a direct link between APN and migration (Figure 3D).

Restoration of cytokine-stimulated APN expression after DAC treatment

Several cytokines have been shown to regulate APN expression in different cell types, e.g. IL-4 increases APN expression in monocytes, endothelial cells and renal cell carcinoma cells (30,31). To investigate an association of APN expression and cytokine production in melanoma cells, the mRNA expression of five cytokines known to control either APN expression or to be involved in melanoma progression was analysed. Whereas EGF and IL-4 transcripts were heterogeneously expressed without any link to APN expression, the mRNA levels of bFGF, TGF- β 1 and IL-6 were higher in APN⁺ melanoma cells compared with APN-negative melanoma cells (Supplementary Figure 4 is available at *Carcinogenesis* Online).

In order to determine whether these cytokines can up-regulate APN expression in melanoma, APN⁺ WM-1552C and GR-M cells were stimulated for 48 h before APN quantitation. TGF- β 1 and IL-4 causes an increase in APN transcription (Figure 4A) and in protein expression, exemplarily shown for GR-M in Figure 4B, whereas bFGF, IL-6 and EGF do not regulate APN expression. Then, APN-negative Colo-794 cells were treated with these cytokines in the presence or absence of DAC. As shown in Figure 4C, not the cytokine treatment alone, but a combination of cytokine with demethylation induces myeloid APN transcripts, suggesting an inhibitory effect of the APN promoter DNA methylation on the cytokine-mediated stimulation. The highest APN protein surface expression with an up to 2-fold increase were found after co-incubation of DAC with TGF- β 1 or IL-4 (Figure 4D). In contrast, bFGF, IL-6 or EGF exerted no or only a marginal additive effect on the activity of the myeloid promoter. These observations could be confirmed with the APN-negative cell line Colo-857 (data not shown).

Differential DNA methylation of the myeloid APN promoter in primary melanoma

To investigate the influence of promoter DNA methylation on APN gene expression in melanoma lesions, the amount of myeloid as well

J. Wulfänger et al.

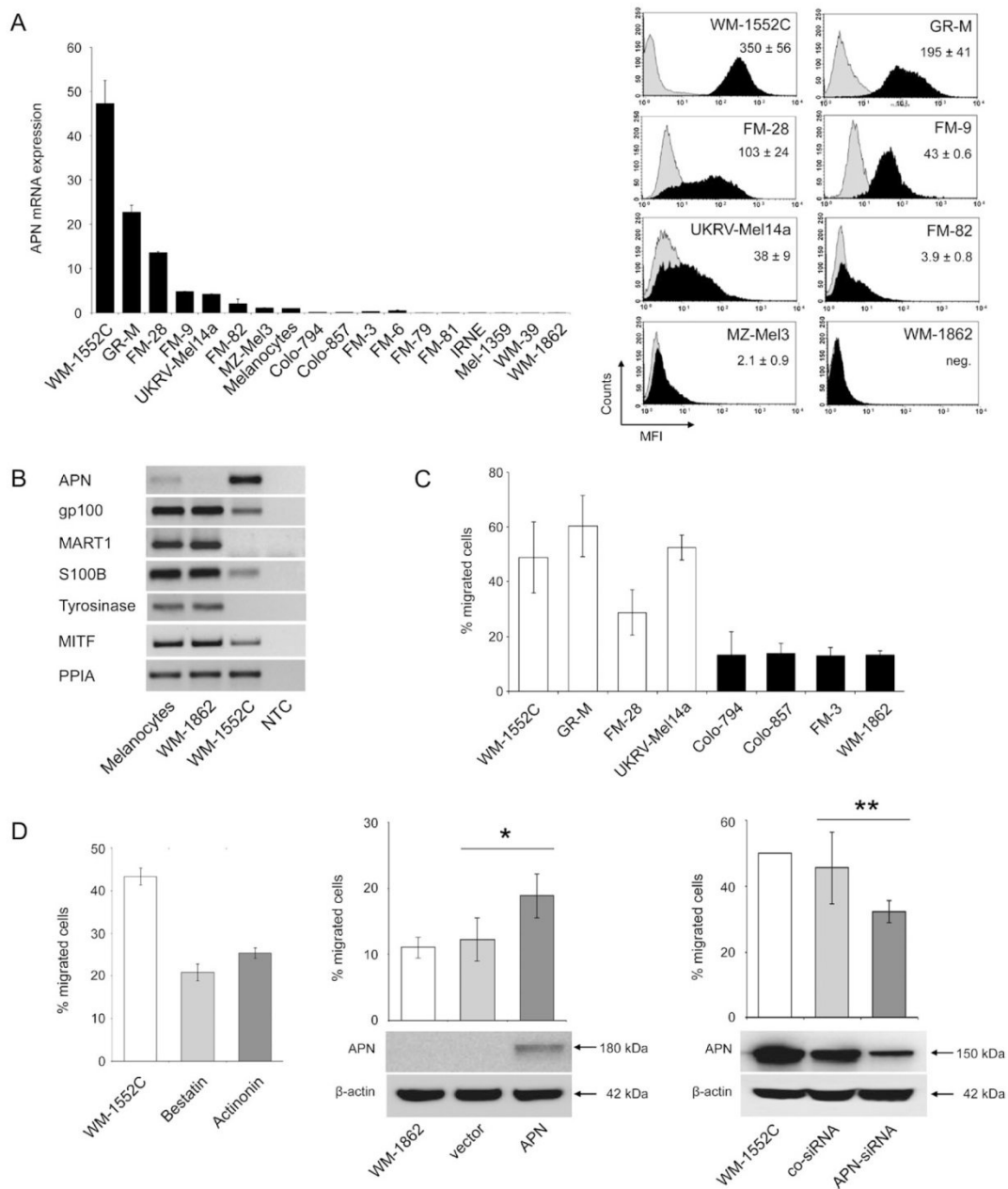


Fig. 1. Loss of melanocytic markers and increased migration in APN⁺ melanoma cells. **(A)** Total APN mRNA levels of 17 melanoma cell lines in relation to the expression of melanocytes (set to 1) as well as representative histograms of APN cell surface expression (black curves) including mean fluorescence intensity of at least three independent experiments are shown (isotype control, grey curves). **(B)** The expression of melanocytic markers was analysed in melanocytes, in APN-negative WM-1862 as well as in APN⁺ WM-1552C cells by end-point RT-PCR. NTC, non-template control. **(C)** APN⁺ melanoma cell lines showed higher migration potentials to collagen type I in comparison with APN-negative cells. **(D)** Migration of APN-overexpressing WM-1862 cells was increased compared with vector control (**P* = 0.008) and could be blocked by aminopeptidase inhibitors or by APN-directed small interfering RNA in APN⁺ WM-1552C cells (***P* = 0.003). Data are expressed as % of migrated cells and represent the mean of three independent experiments.

APN promoter methylation in melanoma

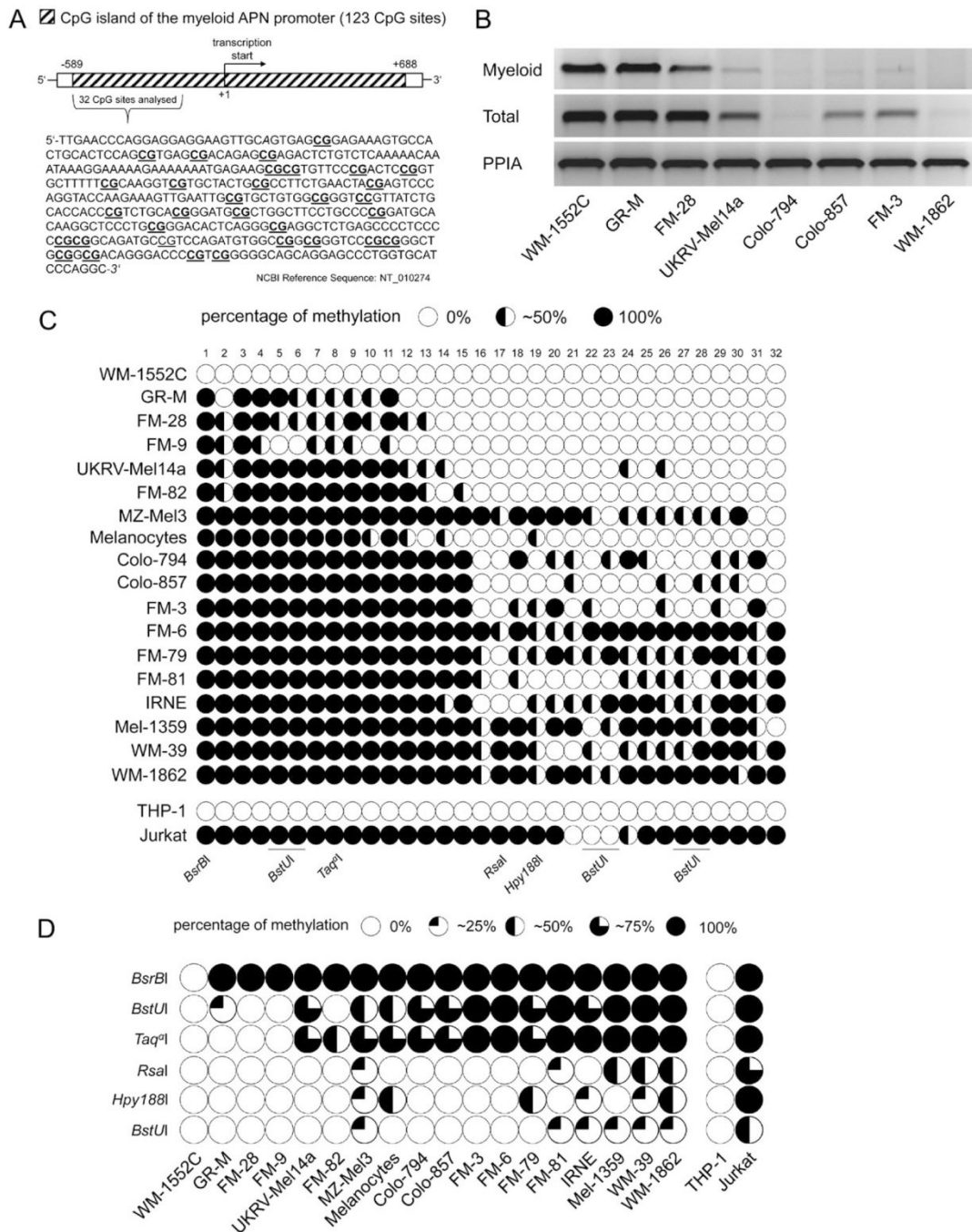


Fig. 2. Structure, transcriptional activity and DNA methylation status of the myeloid APN promoter in melanoma cells. (A) Schematic illustration of the CpG island in the myeloid APN promoter and sequence of CpG region analysed. (B) mRNA of representative melanoma cell lines was subjected to end-point RT-PCR amplifying the myeloid and total APN transcripts. Peptidylprolyl isomerase A (PPIA) served as a control. (C) Methylation pattern of 32 CpG sites in the myeloid APN promoter for the melanoma cell lines analysed are shown. CpG sites and methylation status are marked with circles. (D) Results of COBRA using different restriction enzymes with percentage classification of DNA methylation pattern are summarized.

J. Wulfänger et al.

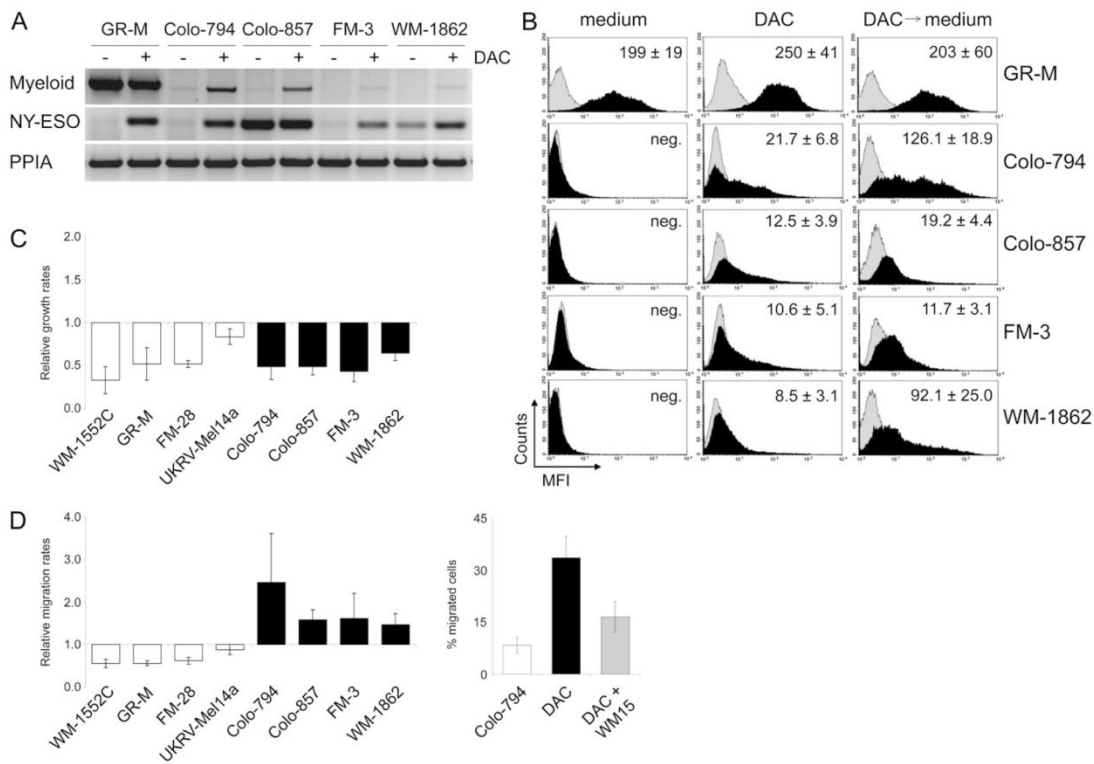


Fig. 3. Induced APN expression and migratory activities after DAC treatment. (A) Induction of myeloid mRNA expression in APN-negative melanoma cell lines. Cells were treated with 5 μ M DAC each day for a period of 4 days before mRNA isolation and end-point RT-PCR. GR-M melanoma cells served as APN⁺ control, NY-ESO as DAC efficacy control and peptidylprolyl isomerase A (PPIA) as complementary DNA quality control. (B) Induced APN surface expression in melanoma cells. Cells were cultured in the presence and absence of 5 μ M DAC each day for 4 days (termed DAC) or prolonged cultivated without DAC for additional 4 days (DAC \rightarrow medium). Representative histograms of APN staining (black curves) with mean fluorescence intensity of at least three independent experiments are shown (isotype control, grey curves). (C) Diminished growth of DAC-treated melanoma cells. Cells were cultivated each of 4 days with or without 5 μ M DAC in duplicates before determination of the cell number. Growth rates relative to medium control of four APN-negative (black bars) as well as of four APN⁺ melanoma cell lines (white bars) are presented. (D) DAC-mediated APN induction caused an increased migration capacity in the APN-negative melanoma cell line Colo-794 in relation to medium control and could be inhibited by the APN-specific mAb WM15. Data are expressed as % of migrated cells and represent the mean of three independent experiments.

as of total APN transcripts of 18 short-term cultures of melanoma lesions (C1–C18) were compared with the methylation status of the myeloid APN promoter analysed by COBRA (Figure 5A and B). High expression of APN transcripts was associated with a low frequency of APN promoter DNA methylation, whereas no or marginal APN expression correlated with a high degree of methylated CpG oligonucleotides ($P < 0.001$). To assess the methylation status of this chromosomal DNA region, three tumours with different APN expression levels were selected and subjected to DNA sequencing of 10 individual bacterial clones as described in Materials and methods. As shown in Figure 5C, APN expression was dependent on the methylation status of the myeloid APN promoter also in melanoma lesions ($P = 0.023$). Whereas C7 with the highest APN expression was marginally methylated, a higher degree of methylation was found in the tumour probe C5 with medium APN expression. Methylation was even more pronounced in the APN-negative tumour probe C4. The highest frequency of methylated CpG oligonucleotides was detected in CpG position 1–11, which was analogous to the results obtained by direct sequencing of the melanoma cell lines. Similar to the data in melanoma cell lines, high APN levels were also associated with a decreased expression of melanocytic markers in these primary

tumours (Supplementary Table 3 is available at *Carcinogenesis* Online). In addition, a heterogeneous methylation pattern of the APN promoter DNA was detected in 13 fresh tumour cell suspensions (T1–13, without any *in vitro* culture), indicating that no culture artefact was responsible for the differences in the APN promoter DNA methylation (Figure 5D).

APN protein expression in a melanoma TMA

To study APN expression in a high number of patient tissues, TMA consisting of 364 primary malignant melanoma lesions, 39 metastases and 62 benign nevi including compound and dermal nevi was stained with an APN-specific mAb. Fifty-eight tissues of total 404 cases exhibited at least a weak membranous and cytoplasmic APN staining. Thereby, primary melanoma showed a higher APN expression (16.9%) when compared with benign nevi (4.1%) and melanoma metastases (5.7%) ($P < 0.001$; Figure 6A). Higher Clark levels, increased tumour thickness >2.0 mm and positive nodal status (pN1–3) were significant prognostic factors (Supplementary Table 4 is available at *Carcinogenesis* Online). However, there existed neither a significant correlation of APN positivity with these factors (Supplementary Table 5 is available at *Carcinogenesis* Online) nor with

APN promoter methylation in melanoma

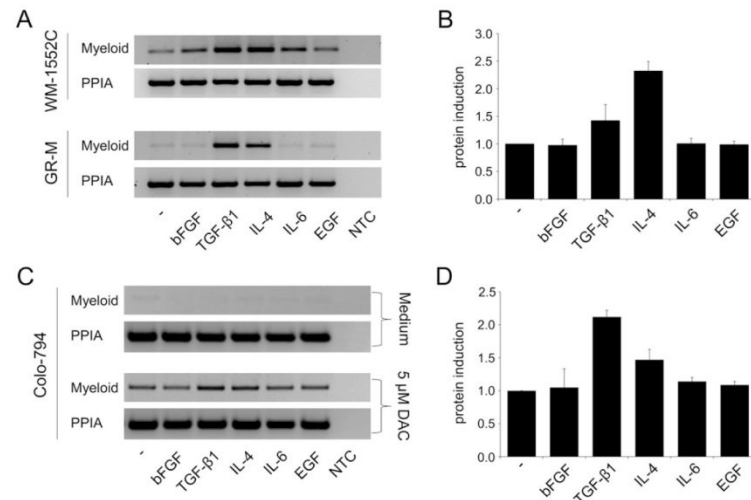


Fig. 4. Cytokine-mediated stimulation of APN expression. (A) Increased myeloid transcript levels after cell stimulation with TGF-β1 or IL-4. APN⁺ WM-1552C and GR-M cells were treated with the indicated cytokines for 48 h before analysing of the myeloid mRNA transcripts by end-point RT-PCR. (B) APN cell surface expression was determined as described in Materials and methods. Results of three independent experiments relative to untreated GR-M cells are presented. (C) APN-negative Colo-794 cells were treated each of 4 days with or without 5 μM DAC; on days 3 and 4, indicated cytokines were additionally supplemented. Then, the myeloid mRNA transcripts were quantified using end-point RT-PCR. (D) Results of flow cytometry of three independent experiments relative to DAC-treated Colo-794 cells without additional cytokine (set to 1) are presented. NTC, non-template control.

overall survival ($P = 0.265$) and RFS ($P = 0.300$) (Supplementary Figure 5 is available at *Carcinogenesis* Online).

C7 and C12 as short-time melanoma cultures with the highest APN expression were both histologically typed as nodular melanoma. This subtype showed the shortest overall survival of all indicated melanoma kinds in the TMA (Figure 6B). However, no association was found for APN positivity with either nodular melanoma or with any of the other subtypes (Figure 6C).

Discussion

APN exerts many biological functions, such as processing biologically active peptides, promotion of invasion and degradation of extracellular matrices as well as modulation of cell motility and angiogenesis (6). Despite an altered APN expression has been described in several tumour types, limited information exists with respect to the regulation mechanism of its gene expression in tumours. A transcriptional control of APN by different transcription factors, such as c-Myb, Ets-2 or c-Maf has been demonstrated in endothelial cells (32–34). Several cytokines are known to up-regulate APN protein expression in different cell types (30,31,35). Furthermore, cell–cell contacts as well as hypoxia have been discussed as factors involved in APN regulation (4,36). With respect to other membrane peptidases often co-localized with APN, an epigenetic control has been described. For example, CpG methylation was detected for the neprilysin/CD10 in lymphoid malignancies and in prostate carcinoma, for dipeptidyl peptidase IV/CD26 in T-cell leukaemia and melanoma (37–40). Since similar data on APN are lacking and a putative CpG island is located in the myeloid APN promoter, methylation-specific PCR and bisulfite sequencing were used by us to determine the DNA methylation status of the myeloid APN promoter in primary and established melanoma cell lines as well as in melanoma lesions. We here show for the first time that (i) the myeloid APN promoter indeed contains a large CpG island; (ii) low CpG methylation frequency is accompanied with higher levels of myeloid promoter-derived APN mRNA as well as protein; (iii) DAC-mediated demethylation restores protein expression, which was accompanied

by an enhanced migration and (iv) these observations are not limited to cell lines but can also be extended to short-term tumour cultures as well as melanoma lesions indicating an *in vivo* relevance of DNA methylation controlling APN expression. Additionally, we could also observe a differential DNA methylation in cells of haematopoietic origin as demonstrated for THP-1 and Jurkat cells. Thus, epigenetic silencing of APN and other aminopeptidases might represent a common mechanism not only in melanoma but also in other tumour or non-tumourous cells to regulate their expression.

In the melanoma cell lines investigated a broad range of DNA methylation of the myeloid APN promoter was observed. Several APN protein-expressing cell lines have clearly demethylated CpG sites compared with the strongly methylated regions of APN-negative cells. As described in literature, melanocytes lack APN expression (15,16,41). In our analysis, the mRNA amounts and the semi-methylated status of the myeloid APN promoter of melanocytes indicate that APN protein expression in these cells should be classified in between positive and negative when compared with the melanoma cells analysed. Interestingly, Seftor *et al.* (41) showed that a 4 day incubation of melanocytes in a matrix preconditioned by highly aggressive melanoma cells resulted in a reversible up-regulation of APN mRNA accompanied by VE-cadherin, urokinase, c-Met as proto-oncogene-encoding hepatocyte growth factor receptor protein and the laminin 5 γ2 chain. These authors discussed an epigenetic transdifferentiation of the benign melanocytic phenotype by the microenvironment and APN expression might represent one link in the chronology of these phenotypic changes.

DNA methylation leads to a more compact chromatin structure of chromosomal promoter regions causing repression of gene activity by disturbing the binding of transcription factors (42). Demethylation might be a precondition for the stimulatory effect of these cytokines on APN expression. Indeed, cytokines alone could not induce APN, but stimulation by recombinant IL-4 and TGF-β1 in combination with DAC restored APN protein expression. IL-4 is known to increase APN expression in monocytes and epithelial cells (30,31); both APN promoters should be involved. In contrast, TGF-β1 increases APN expression on monocytes (35) and melanoma, whereas it has no

J.Wulfänger *et al.*

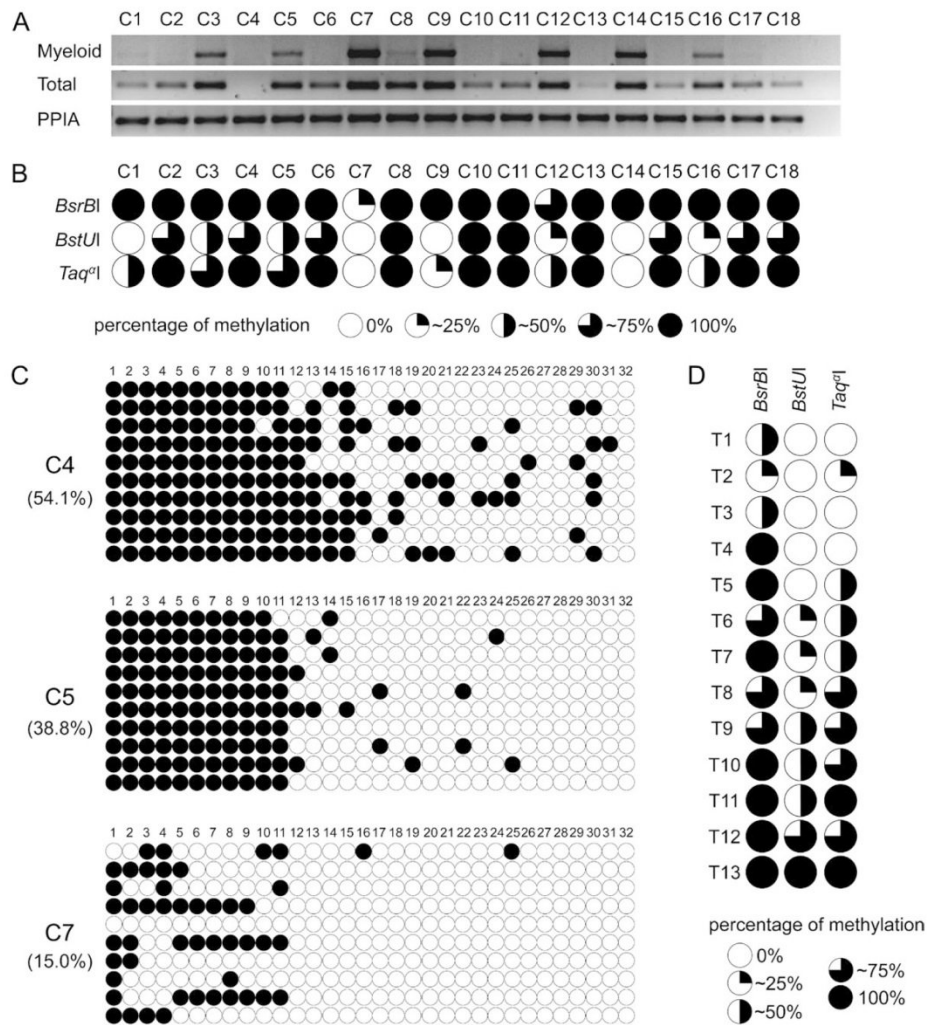


Fig. 5. Different methylation status of the myeloid APN promoter in various short-term melanoma cultures and tumour lesions. (A) Differential APN mRNA expression in short-term cultivated melanoma cells. mRNA expression was analysed by end-point RT-PCR amplifying the myeloid and total APN transcripts. Peptidylprolyl isomerase A (PPIA) served as a control. (B) Distinct DNA promoter methylation pattern in short-term melanoma cultures (C1–C18). Results of COBRA using different restriction enzymes as marked with the percentage of the DNA methylation pattern are summarized. (C) Statistical analysis of the distinct methylation pattern. Amplified bisulfite-treated DNA was cloned into the PCR2.1-Topo vector and 10 individual clones of the cultivated melanoma C4, C5 and C7 were subjected to DNA sequencing. Black circles represent methylated and white unmethylated CpG sites. Percentages of methylation grade over all CpG sites analysed are indicated. (D) COBRA of single-cell suspensions obtained from the melanoma lesions (T1–T13) confirmed heterogeneous promoter methylation in tumours.

influence on renal or thyroid carcinoma (7,31). Therefore, the TGF- β 1 effect might be selectively driven by the myeloid promoter dependent on tumour entities analysed. Interestingly, we found APN up-regulated in melanoma cells after TGF- β 1 treatment as well as a higher expression of this cytokine in APN⁺ compared with APN-negative melanoma. Increased expression of TGF- β has been observed in invasive primary melanomas and in metastatic nodules as compared with normal skin melanocytes (43). Resistance to TGF- β -mediated tumour suppression in melanoma appears to be a crucial step in tumour aggressiveness since it is usually coupled with the ability of TGF- β to drive the oncogenic process via autocrine and paracrine effects (44). Taken together, a dependence of CpG methylation den-

sity and the capability for cytokine stimulation is suggested by us and will be the focus of further studies.

Previous studies discuss APN as a marker of higher migration capacity and aggressiveness in melanoma (19,20,28). Our *in vitro* results are in accordance with the literature since APN expression was associated with loss of melanocytic marker expression in cell lines as well as in tumour lesions. Furthermore, a 2- to 5-fold increased migration rate of APN⁺ versus APN-negative melanoma cells was measured, which could be blocked by RNA interference or aminopeptidase-specific inhibitors. Treatment of APN-negative cells with the demethylating agent DAC could not only induce APN protein but also caused an APN-mediated increase of cell migration.

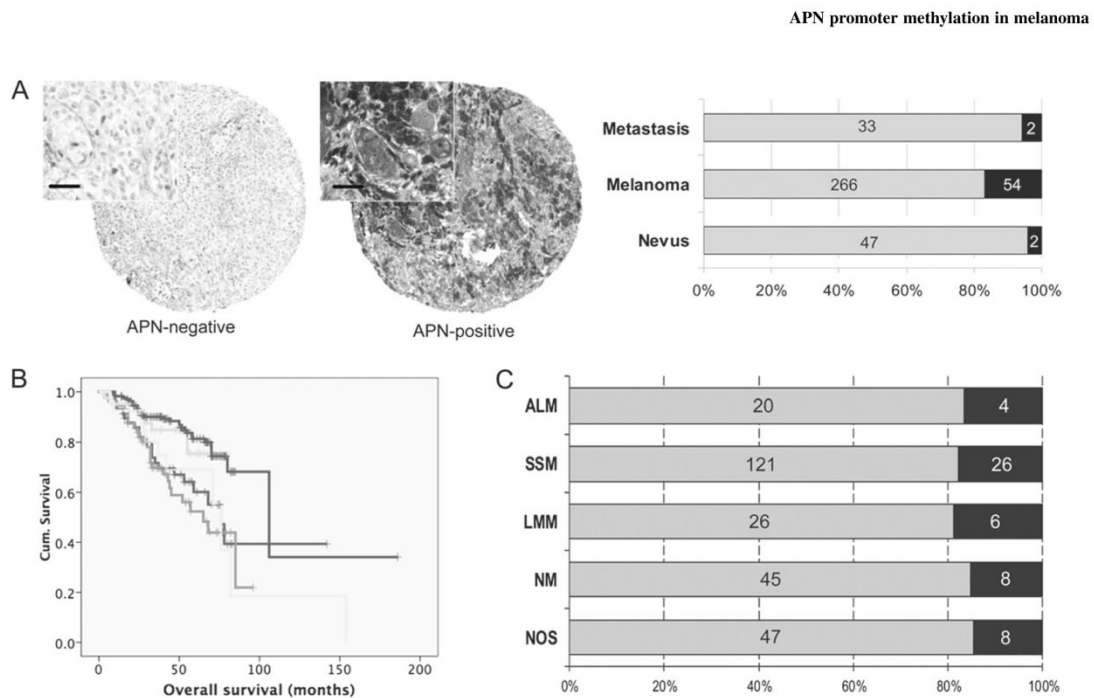


Fig. 6. *In situ* expression of APN. (A) Heterogeneous APN expression in melanoma lesions. Representative APN stainings of melanoma tissues as well as cumulative bar charts including the number of informative cases with negative (grey bars) and strong APN immunoreactivity (black bars) in different melanoma tissue types are shown ($P = 0.018$; original magnification $\times 20$, inserts $\times 200$ with magnification bars of $20 \mu\text{m}$). (B) Kaplan–Meier curves regarding survival of melanoma patients with different melanoma subtypes. (Yellow = ALM, acral lentiginous melanoma; Purple = SSM, superficial spreading melanoma; Light brown = LMM, lentigo maligna melanoma; Green = NM, nodular melanoma; Blue = NOS, not otherwise specified; $P_{\text{Log-rank}} < 0.001$). (C) APN expression in melanoma subtypes (APN-negative, grey bars; APN⁺, black bars).

DAC has been recently implemented into several clinical phase I trials and antitumour efficacy is currently monitored in different solid tumours. Almost all *in vitro* studies demonstrated that promoter demethylation using DAC decreases cell growth by induction of different tumour suppressor genes, but it might also activate silenced prometastatic genes like APN as demonstrated in this study. Consistent with our data, Ateeq *et al.* (45) described an induction of pro-invasive and pro-metastatic genes, e.g. the urokinase-type plasminogen activator, the chemokine receptor CXCR4 as well as the breast cancer-specific gene 1 leading to an increased invasion and migration ability of non-invasive breast cancer cell lines. Based on this knowledge, the implementation of demethylating agents in antitumour therapy of melanoma has to be further evaluated.

When data on the higher motility of APN⁺ melanoma cells are taken into account, an association of APN expression in melanoma tissues with worse patients' prognosis was postulated. However, our data of a TMA consisting of 465 human tissues, including benign melanocytic nevi, malignant melanoma and melanoma metastases did not show an association of APN expression and shorter patients' survival. APN protein could only be detected in 17% of all tumour samples analysed, in particular mainly in primary malignant melanoma. Another explanation would be APN expression as the property of a specific melanoma subtype. Winnepenninckx *et al.* (46) reported high levels of APN but diminished expression of melanocytic markers in 'spindle cell melanoma'. This subtype also known as desmoplastic melanoma represents <2% of all melanoma. Unfortunately, we did not observe a significant association of APN staining with any melanoma subtype indicated. It is noteworthy that desmoplastic melanoma was not designated in the array employed. Additional factors might affect APN protein expression *in vivo* and these factors have to be elucidated yet.

In summary, we demonstrate for the first time that DNA methylation of the myeloid promoter regulates APN transcription in

melanoma and that treatment with demethylating agents causes *de novo* APN protein expression in these cells leading to a migratory phenotype. Therefore, our findings provide a new principle controlling APN expression in cancer. Future studies will have to be extended to tumours of distinct origin to clarify whether epigenetic control is a common APN regulatory mechanism.

Supplementary material

Supplementary Tables 1–5 and Figures 1–5 can be found at <http://carcin.oxfordjournals.org/>.

Funding

This work was partially sponsored by the Wilhelm Roux Program of the Martin-Luther-University Halle-Wittenberg, Halle (Saale), Germany (FKT 17/40) and in part supported by the Deutsche Krebshilfe e.V. (Project 108134).

Acknowledgements

We would like to thank Sylvi Magdeburg for excellent secretarial help and Dr Markus Meissner (University Hospital, Frankfurt, Germany) for providing us with melanocytes. This paper represents parts of the PhD thesis of J.W.

Conflict of Interest Statement: None declared.

References

1. Look, A.T. *et al.* (1989) Human myeloid plasma membrane glycoprotein CD13 (gp150) is identical to aminopeptidase N. *J. Clin. Invest.*, **83**, 1299–1307.
2. Shapiro, L.H. *et al.* (1991) Separate promoters control transcription of the human aminopeptidase N gene in myeloid and intestinal epithelial cells. *J. Biol. Chem.*, **266**, 11999–12007.

J. Wulfänger et al.

3. Olsen, J. et al. (1997) An enhancer with cell-type dependent activity is located between the myeloid and epithelial aminopeptidase N (CD 13) promoters. *Biochem. J.*, **322**, 899–908.
4. Riemann, D. et al. (1999) CD13—not just a marker in leukemia typing. *Immunol. Today*, **20**, 83–88.
5. Mina-Osorio, P. (2008) The moonlighting enzyme CD13: old and new functions to target. *Trends Mol. Med.*, **14**, 361–371.
6. Carl-McGrath, S. et al. (2006) Ectopeptidases in tumour biology: a review. *Histol. Histopathol.*, **21**, 1339–1353.
7. Kehlen, A. et al. (2003) Biological significance of aminopeptidase N/CD13 in thyroid carcinomas. *Cancer Res.*, **63**, 8500–8506.
8. Tokuhara, T. et al. (2010) Clinical significance of aminopeptidase N in non-small cell lung cancer. *Clin. Cancer Res.*, **12**, 3971–3978.
9. Perez, L. et al. (2009) Increased APN/CD13 and acid aminopeptidase activities in head and neck squamous cell carcinoma. *Head Neck*, **31**, 1335–1340.
10. Mawrin, C. et al. (2010) Reduced activity of CD13/aminopeptidase N (APN) in aggressive meningiomas is associated with increased levels of SPARC. *Brain Pathol.*, **20**, 200–210.
11. Gohring, B. et al. (1998) Endopeptidase 24.11/CD10 is down-regulated in renal cell cancer. *Int. J. Mol. Med.*, **2**, 409–414.
12. Varona, A. et al. (2007) Altered levels of acid, basic, and neutral peptidase activity and expression in human clear cell renal cell carcinoma. *Am. J. Physiol. Renal Physiol.*, **292**, F780–F788.
13. Bogenrieder, T. et al. (1997) Expression and localization of aminopeptidase A, aminopeptidase N, and dipeptidyl peptidase IV in benign and malignant human prostate tissue. *Prostate*, **33**, 225–232.
14. Teranishi, J. et al. (2008) Evaluation of role of angiotensin III and aminopeptidases in prostate cancer cells. *Prostate*, **68**, 1666–1673.
15. Elder, D.E. et al. (1989) Antigenic profile of tumor progression stages in human melanocytic nevi and melanomas. *Cancer Res.*, **49**, 5091–5096.
16. Menrad, A. et al. (1993) Biochemical and functional characterization of aminopeptidase N expressed by human melanoma cells. *Cancer Res.*, **53**, 1450–1455.
17. Saiki, I. et al. (1993) Role of aminopeptidase N (CD13) in tumor-cell invasion and extracellular matrix degradation. *Int. J. Cancer*, **54**, 137–143.
18. Aozuka, Y. et al. (2004) Anti-tumor angiogenesis effect of aminopeptidase inhibitor bestatin against B16-BL6 melanoma cells orthotopically implanted into syngeneic mice. *Cancer Lett.*, **216**, 35–42.
19. Saitoh, Y. et al. (2006) A derivative of aminopeptidase inhibitor (BE15) has a dual inhibitory effect of invasion and motility on tumor and endothelial cells. *Biol. Pharm. Bull.*, **29**, 709–712.
20. Fujii, H. et al. (1995) Human melanoma invasion and metastasis enhancement by high expression of aminopeptidase N/CD13. *Clin. Exp. Metastasis*, **13**, 337–344.
21. Wulfaenger, J. et al. (2008) Aminopeptidase N (APN)/CD13-dependent CXCR4 downregulation is associated with diminished cell migration, proliferation and invasion. *Mol. Membr. Biol.*, **25**, 72–82.
22. Daniotti, M. et al. (2004) BRAF alterations are associated with complex mutational profiles in malignant melanoma. *Oncogene*, **23**, 5968–5977.
23. Li, L.C. et al. (2002) MethPrimer: designing primers for methylation PCRs. *Bioinformatics*, **18**, 1427–1431.
24. Simon, R. et al. (2003) Tissue microarray (TMA) applications: implications for molecular medicine. *Expert Rev. Mol. Med.*, **5**, 1–12.
25. Nocito, A. et al. (2001) Microarrays of bladder cancer tissue are highly representative of proliferation index and histological grade. *J. Pathol.*, **194**, 349–357.
26. Bar-Eli, M. (2001) Gene regulation in melanoma progression by the AP-2 transcription factor. *Pigment Cell Res.*, **14**, 78–85.
27. Gould Rothberg, B.E. et al. (2010) Biomarkers: the useful and the not so useful—an assessment of molecular prognostic markers for cutaneous melanoma. *J. Invest. Dermatol.*, **130**, 1971–1987.
28. Fontijn, D. et al. (2006) CD13/Aminopeptidase N overexpression by basic fibroblast growth factor mediates enhanced invasiveness of 1F6 human melanoma cells. *Br. J. Cancer*, **94**, 1627–1636.
29. Fröhlich, E. (2010) Proteases in cutaneous malignant melanoma: relevance as biomarker and therapeutic target. *Cell. Mol. Life Sci.*, **67**, 3947–3960.
30. van Hal, P.T. et al. (1994) Potential indirect anti-inflammatory effects of IL-4. Stimulation of human monocytes, macrophages, and endothelial cells by IL-4 increases aminopeptidase-N activity (CD13; EC 3.4.11.2). *J. Immunol.*, **153**, 2718–2728.
31. Riemann, D. et al. (1995) Stimulation of the expression and the enzyme activity of aminopeptidase N/CD13 and dipeptidylpeptidase IV/CD26 on human renal cell carcinoma cells and renal tubular epithelial cells by T cell-derived cytokines, such as IL-4 and IL-13. *Clin. Exp. Immunol.*, **100**, 277–283.
32. Bhagwat, S.V. et al. (2001) CD13/APN is activated by angiogenic signals and is essential for capillary tube formation. *Blood*, **97**, 652–659.
33. Petrovic, N. et al. (2003) CD13/APN transcription is induced by RAS/MAPK-mediated phosphorylation of Ets-2 in activated endothelial cells. *J. Biol. Chem.*, **278**, 49358–49368.
34. Mahoney, K.M. et al. (2007) CD13/APN transcription is regulated by the proto-oncogene c-Maf via an atypical response element. *Gene*, **403**, 178–187.
35. Kehlen, A. et al. (2004) IL-10 and TGF-beta differ in their regulation of aminopeptidase N/CD13 expression in monocytes. *Int. J. Mol. Med.*, **13**, 877–882.
36. Stockwin, L.H. et al. (2006) Proteomic analysis of plasma membrane from hypoxia-adapted malignant melanoma. *J. Proteome Res.*, **5**, 2996–3007.
37. Taylor, K.H. et al. (2006) Promoter DNA methylation of CD10 in lymphoid malignancies. *Leukemia*, **20**, 1910–1912.
38. Usmani, B.A. et al. (2000) Methylation of the neutral endopeptidase gene promoter in human prostate cancers. *Clin. Cancer Res.*, **6**, 1664–1670.
39. Tsuji, T. et al. (2004) Clinical and oncologic implications in epigenetic down-regulation of CD26/dipeptidyl peptidase IV in adult T-cell leukemia cells. *Int. J. Hematol.*, **80**, 254–260.
40. McGuinness, C. et al. (2008) Dipeptidyl peptidase IV (DPP4), a candidate tumor suppressor gene in melanomas is silenced by promoter methylation. *Front. Biosci.*, **13**, 2435–2443.
41. Sefter, E.A. et al. (2005) Epigenetic transdifferentiation of normal melanocytes by a metastatic melanoma microenvironment. *Cancer Res.*, **65**, 10164–10169.
42. Baylin, S.B. (2002) Mechanisms underlying epigenetically mediated gene silencing in cancer. *Semin. Cancer Biol.*, **12**, 331–337.
43. Van Belle, P. et al. (1996) Melanoma-associated expression of transforming growth factor-beta isoforms. *Am. J. Pathol.*, **148**, 1887–1894.
44. Lasfar, A. et al. (2010) Resistance to transforming growth factor beta-mediated tumor suppression in melanoma: are multiple mechanisms in place? *Carcinogenesis*, **31**, 1710–1717.
45. Ateeq, B. et al. (2008) Pharmacological inhibition of DNA methylation induces proinvasive and prometastatic genes *in vitro* and *in vivo*. *Neoplasia*, **10**, 266–278.
46. Winnepenninckx, V. et al. (2003) New phenotypical and ultrastructural findings in spindle cell (desmoplastic/neurotropic) melanoma. *Appl. Immunohistochem. Mol. Morphol.*, **11**, 319–325.

Received May 26, 2011; revised January 24, 2012; accepted January 29, 2012

Supplementary Table 1

Primer sequences, annealing temperature and product size of different genes used in indicated application.

Application	Gene	RefGene	Primer sequence		Annealing	Product size [bp]	
			Sense	Antisense			
Endpoint- and quantitative RT-PCR	APN	NM_001150	GACGAAGAGAAGCTGGAGGAAGA	CTTCAATCAGGAAGAGGGTGT	60 °C	163	
	gp100	NM_006928	GTATTGAAAGTGCCGAGATCCT	CCAGAGACACATTGAGGCAGTA		240	
	MART-1	NM_005511	TCATCGGCTGTTGGTATTGTAG	TAAGGTGGTGGTACTGTTCTG		223	
	NY-ESO	NM_005511	CGCCTGCTTGAGTTCTACCT	CAGCAGTCAGTCGGATAGCAG		163	
	S100B	NM_006272	GAGACAAGCACAAGCTGAAGAA	CATCATTGTCCAGTGTTCAT		126	
	Tyrosinase	NM_000372	GTGGGAACAAGAAATCCAGAAG	TCCATTGCATAAAGACTGATGG		223	
	MITF	NM_198159	CCTGTATGCAGATGGATGATGT	GCTCTTGCTTCAGACTCTGTGA		241	
	bFGF	NM_002006	CGTTACCTGGCTATGAAGGAAG	CAGCTCTTAGCAGACATTGGAA		227	
	TGF-β1	NM_000680	GACTCGCCAGAGTGGTTATCTT	CTGAAGCAATAGTTGGTGCCA		290	
	IL-4	NM_000589	CAGTTCTACAGCCACCATGAGA	CATGATCGTCTTTAGCCTTTCC		201	
Characterization	IL-6	NM_000600	ACAGACAGCCACTCACCTCTTC	TCTTTGGAAGTTTCAGGTGTT	156		
	EGF	NM_001963	CTACCAAGGAGATGGGATTCAC	CATGCATACCTTCCCAATGCTT	297		
	PPIA	NM_021130	CCATCTATGGGGAGAAATTTGA	CAGTCAGCAATGGTGATCTTCT	254		
	Myeloid APN	NM_001150	GTCCAGGGTCCAGGTCC	AGGTACGGTCTCAGCGTCAC	52 °C	538	
	DNA methylation	1. PCR		TTGAATTTAGGAGGAGGAAGTTGTA	CAACACTAAACTCCTCTTTCC	611	
		2. PCR		TTGAATTTAGGAGGAGGAAGTTGTA	CAATCAACTTTCTTAATACCTAAAAC	207	
	COBRA	2. PCR		GTTTTAGGTATTAAGAAAGTTGAATTG	ACCTAAAATACACAAAACCTCTACTAC	56 °C	241
		2. PCR		TTGAATTTAGGAGGAGGAAGTTGTA	ACCTAAAATACACAAAACCTCTACTAC	420	

Supplementary Table 2

Expression of APN and melanocytic markers as well as methylation pattern of melanoma cell lines and melanocytes.

Cells	Melanocytic marker *					APN		
	gp100	MART-1	NY-ESO	S100B	Tyrosinase	protein †	methylation (%)	DAC induction ‡
WM-1552C	-	-	-	-	-	+++	0.0	1.0 ± 0.2
GR-M	-	-	-	-	-	+++	23.4	0.9 ± 0.1
FM-28	+	++	++	+++	++	+++	28.1	2.0 ± 0.4
FM-9	-	-	+++	-	-	++	15.6	n.d.
UKRV-Mel14a	-	-	+	-	-	++	40.6	2.5 ± 0.7
FM-82	+++	+++	+++	+++	+++	+	39.1	13.0 ± 5.6
MZ-Mel3	-	-	+	+++	++	+	78.1	9.7 ± 4.8
Melanocytes	+++	+++	-	+++	+++	n.d.	37.5	n.d.
Colo-794	+++	+++	+	+++	+++	-	65.6	19.4 ± 4.7
Colo-857	+++	-	+++	+++	+++	-	54.7	22.0 ± 7.3
FM-3	+++	+++	++	+++	+++	-	60.9	9.8 ± 2.1
FM-6	+	++	+++	+++	++	-	92.2	6.4 ± 1.9
FM-79	+++	+++	+++	+++	+++	-	79.7	58.7 ± 0.2
FM-81	+	+++	-	++	++	-	65.6	40.2 ± 9.6
IRNE	++	+++	+++	+++	+++	-	76.6	30.8 ± 18.5
Mel1359	+++	+++	+++	+++	+++	-	85.9	n.d.
WM-39	+++	+++	+	+++	+++	-	78.1	n.d.
WM-1862	+++	+++	-	+++	+++	-	92.2	67.3 ± 19.7

* mRNA quantification of melanocytic marker was performed as described in Materials and Methods. Results are expressed as x-fold expression of the melanoma cell line WM-1552C set to 1 and scored as - <10; + 10-100; ++ 100-1 000; +++ >1 000.

† APN protein expression of melanoma cells was analysed by flow cytometry using an APN-specific mAb. The MFI was determined and scored as: -: not expressed; +: MFI 1-10; ++: MFI 10-100; +++: MFI >100.

‡ APN mRNA induction after cell treatment with 5 µM DAC each day for a period of four days. The results are expressed as x-fold induction in relation to medium control. n.d.: not determined.

Supplementary Table 3

Expression of APN and melanocytic markers in short-term melanoma cultures.

No.	cell source of metastasis	gender	age at diagnosis	primary tumour site	Primary tumour type *	Breslow (mm)	Clark's level	Overall survival from excision (years)	BRAF status	APN †	Melanocytic marker †				
											gp-100	MART-1	NY-ESO	S100B	Tyrosinase
C7	nodal	M	52	Trunk	NM	3.7	III	< 2	V600E	1.000	1.0	1.0	1.0	1.0	
C12	cutaneous	F	59	Leg	NM	1.72	IV	> 17	V600E	0.310	0.0	0.0	n.e.	3.7	
C3	nodal	F	22	Leg	SSM	0.91	IV	> 9	V600E	0.218	0.0	0.7	45.8	45.8	
C14	cutaneous	M	51	Hand	SSM	2.69	IV	4	V600E	0.187	0.0	0.0	2396.5	0.0	
C9	nodal	M	56	Unknown				> 5	V600E	0.145	0.3	1.7	818.7	21.8	
C5	nodal	F	39	Trunk	SSM	2.2	III	< 1	V600E	0.041	5.1	16.4	n.e.	12.9	
C16	cutaneous	M	49	Trunk	SSM	4.8	III	< 1	V600E	0.031	17.9	71.9	n.e.	7.8	
C8	nodal	M	69	Arm	SSM	> 4	IV	< 2	wt	0.021	19.5	33.4	1.3	18.7	
C17	muscles	M	41	Unknown				< 1	wt	0.010	12.1	8.7	n.e.	9.7	
C6	nodal	M	53	Arm	n.a.			< 1	wt	0.004	21.8	38.8	n.e.	8.8	
C1	nodal	M	51	Leg	SSM	15	V	< 1	L597S	0.004	30.0	33.1	n.e.	32.9	
C2	nodal	F	36	Arm	SSM	2.48	IV	> 13	V600E	0.003	6.9	17.9	n.e.	26.3	
C10	nodal	F	45	Trunk	SSM	1.23	IV	> 6	V600E	0.003	18.1	38.4	n.e.	4.7	
C18	nodal	M	24	Trunk	n.a.	3.4	IV	< 1	wt	0.003	34.6	34.7	n.e.	7.5	
C15	lungs	M	56	Trunk	n.a.	1.9	IV	< 2	V600E	0.002	0.6	16.6	18.9	10.5	
C11	cutaneous	F	52	Leg	n.a.			< 2	wt	0.002	9.7	46.4	n.e.	10.5	
C13	cutaneous	M	68	Foot	SSM	2	IV	> 3	wt	0.001	2.0	9.3	1981.1	16.3	
C4	nodal	F	36	Trunk	SSM	0.9	II	> 6	V600E	n.e.	0.4	30.4	63.7	69.4	

* NM: nodular melanoma; SSM: superficial spreading melanoma; n.a.: not available

† mRNA quantification of APN and melanocytic markers was performed as described in Materials and Methods. Results are displayed as x-fold expression of the APN highest expressing short-term cultivated melanoma C7 set to 1.
n.e.: not expressed.

Supplementary Table 4

Univariate analysis of clinicopathological and immunohistochemical variables relative to recurrence-free survival and overall survival.

Variable	Category	Tumour recurrence (RFS)			Overall survival		
		n	events (%)	P*	n	events (%)	P*
Age at diagnosis							
	≤60 years	122	27.9	0.254	180	15.0	0.561
	>60 years	104	19.2		184	10.9	
Gender							
	female	98	20.4	0.816	169	4.7	<0.001
	male	128	26.6		195	20.0	
Clark level							
	I-II	44	6.8	<0.001	77	2.6	<0.001
	III	60	10.0		106	4.7	
	IV-V	111	35.1		163	22.7	
Tumour thickness							
	≤2.0 mm	140	11.4	<0.001	255	7.1	<0.001
	>2.0 mm	80	45.0		103	27.2	
Nodal status							
	pN0	200	21.0	<0.001	319	10.3	<0.001
	pN1-3	20	55.0		23	52.2	
Ki67 labelling index							
	negative	32	31.3	0.002	47	14.9	0.487
	0.5-5%	88	15.9		155	11.6	
	>5%	94	28.7		144	13.2	

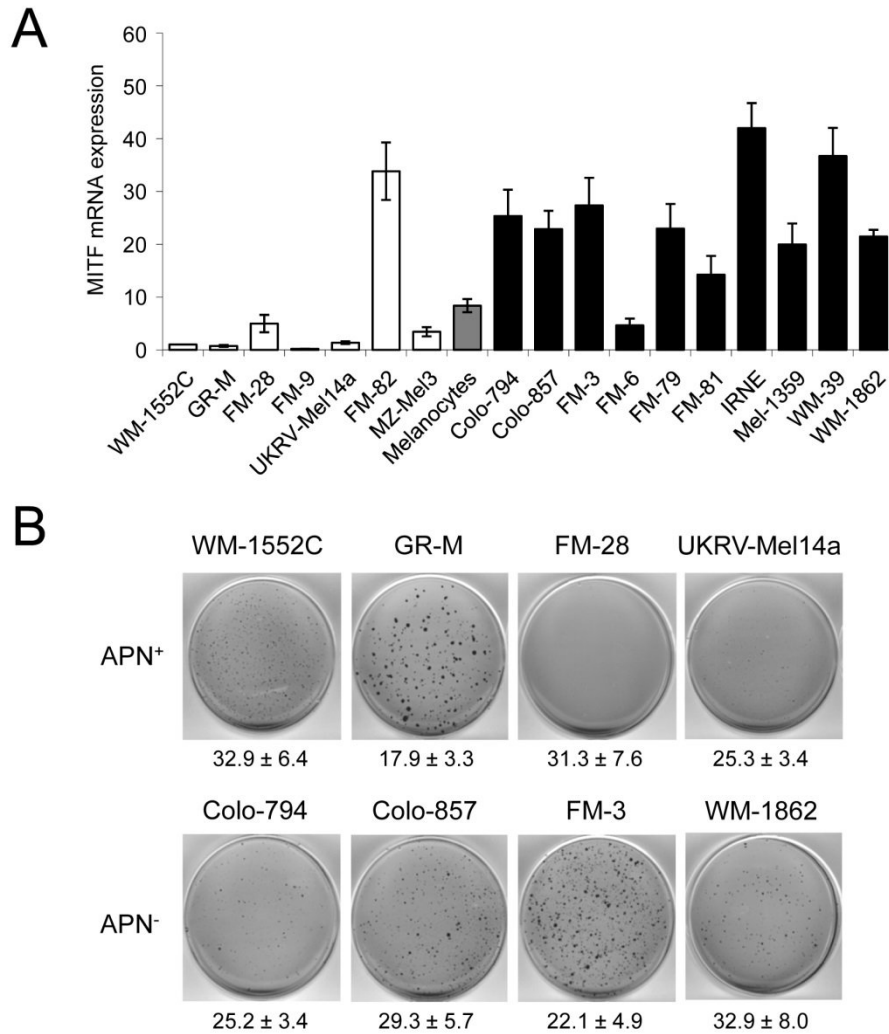
* Log rank test (2-sided), boldface indicates statistical significance.

Supplementary Table 5

Clinicopathological variables and APN expression among TMA.

Variable	Category	APN immunoreactivity		P*
		n analysable	positive (%)	
Primary malignant melanomas				
Age at diagnosis				
	≤60 years	160	26.0	0.100
	>60 years	160	15.1	
Gender				
	female	141	15.6	0.177
	male	179	24.3	
Clark level				
	I	2	0.0	0.479
	II	54	14.9	
	III	93	20.8	
	IV	142	26.8	
	V	14	7.7	
Tumour thickness				
	≤2.0 mm	217	23.3	0.193
	>2.0 mm	98	14.0	
Nodal status				
	pN0	282	22.1	0.550
	pN1-3	21	10.5	
Ki-67 labelling index				
	negative	46	35.3	0.196
	0.5-5%	137	17.1	
	>5%	127	19.8	
Benign nevi				
	compound	27	8.0	0.495
	dermal	22	0.0	

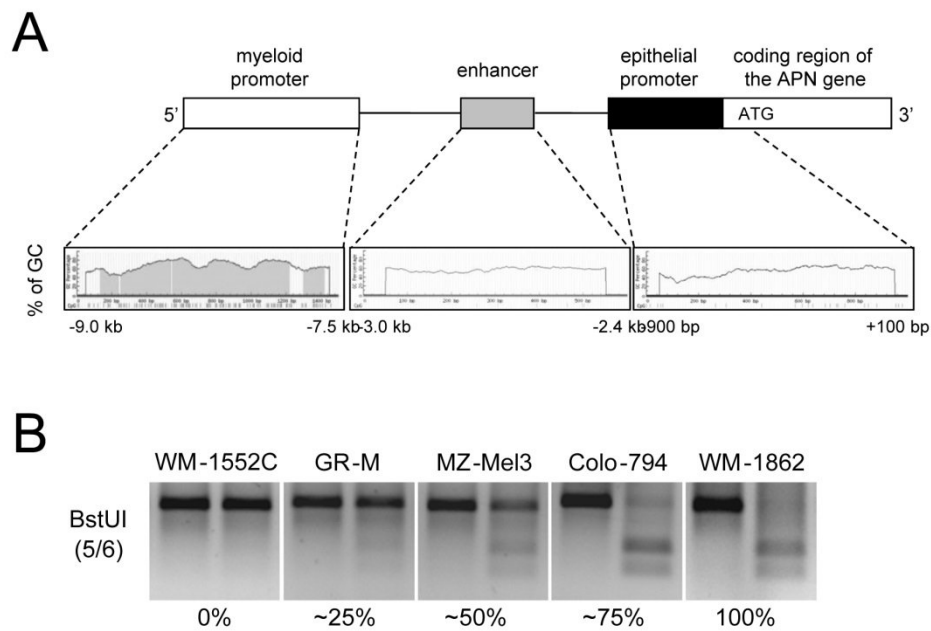
* Fisher's exact test (2-sided), otherwise χ^2 -test.

Wulfänger *et al.* Suppl. 1

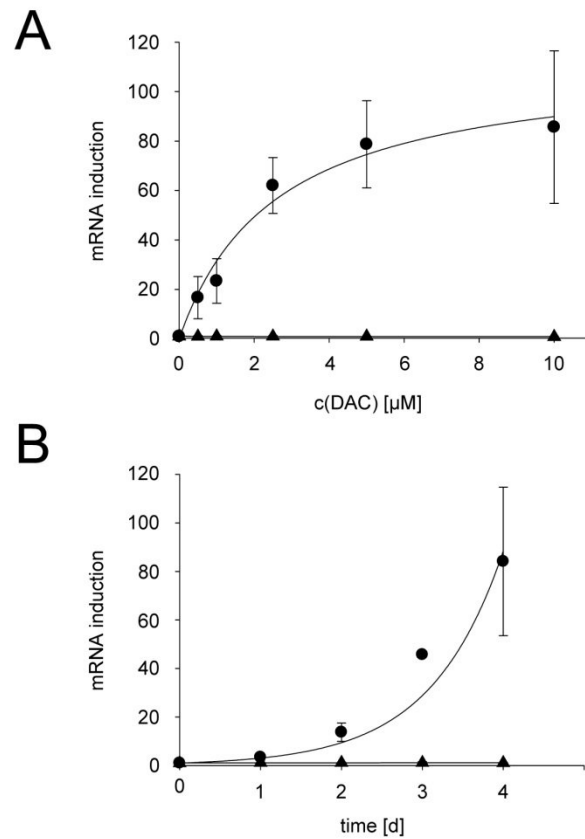
Suppl. Fig. 1: MITF expression and growth properties of melanoma cells.

(A) MITF expression of APN⁺ (white bars) and APN-negative melanoma cells (black bars) was quantified using quantitative RT-PCR. Results of three independent experiments are presented as fold mRNA expression in relation to WM-1552C set to 1.

(B) Anchorage-independent growth and doubling times were analysed as described in Materials and methods. A representative soft agar culture and doubling times of four APN-negative and APN⁺ melanoma cell lines are presented.

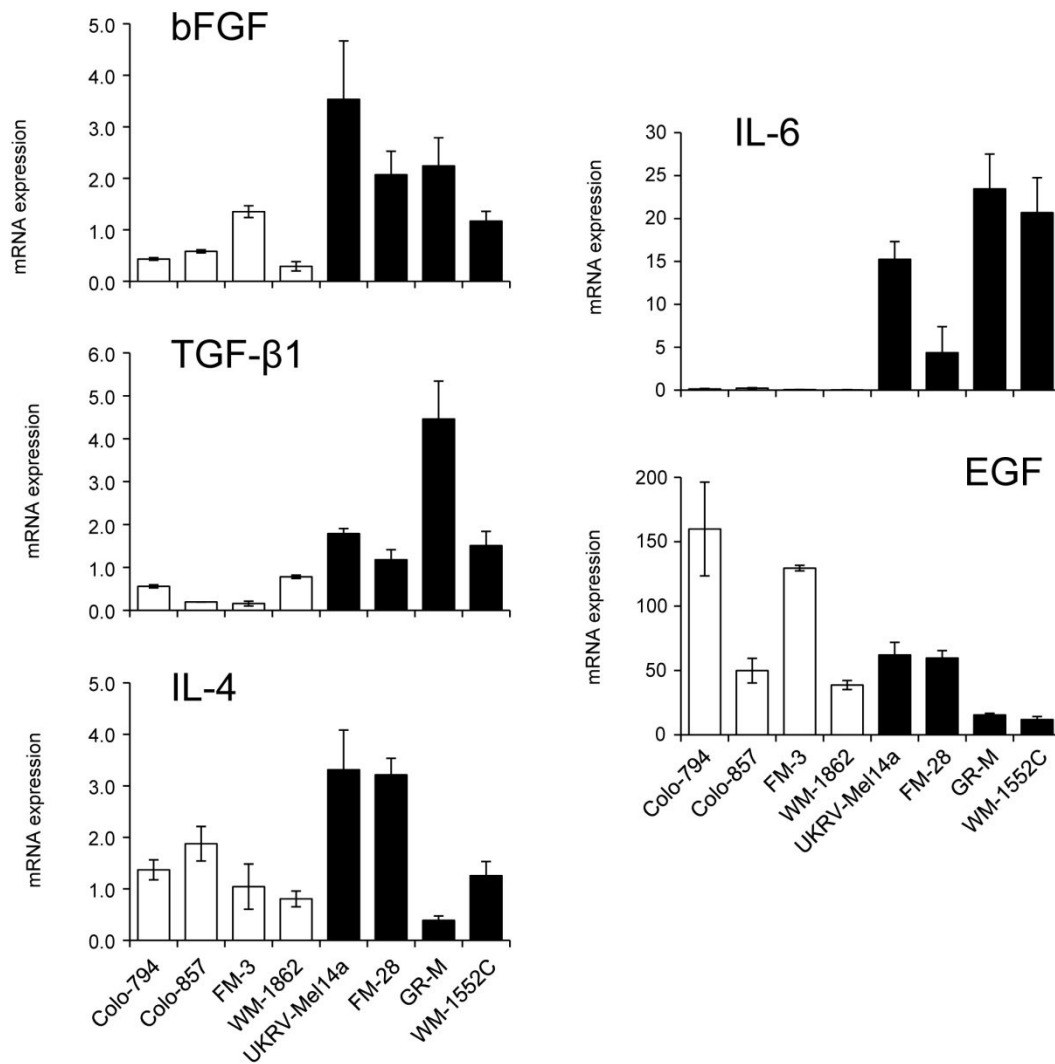
Wulfänger *et al.* Suppl. 2

Suppl. Fig. 2: Structure of the APN gene and categorisation of COBRA results. (A) Schematic illustration of the APN gene and GC content in the different regions of interest using a bioinformatic program. Numbers indicate the position of the sequences in relation to the ATG initiation codon. Grey parts under the curve represent the CpG content. (B) Representative COBRA using *Bst*UI with percentage classification of DNA methylation pattern of melanoma cell lines are shown.

Wulfänger *et al.* Suppl. 3

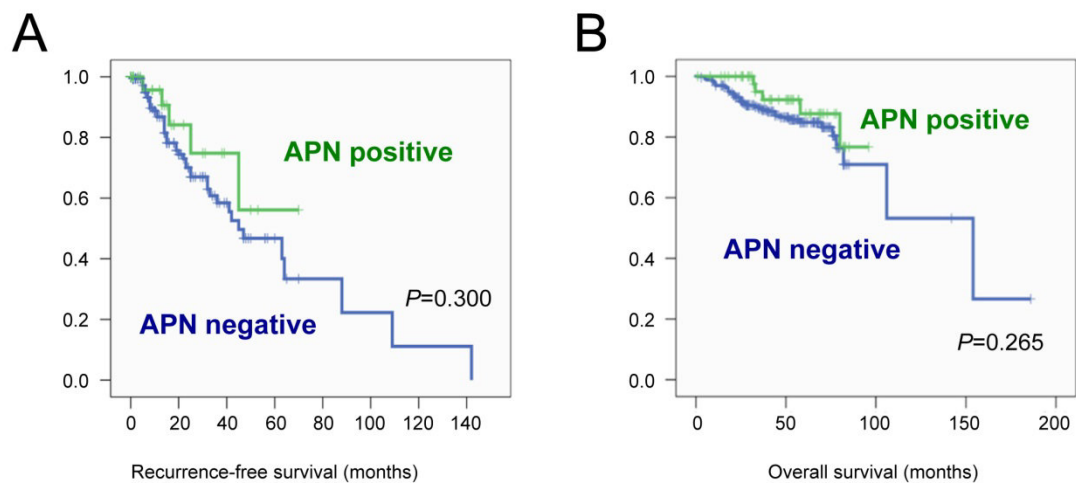
Suppl. Fig. 3 :Dose- and time-dependence of APN mRNA induction after DAC treatment. APN-negative melanoma cell line WM-1862 (-●-) as well as APN⁺ GR-M (-▲-) were treated either (A) with different concentration of DAC each day for a period of four days or (B) with 5 μ M DAC for different time points indicated. Results are expressed as x-fold mRNA induction in relation to medium control of three independent experiments.

Wulfänger *et al.* Suppl. 4



Suppl. Fig. 4: Differential cytokine expression in melanoma cells.

Cytokine expression of APN-negative melanoma cell lines (white bars) as well as APN⁺ (black bars) was quantified using quantitative RT-PCR. Results of three independent experiments are presented as fold mRNA expression in relation to melanocytes set to 1.

Wulfänger *et al.* Suppl. 5

Suppl. Fig. 5: APN and patients' survival.

Kaplan-Meier curves regarding recurrence-free (A) and overall survival (B) of melanoma patients with or without APN expression are displayed.

4.3 **Manuskript 3: Aminopeptidase N (APN)/ CD13-dependent CXCR4 downregulation is associated with diminished cell migration, proliferation and invasion.**

Molecular Membrane Biology, January 2008; 25(1): 72–82

informa
healthcare

Aminopeptidase N (APN)/CD13-dependent CXCR4 downregulation is associated with diminished cell migration, proliferation and invasion

JENS WULFAENGER, SUSANNA NIEDLING, DAGMAR RIEMANN, & BARBARA SELIGER

Institute of Medical Immunology, Martin-Luther-University, Halle-Wittenberg, Germany

(Received 20 November 2006; and in revised form 25 June 2007)

Abstract

Aminopeptidase N (APN/CD13) is a 150 kDa membrane-bound ubiquitously expressed protease with a broad functional repertoire. It hydrolyzes small peptide mediators, modulates cell motility and adhesion to extracellular matrix and also acts as a viral receptor. In order to dissect the function of enzymatically active and inactive APN/CD13, substitutions of different enzymatic active amino acid residues were generated by site-directed mutagenesis and stably transfected into human embryonic kidney cells. All APN variants analyzed exhibited a complete loss of enzymatic activity, whereas wild type APN transfectants exerted a strong aminopeptidase-specific activity. Furthermore, wild type APN expression was associated with a significant decrease in proliferation, migration and also reduced anchorage-independent growth when compared to enzymatically inactive APN variants and controls. This appeared to be due to a downregulated mRNA and protein expression of the chemokine receptor CXCR4 and an inhibition of the stromal cell-derived factor (SDF)-1 α /CXCL12-mediated migration. Thus, high APN enzyme activity may antagonize the cellular properties regulated by the CXCR4/SDF-1 α system in embryonic kidney cells.

Keywords: *Aminopeptidase, APN/CD13, enzyme activity, chemokine receptor, CXCR4, cell motility*

Abbreviations: Ala-pNA, alanine-p-nitroanilide; APN, aminopeptidase N; DPIV, dipeptidyl peptidase IV; ECL, enhanced chemiluminescence; EGFP, enhanced green fluorescence protein; FACS, fluorescence activated cell sorter; FBS, fetal bovine serum; G-CSF, granulocyte colony stimulating factor; HRP, horseradish peroxidase; JAK/STAT3, Janus kinase/signal transducer and activator of transcription 3; MAPK, mitogen-activated protein kinases; HPRT1, hypoxanthine guanine phosphoribosyl transferase 1; mAb, monoclonal antibody; MFI, mean specific fluorescence intensity; PAGE, polyacrylamide gel electrophoresis; PBS, phosphate-buffered saline; RT-PCR, reverse transcriptase-polymerase chain reaction; PE, phycoerythrin; SDF-1, stromal cell-derived factor-1; SDS, sodium dodecyl sulfate; wt, wild type.

Introduction

Aminopeptidase N (APN)/CD13 is a Zn²⁺-dependent ectopeptidase of the superfamily of gluzincins with a molecular weight of approximately 150 kDa (Hooper 1994). The enzyme hydrolyzes oligopeptides and cleaves preferentially neutral amino acids from the N-terminus of various substrates (Turner 1998). APN is expressed on the surface of a broad variety of cell types including fibroblasts, endothelial cells, committed haematopoietic progenitors, osteoclasts, synaptic membranes of the central nervous system, epithelial cells of the placenta,

intestine and kidney as well as on tumors of distinct origin (Look et al. 1989).

Regarding its structure, APN belongs to the type II membrane proteins with a single-spanning helical transmembrane domain and a short cytoplasmic tail. It is a highly glycosylated protein with ten potential glycosylation sites in the large extracellular domain which contains the catalytic active site with the conserved pentapeptide consensus sequence HELAH representing a zinc binding motif (Vallee & Auld 1990). The lack of a 39 amino acid segment including the HELAH motif leads to an intracellular retardation and a complete loss of enzymatic activity

Correspondence: Barbara Seliger, Institute of Medical Immunology, Martin-Luther-University, 06097 Halle, Germany. Tel: +49 345 557 4054. Fax: +49 345 557 4055. E-mail: Barbara.Seliger@medizin.uni-halle.de

ISSN 0968-7688 print/ISSN 1464-5203 online © 2008 Informa UK Ltd
DOI: 10.1080/09687680701551855

(Ashmun et al. 1992). Substitution of the Glu³⁵⁰ residue of the additional consensus sequence GAMEN demonstrated the crucial role of this amino acid for the exopeptidase function of pig APN (Luciani et al. 1998). The involvement of this glutamate in the catalytic process of aminopeptidase A has also been described (Vazeux et al. 1996).

APN plays diverse tissue-specific roles and modulates immune responses and inflammation (Riemann et al. 1999). The enzyme is involved in cell cycle control, cell differentiation, cell motility, degradation of the extracellular matrix, cellular attachment and in the function of immune cells, e.g., by trimming peptides protruding out of the binding groove of MHC class II molecules (Larsen et al. 1996). In pathophysiological processes, APN serves as a receptor for various viruses, such as the cytomegalovirus (Soderberg et al. 1993) and different coronaviruses (Delmas et al. 1992, Yeager et al. 1992). Furthermore, its expression has been associated to tumor angiogenesis and the metastatic potential of tumors (Bauvois 2004, Bhagwat et al. 2001, Fujii et al. 1995).

The biological activity of APN is not only achieved by the cleavage of peptides, such as neuropeptides, vasoactive peptides, chemokines and growth factor molecules, but also by participation in signal transduction processes (Riemann et al. 2002). The involvement of membrane peptidases in multimeric protein complexes and their presence in membrane microdomains like rafts and caveolae is a prerequisite for their signaling capacity. Since there exists limited and controversial information on APN function related to its enzymatic activity, the expression pattern, enzyme activity and the biological function of wild type APN (wt-APN) was compared to that of defined APN mutants with different substitutions in the enzymatic active site. Due to the different migration capacity of the APN mutants, the involvement of chemokine receptors and their ligands was also determined.

Materials and methods

Plasmid construction

The full-length cDNA of the human wild type APN (wt-APN) was isolated from total cellular RNA of U937 cells using the APN-specific primers 5'-ATATTTGAGCTCATGGCCAAGGGCTTCTATATTTCCAAGTC-3' (forward) and 5'-ATATTTGTCGACATTTTGCTGTTTTCTGTGAACCACTGGA-3' (reverse). The cDNA was cloned into the *Sac* I and *Sal* I restriction sites of the mammalian expression vector pEGFP-N1 (Clontech Laboratories Inc., Mountain View, CA, USA), which

Modulation of CXCR4 expression by APN activity 73

results in a C-terminal tagging of APN with the enhanced green fluorescent protein (EGFP). APN mutants with modification of the enzymatic active site such as E354G, E354I, E354Q, H387/391C, H387/391I, E388G and E410G, respectively, were generated with the PCR-based Quik Change XL Site-directed Mutagenesis Kit (Stratagene, La Jolla, CA, USA) according to the instruction manual. The primers used for cloning and their experimental conditions are listed in the supplementary Table I (online version only). In addition, a schematic illustration of the positions of the amino acid substitutions is shown in the supplementary Figure 1 (online version only). The integrity of the vector was confirmed by DNA sequencing.

Cell culture, transfection and selection of clones

The human embryonic kidney cell line HEK293 (Deutsche Sammlung fuer Mikroorganismen und Zellkulturen (DSMZ) ACC 305, Braunschweig, Germany) was maintained in RPMI1640 medium supplemented with 10% fetal bovine serum (FBS), 2 mM L-glutamine, 10 mM HEPES and antibiotics. The different APN plasmids and pEGFP-N1 serving as mock control were stably transfected into HEK293 cells using Lipofectamine 2000 (Invitrogen, Carlsbad, CA, USA) according to the manufacturer's instructions. APN-expressing cells were selected in RPMI1640 medium supplemented with 500 µg/ml G-418 (Invitrogen) 48 h post transfection for a period of 2 weeks. Individual single cell clones have been isolated by cell sorting (FACS Vantage, BD Biosciences, San Jose, CA, USA) after staining for APN expression.

Determination of APN enzymatic activity

For protein extracts cell pellets were resuspended in ice-cold 50 mM Tris/HCl (pH 7.4) containing 0.5% Triton X-100. After 1 h incubation on ice cells were disrupted using ultrasonication and debris was removed by a centrifugation step (10,000 g, 4°C). Protein concentrations were determined using the bicinchoninic acid (BCA) method with bovine serum albumine (BSA) as a standard (Smith et al. 1985). Total cellular APN activity was determined using 8 µg of isolated total protein extracts, whereas surface APN activity was measured employing 5×10^4 cells. The APN substrate alanine-p-nitroanilide (Ala-pNA; Sigma, St. Louis, MO, USA) was added at various concentrations ranging from 40 µM to 4 mM. The incubation was carried out at 37°C for 15 min in PBS. Ala-pNA cleavage was analyzed by the determination of the hydrolysis of Ala-pNA reflecting the p-nitroaniline concentration in the supernatant at an

74 *J. Wulfaenger et al.*

OD of 405 nm using the ELISA reader MRX II (Dynex Technologies GmbH, Berlin, Germany) (Firla et al. 2002). Cell-free and enzyme-free supernatants served as controls. The specificity of the Ala-pNA cleavage was monitored by preincubation of cells with 10 μM of the inhibitor actinonin (Sigma, St. Louis, MO, USA) for 30 min at 37°C before adding the substrate (Tieku & Hooper 1992). All tests were run in duplicates and independently repeated three times. Enzyme rates were used for the determination of the maximal turnover rate by direct fitting to the Michaelis-Menten equation. Statistical analyses were performed using the Sigma-Plot software. Enzyme activities were expressed as $\mu\text{mol} \times \text{min}^{-1} \times 10^{-6}$ cells or $\mu\text{mol} \times \text{min}^{-1} \times \text{mg}^{-1}$.

RNA isolation and real time quantitative RT-PCR

Total cellular RNA was isolated using the RNeasy Mini Kit (Qiagen, Hilden, Germany) according to the manufacturer's protocol. After DNase I (Invitrogen) treatment, 0.5 μg total RNA was transcribed into cDNA using the RevertAid H Minus First Strand cDNA Synthesis kit (MBI Fermentas, Hanover, MD, USA) and oligo(dT)₁₈ primer at a final volume of 20 μl .

Quantification of gene expression was performed by real time quantitative RT-PCR on the Rotor-Gene 2000 system (Corbett Research, Sydney, Australia) employing the QuantiTect SYBR Green PCR kit (Qiagen) and specific primers listed in the supplementary Table II (online version only). Real time quantitative RT-PCR amplifications were performed in a final volume of 20 μl at 95°C for 15 min followed by 40 cycles with denaturation at 95°C for 30 s, annealing at 58°C for 30 s and elongation at 72°C for 30 s. PCR products were finally subjected to a melting curve analysis. The mRNA levels were quantified with the Rotor-Gene analysis software in comparative quantitation mode and normalized to hypoxanthine guanine phosphoribosyl transferase 1 (HPRT1) expression levels. All real time quantitative RT-PCRs were done at least three times using RNA from independent experiments.

Western blot analysis

1×10^6 cells were lysed in RIPA buffer containing protease and phosphatase inhibitor cocktails (Sigma, St. Louis, MO, USA). 25 μg protein cell extract were separated on 8% SDS-polyacrylamide gels and transferred to nitrocellulose membrane (Schleicher & Schuell Bioscience GmbH, Dassel, Germany) using a semi-dry Fastblot™ apparatus (Biometra, Goettingen, Germany). After blocking with 5% dry

milk powder in TBS-T buffer for 1 h, the nitrocellulose membrane was incubated with the primary antibodies anti-CD13 monoclonal antibody (mAb) (clone BF-10), anti-GFP mAb (clone B-2), both purchased from Santa Cruz Biotechnology (Santa Cruz, CA, USA) or the anti-actin-specific mAb (clone 9A1; Abcam Inc., Cambridge, MA, USA), respectively, at 4°C overnight. After three washing steps with TBS-T buffer, blots were incubated with the appropriate horseradish peroxidase (HRP)-conjugated secondary antibodies (DAKO, Hamburg, Germany) at room temperature for 2 h. The membranes were developed employing the enhanced chemiluminescence (ECL)-based system (GE Healthcare Bio-Sciences Corp., Piscataway, NJ, USA).

Flow cytometry

For flow cytometric analysis, 5×10^5 cells were stained either with specific phycoerythrin (PE)-coupled mAb, listed in the supplementary Table II (online version only), or with the appropriated isotype controls at room temperature in the dark for 20 min. For CCR10 immunostaining, cells were first incubated with unlabeled primary antibody or isotype control at 4°C for 30 min followed by an incubation with PE-coupled goat F(ab')₂ anti-rabbit IgG at 4°C for additional 30 min. After fixation with 2% paraformaldehyde/phosphate-buffered saline (PBS) for 10 min, PE-fluorescence intensity was determined with the FACS Calibur flow cytometer and CellQuest software (BD Biosciences, Heidelberg, Germany). The results are expressed both as the percentage of expression and as mean specific fluorescence intensity (MFI) of FL2 of three independent experiments.

Cell growth assay

Cell proliferation was determined using the XTT-based colorimetric assay (Cell Proliferation Kit II (XTT), Roche Applied Science, Mannheim, Germany). Briefly, 7.5×10^3 cells/well were seeded into 96-well micro plates. Cell growth was monitored for the indicated time points by incubation with XTT labeling mixture for 4 h and spectrophotometrically assayed at a wavelength of 492 nm vs. 630 nm. The results of the XTT assay are presented as absorbance at 492 nm. All experiments were performed in triplicates with three independent assays.

Soft agar growth

Anchorage-independent growth was determined by the ability of the transfected cells to form colonies in soft agar as previously described (Courtenay 1976).

Briefly, 2×10^4 cells/60 mm petri-dish were seeded into 0.3% agar on top of a 0.5% agar base layer, both containing 20% FBS-supplemented RPMI1640. The cultures were maintained in humidity at 37°C with an atmosphere of 5% CO₂ for 18 days. The soft agar colonies were visualized by staining each petri-dish with 500 µl iodo-nitrotetrazoliumchloride (5 mg/ml, Sigma, St. Louis, MO, USA) overnight at 37°C and microscopically quantified.

Migration assay

Migration assays were performed in transwell diffusion chambers (Corning Costar, Corning, NY, USA) with a pore size of 8 µm diameter as recently described (Kehlen et al. 2004). 600 µl RPMI1640 medium containing 10% FBS, 2 mM L-glutamine, 10 mM HEPES and antibiotics as well as Collagen type I (8 µg/ml medium, BD Biosciences, Heidelberg, Germany) were added to the bottom of the 24-well plate. 5×10^4 cells were inserted into the top chamber. To analyze CXCR4-specific migration, different concentration of recombinant SDF-1 α (PeproTech, Rocky Hill, NJ, USA) and of CXCR4-specific inhibitor AMD3100 (Sigma) were added to the system. After 22 h at 37°C, all cells remaining in the transwell chamber were removed by scratching with cotton swabs. The number of migrated cells was determined with the CellTiter-Glo Luminescent Cell Viability Assay (Promega, Madison, WI, USA) according to the manufacturer's protocol. Luminescence was measured with a Lumat LB 9507 luminometer (Berthold Technologies, Bad Wildbad, Germany). Assays were run in duplicate in at least three independent experiments and results are expressed as percentage of migrated cells compared to the total cell number.

Results

Generation of APN variants with lack of enzymatic activity

Various APN variants with distinct substitutions in the catalytic domain of the enzyme differentially affecting the catalytic substrate cleavage were generated by site-directed mutagenesis: (i) the glutamate residue at the amino acid position 354 in APN known to interact with the free N-terminus of substrates or inhibitors and to stabilize the transition state was mutated to neutral glycine, hydrophobic isoleucine or uncharged, polar glutamine, (ii) the histidines at positions 387 and 391 in the HELAH motif of APN as well as the glutamate at the amino acid position 410 coordinately binding the zinc ion were substituted either by the hydrophobic isoleucine, by cysteine (aa 387/391) or by glycine (aa 410)

Modulation of CXCR4 expression by APN activity 75

and (iii) the cleavage-associated glutamate E388 was altered to glycine.

Three independent clones of transfectants and parental HEK293 cells were analyzed for APN expression by real time quantitative RT-PCR, Western blot and/or flow cytometry. As representatively shown for APN-E388G, the APN variants exhibited high APN mRNA and protein levels, which were comparable to that of wt-APN clones (Figure 1 A, B). With the exception of the variant APN-H387/

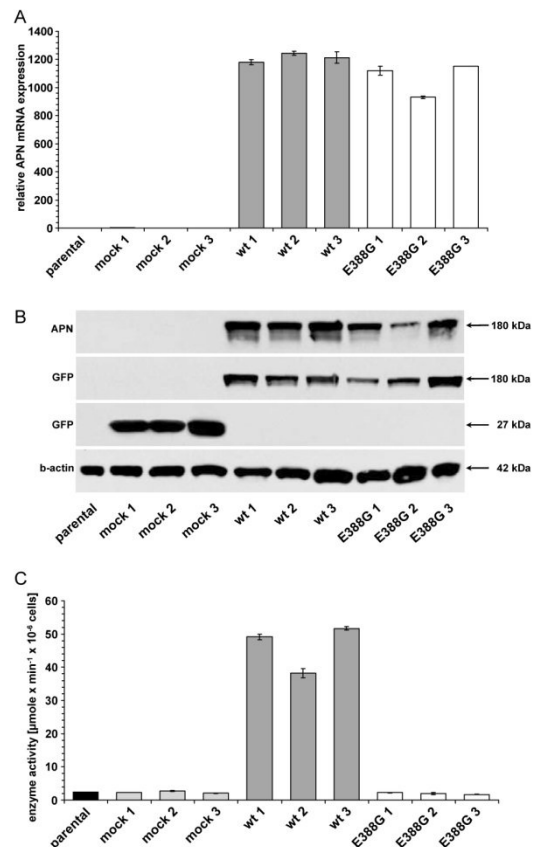


Figure 1. APN expression patterns of representative wt and mutant APN transfectants and respective controls. (A) Determination of the APN mRNA expression. mRNA of cell clones was quantified by real time quantitative RT-PCR (each in triplicate experiments) as described in Materials and methods. The results are expressed as relative APN mRNA expression. HEK293 parental cells are set to 1. (B) APN protein expression in APN transfectants. Equal amounts of proteins were resolved by SDS-PAGE and analyzed by Western blot using APN- and GFP-specific antibodies. Staining of the Western blot with an anti- β -actin mAb served as loading control. (C) Cell surface enzyme activity of APN transfectants. The enzyme activity of HEK293 cells expressing different APN forms was determined by Ala-pNA cleavage as described in Materials and methods. Results are expressed as $\mu\text{mole} \times \text{min}^{-1} \times 10^{-6}$ cells.

76 J. Wulfaenger et al.

Table I. APN cell surface expression and the enzymatic activity of parental HEK293 cells and transfectants as well as cell extracts.

Clone	Flow cytometry	Enzymatic activity	
	MFI ^a	$\mu\text{mole} \times \text{min}^{-1} \times 10^{-6} \text{ cells}^{\text{b}}$	$\mu\text{mole} \times \text{min}^{-1} \times \text{mg}^{-1} \text{ c}$
parental	6 ± 0.4	2.4 ± 0.1	2.7 ± 0.5
mock	n. d.	2.4 ± 0.3	2.2 ± 0.4
WT	5052 ± 334.2	46.4 ± 5.8	105.6 ± 9.1
E354G	3801 ± 571.3	2.9 ± 0.4	2.4 ± 0.5
E354I	3538 ± 881.5	2.7 ± 0.1	2.2 ± 0.3
E354Q	4965 ± 723.7	2.3 ± 0.4	2.8 ± 0.6
H387/391C	3557 ± 183.0	2.7 ± 0.4	2.2 ± 0.4
H387/391I	9 ± 0.3	2.7 ± 0.4	2.3 ± 0.2
E388G	5057 ± 771.3	2.1 ± 0.1	2.0 ± 0.1
E410G	4572 ± 775.3	2.2 ± 0.1	2.2 ± 0.3

^aFlow cytometric analysis was performed as described in Materials and methods using PE-coupled anti-CD13 mAb. The results are expressed as average FL2 mean specific fluorescence intensity (MFI) of three independent clones in three experiments. ^bThe enzymatic activity was determined according to Materials and methods. The results are expressed as $\mu\text{mole} \times \text{min}^{-1} \times 10^{-6} \times \text{cells}$ or as $\mu\text{mole} \times \text{min}^{-1} \times \text{mg}^{-1}$ of extracted proteins. n. d., not determined due to the strong green fluorescence, which interferes with the PE channel.

391I, a CD13 cell surface expression was found in all APN variants as determined by staining with a PE-labeled anti-CD13-specific mAb (Table I). The mock transfectants expressed high levels of intracellular GFP, which interfered with the PE-fluorescence channel. Glycosidase digestion experiments and immunoelectrophoretic blot analysis under reducing conditions demonstrated that most APN variants were present as a 180 kDa polypeptide with a complex glycosylation pattern similar to that of wt-APN. Only the variant APN-H387/391I exhibited a mannose-rich glycosylated protein with a molecular weight of 150 kDa as a result of intracellular retardation in the endoplasmic reticulum (data not shown).

The enzymatic activities of the APN variant expressing HEK293 cells and their respective controls as well as the corresponding cell extracts were analyzed employing different concentrations of Ala-pNA as substrate. Wt-APN exhibited high levels of substrate cleavage of living cells as well as in total cell extracts with a clonal variation between 97–114 $\mu\text{mole} \times \text{min}^{-1} \times 10^{-6} \text{ cells}$ and 40–55 $\mu\text{mole} \times \text{min}^{-1} \times \text{mg}^{-1}$, respectively, whereas all APN variants exerted an approximately 20-fold and 50-fold reduced APN-specific activity with a residual cleavage of the Ala-pNA substrate comparable to that of the parental HEK293 cells and mock controls (Table I; Figure 1C and supplementary Figure I – online version only). The preincubation of cells with the aminopeptidase-specific inhibitor actinonin resulted in a complete inhibition of Ala-pNA cleavage demonstrating the specificity of this assay (data not shown). Since with the exception of APN-H387/391I all other enzymatically inactive APN variants were expressed on the cell surface, APN surface expression is independent of APN enzyme activity.

Functional role of APN enzyme activity

It has been demonstrated that APN overexpression is associated with cell growth and migration capabilities (Kehlen et al. 2003, van Hensbergen et al. 2004). In order to determine whether enzyme activity is involved in these physiological processes, three individual clones of wt-APN, APN-E388G, vector control as well as parental HEK293 cells were selected for further characterization. Overexpression of wt-APN, but not of APN-E388G caused a significant downregulation of the proliferation rate when compared to controls as determined by XTT assay (Figure 2A). This reduced cell growth was accompanied by a diminished migration capacity of wt-APN that was approximately 40% of the migration rate of APN-E388G transfectants (Figure 2B). In addition, the anchorage-independent growth of wt-APN was significantly inhibited when compared to parental HEK293 cells, mock controls and APN-E388G transfectants with a 90% downregulation in the number of soft agar colonies (Figure 2C).

Association of chemokine receptor expression with APN expression

Since chemokine receptor expression is involved in migratory and metastatic processes, it was determined whether there exists a link between APN and chemokine receptor expression. First, the mRNA expression pattern of ten different chemokine receptors was analyzed in wt-APN and APN-E388G transfectants as well as mock controls and parental HEK293 cells using real time quantitative RT-PCR (Table II).

As shown in Figure 3A, the mRNA expression of the chemokine receptors analyzed was extremely heterogeneous in HEK293 cells ranging from a total

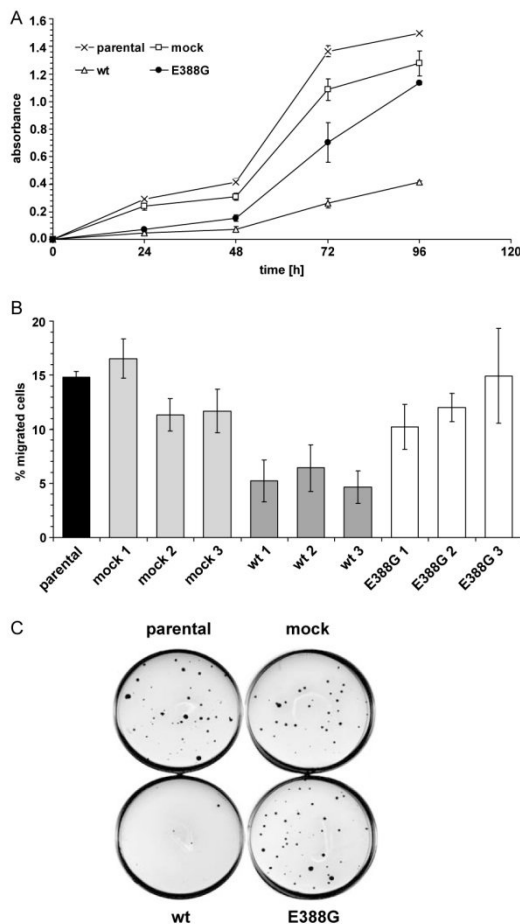


Figure 2. Cell growth and migration are dependent on APN enzyme activity. (A) Cell proliferation of APN transfectants. Proliferation was measured using a XTT-based colorimetric assay (absorbance at 492 nm vs. 630 nm in time-dependence). One out of four representative experiments is shown. (B) Decreased migration properties of wt-APN transfected cells. Cell migration of APN transfectants and respective controls was assessed in transwell diffusion chambers. After 22 h of chemotaxis to collagen type I, total migrated cells were quantified by a luciferase-based system. Values are given as percentage of migrated cells compared to the number of cells employed. Data are pooled from three independent experiments. (C) Soft agar colony formation. Anchorage-independent growth of APN transfectants was determined in soft agar. Double layer agar cultures in 60-mm petri-dishes were established as described in Materials and methods. 2×10^4 cells were cultured in humidity at 37°C for 18 days. After staining of viable cells with iodo-nitrotriazoliumchloride overnight, colonies were microscopically counted. A representative staining pattern of APN transfectants is shown.

lack of CXCR3, CCR2 and CCR5, to low expression levels of CXCR1, 2, 6 and 7 as well as CCR7 and 10 and high expression levels of CXCR4. A distinct chemokine receptor expression was also

Modulation of CXCR4 expression by APN activity 77

detected in wt-APN and the APN variant APN-E388G. CXCR1 and CCR10 were upregulated on the cell surface of wt-APN transfectants, but not on APN-E388G cells. In contrast, wt-APN transfectants exhibited a strong downregulation of the CXCR4 mRNA and cell surface expression, whereas APN-E388G transfectants expressed CXCR4 mRNA levels comparable to that of parental HEK293 cells (Figure 3B, C). It is noteworthy that CXCR2, 6, 7 and CCR7 were not differentially expressed in both transfectants. These data suggest an association between APN enzyme activity and CXCR4 expression. The wt-APN-mediated CXCR4 downregulation was independent of the CXCR4 ligand, the stromal cell-derived factor (SDF)-1 α /CXCL12 since neither mRNA nor protein expression was detected by RT-PCR and a SDF-1 α -specific ELISA, respectively (data not shown).

In order to determine whether CXCR4 is responsible for the altered properties, the migration rates of HEK293 parental cells in the presence of different concentrations of recombinant SDF-1 α were investigated. A dose-dependent correlation between SDF-1 α and migration was observed reaching a maximum with 50 nM SDF-1 α (Figure 4A). The SDF-1 α -induced migration was selectively blocked by the CXCR4-specific inhibitor AMD3100 in a dose-dependent manner (Figure 4B). APN-E388G transfectants as well as mock control cells exhibited similar migration properties as HEK293 cells with a two-fold increase in the presence of 30 nM SDF-1 α and an inhibition of migration by treatment with 25 μ M AMD3100. In contrast, no effect of SDF-1 α on the migration rates of wt-APN transfectants could be demonstrated (Figure 4C).

Discussion

So far, many studies implemented to define APN functions used either microbial aminopeptidase-specific inhibitors, such as bestatin, probestin and actinonin, or the enzyme activity-inhibiting mAb clone WM15 (Marotti et al. 2000, Gabrilovac et al. 2004, Bauvois & Dauzonne 2006). However, these experimental approaches did not lead to a proper dissection between signals obtained by APN inhibition and signals obtained after ligation of the APN molecule independent of the enzyme activity. For example, incubation with the mAb WM15 provokes a calcium increase, phosphorylation of the mitogen-activated protein kinases (MAPK) Erk, JNK and p38 as well as an upregulation of IL-8 mRNA in monocytic cells (Santos et al. 2000), whereas the inhibitor bestatin accesses into the cell via a H⁺-coupled energy-dependent dipeptide transporter

78 J. Wulfaenger et al.

Table II. Relative mRNA and cell surface expression of different chemokine receptors in HEK293 cells and transfectants

Chemokine receptor	mRNA ^a				protein ^b					
	parental	mock	WT	E388G	parental		WT		E388G	
	%	%	%	%	%	MFI	%	MFI	%	MFI
CXCR1	100±0.8	112±3.9	133±3.7	103±3.0	12±2.0	6±1.3	23±2.86	13±0.9	11±2.1	6±0.8
CXCR2	100±0.8	97±7.4	95±1.6	98±7.5	18±5.8	17±2.8	20±1.3	16±0.6	17±3.3	16±2.7
CXCR4	100±1.6	99±5.2	54±1.1	121±1.8	42±5.4	32±4.8	23±3.2	16±0.6	42±5.3	31±4.5
CXCR6	100±3.1	92±22.5	105±19.7	114±9.3			not determined			
CXCR7	100±11.3	72±4.4	87±14.4	89±7.4			not determined			
CCR7	100±2.0	105±9.8	95±3.5	119±8.2	18±4.0	8±0.9	18±3.6	9±0.9	18±2.1	9±1.0
CCR10	100±0.0	97±5.4	102±5.8	120±1.0	9±0.8	2±0.7	22±4.1	6±0.6	9±1.2	3±0.5

^amRNA expression levels were determined by real time quantitative RT-PCR as described in Materials and methods. The chemokine receptor expression of parental HEK293 cells was set to 100%. ^bProtein expression was determined by flow cytometry using the respective PE-coupled anti-chemokine receptor-specific antibodies and data are given as average percentage (%) as well as mean specific fluorescence intensity (MFI) of FL2 of three independent experiments.

(Lee 2000), which affects the protein kinase C pathway (Kumano & Sugawara 1992) and the pp60/c-Src tyrosine kinase activity (Murata et al. 1994). Based on this knowledge, the development of an inhibitor- and antibody-free system is required to characterize the involvement of APN enzyme activity in cellular functions. Therefore, various APN variants with different substitutions in the enzyme active site were generated and stably transfected in HEK293 cells. All single or double substitutions caused a complete loss of APN-specific activity, whereas the wt-APN exhibited high catalytic activity both in protein extracts as well as on the cell surface of intact cells. These data are in accordance with studies of structurally related proteins demonstrating that single amino acid substitutions both in the GAMEN motif and in the zinc-binding motif of human insulin-regulated aminopeptidase resulted in decreased or abolished enzyme activity (Laustsen et al. 2001). Mutations in the histidines in the HELLGH motif of the rat dipeptidyl peptidase III are associated with an abnormal structure and subsequently loss of enzymatic activity (Fukasawa et al. 1999). With the exception of H387/391I all APN variants were expressed on the cell surface and showed the same immunoelectrophoretic behavior as wt-APN. Substitutions of both histidine residues to isoleucine at amino acid position 387 and 391 might disrupt zinc binding causing a destabilization of the APN structure, its intracellular retardation and consequently loss of cell surface expression. In contrast, substitutions of these histidines to cysteines might mimic zinc binding thereby leading to cell surface expression of APN. Thus, each amino acid in the enzymatic active site of APN is essential for the catalytic process and their disruption/substitution always leads to a complete loss of APN-specific

activity. However, despite the lack of enzyme activity, all variants expressed APN-specific mRNA and protein levels comparable to that of wt-APN.

Overexpression of catalytically active APN in HEK293 cells caused a decreased cell proliferation, migration and soft agar colony formation, whereas cells transfected with the APN variant E388G lacking enzyme activity exhibited growth properties similar to untransfected HEK293 cells. These data indicate the importance of APN enzyme activity, rather than signal transduction via ligation of the membrane enzyme for growth properties. One might speculate that APN either cleaves and inactivates a yet unknown proliferation-promoting substrate, or activates by cleavage an inhibiting mediator. Morphological changes such as epithelial-mesenchymal transition or differences in adhesive features could not be detected in our transfection model (data not shown).

The role of APN expression in tumors is controversially discussed. Diminished or lack of APN expression was described in renal cell cancer (Gohring et al. 1998), acute myeloid leukaemia (Dybkaer et al. 2001) as well as in prostate carcinoma (Bogenrieder et al. 1997) which might be accompanied by an improved anchorage-independent growth or migratory potential. In accordance with our results transfection of an APN-negative ovarian cancer cell line with an APN-expression vector resulted in reduced invasion of cells into matrigel, although the *in vitro* growth of these cells was not affected (van Hensbergen et al. 2004). In contrast, a positive correlation of APN with tumor progression was demonstrated in pancreatic (Ikeda et al. 2003) and hepatocellular carcinoma (Rocken et al. 2004). Blocking of APN activity by inhibitors or down-regulation by small interfering RNA caused a

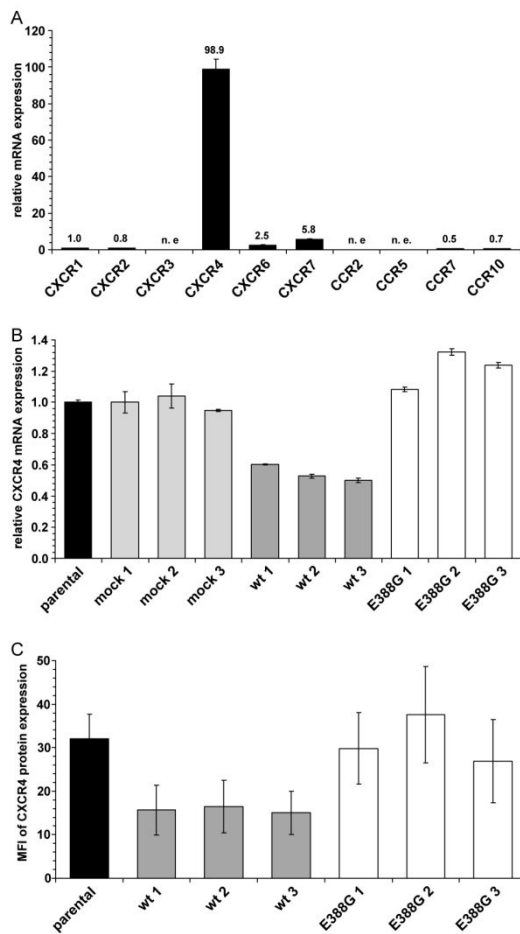


Figure 3. The major expressed chemokine receptor CXCR4 is downregulated in wt-APN transfectants on mRNA and protein levels. (A) mRNA expression levels of different chemokine receptors in HEK293 cells using real time quantitative RT-PCR analysis. Values are given as X-fold mRNA expression with CXCR1 expression set to 1. (B) mRNA from parental HEK293 cells as well as transfectants was subjected to real time quantitative RT-PCR analysis using CXCR4-specific primers. Gene expression levels were normalized to HPRT1 expression and then displayed as X-fold mRNA expression with HEK293 parental cells set to 1. (C) CXCR4 cell surface expression of controls and APN transfectants. Cells were detached and directly stained with PE-coupled anti-CXCR4-specific mAb. After fixation with paraformaldehyde PE-fluorescence intensity of cells was determined by flow cytometry. Values are expressed as mean specific fluorescence intensity (MFI) of FL2. Results are shown as average of three independent experiments.

decreased cell growth or metastatic behavior of cell lines of different origin (Kehlen et al. 2003, Kido et al. 2003, Bauvois & Dauzonne 2006). Contradictory results were obtained for the influence of APN expression in gastric carcinoma: A decreased

Modulation of CXCR4 expression by APN activity 79

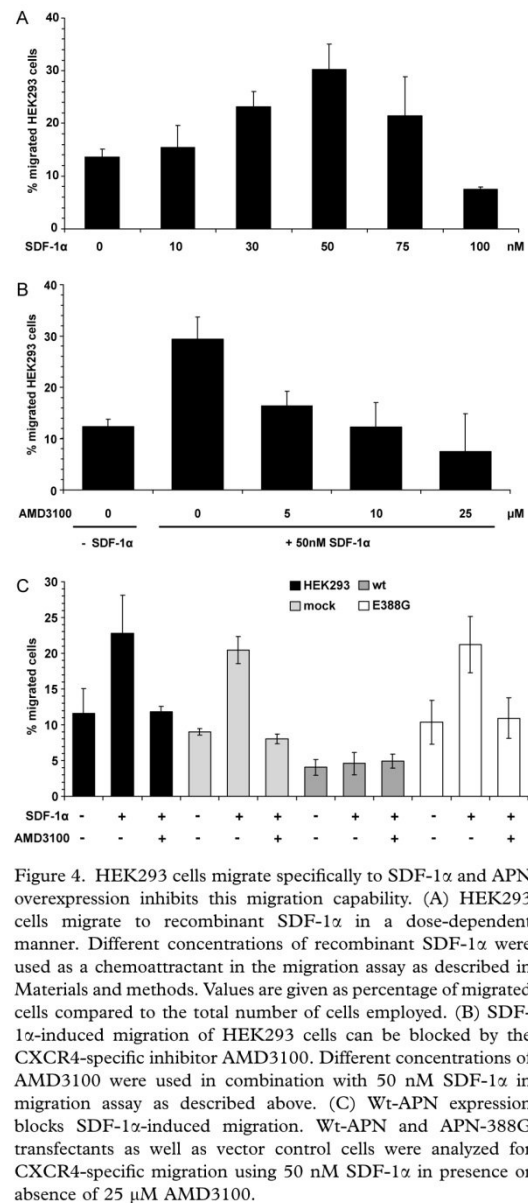


Figure 4. HEK293 cells migrate specifically to SDF-1α and APN overexpression inhibits this migration capability. (A) HEK293 cells migrate to recombinant SDF-1α in a dose-dependent manner. Different concentrations of recombinant SDF-1α were used as a chemoattractant in the migration assay as described in Materials and methods. Values are given as percentage of migrated cells compared to the total number of cells employed. (B) SDF-1α-induced migration of HEK293 cells can be blocked by the CXCR4-specific inhibitor AMD3100. Different concentrations of AMD3100 were used in combination with 50 nM SDF-1α in migration assay as described above. (C) Wt-APN expression blocks SDF-1α-induced migration. Wt-APN and APN-388G transfectants as well as vector control cells were analyzed for CXCR4-specific migration using 50 nM SDF-1α in presence or absence of 25 μM AMD3100.

APN expression associated with a poor prognosis as well as higher metastatic rate in lymph nodes was described by Kawamura and co-authors (Kawamura et al. 2007), whereas an upregulation of APN expression and a correlation of APN with lymph node metastasis were found by others (Carl-McGrath et al. 2004).

In order to dissect the molecular mechanisms leading to the altered growth properties, the chemokine receptor status was analyzed in the different

80 *J. Wulfaenger et al.*

APN transfectants and controls. HEK293 cells and the APN-E388G variant, but not wt-APN highly expressed the chemokine receptor CXCR4 and exhibited an increased SDF1 α -mediated migration. In contrast, the APN enzyme activity-mediated downregulation of CXCR4 expression completely disrupted the transwell migration to recombinant SDF-1 α /CXCL12. These data suggest not only a link between CXCR4 and APN activity, but also the importance of CXCR4 downregulation for the diminished cell proliferation, migration rate as well as the reduced soft agar colony formation. This is in line with a report by Diodovich et al. (2005) in which a reduced cell proliferation and clonogenic capability was accompanied by a downregulation of CXCR4 expression in cord blood cells after acrylonitrile exposure. Since chemokine receptors communicate with each other, thereby cross-regulating their function, an indirect regulation of CXCR4 by other chemokines or cytokines inactivated by APN cannot be excluded. APN has been shown to be able to proteolytically process the chemokine CXCL11 which leads to an impaired CXCR3 and CXCR7 binding and signaling and consistently to a reduced cell migration of lymphocytes and endothelial cells (Proost et al. 2007). However, since SDF-1 α has a proline at the penultimate position of the N-terminus, APN should not be able to cleave this chemokine. Bradykinin and substance P possess the Lys-Pro aminoterminus and are natural inhibitors for APN (Xu et al. 1995). In a cleavage assay of SDF-1 α and APN-wt transfectants followed by mass spectrometry we could not detect a processing of recombinant SDF-1 α , therefore the degradation of SDF-1 α by APN can be excluded (data not shown).

Dipeptidyl peptidase IV (DPIV)/CD26, another member of membrane-bound peptidases known to inactivate SDF-1 α (Shioda et al. 1998), is not expressed on the cell surface of transfected HEK293 cells (data not shown). Therefore, one can exclude a cooperation between APN and DPIV in the cleavage of chemokines. However, it is noteworthy that (i) other proteases in HEK293 cells such as matrix metalloproteinase-9 (MMP-9) or cathepsin G might be involved in the processing of SDF-1 α and affect the diminished migration of wt-APN transfectants and that (ii) ligands of neuropeptide receptors as APN substrates might cross-regulate chemokine receptors (Zhang et al. 2003) resulting in a functionally significant cross-talk between neurohormonal and cytokine signaling.

The molecular mechanisms of the biological functions controlled by CXCR4 are complex. Interaction of SDF-1 α /CXCL12 with its G-protein-coupled receptor CXCR4 activates several cellular

pathways important for the regulation of adhesion, locomotion or chemotaxis (Kucia et al. 2004). The most important pathways include the mitogen-activated protein kinase MAPK, the PI-3 kinase/Akt pathway, release of calcium ions, activation of focal adhesion proteins (e.g., p130Cas, paxillin and focal adhesion kinase) as well as signaling via the Janus kinase/signal transducer and activator of transcription 3 (JAK/STAT3) (Kucia et al. 2004). Our preliminary results demonstrate that binding of SDF-1 α ligand to CXCR4 leads to time-dependent phosphorylation of the MAPK Erk as well as of Akt in all transfectants investigated suggesting that these pathways are not involved in the different migration properties of the wt-APN transfectants in comparison to APN-E388G and control cells (data not shown). Our future investigations have to implement calcium and JAK/STAT3 signaling pathways. Since enzymatically active APN has been associated with membrane protein organization in a recent paper on bradykinin-induced migration of endothelial cells (Petrovic et al. 2007), we will further study on APN location in rafts/caveolae of transfected HEK293 cells.

In conclusion, to the best of our knowledge this is the first report dissecting the independence of APN expression and enzyme activity. Enzymatic active APN significantly affects cell properties, such as cell proliferation, migration and invasion. This is accompanied by diminished CXCR4 expression and a disruption of SDF-1 α -induced migration. However, additional investigations are required to identify APN substrates and to define the molecular mechanism responsible for these effects.

Acknowledgements

This work was supported by the DFG, Bonn, Germany (grant RI 799/2-2) and by the ROUX program of the Martin-Luther-University Halle-Wittenberg, Germany (grant FKZ 4/07). We would like to thank C. Recktenwald for mass spectrometric analysis of cleavage products and C. Stoerr for excellent secretarial help.

References

- Ashmun RA, Shapiro LH, Look AT. 1992. Deletion of the zinc-binding motif of CD13/aminopeptidase N molecules results in loss of epitopes that mediate binding of inhibitory antibodies. *Blood* 79:3344-3349.
- Bauvois B. 2004. Transmembrane proteases in cell growth and invasion: new contributors to angiogenesis? *Oncogene* 23:317-329.
- Bauvois B, Dauzonne D. 2006. Aminopeptidase-N/CD13 (EC 3.4.11.2) inhibitors: chemistry, biological evaluations, and therapeutic prospects. *Med Res Rev* 26:88-130.

- Bhagwat SV, Lahdenranta J, Giordano R, Arap W, Pasqualini R, Shapiro LH. 2001. CD13/APN is activated by angiogenic signals and is essential for capillary tube formation. *Blood* 97:652–659.
- Bogenrieder T, Finstad CL, Freeman RH, Papandreou CN, Scher HI, Albino AP, Reuter VE, Nanus DM. 1997. Expression and localization of aminopeptidase A, aminopeptidase N, and dipeptidyl peptidase IV in benign and malignant human prostate tissue. *Prostate* 33:225–232.
- Carl-McGrath S, Lendeckel U, Ebert M, Wolter AB, Roessner A, Rocken C. 2004. The ectopeptidases CD10, CD13, CD26, and CD143 are upregulated in gastric cancer. *Int J Oncol* 25:1223–1232.
- Courtenay VD. 1976. A soft agar colony assay for Lewis lung tumour and B16 melanoma taken directly from the mouse. *Br J Cancer* 34:39–45.
- Delmas B, Gelfi J, L'Haridon R, Vogel LK, Sjöström H, Noren O, Laude H. 1992. Aminopeptidase N is a major receptor for the entero-pathogenic coronavirus TGEV. *Nature* 357:417–420.
- Diodovich C, Malerba I, Ferrario D, Bowe G, Bianchi MG, Acquati F, Taramelli R, Parent-Massin D, Gribaldo L. 2005. Gene and protein expressions in human cord blood cells after exposure to acrylonitrile. *J Biochem Mol Toxicol* 19:204–212.
- Dybkaer K, Olesen G, Pedersen FS, Kristensen JS. 2001. Stromal-mediated down-regulation of CD13 in bone marrow cells originating from acute myeloid leukemia patients. *Eur J Haematol* 66:168–177.
- Firla B, Arndt M, Frank K, Thiel U, Ansgore S, Tager M, Lendeckel U. 2002. Extracellular cysteines define ectopeptidase (APN, CD13) expression and function. *Free Radic Biol Med* 32:584–595.
- Fujii H, Nakajima M, Saiki I, Yoneda J, Azuma I, Tsuruo T. 1995. Human melanoma invasion and metastasis enhancement by high expression of aminopeptidase N/CD13. *Clin Exp Metastasis* 13:337–344.
- Fukasawa K, Fukasawa KM, Iwamoto H, Hirose J, Harada M. 1999. The HELLLGH motif of rat liver dipeptidyl peptidase III is involved in zinc coordination and the catalytic activity of the enzyme. *Biochemistry* 38:8299–8303.
- Gabrilovac J, Cupic B, Breljak D, Zekusic M, Boranic M. 2004. Expression of CD13/aminopeptidase N and CD10/neutral endopeptidase on cultured human keratinocytes. *Immunol Lett* 91:39–47.
- Gohring B, Holzhausen HJ, Meye A, Heynemann H, Rebmann U, Langner J, Riemann D. 1998. Endopeptidase 24.11/CD10 is down-regulated in renal cell cancer. *Int J Mol Med* 2:409–414.
- Hooper NM. 1994. Families of zinc metalloproteases. *FEBS Lett* 354:1–6.
- Ikeda N, Nakajima Y, Tokuhara T, Hattori N, Sho M, Kanehiro H, Miyake M. 2003. Clinical significance of aminopeptidase N/CD13 expression in human pancreatic carcinoma. *Clin Cancer Res* 9:1503–1508.
- Kawamura J, Shimada Y, Kitaichi H, Komoto I, Hashimoto Y, Kaganoi J, Miyake M, Yamasaki S, Kondo K, Imamura M. 2007. Clinicopathological significance of aminopeptidase N/CD13 expression in human gastric carcinoma. *Hepato-gastroenterology* 54:36–40.
- Kehlen A, Englert N, Seifert A, Klönisch T, Dralle H, Langner J, Hoang-Vu C. 2004. Expression, regulation and function of autotaxin in thyroid carcinomas. *Int J Cancer* 109:833–838.
- Kehlen A, Lendeckel U, Dralle H, Langner J, Hoang-Vu C. 2003. Biological significance of aminopeptidase N/CD13 in thyroid carcinomas. *Cancer Res* 63:8500–8506.
- Kido A, Krueger S, Haecckel C, Roessner A. 2003. Inhibitory effect of antisense aminopeptidase N (APN/CD13) cDNA transfection on the invasive potential of osteosarcoma cells. *Clin Exp Metastasis* 20:585–592.
- Kucia M, Jankowski K, Reza R, Wysoczynski M, Bandura L, Allendorf DJ, Zhang J, Ratajczak J, Ratajczak MZ. 2004. CXCR4-SDF-1 signalling, locomotion, chemotaxis and adhesion. *J Mol Histol* 35:233–245.
- Kumano N, Sugawara S. 1992. Ubenimex (Bestatin), an aminopeptidase inhibitor, modulates protein kinase C in K562 cells. *J Biol Regul Homeost Agents* 6:116–120.
- Larsen SL, Pedersen LO, Buus S, Stryhn A. 1996. T cell responses affected by aminopeptidase N (CD13)-mediated trimming of major histocompatibility complex class II-bound peptides. *J Exp Med* 184:183–189.
- Laustsen PG, Vang S, Kristensen T. 2001. Mutational analysis of the active site of human insulin-regulated aminopeptidase. *Eur J Biochem* 268:98–104.
- Lee VH. 2000. Membrane transporters. *Eur J Pharm Sci* 11 Suppl 2:S41–50.
- Look AT, Ashmun RA, Shapiro LH, Peiper SC. 1989. Human myeloid plasma membrane glycoprotein CD13 (gp150) is identical to aminopeptidase N. *J Clin Invest* 83:1299–1307.
- Luciani N, Marie-Claire C, Ruffet E, Beaumont A, Roques BP, Fournie-Zaluski MC. 1998. Characterization of Glu350 as a critical residue involved in the N-terminal amine binding site of aminopeptidase N (EC 3.4.11.2): insights into its mechanism of action. *Biochemistry* 37:686–692.
- Marotti T, Balog T, Munic V, Sobocanec S, Abramic M. 2000. The link between met-enkephalin-induced down-regulation of APN activity and the release of superoxide anion. *Neuropeptides* 34:121–128.
- Murata M, Kubota Y, Tanaka T, Iida-Tanaka K, Takahara J, Irino S. 1994. Effect of ubenimex on the proliferation and differentiation of U937 human histiocytic lymphoma cells. *Leukemia* 8:2188–2193.
- Petrovic N, Schacke W, Gahagan JR, O'Connor C A, Winnicka B, Conway RE, Mina-Osorio P, Shapiro LH. 2007. CD13/APN regulates endothelial invasion and filopodia formation. *Blood* 110:142–150.
- Proost P, Mortier A, Loos T, Vandercappellen J, Gouwy M, Ronse I, Schutyser E, Put W, Parmentier M, Struyf S, Van Damme J. 2007. Proteolytic processing of CXCL11 by CD13/aminopeptidase N impairs CXCR3 and CXCR7 binding and signalling and reduces lymphocyte and endothelial cell migration. *Blood* 110:37–44.
- Riemann D, Blosz T, Wulfaenger J, Navarrete Santos A. 2002. Signal transduction via membrane peptidases. In: Langner J, Ansgore S, editors. *Ectopeptidases*. New York: Academic/Plenum Publishers. p. 141–170.
- Riemann D, Kehlen A, Langner J. 1999. CD13—not just a marker in leukemia typing. *Immunol Today* 20:83–88.
- Rocken C, Carl-McGrath S, Grantzdorffer I, Mantke R, Roessner A, Lendeckel U. 2004. Ectopeptidases are differentially expressed in hepatocellular carcinomas. *Int J Oncol* 24:487–495.
- Santos AN, Langner J, Herrmann M, Riemann D. 2000. Aminopeptidase N/CD13 is directly linked to signal transduction pathways in monocytes. *Cell Immunol* 201:22–32.
- Shioda T, Kato H, Ohnishi Y, Tashiro K, Ikegawa M, Nakayama EE, Hu H, Kato A, Sakai Y, Liu H, Honjo T, Nomoto A, Iwamoto A, Morimoto C, Nagai Y. 1998. Anti-HIV-1 and chemotactic activities of human stromal cell-derived factor 1alpha (SDF-1alpha) and SDF-1beta are abolished by CD26/dipeptidyl peptidase IV-mediated cleavage. *Proc Natl Acad Sci USA* 95:6331–6336.
- Smith PK, Krohn RI, Hermanson GT, Mallia AK, Gartner FH, Provenzano MD, Fujimoto EK, Goeke NM, Olson BJ, Klenk DC. 1985. Measurement of protein using bicinchoninic acid. *Anal Biochem* 150:76–85.

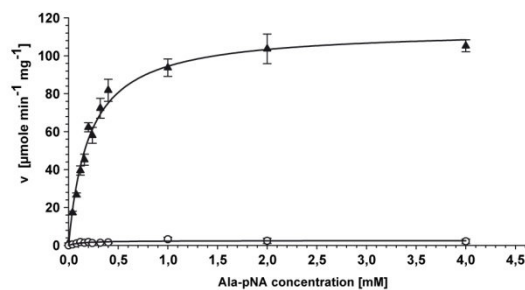
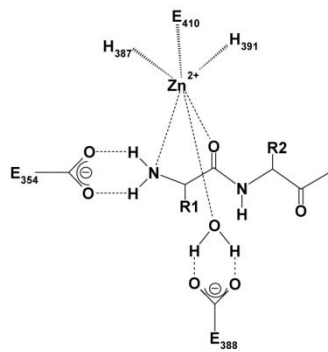
82 *J. Wulfaenger et al.*

- Soderberg C, Giugni TD, Zaia JA, Larsson S, Wahlberg JM, Moller E. 1993. CD13 (human aminopeptidase N) mediates human cytomegalovirus infection. *J Virol* 67:6576–6585.
- Tieku S, Hooper NM. 1992. Inhibition of aminopeptidases N, A and W. A re-evaluation of the actions of bestatin and inhibitors of angiotensin converting enzyme. *Biochem Pharmacol* 44:1725–1730.
- Turner AJ. 1998. Membrane alanyl aminopeptidase. In: Barrett AJ, Rawlings ND, Woessner JF, editors. *Handbook of proteolytic enzymes*. London: Academic Press. p. 996–1000.
- Vallee BL, Auld DS. 1990. Zinc coordination, function, and structure of zinc enzymes and other proteins. *Biochemistry* 29:5647–5659.
- van Hensbergen Y, Broxterman HJ, Rana S, van Diest PJ, Duyndam MC, Hoekman K, Pinedo HM, Boven E. 2004. Reduced growth, increased vascular area, and reduced response to cisplatin in CD13-overexpressing human ovarian cancer xenografts. *Clin Cancer Res* 10:1180–1191.
- Vazeux G, Wang J, Corvol P, Llorens-Cortes C. 1996. Identification of glutamate residues essential for catalytic activity and zinc coordination in aminopeptidase A. *J Biol Chem* 271:9069–9074.
- Xu Y, Wellner D, Scheinberg DA. 1995. Substance P and bradykinin are natural inhibitors of CD13/aminopeptidase N. *Biochem Biophys Res Commun* 208:664–674.
- Yeager CL, Ashmun RA, Williams RK, Cardellicchio CB, Shapiro LH, Look AT, Holmes KV. 1992. Human aminopeptidase N is a receptor for human coronavirus 229E. *Nature* 357:420–422.
- Zhang N, Hodge D, Rogers TJ, Oppenheim JJ. 2003. Ca²⁺-independent protein kinase Cs mediate heterologous desensitization of leukocyte chemokine receptors by opioid receptors. *J Biol Chem* 278:12729–12736.

This paper was first published online on iFirst on 5 October 2007.

Supplementary Table I. Primer sequences used for real time quantitative RT-PCR and antibodies for flow cytometry.

APN form	Primers	
	Sense	Antisense
E354G	GCCATGGGCAACTGGGG	CCCCAGTTGCCCATGGC
E354I	GCCGGCGCCATGATCAACTGGGGACT GGTGACCTAC	GTAGGTACCAGTCCCCAGTT GATCATGGCGCCGGC
E354Q	GCCATGCAGAACTGGGGA	TCCCCAGTTCTGCATGGC
H387/391C	GGTCACTGTGATTGCTTGCGAGCTGGCCTG CCAGTGGTTCGGG	CCCGAACCCTGGCAGGCCAGCTCGCAAGC AATCACAGTGACC
H387/391I	GGTGGTCACTGTGATTGCTATCGAGCTGG CCATCCAGTGGTTCGGG	CCCGAACCCTGGATGGCCAGCTCGATAGCAA TCACAGTGACCACC
E388G	GCTCATGGCCTGGCCAC	GTGGGCCAGGCCATGAGC
E410G	TGTGGCTGAACGGCGGCTTCGCCTCCTAC GTGGAGT	ACTCCACGTAGGAGGCGAAGCCGCCGTTTCAG CCACA



Supplementary Figure 1. All amino acid substitutions in the enzymatic active site of APN cause a complete loss of APN-specific activity. (A) Schematic illustration of the initial step of peptide cleavage by APN. Histidines H387 and H391 as well as glutamate E410 complex the zinc ion. E354 is involved in the polarization of the amino terminus of peptides, whereas E388 polarizes a water molecule, which attacks the carboxyl group of peptide bond. (B) Kinetic plot of cell extracts of APN-WT and APN-E388G expressing transfectants using Ala-pNA as substrate. Replicate determination for APN-WT (\blacktriangle) and E388G (\circ) using different substrate concentration and enzyme activities are directly fitted to Michaelis-Menten curves. The curve of the APN-E388G transfectants is characteristic for the other variants exhibiting loss of enzymatic activity.

Supplementary Table II. Primer sequences used for real time quantitative RT-PCR and antibodies for flow cytometry.

Gene	RefGene	Primers		Antibody	
		Sense	Antisense	Clone	company
APN	NM_0011150	GACGAAGAGAACTGGAGGAAGA	CTTCAATCAGGAAGAGGGTGTT	Leu-M7	BD Pharmingen (San Jose, CA)
CXCR1	NM_000634	CTCCGTCCTGATGTCTACCTG	CAGGATGCCACTGTAGAAGTTG	427,05	R&D Systems (Minneapolis, MN)
CXCR2	NM_001557	CATGGAGAGTGACAGCTTTGAA	CAGGGCATAGATAATGACCACA	6C6	BD Pharmingen (San Jose, CA)
CXCR4	NM_003467	CCTTATCCTGCCTGGTATTGTC	CGATGCTGATCCCAATGTAGTA	12G5	BD Pharmingen (San Jose, CA)
CCR2	NM_000648	ACTCTTGGGATGACTCACTGCT	CATTCTTTCCTGGTCTCACTCC	48607	R&D Systems (Minneapolis, MN)
CCR5	NM_000579	GCTTGTCATGGTCATCTGCTAC	AAGGTGTTTCAGGAGAAGGACAA	2D7/ CCR5	BD Pharmingen (San Jose, CA)
CCR7	NM_001838	CACTTTGTTTCGAGTCTTTGTGC	CCAGGTTGAGCAGGTAGGTATC	150503	R&D Systems (Minneapolis, MN)
CCR10	NM_016602	CTCAATCCCGTTCTCTACGC	GTTGTCCCAGGAGAGACTGTG	AP2012a	Abgent (San Diego, CA)
HPRT1	NM_000194	GCTGGATTACATCAAAGCACTG	CTGACCAAGGAAAGCAAAGTCT		

4.4 Manuskript 4: Functional co-localization of monocytic aminopeptidase N/ CD13 with the Fc gamma receptors CD32 and CD64.



ELSEVIER

Available online at www.sciencedirect.com

SCIENCE @ DIRECT®

Biochemical and Biophysical Research Communications 331 (2005) 1408–1412

BBRC

www.elsevier.com/locate/ybbrc

Functional co-localization of monocytic aminopeptidase N/CD13 with the Fc γ receptors CD32 and CD64

Dagmar Riemann^{a,*}, Anatolij Tcherkes^a, Gert H. Hansen^b, Jens Wulfaenger^a,
Tanja Blosz^a, E. Michael Danielsen^b

^a Institute of Medical Immunology, Martin Luther University Halle/Wittenberg, Magdeburger Straße 2, D-06097 Halle, Germany

^b Department of Medical Biochemistry, Panum Institute, University Copenhagen, Denmark

Received 12 April 2005

Available online 22 April 2005

Abstract

Information about the function of aminopeptidase N/CD13 on monocytes is limited. In order to gain more insight into its interaction with other proteins, we have identified molecules that co-localize with the membrane ectoenzyme at the cell surface of monocytes. Using laser scanning and electron microscopy as well as fluorescence resonance energy transfer (FRET) measured by flow cytometry we show that monocytic CD13 co-localized with the Fc γ receptor II/CD32 after Fc receptor ligation by a CD32-specific antibody. FRET was also observed between CD13 and the Fc γ receptor I/CD64, but not with the myeloid marker CD33 representing a member of the sialoadhesin family. Our results imply a novel functional role of CD13 and Fc γ receptors as members of a multimeric receptor complex. Further studies have to be done to elucidate common signaling pathways of these molecules.

© 2005 Elsevier Inc. All rights reserved.

Keywords: Monocytes; Aminopeptidase; Fc receptor; CD13; CD32; CD64; FRET; Electron microscopy

Aminopeptidase N (APN)/CD13 (EC 3.4.11.2) belongs to a group of transmembrane ectoenzymes which are all ubiquitously expressed in cells of different origin and exhibit a broad functional repertoire. These membrane peptidases hydrolyze small peptide mediators, function as receptors, and participate in cell motility and in the control of growth and differentiation of various cellular systems [1]. Recent observations point to a direct involvement of membrane peptidases as part of multimeric protein complexes in signal transduction processes [2].

Human CD13 exists as a heavily glycosylated non-disulfide-linked homodimer with an apparent subunit molecular weight of 140–160 kDa, of which carbohydrate accounts for at least 20% of the mass. The coding

sequence predicts that CD13 is a type II-integral membrane protein of 967 amino acids with a short (8–10 amino acids) cytoplasmic domain and a 24-residue hydrophobic transmembrane region [3]. The large extracellular domain contains the catalytically active site with the pentapeptide signature sequence His-Glu-Leu-Ala-His revealing the metalloprotease nature. CD13 is significantly expressed on human monocytes and might play a role in the processing of biologically active peptides controlling local concentrations available for receptor binding. Despite the short cytoplasmic tail ligation or cross-linking of the monocytic peptidase by monoclonal antibodies (mAb) results in activation of mitogen-activated protein (MAP) kinases and an increase in IL-8 mRNA expression [4]. In order to understand the function of CD13 on monocytes molecules co-localized with the ectoenzyme have to be identified. In 1989, McIntyre et al. [5] proposed that signal transduction by CD13-specific mAb could be the result of the formation of

* Corresponding author. Fax: +49 345 5574055.

E-mail address: dagmar.riemann@medizin.uni-halle.de (D. Riemann).

complexes between APN and receptors for the Fc portion of antibodies. Therefore, it was investigated whether CD13 is co-localized with Fc γ receptors using laser scanning microscopy, electron microscopy, and the fluorescence resonance energy transfer (FRET) technique combined with flow cytometry.

Methods

Cells. The human monocytoid leukemia cell line THP-1 was obtained from the German Collection of Microorganisms and Cell Cultures (Braunschweig, Germany). These suspension cells were maintained in RPMI 1640 medium supplemented with 10% heat-inactivated fetal calf serum (FCS, Biochrom KG, Berlin, Germany), 2 mM L-glutamine, and antibiotics. A 30-min preincubation of cells (washed serum-free in PBS) with actinomycin (5×10^{-5} M final concentration, Sigma-Aldrich, München, Germany) at room temperature was carried out to inhibit APN enzyme activity. Heparinized venous blood was obtained from healthy volunteers (laboratory staff).

Immunofluorescence staining and confocal laser microscopy. Co-localization of membrane species at the few hundred nanometer scale was studied on a Zeiss META 510 confocal microscope (Jena, Germany). Cells were doubly labeled with antibodies specific for the distinct molecular species and carrying spectrally different fluorophores that can be excited and separately detected. Alexa Fluor 488 was excited at 488 nm; Cy3 at 543 nm. Fluorescence emission was detected through 505–550 band-pass and 560 LP filters. Confocal optical sections ($<0.6 \mu\text{m}$ thick, image stacks of 1024×1024 pixel) were taken with a 63 \times Plan Apochromat water immersion objective.

THP-1 cells were washed and pre-incubated with 100 $\mu\text{g}/\text{ml}$ human IgG as Fc receptor blocking reagent (Sigma-Aldrich) for 10 min on ice and incubated with saturating concentrations of a mouse anti-Fc γ RII antibody clone IV.3 (Stem Sep, StemCell Technologies, Vancouver, Canada), and a rabbit polyclonal anti-CD13 mAb (kindly provided by Irene Moerk, Panum Institute, Copenhagen) on ice for 30 min, followed by incubation with an Alexa 488-conjugated chicken anti-mouse IgG (Molecular Probes, Eugene, OR, USA) and a Cy3-labeled goat anti-rabbit secondary antibody (Coulter-Beckmann, Krefeld, Germany). Control cells were incubated with IgG1 isotype control (DAKO, Hamburg, Germany) and rabbit serum (Dianova GmbH, Hamburg, Germany), followed by the incubation with both secondary antibodies. Upon washing cells were fixed in 2% paraformaldehyde in PBS and mounted onto slides.

Electron microscopy. THP-1 cells were pre-incubated with human IgG for 10 min on ice. Upon washing with cold PBS (pH 7.2) cells were fixed in 4% paraformaldehyde in PBS for 2 h at 4 $^{\circ}\text{C}$, washed again, and then stored in PBS containing 1% paraformaldehyde. Pre-embedding and indirect immunogold double labeling of CD32 and CD13 were performed as previously described [6]. Briefly, cells were first incubated with a primary polyclonal goat antibody directed against CD32 (R&D Systems, Wiesbaden, Germany) and a secondary gold-labeled (7 nm gold particles) rabbit anti-goat antibody [7]. After fixation in 2% paraformaldehyde/0.1% glutaraldehyde in 0.1 M sodium phosphate buffer, pH 7.2 (PB) for 1 h at 4 $^{\circ}\text{C}$ to destroy the antigenicity in the antibody complex, the cells were incubated with a primary polyclonal rabbit anti-CD13 (1:50) and a secondary gold-labeled (13 nm gold particles) goat anti-rabbit antibody. For ultrastructural analysis, the cells were fixed in 2.5% glutaraldehyde in PB for 15 min, treated with 1% osmium tetroxide in PB for 1 h, dehydrated in acetone, and then embedded in Epon according to standard procedures. Ultrathin sections were cut on an LKB Ultratome III ultramicrotome, stained in 1% uranyl acetate in water and in lead citrate, and finally examined in a Zeiss EM 900 electron microscope equipped with a Mega View camera system.

Flow cytometry and fluorescence resonance energy transfer. The antibodies used for flow cytometry and FRET were the phycoerythrin (PE)-conjugated IgG1 isotype control, anti-CD13 clone Leu-M7, anti-CD32 clone FL18.26, and anti-CD33 clone P67.6 (all from BD Biosciences, Heidelberg, Germany), anti-CD64 clone 10.1 (DAKO, Hamburg, Germany), the biotinylated anti-CD13 clone Leu-M7 (customer service, BD Biosciences), and a biotinylated IgG1 isotype control (Serotec GmbH, Düsseldorf, Germany). Streptavidin (SA)-Cy5 (Dianova, Hamburg, Germany) was used as a fluorophore for biotinylated antibodies.

The expression of CD13, CD32, CD64, and CD33 was evaluated by FACS analysis on peripheral blood monocytes and THP-1 cells. Fifty microliters of EDTA blood sample was incubated with the PE-labeled antibody at room temperature for 15 min, treated with FACS lysing solution (BD Biosciences) for lysis of erythrocytes and fixation of leucocytes, and measured after two washing steps with PBS. THP-1 cells were incubated with the PE-labeled antibodies at room temperature for 15 min after pre-incubation with human IgG. After fixation of the cells with 1% paraformaldehyde, cells were washed with PBS.

Measurements were performed with a dual-laser FACSCalibur flow cytometer and CellQuest software (BD Biosciences, Heidelberg, Germany). At least 3000 cells were acquired in list mode, monocytes were identified on the basis of their forward scatter and side scatter patterns. All data were corrected for background by subtracting the binding of the isotype control antibody.

FRET efficiency is a very sensitive indicator of the molecular co-localization on a scale of 2–10 nm due to its inverse sixth-power dependence on the actual donor-acceptor distance [8]. FRET is a nonradiating energy that is tunneled from a donor fluorophore (PE) excited with the 488-nm argon laser line to an acceptor fluorophore (Cy5). The acceptor fluorophore Cy5 that we used was not directly excited at 488 nm. Efficient energy transfer results in an increased acceptor emission. For determination of FRET efficiency, changes in fluorescence intensities of donor plus acceptor labeled cells were related to emission signals from donor-only and acceptor-only labeled cells.

THP-1 cells or peripheral blood mononuclear cells were washed twice with PBS containing 0.5% BSA. Cells were preincubated with 100 $\mu\text{g}/\text{ml}$ human IgG (Sigma-Aldrich) at room temperature for 10 min for occupation of Fc receptors, and thereafter, incubated with saturating concentrations of the PE-conjugated and biotinylated CD13 mAb on ice for 30 min. Blood erythrocytes were lysed by a fixative-free lysing buffer containing ammonium chloride. After washing twice with PBS containing BSA and azide at 4 $^{\circ}\text{C}$, samples were divided into equal parts, with only one part of each sample incubated with a saturating amount of SA-Cy5 (0.6 $\mu\text{g}/\text{ml}$) for 15 min on ice. Both parts were washed as described above. Measurements at the FACSCalibur were performed without compensation.

The energy transfer parameter (ET_p) which is proportional to FRET efficiency (ET) was calculated according to Heine et al. [9], where A is the acceptor, D is the donor, FL2 is the mean fluorescence in channel 2 (488–530 nm) (donor, R-PE), FL3 is the mean fluorescence in channel 3 (488–585 nm), and FL4 is the mean fluorescence in channel 4 (633–670 nm, acceptor, Cy5) (each value was obtained after autofluorescence subtraction):

$$\text{ET}_p = [\text{FL3}(\text{D}, \text{A}) - \text{FL2}(\text{D}, \text{A})/a - \text{FL4}(\text{D}, \text{A})/b]/\text{FL3}(\text{D}, \text{A}),$$

where $a = \text{FL2}(\text{D})/\text{FL3}(\text{D})$ and $b = \text{FL4}(\text{A})/\text{FL3}(\text{A})$. An $\text{ET} = 5\text{--}8\%$ was defined as threshold level for significant transfer efficiency. This value is comparable to the ET of 5% given by Szöllösi et al. [10].

Results and discussion

In this paper, we provide evidence for a co-localization of CD13 with Fc γ receptors in monocytes. The receptors for the Fc portion of immunoglobulin (Ig) G

are important immune-response modulating molecules. Engagement of monocyte Fc γ receptors by IgG-opsonized particles or by IgG-containing immune complexes triggers different effector and inflammatory functions, such as phagocytosis, respiratory burst, as well as secretion of inflammatory cytokines thereby modulating inflammatory responses. Fc γ receptor I/CD64 is a high affinity receptor ($K_d = 10^{-8}$ M for monomeric IgG), whereas Fc γ receptor II/CD32 exhibits low affinity for monomeric IgG [11,12].

Using multicolor confocal laser scanning microscopy we demonstrated a large-scale (≈ 200 nm) co-localization of CD13 and CD32 in THP-1 cells (Fig. 1). A sub-

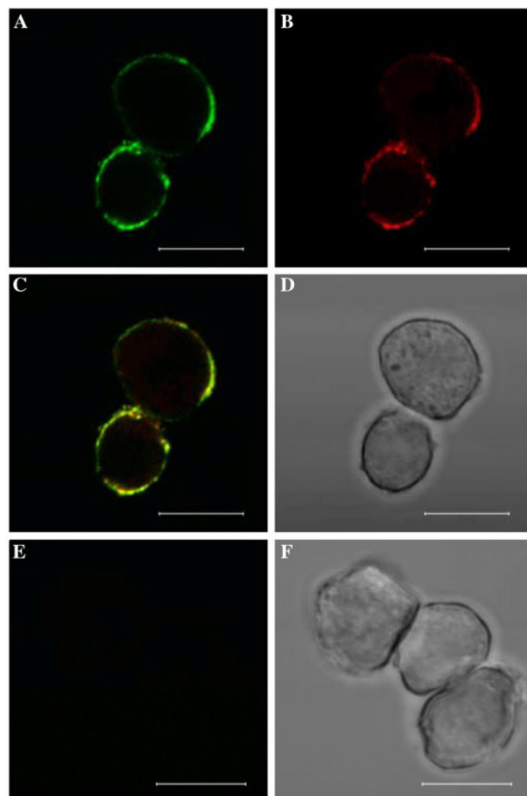


Fig. 1. Co-localization of CD32, and CD13 proteins on THP-1 cells, as detected by confocal laser scanning microscopy. Cells were indirectly stained with a CD32-specific mAb (Alexa 488, green; A) and a CD13-specific polyclonal antibody (Cy3, red; B). Membrane areas where two membrane molecules co-localize are indicated with mixed colors in the overlay image (C). Control staining with IgG1 isotype control and rabbit serum followed by both secondary antibodies is shown as overlay image (E), with identical magnification, illumination, and signal processing conditions as in (A–C). Frames in D and F were captured from transmitted light. The applied colors are pseudocolors. Scale bar, 10 μ m. (For interpretation of the references to color in this figure legend, the reader is referred to the web version of this paper.)

stantial overlap between membrane areas rich in CD13 molecules and CD32 was found, suggesting that these proteins were mostly confined to identical membrane domains on these cells. Though we performed all incubation steps on ice, we cannot exclude the fact that the observed co-localization is the result of antibody ligation of Fc γ receptors. Receptor clustering is thought to be the first step of a signaling pathway that targets the adjacent submembranous cytoskeleton. Kwiatkowska et al. showed that cross-linking of CD32 with specific mouse antibody, followed by anti-mouse IgG at 0 $^{\circ}$ C, led to clustering of the receptor on the surface of U937 monocytes; the formed receptor clusters (patches) were uniformly distributed over the cell surface. At this temperature, no internalization of cell surface receptor took place [13]. Another study showed that monomeric IgG, which is commonly used for blocking unspecific antibody binding, can induce the monocyte secretion of small amounts of the chemokine monocyte chemoattractant protein (MCP)-1, thus suggesting that the natural ligand of the high affinity receptor CD64 may elicit productive binding and initiate signal transduction [14].

Data of laser scanning microscopy were confirmed by us by electron microscopy. THP-1 cells were pre-incubated with human IgG and a CD32-specific antibody on ice before fixation, to make both methods comparable. Using immunogold labeling, both CD32 and CD13 were localized at the cell surface. The labeling of CD32 was detected both as single gold particles, but more frequently as large aggregates of gold particles indicating the clustering of CD32 in the plasma membrane (Fig. 2). An intense labeling of CD13 was found at the surface of THP-1 cells with a co-localization of CD32 and CD13 in the areas of the plasma membrane containing a high concentration of CD32 receptors.

FRET measurements were performed to investigate whether the microscopically observed clusters of CD13 and CD32 also display molecular proximity at the 2–10 nm scale, whereby energy transfer values are expressed as FRET efficiency. The use of flow cytometry allows FRET data to be gathered from a large number of individual cells. Fc γ receptor I/CD64 was additionally included in these experiments, since monocytes of peripheral blood as well as THP1 cells express both CD32 and CD64 molecules. Table 1 demonstrates a heterogeneous fluorescence intensity of both THP-1 cells and peripheral blood monocytes incubated with PE-conjugated antibodies against CD13, CD32, CD33, and CD64, respectively. In blood monocytes, but not in THP1 cells, CD32 expression often exceeded CD13 expression with the antibody clones used, whereas the intensity of CD64 expression was weaker compared to CD32 expression.

The results of flow cytometric FRET measurements are summarized in Table 2. To establish a positive

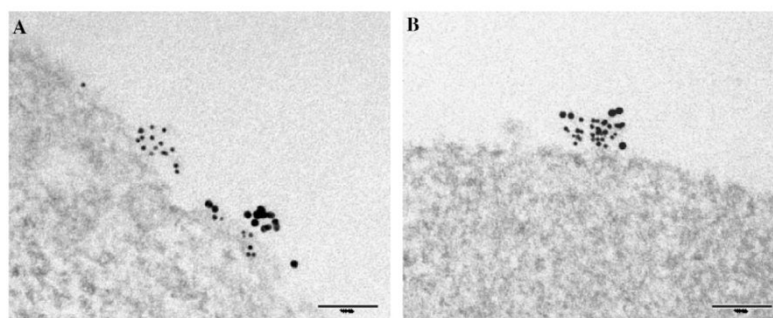


Fig. 2. Immunogold double labeling of CD32 (7 nm gold particles) and CD13 (13 nm gold particles). CD32 labeling was seen both as single particles (A) and in clusters (B). Clustered CD32 was often found to be co-clustered with CD13. Bars; 100 nm.

Table 1
Heterogeneous levels of CD13, CD32, CD33, and CD64 on monocytes and THP-1 cells

	Fluorescence intensity			
	CD13	CD32	CD64	CD33
THP-1	1005 ± 124	136 ± 10	36 ± 9	213 ± 35
Monocytes	765 ± 296	1031 ± 231	296 ± 238	703 ± 371

Flow cytometry was performed as described under Methods using anti-CD13, anti-CD32, anti-CD64, and anti-CD33 antibodies on peripheral blood monocytes and THP-1 cells. Data are given as mean values of fluorescence intensity of PE-conjugated antibodies with the mean ± SD of five independent experiments measured with the same instrument settings.

Table 2
FRET efficiencies between donor/acceptor pairs bound to CD13, CD32, CD64, and CD33 molecules

FRET pairs		FRET efficiencies (%)	
Donor	Acceptor	THP-1 cells	Monocytes
CD13	CD13	60.1 ± 5.7	51.6 ± 6.4
CD32	CD13	23.8 ± 5.6	10.3 ± 3.9
CD64	CD13	14.3 ± 4.3	12.8 ± 5.1
CD33	CD13	6.3 ± 0.6	4.3 ± 0.97

The mean energy transfer efficiencies for THP-1 cells and peripheral blood monocytes are expressed in terms of emission of Cy5 excited by 488 nm (ET_p, acceptor sensitized emission). Data are means ± SD of five independent experiments. An ET = 5–8% was defined as the threshold level for significant transfer efficiency.

control for our system, we measured FRET between CD13 homodimers. According to our FRET data CD13 molecules exhibited a high degree of homodimerization. CD13 forms homodimers intracellularly before Golgi-associated processing, suggesting that dimerization may be required for the export from the endoplasmic reticulum [15]. Our FRET experiments revealed that both CD32 and CD64 showed significant energy transfer with CD13. FRET efficiency values for CD32–CD13 were obviously lower in monocytes compared to THP1 cells, with a high interindividual range, although

CD32 expression of monocytes exceeded CD32 expression of THP1 cells. Similar FRET values were obtained for the pair CD64–CD13 in THP1 cells and monocytes. FRET between CD33, a member of the sialoadhesin family on monocytes, and CD13 served as negative control with no energy transfer detectable. FRET appeared to be independent of enzyme activity, since a 30-min preincubation of THP1 cells and monocytes with actinonin as inhibitor of APN enzyme activity did not affect FRET between both Fcγ receptors and CD13 (data not shown).

Our results imply a new functional role of CD13 and Fcγ receptors as members of a multimeric receptor complex. Several parallels can be found in the expression and function of CD13 and Fcγ receptors. For example, stimulation of monocytes with immune complexes induces a rapid expression of chemokines, such as MCP-1 and IL-8 [14]. Chemokines can be inactivated by membrane peptidases as suggested for MCP-1 as putative CD13 substrate [16]. Monocytic CD13 molecules [17] as well as ligated Fcγ receptors [13] are located in cholesterol-enriched membrane microdomains, also called lipid rafts or caveolae, which play a role in ligand-induced signaling. The ligand-binding subunit of Fcγ receptors has been proposed to be responsible for raft coalescence which is independent of Src family kinase activity [18]. Cross-linking of both CD32 [19] and CD13 [4] with antibodies can induce activation of the mitogen-activated protein (MAP) kinase cascade. Furthermore, results from the literature show that the human cytomegalovirus as CD13 ligand induces a rise in intracellular Ca²⁺ levels by binding to the molecule [20]. Enzyme activity of CD13 is involved in antigen processing by monocytes and dendritic cells [21,22], whereas peptidase activity seems not to be required for signal transduction via CD13, e.g., after cytomegalovirus binding [20].

In summary, our results suggest Fcγ receptors as colocalization partners of CD13 on monocytes. Several studies suggest that signaling induced by Fcγ receptors is susceptible of modulation by other membrane pro-

teins as signaling regulators [23]. In addition to functional implications, the different signal pathways engaged by CD13 and other receptors that are part of the Fc receptor complex have to be dissected in future work.

Acknowledgments

This work was supported by the Deutsche Forschungsgemeinschaft (DFG RI799/2-1, 2-2) and the Roux program of the Medical Faculty of the Martin Luther University Halle/Wittenberg (FKZ 07/06). We gratefully thank Bettina Hause for help with laser scanning microscopy, and Alexandra Pfeiffer (Institute for Clinical Chemistry and Laboratory Medicine, University of Regensburg, Germany) for help with flow cytometric FRET analysis. Sabrina Kießling, Anja Müller, and Christine Hamann are gratefully acknowledged for their excellent technical assistance.

References

- [1] D. Riemann, A. Kehlen, J. Langner, CD13—not just a marker in leukemia typing, *Immunol. Today* 20 (1999) 83–88.
- [2] D. Riemann, T. Blosz, J. Wulfänger, J. Langner, A. Navarrete Santos, Signal transduction via membrane peptidases, in: J. Langner, S. Ansorge (Eds.), *Ecto-peptidases*, Kluwer Academic/Plenum Publishers, New York, 2002, pp. 141–170.
- [3] J. Olsen, G.M. Cowell, E. Königshofer, E.M. Danielsen, J. Møller, L. Laustsen, O.C. Hansen, K.G. Welinder, J. Engberg, W. Hunziker, et al., Complete amino acid sequence of human intestinal aminopeptidase N as deduced from cloned cDNA, *FEBS Lett.* 238 (1988) 307–314.
- [4] A. Navarrete Santos, J. Langner, M. Herrmann, D. Riemann, Aminopeptidase N/CD13 is directly linked to signal transduction pathways in monocytes, *Cell. Immunol.* 201 (2000) 22–32.
- [5] E.A. MacIntyre, P.J. Roberts, M. Jones, C.E. Van der Schoot, E.J. Favalaro, N. Tidman, D.C. Linch, Activation of human monocytes occurs on cross-linking monocytic antigens to an Fc receptor, *J. Immunol.* 142 (1989) 2377–2383.
- [6] G.H. Hansen, L. Immerdal, E. Thorsen, L.L. Niels-Christiansen, B.T. Nystrom, E.J. Demant, E.M. Danielsen, Lipid rafts exist as stable cholesterol-independent microdomains in the brush border membrane of enterocytes, *J. Biol. Chem.* 276 (2001) 32338–32344.
- [7] G.H. Hansen, L.L. Wetterberg, H. Sjöström, O. Noren, Immunogold labelling is a quantitative method as demonstrated by studies on aminopeptidase N in microvillar membrane vesicles, *Histochem. J.* 24 (1992) 132–136.
- [8] L. Stryer, Fluorescence energy transfer as a spectroscopic ruler, *Annu. Rev. Biochem.* 47 (1978) 819–846.
- [9] H. Heine, E.T. Rietschel, A.J. Ulmer, The biology of endotoxin, *Mol. Biotechnol.* 19 (2001) 279–296.
- [10] J. Szöllösi, L. Tron, S. Damjanovich, S.H. Helliwell, D. Arndt-Jovin, T.M. Jovin, Fluorescence energy transfer measurements on cell surfaces: a critical comparison of steady-state fluorimetric and flow cytometric methods, *Cytometry* 5 (1984) 210–216.
- [11] J.F. Cohen-Solal, L. Cassard, W.H. Fridman, C. Sautes-Fridman, Fc gamma receptors, *Immunol. Lett.* 92 (2004) 199–205.
- [12] R. Clynes, J.S. Maizes, R. Guinamard, M. Ono, T. Takai, J.V. Ravetch, Modulation of immune complex-induced inflammation in vivo by the coordinate expression of activation and inhibitory Fc receptors, *J. Exp. Med.* 189 (1999) 179–185.
- [13] K. Kwiatkowska, A. Sobota, The clustered Fc gamma receptor II is recruited to Lyn-containing membrane domains and undergoes phosphorylation in a cholesterol-dependent manner, *Eur. J. Immunol.* 31 (2001) 989–998.
- [14] C.B. Marsh, M.D. Wewers, L.C. Tan, B.H. Rovin, Fc(gamma) receptor cross-linking induces peripheral blood mononuclear cell monocyte chemoattractant protein-1 expression: role of lymphocyte Fc(gamma)RIII, *J. Immunol.* 158 (1997) 1078–1084.
- [15] E.M. Danielsen, Perturbation of intestinal microvillar enzyme biosynthesis by amino acid analogs. Evidence that dimerization is required for the transport of aminopeptidase N out of the endoplasmic reticulum, *J. Biol. Chem.* 265 (1990) 14566–14571.
- [16] M. Weber, M. Ugucioni, M. Baggiolini, I. Clark-Lewis, C.A. Dahinden, Deletion of the NH₂-terminal residue converts monocyte chemoattractant protein 1 from an activator of basophil mediator release to an eosinophil chemoattractant, *J. Exp. Med.* 183 (1996) 681–685.
- [17] A. Navarrete Santos, J. Roentsch, E.M. Danielsen, J. Langner, D. Riemann, Aminopeptidase N/CD13 is associated with raft membrane microdomains in monocytes, *Biochem. Biophys. Res. Commun.* 269 (2000) 143–148.
- [18] H. Kono, T. Suzuki, K. Yamamoto, M. Okada, T. Yamamoto, Z. Honda, Spatial raft coalescence represents an initial step in Fc gamma R signaling, *J. Immunol.* 169 (2002) 193–203.
- [19] Z. Banki, L. Kacani, B. Mullauer, D. Wilflingseder, G. Obermoser, H. Niederegger, H. Schennach, G.M. Sprinzl, N. Sepp, A. Erdei, M.P. Dierich, H. Stoiber, Cross-linking of CD32 induces maturation of human monocyte-derived dendritic cells via NF-kappa B signaling pathway, *J. Immunol.* 170 (2003) 3963–3970.
- [20] S. Gredmark, W.B. Britt, X. Xie, L. Lindbom, C. Soderberg-Naucler, Human cytomegalovirus induces inhibition of macrophage differentiation by binding to human aminopeptidase N/CD13, *J. Immunol.* 173 (2004) 4897–4907.
- [21] S.L. Larsen, L.O. Pedersen, S. Buus, A. Stryhn, T cell responses affected by aminopeptidase N (CD13)-mediated trimming of major histocompatibility complex class II-bound peptides, *J. Exp. Med.* 184 (1996) 183–189.
- [22] X. Dong, B. An, L. Salvucci Kierstead, W.J. Storkus, A.A. Amoscatto, R.D. Salter, Modification of the amino terminus of a class II epitope confers resistance to degradation by CD13 on dendritic cells and enhances presentation to T cells, *J. Immunol.* 164 (2000) 129–135.
- [23] P. Mina-Osorio, E. Ortega, Signal regulators in FcR-mediated activation of leukocytes? *Trends Immunol.* 25 (2004) 529–535.

5 Diskussion

Der Schwerpunkt der Forschungen des Instituts für Medizinische Immunologie der Martin-Luther-Universität Halle-Wittenberg ist seit Jahren die Identifizierung und anschließende Charakterisierung potentieller Biomarker als neue Zielstrukturen für Therapieformen vor allem bei der Behandlung des Melanoms und des NZK. In der vorliegenden Arbeit wurden die molekularen und zellulären Funktionen von UCHL1 und APN näher charakterisiert und die klinische Relevanz derer Expression im malignen Melanom untersucht. In den nachfolgenden Abschnitten werden die jeweiligen publizierten Ergebnisse mit der aktuellen Literatur diskutiert.

5.1 UCHL1, ein interessanter Kandidat für die Generierung/ Etablierung neuer Therapieformen des malignen Melanoms

Aufgrund der differentiellen Genexpression und der vielfältigen molekularen bzw. zellulären Funktionen in tumorrelevanten Prozessen, wie Proliferation, Migration/ Invasion, Apoptose und Signaltransduktion, ist UCHL1 ein interessantes Kandidatenprotein für die Entwicklung einer neuen zielgerichteten Krebsbehandlung bzw. für eine T-Zell-basierende Immuntherapie [149]. Die vorliegende Arbeit unterstützt die Hypothese, die Hydrolase als mögliche Zielstruktur für den Einsatz bei Melanomerkkrankungen in Betracht zu ziehen, da

- (i) UCHL1 in frühen Stadien der Melanomprogression stark herunterreguliert ist,
- (ii) UCHL1-positive Melanomzellen schnellere Proliferationscharakteristika aufweisen,
- (iii) die Hydrolase wichtige zelluläre Signaltransduktionswege beeinflusst
- (iv) und dadurch auch das Resistenzverhalten gegenüber ROS moduliert.

UCHL1-Expression und –Regulation während der Melanomprogression

In der vorliegenden Arbeit konnte unter Verwendung von etablierten TMA erstmalig gezeigt werden, dass bereits in sehr frühen Stadien der melanozytären Transformation die UCHL1-Expression stark herunterreguliert ist. Melanozyten sind definitiv UCHL1-positiv. Sowohl vier unabhängig isolierte reine Melanozyten-Populationen in dieser Arbeit als auch drei unabhängige Studien bestätigten eine UCHL1-Positivität auf mRNA- und

Proteinebene [150-152]. Da in keinem der 50 immunhistochemisch untersuchten benignen Nävi entsprechendes Protein detektiert wurde, ist davon auszugehen, dass die Expression der Hydrolase bereits in diesen Vorstufen der malignen Transformation reprimiert wird. Dieses neue Ergebnis lässt eine stark tumorsupprimierende Rolle von UCHL1 postulieren.

In den insgesamt 331 Melanomläsionen wurde das UCHL1-Protein mit einer Häufigkeit von ca. 7,2 % nachgewiesen. Es bestand kein signifikanter Zusammenhang der UCHL1-Expression mit klinisch-pathologischen Parametern oder mit den histologischen Subtypen des Melanoms. Die Herunterregulation der Hydrolase ist durch die Ergebnisse einer früheren unabhängigen Studie bestätigt [152]. In dieser Untersuchung von Hoek *et al.* wurden insgesamt 553 Melanomproben mittels TMA und mittels polyklonaler UCHL1-Antikörper analysiert. Dabei wurde ein putativer, aber nicht-signifikanter Zusammenhang zwischen schlechterem Überleben der Patienten bei UCHL1-Verlust nachgewiesen. Bei Betrachtung von ausschließlich primären Melanomen war diese Korrelation signifikant. Am häufigsten war UCHL1 in den primären Tumoren mit einem Durchmesser von weniger als 2 mm exprimiert. Aufgrund der geringeren Frequenz in metastasierten Melanomen interpretierten die Autoren insgesamt einen Verlust der UCHL1-Expression in progressiveren Tumorstadien. Keine Korrelation von UCHL1 war mit dem Patientenalter, Geschlecht, Ulzerationen bzw. dem Clark-Level (Eindringtiefe der Tumormasse) nachweisbar. In der gleichen Analyse wurde eine starke mRNA-Herunterregulation von UCHL1 in metastasierenden Melanomzelllinien im Vergleich zu Melanozyten mittels Affymetrix-Mikroarrays bestätigt. Dies korreliert mit den Ergebnissen der vorliegenden Arbeit. Mit ungefähr 10 % Vorkommen in den 18 Kurzzeitkulturen bzw. in den 19 untersuchten Zelllinien war die Frequenz stark vermindert. Relativ homogene Expressionsraten wurden für die UCH-Familienmitglieder UCHL3 und UCHL5 bestimmt (Daten nicht gezeigt). Bei einem Vergleich der Expression von insgesamt 1300 Genen des Ubiquitin-Proteasom-Systems in drei Proben primärer Melanomzellen versus einer benignen Melanozytenkultur wurde UCHL1 als das Gen mit der signifikantesten differentiellen Expression detektiert [151]. In allen Tumorproben war die Hydrolase sehr stark herunterreguliert. UCHL3-Mengen waren in dieser Studie im Vergleich zu den Melanozyten ebenfalls nicht verändert.

In der wissenschaftlichen Literatur ist belegt, dass die Promotor-DNA-Methylierung ein entscheidender Regulationsmechanismus für die verminderte UCHL1-Expression in verschiedenen Tumorentitäten darstellt. So wurde eine inverse Korrelation des Methylierungsgrads mit der Genaktivität in Karzinomzellen der Niere, der Prostata, des Darms, des Ösophagus und des Brustgewebe nachgewiesen [2, 36, 50, 153, 154]. In

einer Melanom-Studie wurde mittels verschiedener Array-basierender Experimentalansätze ein durchschnittlicher Methylierungsgrad von 42 % aller CpG-Stellen in den 23 untersuchten Zelllinien nachgewiesen [150]. Zellen mit keiner detektierbaren mRNA hatten einen größeren Prozentsatz (79 %), die mit hohen mRNA-Mengen einen geringeren (20 %). In UCHL1-positiven Melanozyten waren mit ca. 5 % die wenigsten CpG-Stellen methyliert. Diese Ergebnisse konnten durch die vorliegende Arbeit sowohl für Zelllinien als auch für Kurzzeitkulturen bestätigt werden. Hohe UCHL1-mRNA-Mengen in Melanozyten, in den Kurzzeitkulturen T9 bzw. T14 und der stark positiven Linie Buf1286 wiesen keine DNA-Methylierung auf, marginale Mengen bzw. UCHL1-Negativität waren mit einem stark erhöhten Prozentsatz an methylierten CpG-Stellen assoziiert. Unter Verwendung des DNA-Methyltransferase-inhibierenden Nukleotid-Analogons DAC in der Zellkultur konnte eine zumindest partielle Demethylierung der genomischen DNA und eine dosis- und zeitabhängige gesteigerte Transkription in verschiedenen UCHL1-negativen Zelllinien belegt werden. Nach DAC-Behandlung wurde eine erhöhte Proteinmenge nur in der konstitutiv schwach positiven Zelllinie FM-6 nachgewiesen. Dies kann verschiedene Gründe haben. Der demethylierende Effekt von DAC kommt nur während der DNA-Replikation der Zellteilung zu tragen. Aufgrund der proliferationsinhibierenden Wirkung des DNA-Analogons in Kombination mit den hohen CpG-Methylierungsgraden war die gemessene Demethylierung unvollständig. So könnten folglich die erhöhten mRNA-Mengen in den auf Proteinebene negativen Zellen unterhalb der für die Translation notwendigen Mengen liegen. Es kann auch nicht vollständig ausgeschlossen werden, dass Histonmodifikationen, transkriptionelle Suppressoren bzw. miRNA der Expression entgegenwirken.

Proliferationssteigernde Wirkung von UCHL1 in Melanomzellen

Bis zur vorliegenden Arbeit waren keine funktionellen Daten über die UCHL1-Expression in Melanomzelllinien bekannt. Unter Verwendung diverser Transfektionsmodelle der Genüberexpression und der –stilllegung konnte erstmalig eine proliferationsfördernde Wirkung der Hydrolase in Melanomzellen sowohl unter Zellkulturbedingungen, bei Serumdepletion und im verankerungsunabhängigen Wachstum belegt werden. Migrations- und Wundheilungscharakteristika waren im Vergleich zu den entsprechenden Kontrollen nicht verändert. Obwohl das Expressionsprofil der immunhistochemischen Analysen eine tumorsupprimierende Wirkung vermuten ließ, scheint UCHL1 in malignen transformierten Zellen eher tumorfördernde Funktionen auszuüben. Die genauen molekularen Mechanismen sind zwar bisher unvollständig untersucht, lassen aber folgende Interpretationen zu:

- (i) *Hydrolytische UCHL1-Aktivität.* Bei diesen Prozessen ist höchstwahrscheinlich die enzymatische Aktivität involviert, da der Gesamtgehalt an polyubiquitinierten Proteinen signifikant verringert ist und die inaktive C90S-Variante keine wachstumsbezogenen Veränderungen im Vergleich zu den entsprechenden Vektorkontrollzelllinien aufwies. Wildtypische UCHL1 reduzierte die Menge polyubiquitiniertes Protein über einen Molekulargewichtsbereich von 10-300 kDa und scheint damit eher substratspezifisch vorwiegend hydrolytisch aktiv zu sein. Die exakten Funktionen der UCHL1-Enzymaktivitäten sind unvollständig aufgeklärt. Vorwiegend fungiert die Hydrolase in der Generierung bzw. dem Recycling von monomeren Ubiquitin-Bausteinen. Als Substrate können die multimeren Ubiquitin-Genprodukte, wie das Ubiquitin B und C bzw. das ribosomale Ubiquitin-Fusionsprotein UbA80, dienen [155]. In Mäusen mit UCHL1-Defizienz wurden verringerte monomere Ubiquitin-Konzentrationen detektiert [156]. Durch Bindung kann UCHL1 ebenfalls Monoubiquitin stabilisieren und somit dessen lysosomalen Abbau verhindern [156]. Diese Assoziation ist unabhängig von der Enzymaktivität, da inaktives C90S ebenso dazu befähigt ist [156]. Weiterhin wird postuliert, dass UCHL1 Polyubiquitin-Ketten von Proteinen, die zur proteasomalen Degradation markiert wurden, hydrolysiert [19, 155]. Jedoch konnte eine weitere Studie eine direkte Hydrolase-vermittelte Deubiquitinierung von Proteinen nicht nachweisen [157]. Die Ligaseaktivität von UCHL1 zur K63-Ubiquitinverknüpfung mit Proteinen, die zur Stabilisierung dieser führt, ist bisher nur am Beispiel des neuronalen Proteins α -Synuclein *in vitro* nachgewiesen [26]. Direkte *in vivo*-Belege für die Implementierung beider UCHL1-Enzymaktivitäten in (patho-)physiologischen Prozessen fehlen und bedürfen weiterer Untersuchungen.
- (ii) *Aktivierter MAPK-Signalweg.* Durch Mutationen in den Genen signaltransduzierender Kinasen (z. B. N-Ras, B-Raf) ist der MAPK-Signalweg in den Melanomzellen sehr oft hyperaktiviert [158]. Dieses konstitutive Anschalten fördert die Karzinogenese [158]. In den analysierten Transfektionsmodellen dieser Arbeit wurde eine signifikante positive Korrelation zwischen wildtypischer UCHL1 und des Phosphorylierungsgrads der *extracellular signal-regulated kinase* ERK1 und ERK2 detektiert. Hemmung dieser Hyperaktivierung mittels des Inhibitors U0126 führte zu verringerten Proliferationsraten in den Wildtyp (WT)-Transfektanten, hatte jedoch keinen Einfluss auf die Vektorkontrollzellen. Da inaktives C90S nur marginale/ keine Veränderungen gegenüber den Kontrollen zeigte, ist die UCHL1-

Enzymaktivität in diesen Prozess involviert. Die molekularen Hintergründe bzw. die Wirkungsorte der Hydrolase auf den MAPK-Signalweg sind jedoch weitestgehend unbekannt. Im Transfektionsmodell der UCHL1-Überexpression von vaskulären glatten Muskelzellen wurde eine verminderte Aktivierung der ERK-Kinasen nach exogener Stimulation mit TNF α im Vergleich zu den Vektorkontrollen beobachtet [159]. Nach UCHL1-Genstilllegung in HEK293-Zellen wurde eine beeinträchtigte MAPK-Aktivierung sowohl nach c-Met-Rezeptorstimulation durch HGF als auch durch direkte Interaktion mit dem α 2-adrenergen Rezeptor gemessen [57, 160]. Somit lassen sich stromaufwärts von ERK vermittelte Regulationen durch die Hydrolase postulieren.

- (iii) *Zusätzlicher aktivitäts- und MAPK-unabhängiger Mechanismus.* Kabuta *et al.* zeigten im Jahr 2013, dass UCHL1 auch unabhängig der Enzymaktivitäten zellbiologische Prozesse steuern kann [161]. Durch die Interaktion mit den Cyclin-abhängigen Kinasen CDK1, CDK4 und CDK5 werden deren zellproliferationssteigernden Eigenschaften wahrscheinlich durch induzierte intramolekulare Konformationsänderungen verstärkt. Dabei scheint UCHL1 weder mit der Bindungsstelle für die zellulären Inhibitoren p27 und p21 zu konkurrieren, noch das Phosphorylierungsmuster zu verändern. In diversen Transfektionsansätzen konnte eine positive Korrelation der UCHL1 mit der Zellproliferation verschiedener Tumorentitäten (z. B. Neuroblastom und Lungenkarzinom) bestimmt werden [161]. In der gleichen Arbeit wurde in einem Xenograft-Modell nach UCHL1-Genstilllegung mit spezifischer siRNA ein verringertes Wachstum nachgewiesen [161]. Caballero *et al.* belegten, dass UCHL1 über Interaktion mit JAB-1 ebenfalls befähigt ist, die proteasomale Degradation des zellzyklusinhibierenden p27 zu beschleunigen [16]. Folglich würden aktivierte CDK in Kombination mit stärker degradiertem p27 einen proliferationsfördernden Effekt auf Melanomzellen ausüben. Weiterhin könnten Wechselwirkungen und Modulationen der Hydrolase mit den α/β -Tubulinen ursächlich für einen veränderten Aufbau des Spindelapparates während der Mitose sein [17].

UCHL1-dosisabhängige Regulation der ROS-Sensitivität in Melanomzellen

Viele Chemotherapeutika, z. B. Vinblastin, Cisplatin, Mitomycin C und Doxorubicin, entfalten ihre antitumorale Wirkung durch ROS-abhängige Aktivierung des apoptotischen Zelltods, da hohe ROS-Konzentrationen zur Inaktivierung/ Denaturierung lebenswichtiger zellulärer Proteine führen [162]. Tumorzellen sind jedoch über diverse

Resistenzmechanismen befähigt, dem Erfolg der Chemotherapie entgegenzuwirken [163]. Ein besseres Verständnis über die zellulären Vorgänge der (De-)Sensibilisierung der Tumorzellen gegenüber ROS wäre somit ein entscheidender Vorteil für die Optimierung von Behandlungsmöglichkeiten von Patienten u. a. mit malignem Melanom. Zum ersten Mal konnte mittels der vorliegenden Arbeit belegt werden, dass UCHL1 das Resistenzverhalten von Melanomzellen gegenüber Wasserstoffperoxid (H_2O_2) beeinflusst. Während die beiden konstitutiv UCHL1-positiven Zelllinien Buf1286 und FM-6 im Vergleich zu drei negativen Zelllinien (Colo-794, Colo-857, WM-1552C) eine deutlich höhere Toleranz aufwiesen, waren die veränderten ROS-Sensitivitäten in den jeweiligen Transfektionsmodellen abhängig von der Stärke der UCHL1-Expression oder von der untersuchten Zelllinie. Drei transfizierte Zelllinien mit hoher Genüberexpression (Buf1280, FM-82, Colo-857) waren resistenter, drei mit schwächerer UCHL1-Expression (WM-1552C, IRNE, Colo-794) sensitiver als die korrespondierenden Vektorkontrollen. Bei Buf1286-Klonen der Genstilllegung bzw. bei Zellklonen der FM-6-Parentalzelllinie mit jeweils unterschiedlicher Expression zeigten die Zellen mit mittleren UCHL1-Mengen signifikant größere Toleranzen gegenüber H_2O_2 als Zellen mit stärkerer bzw. schwächerer Expression. Obwohl die genauen molekularen Hintergründe des unterschiedlichen Toleranzverhaltens unbekannt sind, lassen sich aufgrund weiterer Ergebnisse bzw. der bestehenden wissenschaftlichen Literatur folgende Hypothesen aufstellen:

- (i) *Modulation durch UCHL1-Enzymaktivität.* In den Transfektionsmodellen der Genüberexpression beeinflusste inaktives C90S kaum/ nicht den Aktivierungsstatus der Akt-Kinase, was ein weiterer Beleg für die funktionelle Ausprägung der Enzymaktivität in Melanomzellen ist. Je nach Effektivität der Genüberexpression/ -stilllegung in dem untersuchten Zellsystem würden konsekutiv die Mengen enzymatischer UCHL1-Aktivitäten moduliert. Da die hydrolytische Funktion einen stärkeren Einfluss in den Melanomzellen hatte, würde eine stärkere Deubiquitinierung von Proteinen zu einem veränderten Gleichgewicht von beispielsweise pro- vs. antiapoptotischen Proteinen führen.
- (ii) *Assoziation mit dem PI_3K / Akt-Signalweg.* Eine Akt-Aktivierung korrelierte positiv mit einer höheren Apoptoseresistenz, während Zellen mit verringerten phosphorylierten Akt-Konzentrationen im Vergleich zu den entsprechenden Vektorkontrollen sensitiver gegenüber H_2O_2 reagierten. Ob UCHL1 mit Akt direkt interagiert oder beispielsweise den zellulären Inhibitor PHLPP1 in den Melanomzellen moduliert, ist bisher unbekannt. Weiterhin könnte eine UCHL1-vermittelte Destabilisierung des *Mammalian target of rapamycin* (mTOR) Komplex 1 zu einer Akt-Aktivierung führen [164].

- (iii) *p53-vermittelte Apoptose.* Einige Studien belegten, dass UCHL1 seine zellulären Funktionen durch direkte Modulation des Tumorsuppressors p53 ausübt [50-52]. Jedoch sind die bisherigen Ergebnisse widersprüchlich. So förderte UCHL1 in der zervikalen Karzinomzelllinie HeLa die proteasomale Degradation [55], die Genstilllegung in HEK293 bewirkte eine p53-Akkumulation [165]. Eine UCHL1-Überexpression führte in der Mammakarzinomzelllinie MDA-MB-231 bzw. in der Tumorzelllinie des Nasenrachenraums HONE1 zu verstärkten p53-Mengen [50, 51]. Dies könnte sich unter anderem durch den unterschiedlichen Genstatus in den untersuchten Zelllinien erklären (siehe nächster Abschnitt). In der Prostatakarzinomzelllinie LNCaP war der Polyubiquitinierungsgrad und konsekutiv der proteasomale Abbau stark vermindert [38]. Ebenfalls konnte p53 durch die Komplexbildung von UCHL1 mit der E3-Ubiquitin-Proteinligase *mouse double minute 2 protein* (MDM2), die für die Proteinmarkung zur proteasomalen Degradation des Tumorsuppressors verantwortlich ist, stabilisiert werden [38]. Weiterhin führte die Aktivierung der Akt-Kinase zu einer K48-Ubiquitinierung von p53 und konsekutiv zu einem verstärkten Abbau des Tumorsuppressorproteins [56, 166].
- (iv) *Genetische Status der verwendeten Zelllinien.* Ein weiterer Erklärungsansatz für die bivalenten Eigenschaften von UCHL1 könnte die Selektion der Zellen/ Zelllinien sein. So wurde in Studien, die eine supprimierende UCHL1-Funktion beim Prostatakarzinom belegten [38, 167], schwach-metastasierende Zellen analysiert, während progressive Charakteristika in Zelllinien mit höherem Metastasierungspotential bestimmt wurden [48, 168]. Die Autoren spekulierten, dass sich (epi-)genetische Aberrationen (Mutation, Promotor-DNA-Methylierung, miRNA) während des Fortschreitens des Tumors in spätere Phasen bzw. während der Langzeitkultur von Zelllinien anhäufen. So sind Mutationen im p53-Gen in späteren Tumorstadien stärker frequentiert [169, 170]. Es wurde geschlussfolgert, dass wildtypisches p53 der frühen Phasen durch UCHL1 deubiquitiniert und damit stabilisiert wird, mutiertes p53 der späteren Phasen aufgrund struktureller Alterationen jedoch nicht [30]. Bisher ist der p53-Status in den verwendeten Melanomzelllinien der vorliegenden Arbeit unbekannt. Es ist zu erwähnen, dass mit Ausnahme von FM-6 (N-Ras Q61L) alle anderen untersuchten Zelllinien V600E-mutiertes B-Raf exprimierten. Die Zelllinie Colo-857 hatte zusätzlich eine Gen-Deletion der Janus-Kinase 2, die sowohl zu einer verminderten MHC-Klasse I-Expression als auch zur einer Resistenz gegenüber der IFN- γ -Stimulation

fürte [171], und eine aktivierende Punktmutation in der Rezeptor-Tyrosinkinase c-Met (T992N-Variante). Dies könnte sich ebenfalls auf das Resistenzverhalten auswirken. Weiterhin könnte die unterschiedliche Akt-Beeinflussung in den Zelllinien in dem genetischen Status des zellulären Gegenspielers *Phosphatase and Tensin homolog* (PTEN) begründet sein. In bis zu 40 % aller Melanome wurden Gendeletionen bzw. inaktivierende Substitutionen detektiert [172, 173]. Der p53- und PTEN-Gensequenz-Status wird in gegenwärtigen Arbeiten am Institut ermittelt.

- (v) *Differentielle Genexpression/ Stabilisierung apoptoseinvolvierter Proteine.* Die Genstilllegung der Hydrolase in HEK293-T-Zellen bewirkte nicht nur verminderte Proliferations- und Migrationseigenschaften und verbesserte Apoptoseinduktionsraten, sondern war auch begleitet von differentieller Genexpression [165]. Proapoptotische Gene wie das *BCL2-associated X protein* BAX und der *BCL2-interacting killer* BIK waren verstärkt exprimiert, antiapoptotische und migratorisch involvierte Gene (Paxillin, Rho A bzw. Janus-Kinase 1) transkriptionell reduziert. UCHL1-Überexpression in kolorektalen Karzinomzellen bewirkte eine Akkumulation der Caspase 9 und konsekutiv zu einem verstärkten Auslösen der Apoptose in diesen Zellen [39]. UCHL1 kontrollierte die mittels des Zytostatikums Doxorubicin induzierte Apoptose durch die Stabilisierung des proapoptotischen Proteins NOXA in Melanomzelllinien und Tumorgewebe [151]. Dies erfolgte posttranskriptionell durch die Deubiquitinierung des NOXA-Proteins. Andere in die Apoptose involvierte Proteine wie XIAP oder PUMA waren durch UCHL1 nicht beeinflusst. Die Autoren schlussfolgerten daraus, dass UCHL1 in Kombination mit NOXA ein interessanter Ansatzpunkt für die Tumorbehandlung mittels DNA-schädigenden Chemotherapeutika ist.

Aufgrund der Beeinflussung des Wachstums- und ROS-Resistenzverhaltens durch Modulation tumorrelevanter Signalwege in einer Vielzahl der untersuchten Zelllinien und der damit zu interpretierenden Globalität der in dieser Arbeit dargestellten Ergebnisse könnte UCHL1 ein interessanter Ansatzpunkt/ Tumormarker für die Entwicklung von neuen Therapiestrategien zur Behandlung von Patienten mit malignem Melanom sein. Jedoch müssen weitere Studien folgen, um die genauen regulatorischen Mechanismen detailliert aufzuklären.

5.2 DNA-Methylierung des myeloischen Promotors als neuer epigenetischer Regulationsmechanismus der APN-Genexpression

APN ist in Tumoren im Vergleich zu den gesunden Ursprungsgeweben oft dereguliert. Obwohl die APN-Konzentrationen im Mamma- bzw. im Ovarialkarzinom erhöht sind, wurde keine Korrelation zu einem klinisch-pathologischen Parameter detektiert [140, 174]. Signifikant schlechtere Überlebensraten bei APN-Positivität im Vergleich zu APN-negativen Tumoren wurden für Kolon- und Pankreaskarzinome beschrieben [126, 130]. Für nicht-kleinzellige Lungentumore dient APN als unabhängiger prognostischer Faktor für ein schlechtes Überleben [129, 131]. Eine signifikante negative Korrelation mit dem Auftreten von Lymphknotenmetastasen und mit dem Überleben wurde für APN-positive Magentumore nachgewiesen [137]. Ubenimex, Synonym für den aminopeptidasenspezifischen Inhibitor Bestatin, zeigte für AML und Lymphome ebenso therapeutische Wirksamkeit im Hinblick auf das Überleben wie in soliden Tumoren der Lunge und des Magens [175-177]. Weiterhin konnte Ubenimex die Sensitivität von zervikalen Krebszellen gegenüber einer Strahlentherapie erhöhen [148]. Ein besonderes Augenmerk liegt jedoch in der Funktion von APN als therapeutische Zielstruktur bei der Neovaskularisation, der Neubildung von Blutgefäßen. Peptide mit einem NGR-Motiv binden an APN von neuentstehenden Blutgefäßen, jedoch nicht in ruhenden Gefäßen [178]. Gekoppelt mit dem Apoptose induzierenden TNF α bzw. einer verkürzten Form des Gewebefaktors (tTF), werden die NGR-Fusionsproteine derzeit in klinischen Studien in Bezug auf ihre antiangiogenetische und folglich antitumorale Wirkung überprüft [179-182].

Vor der Veröffentlichung der vorliegenden Arbeit waren die Informationen zur Expression und deren klinischen Relevanz, der Genregulation und Funktionen der Aminopeptidase während der Melanomprogression begrenzt. Elder *et al.* beschrieben die Expression des später als APN identifizierten Antigens 452 in Melanomzellen [183]. Hypoxie-adaptierte murine Melanomzellen B16F10 exprimierten erhöhte APN-Mengen auf mRNA- und Proteinebene [184], obwohl keine Konsensussequenz für die Bindung des Transkriptionsaktivators Hypoxie-induzierter Faktor (HIF)-1 in den APN-Promotoren kodiert ist [185]. Unter Verwendung von mikrobiellen aminopeptidasenspezifischen Inhibitoren bzw. blockierenden Antikörpern konnte eine wichtige Funktion von APN in der Invasion, in der Degradation der extrazellulären Matrix und bei angiogenetischen Prozessen während des Tumorfortschreitens belegt werden [145, 146, 186, 187]. Im Transfektionsmodell der Genüberexpression zeigten APN-Transfektanten im Vergleich zu den korrespondierenden Vektorkontrollen schnellere Migrationsraten, verstärkten MMP-

unabhängigen Kollagenabbau und eine erhöhte Frequenz der Bildung von Lungentumoren in einem Mausmodell [142]. bFGF-Transfektanten wiesen eine deutliche Erhöhung der APN-Konzentrationen mit Zunahme der invasiven Zellcharakteristika auf [97]. Weiterhin deutete die Koexpression der Aminopeptidase mit dem *intercellular adhesion molecule 1* (ICAM1) auf ein eher hoch-metastatisches Verhalten der Melanomzellen hin [188]. Daten zur klinischen Relevanz der APN-Expression in Melanomen sowie groß angelegte Studien mit einer Vielzahl von zu charakterisierenden Zelllinien fehlten.

Expressionshäufigkeit, Funktion und klinische Relevanz von APN im Melanom

In der vorliegenden Arbeit konnte APN-Protein in 41 % aller verwendeten Melanomzelllinien (n=17) durch durchflusszytometrische Messungen und in ca. 16 % aller 355 Tumorförsionen durch immunhistochemische TMA-Analysen nachgewiesen werden. Dagegen waren nur ungefähr 4 % aller benignen Nävi (n=49) positiv für die Aminopeptidase. Somit ist von einer induzierten APN-Expression während der Melanomprogression auszugehen. Es sei zu erwähnen, dass die exprimierten mRNA- und Proteinmengen zueinander koordiniert vorlagen, so dass posttranskriptionelle Regulationsmechanismen nahezu ausgeschlossen werden konnten. Erstmals wurde gezeigt, dass APN-Positivität mit einem totalen Verlust bzw. einer verringerten Expression einer Vielzahl melanozytärer Markerproteine (z. B. gp100, Tyrosinase und MART1) in Zelllinien und in Kurzzeitkulturen entsprechender Melanomförsionen assoziiert ist. Begründet werden konnte dieser Befund mit herunterregulierten Konzentrationen des involvierten Transkriptionsfaktors MITF. Die Expression proinvasiver bzw. prometastasierender Zytokine wie bFGF und TGF- β 1 lag erhöht vor. Der Vergleich von vier APN-positiven mit vier negativen Zelllinien ergab bis zu 5-fach schnellere Migrationsraten bei Expression der Aminopeptidase. Inhibitorversuche mit Bestatin und Actinonin in APN-positiven Zellen sowie diverse Transfektionsmodelle der Genstilllegung mittels siRNA und der vektoriiellen Überexpression belegten eine migrationssteigernde Funktion der Aminopeptidase in Melanomzellen und bestätigten in einer Vielzahl von Zellmodellen die zuvor publizierten Daten anderer Arbeitsgruppen [97, 142, 187]. Proliferationscharakteristika wie Verdopplungszeiten und das verankerungsunabhängige Wachstum waren unabhängig vom APN-Status. Eine migrations- und invasionsfördernde Wirkung von APN konnte auch in anderen Tumorentitäten belegt werden. Kido *et al.* belegten in Osteosarkomzellen, dass durch Genstilllegung der Aminopeptidase mit komplementären shRNA-Konstrukten das Invasionspotential der Zellen zu Matrigel inhibiert wird [144]. Das APN-inhibierende Hydroxamsäure-Derivat 24F konnte die

Migrationsfähigkeit hepatozellulärer Karzinomzellen supprimieren [189]. Ein migrationsförderndes Potential von APN wurde weiterhin in Schilddrüsenkarzinomzellen und in Osteosarkomen bestimmt [127, 190]. Negativ auf invasive Zellcharakteristika wirkte sich die APN-Expression in Zellen des aggressiven Meningeoms und von Eierstocktumoren aus [133, 147].

Winnepenninckx *et al.* postulierten, dass APN als spezifischer Marker für das Spindelzellmelanom dienen könnte [191]. Dieser desmoplastische Subtyp des malignen Melanoms ist gekennzeichnet durch spindelzellförmige Zellen mit großem Zellkern, mit ausgeprägter interzellulärer Kollagenablagerung und hohem Metastasierungsgrad bei schlechter Prognose für die Patienten [191]. In Kombination mit den verstärkten *in vitro*-Migrationsraten der APN-positiven Zellen in der vorliegenden Arbeit ließ sich eine Assoziation der Aminopeptidase-Expression mit klinischen Parametern erwarten. Obwohl ein erhöhter Clark-Level und die größere Tumordicke bzw. das Vorhandensein von Lymphknotenmetastasen signifikante prognostische Marker in der verwendeten Kohorte waren, konnte keine Korrelation mit dem APN-Status detektiert werden. Auch das Gesamtüberleben und das rezidivfreie Überleben der Patienten waren APN-unabhängig. Die Aminopeptidase wurde vorwiegend in primären malignen Melanomen mit einer Häufigkeit von ca. 17 % positiv immunhistochemisch gefärbt, während metastasierte Tumore nur eine Frequenz von 6 % aufwiesen. Zusätzlich wurden keine näheren Anhaltspunkte für eine mögliche Assoziation der APN-Expression mit einem zellulären Subtypen des Melanoms gefunden. Jedoch sei zu erwähnen, dass das Spindelzellmelanom in der vorliegenden Kohorte nicht näher in dem Gewebe-Mikroarray charakterisiert wurde. Zusammenfassend kann festgestellt werden, dass obwohl APN-positiv Melanomzellen *in vitro* multiple Charakteristika von metastasierenden Tumoren besaßen, keine *in vivo*-Relevanz der APN-Expression in Verbindung mit klinisch-pathologischen Parametern in der verwendeten Kohorte nachweisbar war.

Epigenetische CpG-Methylierung des myeloischen APN-Promotors – Ein neuer genregulatorischer Mechanismus zur Kontrolle der APN-Expression in Tumoren

Differentielle Genexpression von verschiedenen Proteasen während der Initiation und Progression des malignen Melanoms ist mit epigenetischen Veränderungen assoziiert. So ist die DPIV-Expression mittels CpG-Methylierung des entsprechenden Promotors in frühen Stadien der Melanomprogression stark herunterreguliert [192]. In der vorliegenden Arbeit konnte von unserer Arbeitsgruppe als wissenschaftliche Erstbeschreibung eine epigenetische Regulation der APN-Expression durch Promotor-DNA-Methylierung in einer

Vielzahl von Melanomen charakterisiert werden. Durch das bioinformatische Programm MethPrimer wurde eine CpG-Insel mit insgesamt 132 CpG-Stellen in einer 1,3 kb langen Sequenz des myeloischen Promotors (im Bereich von -589 bis +688 relativ zum Transkriptionsstart) identifiziert (Abbildung 5, [193]). Weder im epithelialen Promotor, in der transkriptionellen Enhancer-Region noch in den dazwischen liegenden DNA-Sequenzen konnten weitere CpG-Inseln bestimmt werden. Mit Hilfe von diskriminierenden Oligonukleotidsequenzen in der PCR wurde nachgewiesen, dass der myeloische Promotor in Melanomzelllinien und in Tumoraläsionen aktiv ist, da entsprechende Transkripte in den APN-positiven Zellen detektierbar waren. Die epigenetischen Untersuchungen (COBRA, DNA-Sequenzierung) belegten einen heterogenen CpG-Methylierungsgrad in signifikanter Abhängigkeit von der exprimierten APN-Menge. So korrelierten hohe mRNA-Mengen mit verminderter, keine oder marginale Expression mit starker Methylierung. Bei APN-Positivität war der durchschnittliche Methylierungsgrad des myeloischen Promotors bei ca. 32,1 %, bei Negativität bei ca. 75,2 % (Abbildung 5). In diesen Untersuchungen wurde ein 412 bp-langer Bereich mit insgesamt 32 verschiedenen CpG-Stellen kurz vor dem Transkriptionsstart analysiert (Abbildung 5). Davon zeigten die ersten 15 CpG-Stellen mit Ausnahme von WM-1552C im Vergleich zu den 17 anderen eine deutlich erhöhte Methylierungsdichte. Diese Ergebnisse wurden sowohl für diverse Tumore als auch für Kurzzeitkulturen von Melanomen bestätigt und bekräftigen erstmalig eine *in vivo*-Relevanz der epigenetischen Kontrolle der APN-Expression. Für die anderen putativen CpG-Stellen im myeloischen Promotorbereich kann bisher keine Aussage über deren Methylierungszustand getätigt werden, da die Amplifikation von PCR-Produkten aufgrund der Inkompatibilität der jeweiligen Sequenzbereiche fehlschlug.

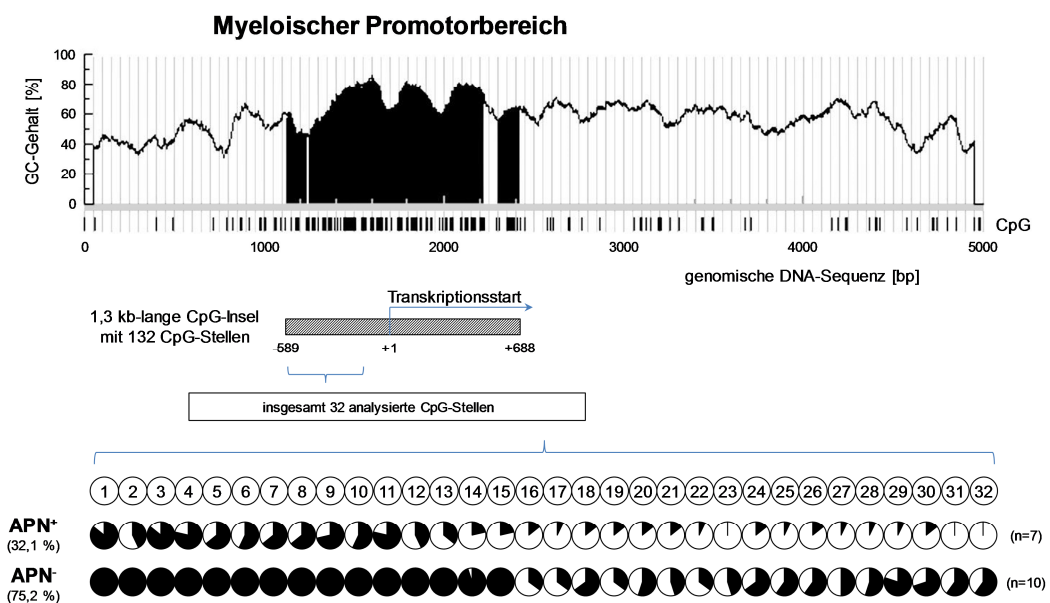


Abbildung 5: Differenzielle CpG-Methylierung des myeloischen APN-Promotors.

Der semimethylierte Promotorbereich und die mittleren exprimierten mRNA-Mengen in den verwendeten Melanozytenkulturen deuten auf eine intermediäre Expression zwischen APN-Positivität und -negativität auf Proteinebene hin. Während einige Studien Melanozyten als APN-negativ klassifizierten [145, 183, 188], konnten Seftor *et al.* belegen, dass die viertägige Kultivierung von Melanozyten in einer von aggressiv metastasierenden Melanomzellen präkonditionierten extrazellulären Matrix zu einer erhöhten APN-Expression führt [194]. Die Autoren spekulierten eine mögliche epigenetische Transdifferenzierung des benignen Charakters der Melanozyten durch das umgebene Mikromilieu, bei dem APN induziert vorliegt.

Bisher unveröffentlichte Ergebnisse weiterführender Experimente unserer Arbeitsgruppe konnten belegen, dass die DNA-Methylierung des myeloischen Promotors als genregulatorischer Mechanismus nicht nur auf das Melanom beschränkt ist. So wiesen die APN-negativen Kolonkarzinomzelllinien HT-29, Colo206F und Colo320 eine hohe Dichte an methylierten CpG-Stellen auf. Drei APN-positive NZK-Zelllinien hatten einen deutlich geringeren Methylierungsgrad als drei negative Zellen. Die Abhängigkeit des Methylierungsmusters von der Expressionsstärke der Aminopeptidase in Zelllinien des Prostatakarzinoms konnte ebenfalls nachgewiesen werden. Durch Sørensen *et al.* wurde 2013 bestätigt, dass die im Vergleich zu den APN-positiven benignen Prostatagewebebeurproben herunterregulierte Expression von APN in den korrespondierenden Karzinomläsionen mit einer verstärkten CpG-Methylierung des myeloischen Promotors einherging [132]. Da diese inverse Korrelation keinen signifikanten Prognosefaktor in der verwendeten Kohorte darstellte, postulierten die Autoren, dass zusätzlich zur CpG-Methylierung die Abwesenheit von APN-relevanten Transkriptionsfaktoren der Myb- und Ets-Familie oder von Enhancer-Proteinen die verringerte Genexpression der Aminopeptidase im Prostatakarzinom begründen. Im hämatopoetischen System wurde in den APN-exprimierenden myeloischen Leukämiezelllinien THP-1, MonoMac-6, HL-60, U937 und K562 keine Methylierung des myeloischen Promotors nachgewiesen (Daten nicht gezeigt). Die negativen Burkitt-Lymphomzellen Raji sowie die T-Zell-Leukämiezelllinie Jurkat wiesen dagegen jeweils einen sehr hohen Methylierungsgrad auf. Interessanterweise exprimierten sowohl die akute lymphatische B-Zellleukämiezelllinie Reh als auch niedrigmaligne B-Zell-*Non-Hodgkin*-Lymphome keine APN auf ihrer Zelloberfläche, hatten aber auch keine methylierten CpG-Stellen im untersuchten Promotorbereich. Vergleichende Methylierungsstudien konnten belegen, dass während der Differenzierung von mononukleären Zellen des peripheren Blutes aus den entsprechenden APN-positiven Progenitorzellen die Promotormethylierung für die Genstilllegung der Aminopeptidase in reifen T- und B-Lymphozyten keine signifikante Rolle spielt (Daten bisher

unveröffentlicht). Dies ist ein zusätzlicher Beleg für die Komplexität der Genexpressionsregulation von APN. Weiterführende Studien werden sich zukünftig darauf fokussieren, in welchen (patho-)physiologischen Prozessen die Promotor-DNA-Methylierung des myeloischen Promotors eine Rolle in der Genregulation von APN spielt.

Wiederherstellung der APN-Expression und –Funktion sowie der Zytokinstimulierbarkeit durch Promotor-DNA-Demethylierung in Melanomzellen

Das Cytidin-Analogon DAC inhibiert durch dessen DNA-Inkorporation während der Replikation die entsprechenden Methyltransferasen, wodurch so generierte hypomethylierte Promotorbereiche wieder zugänglich für die transkriptionelle Regulation werden. Als Supplement im Zellkulturmedium eingesetzt, konnte eine konzentrations- und zeitabhängige Induktion der APN-Expression in zuvor negativen Melanomzelllinien nachgewiesen werden. Mittels hochauflösender Schmelzpunktanalysen konnte zumindest eine partielle Demethylierung des myeloischen Promotorbereiches bestimmt werden (Daten nicht gezeigt), die konsekutiv zu einer Transkriptsteigerung myeloischer mRNA-Spezies und zu einem verstärkten Zelloberflächentransport von APN-Antigenen führte. Die DAC-Behandlung von APN-positiven Zellen hatte nur einen marginalen Einfluss auf die APN-Expression. Weiterhin konnte nachgewiesen werden, dass die DAC-vermittelte Demethylierung in den Melanomzelllinien zu einer Restauration des transkriptionellen Ansprechens gegenüber den Zytokinen IL-4 und TGF- β und zu einer vermehrten additiven Oberflächenexpression von APN-Protein führte. Alleinige Zytokinbehandlung hatte keine veränderte transkriptionelle Aktivität in den APN-negativen Zellen zur Folge.

Als Therapeutikum auch Decitabin genannt, wird DAC momentan in klinischen Studien der Phase I bzw. II bei der Behandlung einer Vielzahl von Tumorerkrankungen, z. B. beim myelodysplastischen Syndrom oder nicht-kleinzelligen Lungentumoren eingesetzt [195, 196]. Bei der Behandlung des metastasierenden Melanoms führte Decitabin beispielsweise in Kombination mit dem Zytostatikum Temozolomid zu objektiven Ansprechraten und zu verlängerten Überlebensraten [197]. Durch die verstärkte Expression melanomassoziierten Antigens (z. B. HMW-MAA) nach Decitabin-Behandlung waren die Tumorzellen für zytotoxische T-Lymphozyten im Rahmen einer Immuntherapie besser erkennbar [198]. Fast alle *in vitro*-Studien konnten vor allem eine antiproliferative Wirkung von DAC nachweisen. Dies wird vor allem mit der Heraufregulation von Tumorsuppressoren begründet [199]. In der vorliegenden Arbeit konnten nach DAC-Behandlung die verschlechterten Wachstumseigenschaften anhand von acht verschiedenen Melanomzellen belegt werden. Während APN-positive Zellen nach Behandlung langsamer migrierten, wiesen behandelte negative Zellen nach APN-

Induktion verstärkte Migrationsraten auf. Da der APN-spezifische Antikörper WM-15 blockierend auf die Migration wirkte, ist von einer APN-vermittelten Steigerung auszugehen. Im Hinblick auf den Therapiererfolg bei der Behandlung des metastasierenden Melanoms mit Decitabin würde das erhöhte Migrationspotential kontraproduktiv sein. Ateeq *et al.* charakterisierten im Brustkarzinom eine DAC-induzierte Expression von prometastasierenden Genen (wie z. B. CXCR4, *breast cancer-specific gene 1* und *urokinase plasminogen activator surface receptor*) und ebenfalls ein gesteigertes Migrations- bzw. Invasionsverhalten von nicht-invasiven Mammakarzinomzellen [200]. Somit lässt sich schlussfolgern, dass das Konzept des Einsatzes von global-demethylierenden Agentien wie Decitabin in der Antitumorthherapie überdacht bzw. in Einzelfällen angepasst werden sollte.

5.3 Etablierung und Charakterisierung eines Modellsystems zur Funktionsanalyse der APN-Enzymaktivität

Bisherige Studien untersuchten die Funktion der APN-spezifischen Enzymaktivität in tumorrelevanten Prozessen unter Verwendung mikrobieller kompetitiver Inhibitoren (z. B. Bestatin, Actinonin und Probestin) [175, 201, 202]. Aufgrund der Kreuzreaktivität dieser mit anderen Aminopeptidasen ist es schwierig abzuschätzen, ob die resultierenden zellulären Konsequenzen der Inhibition auf APN restringiert oder das Zusammenspiel verschiedener Inhibitionen unterschiedlicher Peptidasen ist. So ist beispielsweise Bestatin befähigt, neben APN die ubiquitär exprimierten Aminopeptidase B sowie die Leukotrien-A4-Hydrolase LTA4H zu hemmen [203, 204]. Actinonin inhibiert lösliche oder membranständige Matrixmetalloproteinasen [205]. Weiterhin können diese Inhibitoren nicht nur durch die Zellmembran diffundieren, zytosolische Peptidasen inhibieren und somit beispielsweise die Apoptose der Zellen induzieren [206-208], sondern auch die Signalwege der Proteinkinase C oder pp60-SRC beeinflussen [209, 210]. Studien zur Funktionsbestimmung der APN-Enzymaktivität unter Verwendung des APN-spezifischen monoklonalen Antikörpers WM-15, der durch Bindung an das aktive Zentrum die enzymatische Katalyse beeinträchtigt, zeigten ebenfalls Nebeneffekte [211]. So führte WM-15 in APN-positiven monozytären Zelllinien nicht nur zur Hemmung der entsprechenden Enzymaktivität, sondern induzierte ebenfalls signaltransduzierende Prozesse, wie Calcium-Freisetzung, verstärkte Phosphorylierungen der MAPK ERK, p38 und Jnk, was konsekutiv in erhöhte Transkriptmengen von IL-8 resultierte [212]. Aufgrund der Limitierungen in der Interpretierbarkeit der Ergebnisse in Bezug auf die APN-Enzymaktivität war es notwendig, ein Modellsystem zu entwickeln, das ohne den Einsatz

von Inhibitoren bzw. Antikörpern die Funktion der hydrolytischen APN-Aktivität analysiert. In dieser Arbeit wurden mittels ortsgerichteter Mutagenese diverse Substitutionen in den Sequenzen des GAMEN- (z. B. E354G) und des HELAH-Motivs (H387/391C, H387/391I, E388G) sowie in das Glutamat an Position 410 (E410G) des katalytischen Zentrums eingeführt und die Vektorkonstrukte in HEK293-Zellen transfiziert. Diese humane embryonale Nierenepithelzelllinie wurde ausgewählt, da sie durch eine gute Transfizierbarkeit mit hoher Expressionsrate unter anspruchslosen Kultivierungsbedingungen gekennzeichnet ist. Durch die Verwendung von Chimären aus APN und dem grün-fluoreszierenden Protein (GFP) war es nicht nur möglich, die zelluläre Lokalisation der exprimierten APN-Varianten zu bestimmen, sondern auch stabil exprimierende Zellklone mittels Fluoreszenz-aktivierten Zellsortierens schnell und einfach zu generieren. Jegliche Substitutionen im aktiven Zentrum führten zu einem kompletten Verlust der APN-Enzymaktivität, während die wildtypische Form eine hohe Hydrolaserate des Substrats Ala-*p*-Nitroanilid sowohl im Proteinlysat als auch unter Verwendung intakter Zellen aufwies. Da außer die Mutante H387/391I alle Varianten auf der Zelloberfläche exprimiert wurden und das gleiche gelelektrophoretische Laufverhalten aufwiesen, konnte interpretiert werden, dass die enzymatische Aktivität nicht ursächlich für Glykosylierungsprozesse und den Transport von APN zur Zelloberfläche ist. Weiterführende Experimente konnten zusätzlich nachweisen, dass inaktive APN ebenfalls mit MMD assoziiert ist (bisher nicht publizierte Daten). Aufgrund der intrazellulären Retardierung mit abnormalem Glykosylierungsmuster wurde für H387/391I angenommen, dass die Mutation der beiden Histidine zu Isoleucinen zu einer defizienten Zink-Bindung und konsekutiv zu einer abnormalen Faltung der Peptidase führt, während die Mutation zu Cysteinen die Zink-Bindung höchstwahrscheinlich ermöglicht, die Faltung und weitere Prozessierungsschritte aufrecht erhält, jedoch die Katalyse beeinträchtigt. Somit konnte durch unsere Arbeitsgruppe zum ersten Mal in einer Arbeit belegt werden, dass alle AS in die enzymatische Reaktion von humanen APN involviert sind, dass Substitutionen dieser jedoch nicht die Expression bzw. zelluläre Lokalisation beeinträchtigen. Abbildung 6 zeigt die postulierte Michaelis-Menten-Reaktion der APN-vermittelten N-terminalen Degradation von Peptiden.

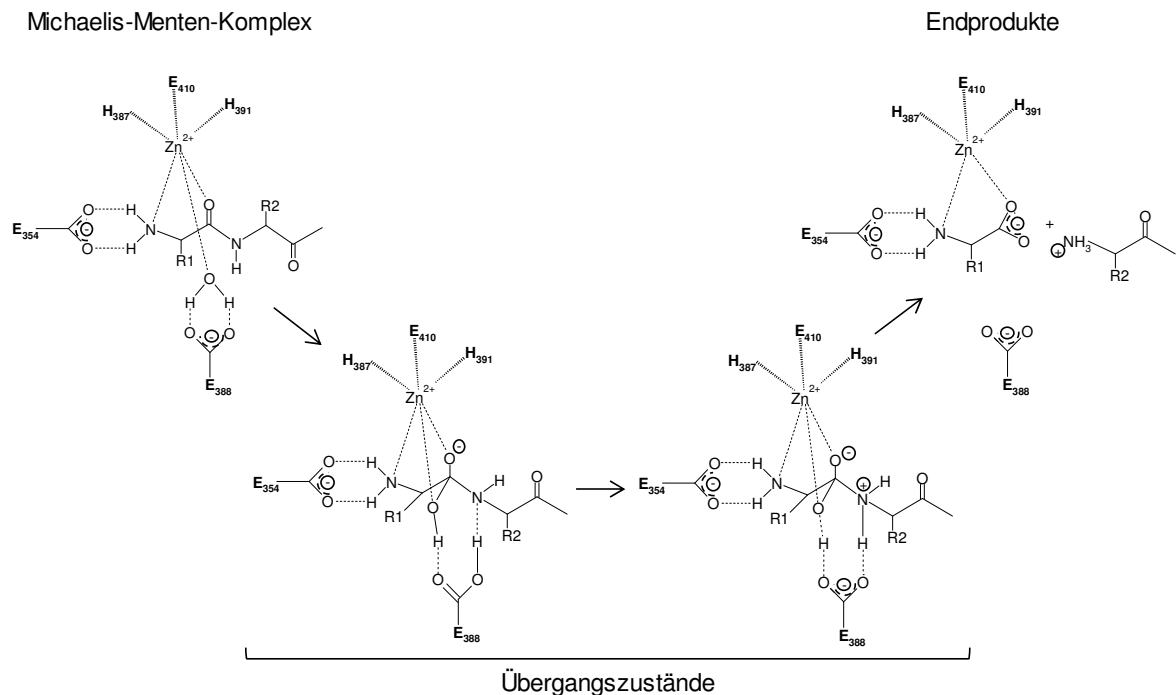


Abbildung 6: Mechanismus der hydrolytischen Peptidspaltung durch APN.

(modifiziert nach Luciani *et al.* [74])

Diese Ergebnisse bestätigen die strukturellen APN-Arbeiten anderer Arbeitsgruppen und stimmen mit Untersuchungen zu anderen Peptidasen überein. So wurde durch Lautsen *et al.* gezeigt, dass Substitutionen im GAMEN-Motiv der Insulin-regulierten Aminopeptidase LNPEP zu einem reduzierten bzw. vollständigen Verlust der Substrat-Katalyse führen [213]. Fukasawa *et al.* belegten für die Dipeptidyl-Peptidase III, Olsen *et al.* für humane APN, dass Mutationen der Histidine im HExxH-Motiv eine abnormale Struktur und folglich einen Verlust der Enzymaktivität bewirken [214].

Anhand des generierten HEK293-Transfektionsmodells konnte in einem antikörper- und inhibitorfreien Zellsystem nachgewiesen werden, dass die APN-Enzymaktivität zellbiologische Prozesse beeinflusst. So wurden in den aktiven APN-WT-Transfektanten erhöhte Verdopplungszeiten bzw. verringerte Proliferationseigenschaften nicht nur unter Zellkulturbedingungen, sondern auch für das verankerungsunabhängige Wachstum bestimmt. Die Expression von inaktiver APN-E388G zeigte im Vergleich zu den Kontrollzellen (parentale und Vektorkontrolle) keine Veränderungen. Ferner beeinträchtigt nur APN-WT mit einer Verminderung um ca. 50 % die Migrationsfähigkeit der Zellen zu Kollagenen. Es sei zu erwähnen, dass die APN-Expression auf mRNA- und Proteinebene in den spezifischen Transfektanten vergleichbar waren. Somit kann eine dosisabhängige veränderte Funktion in dem untersuchten System ausgeschlossen werden. Die genauen molekularen Mechanismen, die diese zellbiologischen Konsequenzen bei vorhandener APN-Enzymaktivität erklären, sind bisher unbekannt. Zellmorphologische Veränderungen

durch beispielsweise den EMT bzw. eine veränderte Zelladhäsion wurden nicht beobachtet. Weiterführende unveröffentlichte Experimente und Ergebnisse lassen in Kombination mit der bestehenden Literatur folgende Hypothesen zu:

- (i) *Veränderte Signaltransduktion.* In den APN-WT-Transfektanten wurde mittels Immunblot eine verstärkte Tyrosinphosphorylierung eines oder mehrerer unbekannter Proteine mit einem geschätzten Molekulargewicht von 130 kDa beobachtet. Somit verändert die Expression aktiver APN den Aktivierungsgrad von Signalwegen mit möglicher Interferenz zellbiologischer Eigenschaften.
- (ii) *Differentielle Genexpression.* Mikroarray-Analysen mit anschließender Validierung belegten unterschiedliche mRNA-Mengen in APN-WT im Vergleich zu APN-E388G und den Kontrollzellen. So waren beispielsweise die Expression der promigratorischen/ invasiven Gene *engulfment and cell motility 1* (ELMO1) bzw. MMP2 nur in den APN-WT-Transfektanten stark vermindert. Zukünftige Untersuchungen, welche die Konsequenzen dieser veränderten Expression auf Zellproliferation und Migration analysieren, könnten APN-vermittelte genregulatorische Mechanismen näher charakterisieren.
- (iii) *Unterschiedliches Potential zur Interaktion mit anderen Rezeptoren.* Substitutionen im aktiven Zentrum könnten bisher undefinierte Auswirkungen auf strukturelle Komponenten im APN-Protein haben, die die Interaktion der jeweiligen Variante mit anderen Oberflächenmolekülen beeinträchtigt. APN ist mit einer Vielzahl von Rezeptoren kolokalisiert. So besitzt die Aminopeptidase in Synergie mit dem *tumor-associated antigen L6* eine migrationsfördernde Wirkung in Lungentumorzellen [215]. Weiterhin kann die gleichzeitige Expression/ Interaktion des *reversion-inducing cysteine-rich protein with Kazal motifs* (RECK) oder von Galektinen mit APN entweder die physiologischen Funktionen (z. B. Internalisierung) oder die Quervernetzung mit anderen Rezeptoren beeinflussen und damit Einfluss auf zelluläre Prozesse nehmen [216-218].
- (iv) *Unbekannter Ligand.* Weiterhin kann spekuliert werden, dass im verwendeten fötalen Kälberserum bei den Experimentalansätzen ein bisher nicht definierter Ligand/ Substrat vorhanden ist, der durch APN (in-)aktiviert wird und die zellulären Resultate erklären lässt.

5.4 Deregulation der SDF-1 α / CXCR4-vermittelten Zellmigration durch APN

Die chemotaktische Migration ist ein wichtiger zellulärer Prozess vor allem bei der Embryogenese und im Immunsystem, um Zellen mittels eines Lockstoffgradienten zielgerichtet zu ihren Bestimmungsort zu dirigieren. Gesteuert wird dieser Prozess hauptsächlich durch die Bindung von Chemokinen an die entsprechenden Chemokinrezeptoren auf der Zelloberfläche [219]. Bisher wurden ca. 20 verschiedene Rezeptoren identifiziert [220]. Ein Rezeptor kann mehrere Liganden besitzen bzw. ein Ligand kann auch an mehreren Rezeptoren binden. Die G-Protein-gekoppelten Rezeptoren besitzen sieben Transmembrandomänen mit jeweils drei intra- bzw. extrazellulären *Loop*-Domänen [221]. Eine extrazelluläre Ligandenbindung N-terminal an den Rezeptor führt zu räumlichen Strukturveränderungen, die über die Transmembrandomänen zu einer veränderten Konformation des intrazellulären C-terminalen Teils und meist zur Aktivierung durch Tyrosinphosphorylierung führen [222]. Dadurch werden in der Zelle diverse Signaltransduktionswege ausgelöst, die u. a. eine Umorganisation von Zytoskelettkomponenten mit morphologischen Veränderungen bewirken und somit die Zellen zum migratorischen Potential befähigen [221].

Der Chemokinrezeptor CXCR4 und sein Ligand SDF-1 α spielen eine wichtige Rolle bei der gerichteten Migration CXCR4-positiver embryonaler Stammzellen während der Embryogenese [223, 224]. Adulte pluripotente Stammzellen benutzen ebenfalls das SDF-1 α / CXCR4-chemotaktische System, um im jeweiligen Zielgewebe lebenserhaltende Funktionen, z. B. Wundheilung und Geweberegeneration, zu fördern [225]. CXCR4- positive Lymphozyten werden durch die Sekretion von SDF-1 α in den Lymphknoten chemotaktisch angezogen, um dort Differenzierungs- bzw. Selektionsprozesse zu durchlaufen [226]. Dieser Vorgang wird auch als *Homing* bezeichnet.

Aufgrund seiner Überexpression in mehr als 20 Tumorarten ist CXCR4 einer der interessantesten Angriffspunkte für eine zielgerichtete Therapieform. Eine induzierte Expression von CXCR4 in Tumorzellen mit verstärkter Metastasenbildung und geringeren Überlebensraten wurde u. a. im Prostatakarzinom, im NZK und im Melanom nachgewiesen [227-229]. Der Chemokinrezeptor ist für Leukämien, für das Mammakarzinom und für das Glioblastom ein prognostischer Marker [230]. Die genregulatorische CXCR4-Induktion kann beispielsweise durch Promotor-Demethylierung, Stimulation mit dem vaskulären endothelialen Wachstumsfaktor (VEGF) oder durch Hypoxie erfolgen [229, 231, 232]. Durch parakrine SDF-1 α -Stimulation sind das Knochenmark, die Lymphknoten, die Leber und die Lunge oft Zielgewebe von CXCR4-positiven Metastasen (Abbildung 7 A, [233]). Zum Mikromilieu des Knochenmarks

angelockt, erfahren die Tumorzellen durch dieses *Homing* bessere Überlebenschancen und schnellere Proliferationsraten [221]. In einer zielgerichteten Tumorthherapie soll eine CXCR4-Hemmung zu einer Mobilisierung der Tumorzellen aus dem protektiven Knochenmark führen und diese dadurch gegenüber einer Chemotherapie sensibilisieren (Abbildung 7 B, [221]). Diverse CXCR4- oder SDF-1 α -Antagonisten sowie CXCR4-spezifische Antikörper werden derzeit in verschiedenen klinischen Studien auf ihre Wirksamkeit überprüft (Informationen erhältlich unter www.clinicaltrials.org). Jedoch sind die bisherigen Ergebnisse nicht zufriedenstellend. Weiterhin können CXCR4-exprimierende und Angiogenese fördernde Progenitorzellen durch hohe SDF-1 α -Konzentrationen in das Tumorgewebe angelockt werden und durch Sekretion von vaskulären Wachstumsfaktoren bzw. Zytokinen das Wachstum bzw. die Blutversorgung des Tumors deutlich verbessern (Abbildung 7 C, [221]). Beim Ovarialkarzinom sind hohe SDF-1 α -Mengen mit reduzierten Überlebensraten assoziiert [234].

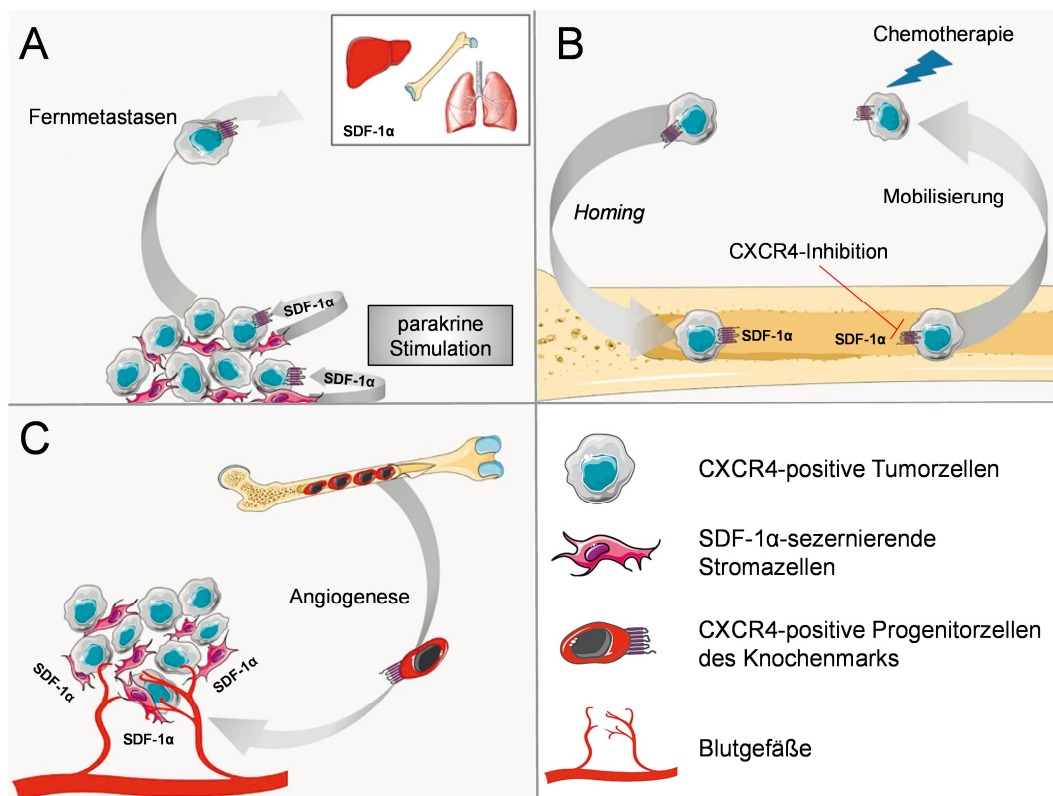


Abbildung 7: Multiple Funktionen der SDF-1 α / CXCR4-Achse in der Tumorbilogie.

(modifiziert nach Domanska *et al.* [221])

In der vorliegenden Arbeit konnte zum ersten Mal gezeigt werden, dass die Expression von aktiver APN in transfizierten HEK293-Zellen zu einer starken Herunterregulation der CXCR4-mRNA- und Proteinmengen führte. Da CXCR4 in den E388G-Transfektanten

vergleichbar mit denen der Kontrollzellen war, muss die Enzymaktivität eine Rolle bei der Regulation spielen. Die reduzierte Expression könnte ursächlich für die erhöhten Verdopplungszeiten und die verschlechterten proliferativen Zellcharakteristika der APN-WT-Zellen sein. So beschrieben Diodovich *et al.* für Zellen des Nabelschnurbluts, dass nach Akrylnitril-Behandlung verminderte CXCR4-Mengen mit verringerten Wachstumseigenschaften und Klonierbarkeit einhergehen [235]. Da Chemokinrezeptoren oft miteinander kreuzvernetzt reguliert sind [236], kann nicht ausgeschlossen werden, dass APN durch enzymatische Spaltung anderer Zytokine/ Chemokine indirekt CXCR4 beeinträchtigt.

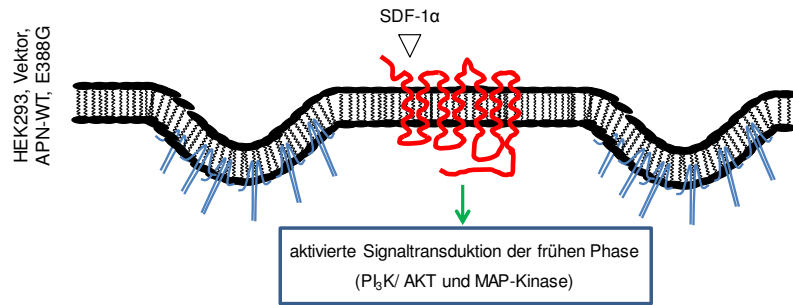
Unter Einsatz von Transwell-Platten konnte nicht nur eine verminderte Migrationsleistung gegenüber Kollagen, sondern auch eine deregulierte Wanderung von APN-WT-Transfektanten zu SDF-1 α detektiert werden. Die inaktive Variante APN-E388G und die Kontrollen zeigten Chemotaxis gegenüber dem Liganden, welche sich komplett mit dem Antagonisten AMD3100 blockieren ließ. Eine hydrolytische Spaltung und folglich eine Inaktivierung von SDF-1 α durch wildtypische APN konnte in einem Spaltungstest mit anschließender massenspektrometrischer Analyse unter Verwendung intakter transfizierter HEK293-Zellen nicht nachgewiesen werden. Dies könnte entweder in der globulären Struktur oder in der N-terminalen AS-Sequenz von SDF-1 α begründet sein. So ist nach Abspaltung der Signalsequenz ein Prolin an vorletzter Stelle kodiert, welches sich stark inhibierend auf die APN-Enzymaktivität auswirkt. Tatsächlich sind Bradykinin und Substanz P mit der gleichen N-terminalen Lysin-Prolin-Sequenz natürliche Inhibitoren für APN [237].

Die SDF-1 α -Bindung an CXCR4 führt zum Aktivieren diverser Signalwege (z. B. MAPK, PI₃K/ Akt und Calcium-Freisetzung) und zur Homodimerisierung des Chemokinrezeptors [238]. Intramolekulare Konformationsänderungen verstärken die Bindungsaffinität zu weiteren SDF-1 α -Liganden [239]. Anschließend kolokalisiert der Rezeptor-Liganden-Komplex mit MMD, worauf dieser internalisiert und entweder lysosomal degradiert wird oder freier CXCR4 nach Liganden-Abspaltung zur Oberfläche transportiert wird [240, 241]. Da nach 10-minütiger Inkubation mit SDF-1 α in allen Transfektanten sowie in den parentalen HEK293-Zellen verstärkte Phosphorylierungen der MAPK ERK1/2 und Akt gemessen wurden (Daten nicht gezeigt), ist davon auszugehen, dass der Ligand unabhängig vom APN-Status an die CXCR4-positiven Zellen bindet und zur Aktivierung der Signalwege befähigt ist. Weiterführende bisher unveröffentlichte Ergebnisse konnten belegen, dass in späteren Phasen der Signaltransduktion (≥ 3 h) der MAPK-Signalweg in den APN-WT-Transfektanten abgeschaltet ist, während in APN-E388G und den Kontrollzellen erhöhte Konzentrationen

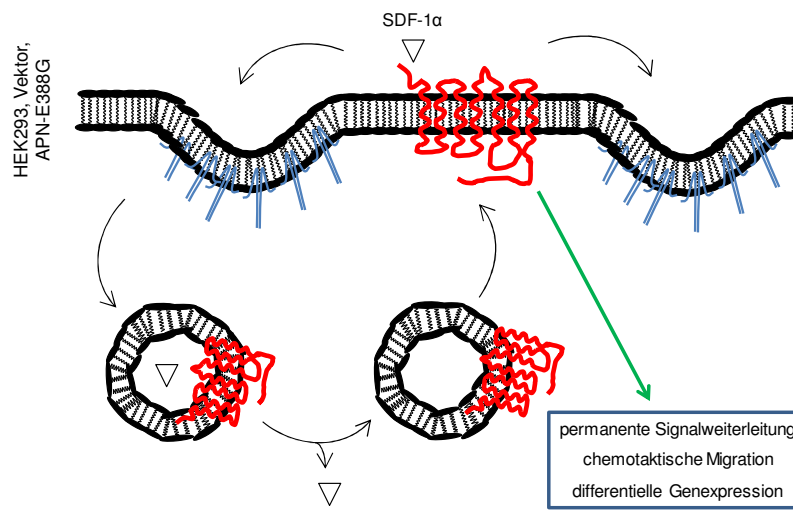
im Vergleich zu den entsprechenden unbehandelten Proben nachweisbar waren. In Kombination mit der vorhandenen Literatur konnten drei Zielgene BAX, *megakaryocyte-associated tyrosine kinase* MATK und Keratin 19 identifiziert werden, die nach 24-stündiger SDF-1 α -Stimulation in APN-E388G und den Kontrollzellen differentiell exprimiert wurden, während keine transkriptionellen Veränderungen in APN-WT gemessen wurden. Dabei könnte die Herunterregulation des epithelialen Markers Keratin 19 den EMT und vor allem die Mobilisierung der embryonalen HEK293-Epithelzellen begünstigen [242, 243]. Die transkriptionelle Steigerung der exprimierten BAX-Mengen würde laut Literatur die Apoptose begünstigen [244, 245]. Jedoch ist die Induktion der Apoptose von einer Vielzahl involvierter Proteine abhängig, so dass die Konsequenzen der veränderten BAX-mRNA-Mengen im System unklar sind. Aufgrund unzureichender Informationen können keine Aussagen über die physiologischen Konsequenzen bzw. über die Funktionen von MATK im HEK293-System getätigt werden.

Das Abschalten der SDF-1 α -vermittelten Signaltransduktion/ Genregulation kann durch die verminderte CXCR4-Internalisierung von nur ca. 15 % des oberflächlich exprimierten CXCR4-Gesamtproteins in den APN-WT-Transfektanten erklärt werden. In APN-E388G und den Kontrollen führte die SDF-1 α -Stimulation in einem Zeitraum von 0,5 – 48 h zu einer konstanten Herunterregulation von ca. 70 % des CXCR4-Proteins auf der Zelloberfläche. Mittels GFP-gekoppelten CXCR4 konnte in der Echtzeit-Fluoreszenzmikroskopie von HEK293-Zellen bewiesen werden, dass CXCR4 hauptsächlich über die MMD nach SDF-1 α -Ligandierung internalisiert, was literarisch in verschiedenen Studien belegt ist [246-248]. Interessanterweise wurde nur in den APN-WT-Transfektanten eine signifikante Verminderung des MMD-assoziierten Strukturproteins Caveolin-1 detektiert. Da die Caveolin-1-mRNA-Mengen unverändert vorlagen, ist von einem bisher unbekanntem posttranskriptionellen Regulationsweg auszugehen. Inaktives APN-E388G ist zwar ebenfalls in MMD lokalisiert, hatte jedoch eine vergleichbare Caveolin-1-Konzentration wie die Kontrollzellen. Andere Markerproteine, wie die Raft-assoziierten Flotilline 1 und 2 oder die SRC-Kinasen Lyn und Fyn, wurden nicht durch APN beeinflusst. Genstilllegung von Caveolin-1 in parentalen HEK293-Zellen mittels vektorbasierender Überexpression spezifischer shRNA-Moleküle führte zu einer signifikanten Herunterregulation der CXCR4-Oberflächenexpression. Zum jetzigen Kenntnisstand lässt sich das in Abbildung 8 dargestellte Modell der APN-vermittelten Beeinträchtigung der SDF-1 α / CXCR4-Achse postulieren.

SDF-1 α -Bindung und Signalweiterleitung



Caveolae-abhängige CXCR4-Internalisierung und Rezeptor-Recycling



Inhibierung der Caveolae-abhängigen CXCR4-Internalisierung durch aktive APN

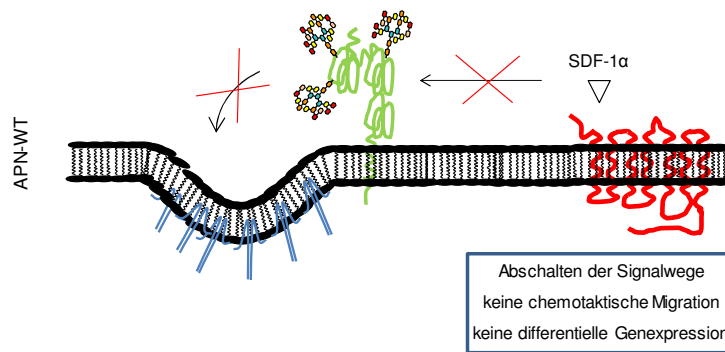


Abbildung 8: Modell der SDF-1 α / CXCR4-Blockade durch APN-WT.

Die SDF-1 α -Bindung an CXCR4 führt zunächst zu einer Aktivierung diverser Signalwege. Anschließend internalisiert der Komplex endozytotisch über Caveolae. Durch den pH-Wechsel in den Endosomen diffundiert der Ligand vom Rezeptor ab. Freier Rezeptor wird zur Zelloberfläche transportiert, wo er erneut für eine Ligandenbindung zur Verfügung steht. Dies führt zur dauerhaften Anschaltung der Signalwege, die konsekutiv zu transkriptionellen Veränderungen und zur chemotaktischen Zellmigration führen. Enzymatisch aktiver APN-WT verringert nicht nur die Caveolin-1-Menge, sondern blockiert den CXCR4-Rezeptor-Recycling-Prozess. Permanent mit SDF-1 α gebundener CXCR4-Komplex ist nicht mehr in der Lage, die Signalweiterleitung aufrecht zu erhalten. Dadurch werden sowohl das SDF-1 α -vermittelte migratorische Potential als auch die differentielle Genexpression inhibiert.

Die zugrundeliegenden Mechanismen sind im Detail unklar. Zum jetzigen Zeitpunkt konnte weder eine direkte Interaktion von CXCR4 oder Caveolin-1 mit APN noch die genauen molekularen Mechanismen der durch die Enzymaktivität inhibierten zellulären Chemotaxis zum SDF-1 α aufgeklärt werden. APN könnte entweder direkt den intrazellulären Oberflächentransport, die signaltransduzierende Homodimerisierung und/oder die Caveolae-Assoziation von CXCR4 blockieren oder durch die Modulation anderer Mediatoren indirekt auf die SDF-1 α / CXCR4-Chemotaxis Einfluss nehmen. So hat beispielsweise der Caveolin-1/ Cavin-1-Komplex tumorprogressive Eigenschaften, während Caveolin-1 bei Cavin-Negativität eine tumorsupprimierende Wirkung ausübt [249]. Es existieren bisher nur wenige Studien, die die veränderte Caveolin-1-Konzentration mit differentieller CXCR4-Genexpression in Zusammenhang bringen. Es wird vermutet, dass vermindertes Caveolin-1 in Leukozyten zu einer erhöhten CXCR4-Menge führt, was zum Fortschreiten einer Lungenfibrose beiträgt [250]. Behandlung der metastasierenden Mammakarzinomzelllinie MDA-MB-231 mit Omega-3-Fettsäuren resultierte in einem strukturellen Auflösen der MMD, wodurch die SDF-1 α -vermittelte Migration der CXCR4-positiven Zellen stark beeinträchtigt wurde [251]. Weiterhin spielt Caveolin-1 eine wichtige Rolle bei der Mobilisierung und dem *Homing* von CXCR4-positiven endothelialen Progenitorzellen zu SDF-1 α -Konzentrationsgradienten während der Vaskulogenese [247].

Die vorliegende Arbeit beschreibt erstmalig einen Zusammenhang zwischen APN, CXCR4 und Caveolin-1. Jedoch sollten zukünftig weitere Untersuchungen erfolgen, um ein besseres Verständnis der molekularen Mechanismen dieser Rezeptortriade auf pathophysiologische Prozesse zu erlangen. Dieses wäre jedoch aufgrund folgender Tatsachen von besonderem Interesse:

- (i) *APN als Rezeptor für Pathogene.* Die Aminopeptidase ist der Rezeptor für diverse Virusarten und fördert den Zelleintritt des *Mycobacterium tuberculosis* [252]. Nach pathogener Bindung internalisiert der jeweilige Komplex meist über MMD [113]. Daher wäre ein interessanter molekularer Therapieansatz zu wissen, wie APN in den jeweiligen Geweben die MMD so modifiziert, damit der Eintritt der Erreger ermöglicht wird.
- (ii) *CXCR4 in der Tumorthherapie.* CXCR4-Überexpression wurde bisher in mehr als 20 verschiedenen Tumorentitäten in Verbindung mit verstärktem Tumorwachstum bzw. höherem Metastasierungsgrad und schlechteren Prognosen für die Patienten beschrieben [221]. CXCR4-spezifische Antikörper bzw. SDF-1 α -Antagonisten werden bereits in diversen klinischen Studien auf deren Funktionalität in der Krebsbehandlung getestet [222, 253]. Da in bisher

unveröffentlichten Arbeiten unserer Arbeitsgruppe eine posttranskriptionelle intrazelluläre CXCR4-Retardierung bei APN-Positivität ebenfalls in NZK- und AML-Zelllinien nachgewiesen wurde, wird durch uns postuliert, dass die publizierten Effekte aus dem HEK293-Zellmodell tumorrelevant sind. Folglich könnte ein besseres molekulares Verständnis des APN-inhibierende Effekts auf die SDF-1 α -vermittelte Chemotaxis CXCR4-positiver Zellen einen wesentlichen Beitrag zur Behandlung von Krebserkrankungen leisten.

- (iii) *Bivalentes Caveolin-1 in der Tumorbilogie.* Lange Zeit galt Caveolin-1 als Tumorsuppressorprotein. So wurden verringerte Konzentrationen im Pankreas-, Lungen-, Schilddrüsen- und Ovarialkarzinom vergleichend zu den korrespondierenden gesunden Geweben bestimmt [254-257]. Jedoch zeigten neuere Studien ebenfalls eine krebsfördernde Wirkung in anderen Geweben wie im Melanom, im Prostata- und Mammakarzinom sowie in den Tumoren des Ösophagus bzw. Nasenrachenraums [258-262]. Erhöhte Genexpression ist dabei assoziiert mit verstärkten Migrationsraten, fortgeschrittenen Tumorstadien und schlechteren Prognosen. Posttranslationelle Modifikationen (z. B. Tyrosinphosphorylierungen) sowie die Interaktion mit Cavin-1 können die Charakteristika von Caveolin-1 beeinflussen [249, 262]. Die APN-vermittelte Herunterregulation von Caveolin-1 ist ein bisher unbekannter Mechanismus, dessen molekulares Verständnis neue weitreichende tumorrelevante Sichtweisen ermöglichen würde.

5.5 Interaktion von APN und Fc γ -Rezeptoren in der Phagozytose und Signaltransduktion

In früheren Arbeiten unserer Arbeitsgruppe wurde gezeigt, dass nach Kreuzvernetzung von APN mittels monoklonaler Antikörper diverse zelluläre Signalkaskaden in monozytären Zellen ausgelöst werden [212]. Neben einem starken biphasischen Ca²⁺-Anstieg durch die Freisetzung der Ionen aus dem endoplasmatischen Retikulum, gefolgt von einem extrazellulären Einstrom in die Zelle, wurde eine verstärkte Phosphorylierung der MAPK ERK1/2, p38 und *c-Jun N-terminal kinase* Jnk gefunden. Zusätzlich wurde eine heraufregulierte mRNA-Menge des chemotaktischen Zytokins IL-8 nach APN-Ligation nachgewiesen. Weiterhin konnte belegt werden, dass APN partiell in MMD der Monozyten lokalisiert ist [117]. Aufgrund der aus nur sieben AS bestehenden zytoplasmatischen Domäne der Aminopeptidase wurde postuliert, dass APN nicht allein, sondern in Assoziation mit anderen Rezeptoren signaltransduzierend aktiv ist. MacIntyre *et al.* zeigten, dass möglicherweise Fc γ -Rezeptoren in diese Prozesse involviert sind [263]. Um

diese Hypothese näher zu untersuchen, wurden bildgebende Verfahren und durchflusszytometrische Messungen der Kollokalisierung von APN mit den Fc γ -Rezeptoren II (CD32) bzw. I (CD64) in der monozytären Leukämiezelllinie THP-1 sowie in isolierten humanen peripheren Blutmonozyten durchgeführt. CD64 ist der hoch affine Rezeptor für monomere Immunglobuline der Klasse G (IgG), während CD32 schwächere Affinitäten besitzt. Diese Rezeptoren sind vorwiegend auf phagozytären Zellen (z. B. Monozyten/ Makrophagen und dendritischen Zellen) exprimiert. Lokal gehäufte antigenkomplexierte Immunglobulin-Bindung über den Fc-Teil des Antikörpers an die entsprechenden Fc γ -Rezeptoren führt zum Auslösen diverser Signaltransduktionen, infolgedessen die Phagozytose durch Zytoskelett-Umorganisationen eingeleitet und durch Sekretion proinflammatorischer Zytokine das Immunsystem aktiviert wird. Mittels der konfokalen Laser-Scanning-Mikroskopie, der Elektronenmikroskopie mit Nano-Goldpartikeln und durchflusszytometrischen FRET-Analysen konnte in der vorliegenden Arbeit eine Kollokalisierung von APN mit CD32 belegt werden. Mit einem signifikanten Energietransfer zwischen CD32 bzw. CD64 jeweils mit APN konnte erstmalig nachgewiesen werden, dass die Aminopeptidase sehr eng mit den beiden Fc γ -Rezeptoren auf der Zelloberfläche von monozytären Zellen kollokalisiert ist und zusammen einen multifunktionellen Komplex bilden. Da eine Vorinkubation mit dem aminopeptidasenspezifischen Inhibitor Actinonin den FRET nicht beeinträchtigt, scheint die APN-Enzymaktivität nicht für das Interagieren verantwortlich zu sein. Diese Ergebnisse stehen im Einklang mit einer weiteren Studie von Mina-Osorio *et al.* [264]. Sie zeigten, dass APN sich auf Bereiche der Fc γ -medierten Phagozytose konzentriert und anschließend in Phagosomen internalisiert wird. In diesen polarisierten Regionen ist APN mit CD32 stark kollokalisiert. Die Phagozytoserate ist bei Kreuzvernetzung von APN mit CD32 im Vergleich zu den jeweiligen Homodimerisierungen am höchsten. Ebenfalls führt das Ligieren beider Rezeptoren zu einer verlängerten Aktivierung der SRC-Kinase Syk, während homodimerisierendes APN-Kreuzvernetzen keine Signalkaskade über Syk auslöst. Die Autoren postulierten, dass sowohl die lokale Anhäufung von APN und CD32, der induzierte phagosomale Prozess als auch die Syk-Aktivierung in den MMD der Zellen stattfinden. So war der Cholesterolinhibitor Ezetimib befähigt, in monozytären Zellen die Interaktion von APN mit den Fc γ -Rezeptoren zu verhindern [265]. Eine weiterführende Studie belegte, dass APN die Phagozytose in Makrophagen und dendritischen Zellen mit anderen Rezeptoren steuern kann [266]. Zwar wurden die interagierenden Rezeptoren nicht näher charakterisiert, aufgrund der vorhandenen Literatur wurde den Galektinen eine wichtige Rolle bei den APN-vermittelten molekularen und zellulären Funktionen in einer Vielzahl von Geweben/ Tumoren zugesprochen [217, 218, 267]. So ist das extrazellulär sezernierte und laktosebindende Galektin-3 in monozytären Zellen konstitutiv

mit APN assoziiert [218]. Die Bindung von quervernetzenden Antikörpern bewirkt eine Dissoziation von Galektin-3 mit Auslösen von Signaltransduktion und zellulärer Aggregation. Auch könnte die Interaktion mit den Mannose-Rezeptoren ursächlich für die Phagozytose sein [268].

Die strukturellen Voraussetzungen von APN bei der Phagozytose bzw. bei der Signaltransduktionsinitiierung sind noch unvollständig aufgeklärt. Die meisten Studien definieren übereinstimmend, dass die enzymatische Aktivität bzw. das aktive Zentrum in diesen Prozess nicht involviert sind [90, 121, 269]. Bis vor kurzem wurde angenommen, dass die zytoplasmatische Domäne der Aminopeptidase inert ist und der signaltransduzierende Prozess nach Kreuzvernetzen von APN-Molekülen mit anderen Rezeptoren und deren zytoplasmatischen Strukturen ausgelöst wird [90, 212, 266]. Die starke Assoziation von APN mit MMD in einer Vielzahl von Geweben könnte die Kolokalisation bzw. die räumliche Nähe zu den Rezeptoren unterstützen/ begründen. Als signalweiterleitende Proteine wurden die Adaptorproteine *growth factor receptor-bound protein 2* (Grb2) und *Son of sevenless* (Sos) mittels Immunpräzipitationsstudien identifiziert, die über Ras den MAPK-Signalweg aktivieren [90]. Die direkte Bindung der Adaptoren an APN wird jedoch ausgeschlossen. Erst kürzlich wurde durch Subramani *et al.* erstmals der Beweis getätigt, dass die kurze zytoplasmatische Domäne von APN nach eigenen Kreuzvernetzen eine signaltransduzierende Funktion in Monozyten ausübt [270]. Es konnte belegt werden, dass das Tyrosin an Position 6 (Abbildung 8) SRC-Kinase-abhängig phosphoryliert werden kann. Ortsgerichtete Mutagenese zu Y6F verhinderte nicht nur eine Phosphorylierung, sondern reduzierte signifikant das Auslösen diverser Signalkaskaden (SRC, *focal adhesion kinase*, ERK1/2) und die adhäsiven Eigenschaften der Monozyten zu epithelialen zervikalen Karzinomzellen durch die verminderte Komplexbildung mit den Zytoskelettkomponenten *IQ motif containing GTPase activating protein 1* (IQGAP1) bzw. α -Actinin.

6 Zusammenfassung

Das Institut für Medizinische Immunologie der Martin-Luther-Universität Halle-Wittenberg beschäftigt sich seit Jahren mit der Identifizierung und Charakterisierung von putativen Biomarkern, die als neue Strukturen für eine zielgerichtete Therapie des metastasierenden Melanoms angewendet werden können. In der vorliegenden Arbeit wurden Expressions- und Funktionsanalysen von APN und UCHL1 in diversen Melanomzelllinien und Tumorkläsionen beschrieben. Dabei konnte erstmalig gezeigt werden, dass die UCHL1-Expression hauptsächlich durch Promotor-DNA-Methylierung bereits im frühen Stadium von benignen Nävi reprimiert vorliegt. Mit 7 % in Melanomkläsionen bzw. 10 % in (Kurzzeit-)Zellkulturen war die Hydrolase relativ selten in Tumoren exprimiert. Jedoch waren UCHL1-positive Zelllinien/ Transfektanten durch Aktivierung des MAPK-Signalwegs mit verbesserten Proliferationseigenschaften gekennzeichnet. Da die Hydrolase zusätzlich das Resistenzverhalten gegenüber ROS über Modulierung des PI₃K/ Akt-Signalwegs beeinflusste, wäre ein besseres Verständnis der genauen regulatorischen Mechanismen ein interessanter Ansatzpunkt, UCHL1 als mögliche Zielstruktur bei der Generierung und Etablierung neuer Therapieformen für zumindest ein Teil von Patienten mit metastasierendem Melanom einzusetzen.

Die gegenüber Melanozyten induzierte APN-Expression in 16 % der Melanomkläsionen und 41 % der Melanomzellkulturen war assoziiert mit einer verringerten Expression melanozytärer Markerproteine und dem Transkriptionsfaktor MITF. Obwohl APN-positive Melanomzellen *in vitro* multiple Charakteristika von metastasierenden Tumoren besaßen, konnten in immunhistochemischen Analysen einer Vielzahl von malignen Primärkläsionen und benignen Nävi keine klinische Relevanz der APN-Expression in der verwendeten Kohorte nachgewiesen werden. Zum ersten Mal wurde die DNA-Methylierung des myeloischen Promotors als neuer epigenetischer Regulationsmechanismus für die Aminopeptidase wissenschaftlich belegt. Ein hoher CpG-Methylierungsgrad war invers korrelierend mit der APN-Expression. Demethylierung mittels des DNA-Analogons DAC führte nicht nur zu einer transkriptionellen und translationellen Induktion der Aminopeptidase, sondern stellte sowohl die Zytokinstimulierbarkeit des myeloischen Promotors als auch die promigratorischen Funktionen des APN-Proteins wieder her.

In einem Transfektionsmodell humaner embryonaler Nierenepithelzellen konnte eine proliferations- und migrationshemmende Wirkung der APN-Enzymaktivität nachgewiesen werden. Ein möglicher Erklärungsansatz war die verringerte Expression des Chemokinrezeptors CXCR4 in den APN-WT-Transfektanten. Zusätzlich konnte erstmalig

gezeigt werden, dass enzymatisch aktive APN die chemotaktische Migration der CXCR4-positiven Zellen zu dem korrespondierenden Liganden SDF-1 α komplett inhibiert. Weiterführende bisher unveröffentlichte Arbeiten lassen vermuten, dass APN-WT über Modifikationen des Caveolae-Strukturproteins Caveolin-1 die Internalisierung, Signalweiterleitung und differentielle Genexpression des SDF-1 α / CXCR4-Komplexes blockiert. Da APN, CXCR4 und Caveolin-1 in multiplen Prozessen der Kanzerogenese und -progression involviert sind, ist ein besseres molekulares Verständnis der in dieser Arbeit beschriebenen Prozesse von besonderem Interesse.

Des Weiteren wurde in monozytären Zellen unter Verwendung verschiedener immunologischer Analysemethoden eine starke Kolokalisation von APN mit dem Fc γ -Rezeptor II/ CD32 bzw. mit dem Fc γ -Rezeptor I/ CD64 nachgewiesen. Es wird postuliert, dass die Komplexbildung von APN mit den in der Phagozytose aktiven Rezeptoren einen neuen funktionellen Signaltransduktionsmechanismus darstellt.

7 Summary

Since many years the Institute of Medical Immunology (Medical Faculty, Martin Luther University Halle-Wittenberg, Halle (Saale), Germany) is focusing on the identification and characterization of new biomarkers as putative structures in molecular-targeted therapies for the treatment of metastatic malignant melanoma. In the present dissertation, comprehensive analyses of the expression and functional pattern of aminopeptidase N (APN)/ CD13 and the ubiquitin carboxyl-terminal hydrolase L1 (UCHL1) in a series of melanoma lesions and cell lines are described.

For the first time, it was demonstrated that the UCHL1 expression is strongly impaired by promoter DNA methylation already in benign nevi, the pre-stages of malignant melanoma transformation. In contrast to UCHL1-expressing melanocytes, the hydrolase was rarely detectable in approximately 7 % of all melanoma lesions as well as in 10 % of all (short-term) cell cultures analyzed. However, UCHL1-positive cell lines as well as respective transfectants were distinguished by improved proliferation rates through activated MAP-kinase signaling compared to UCHL1-negative cells. Since the hydrolase has also affected the cellular ROS resistance by interfering with the PI₃K/ Akt signal transduction pathway in a dose-dependent manner, UCHL1 might serve as an interesting protein candidate for the generation and establishment of a new therapy form for the treatment at least for a subset of malignant melanoma patients.

Compared to melanocytes, the induced APN expression in about 16 % of all melanoma lesions and 41 % of all cell cultures was associated with decreased amounts of diverse melanocytic markers as well as the corresponding transcription factor MITF, respectively. Although APN-positive cells shared multiple characteristics of metastatic melanoma in *in vitro*-analysis, no clinical relevance of its expression could be confirmed using IHC staining of a large series of malign tumor lesions and respective benign nevi. However, for the first time, an epigenetic regulatory mechanism by DNA methylation of the myeloid APN promoter could be recorded. Thereby, high density of CpG methylation was inversely correlated with the APN expression. Demethylation using the DNA analogue DAC in cell culture led not only to a transcriptional and translational induction of the aminopeptidase, but also restored the capability for cytokine stimulation of the respective promoter region as well as facilitated the promigratory function of the APN protein.

By characterization of a generated *in vitro*-transfection model of human embryonic kidney 293 cells it could be shown that APN with its enzymatic activity has an inhibitory potential on cellular proliferation and migration. One explanation could be the diminished

expression of the chemokine receptor CXCR4 in the wild type APN-transfectants compared to mock controls as well as to HEK293 cells expressing mutated APN-forms, respectively. Furthermore, active APN led to a complete disruption of the cell migration to the chemoattractive factor SDF-1 α , the natural CXCR4-ligand. Initial, unpublished results showed a wild type APN-mediated down-modulation of caveolin-1, the scaffolding protein within caveolar membranes, which could be causative for the interrupted CXCR4 internalization, signaling and differential gene expression after SDF-1 α stimulation. Since APN, CXCR4 and caveolin-1 are involved in manifold processes of tumorigenesis and oncogenic progression, future researches could lead to a better understanding of molecular mechanisms underlying several human carcinosis.

Using different methodological approaches a strong colocalization of APN with the Fc γ receptors CD32 and CD64 in monocytes could be verified. It was postulated by us, that the complex formation of the aminopeptidase with these receptors represents a new functional signal transduction mechanism during cellular processes such as phagocytosis.

8 Literaturverzeichnis

- [1] Nijman SM, Luna-Vargas MP, Velds A, Brummelkamp TR, Dirac AM, Sixma TK, Bernards R (2005) A genomic and functional inventory of deubiquitinating enzymes. *Cell* **123**, 773-786.
- [2] Seliger B, Handke D, Schabel E, Bukur J, Lichtenfels R, Dammann R (2009) Epigenetic control of the ubiquitin carboxyl terminal hydrolase 1 in renal cell carcinoma. *J Transl Med* **7**, 90.
- [3] Tokumaru Y, Yamashita K, Kim MS, Park HL, Osada M, Mori M, Sidransky D (2008) The role of PGP9.5 as a tumor suppressor gene in human cancer. *Int J Cancer* **123**, 753-759.
- [4] Wang R, Zhang M, Zhou W, Ly PT, Cai F, Song W (2011) NF-kappaB signaling inhibits ubiquitin carboxyl-terminal hydrolase L1 gene expression. *J Neurochem* **116**, 1160-1170.
- [5] Bheda A, Yue W, Gullapalli A, Shackelford J, Pagano JS (2011) PU.1-dependent regulation of UCH L1 expression in B-lymphoma cells. *Leuk Lymphoma* **52**, 1336-1347.
- [6] Bheda A, Yue W, Gullapalli A, Whitehurst C, Liu R, Pagano JS, Shackelford J (2009) Positive reciprocal regulation of ubiquitin C-terminal hydrolase L1 and beta-catenin/TCF signaling. *PLoS One* **4**, e5955.
- [7] Guglielmotto M, Monteleone D, Boido M, Piras A, Giliberto L, Borghi R, Vercelli A, Fornaro M, Tabaton M, Tamagno E (2012) Abeta1-42-mediated down-regulation of Uch-L1 is dependent on NF-kappaB activation and impaired BACE1 lysosomal degradation. *Aging Cell* **11**, 834-844.
- [8] Shen H, Sikorska M, Leblanc J, Walker PR, Liu QY (2006) Oxidative stress regulated expression of ubiquitin Carboxyl-terminal Hydrolase-L1: role in cell survival. *Apoptosis* **11**, 1049-1059.
- [9] Carrieri C, Cimatti L, Biagioli M, Beugnet A, Zucchelli S, Fedele S, Pesce E, Ferrer I, Collavin L, Santoro C, Forrest AR, Carninci P, Biffo S, Stupka E, Gustincich S (2012) Long non-coding antisense RNA controls Uchl1 translation through an embedded SINEB2 repeat. *Nature* **491**, 454-457.
- [10] Peng Z, Li J, Li Y, Yang X, Feng S, Han S (2013) Downregulation of miR-181b in mouse brain following ischemic stroke induces neuroprotection against ischemic injury through targeting heat shock protein A5 and ubiquitin carboxyl-terminal hydrolase isozyme L1. *J Neurosci Res* **91**, 1349-1362.
- [11] Boudreaux DA, Maiti TK, Davies CW, Das C (2010) Ubiquitin vinyl methyl ester binding orients the misaligned active site of the ubiquitin hydrolase UCHL1 into productive conformation. *Proc Natl Acad Sci U S A* **107**, 9117-9122.
- [12] Cole RN, Hart GW (2001) Cytosolic O-glycosylation is abundant in nerve terminals. *J Neurochem* **79**, 1080-1089.
- [13] Meray RK, Lansbury PT, Jr. (2007) Reversible monoubiquitination regulates the Parkinson disease-associated ubiquitin hydrolase UCH-L1. *J Biol Chem* **282**, 10567-10575.
- [14] Guingab-Cagmat JD, Stevens SM, Jr., Ratliff MV, Zhang Z, Gold MS, Anagli J, Wang KK, Kobeissy FH (2011) Identification of tyrosine nitration in UCH-L1 and GAPDH. *Electrophoresis* **32**, 1692-1705.
- [15] Lowe J, McDermott H, Landon M, Mayer RJ, Wilkinson KD (1990) Ubiquitin carboxyl-terminal hydrolase (PGP 9.5) is selectively present in ubiquitinated inclusion bodies characteristic of human neurodegenerative diseases. *J Pathol* **161**, 153-160.
- [16] Caballero OL, Resto V, Patturajan M, Meerzaman D, Guo MZ, Engles J, Yochem R, Ratovitski E, Sidransky D, Jen J (2002) Interaction and colocalization of PGP9.5 with JAB1 and p27(Kip1). *Oncogene* **21**, 3003-3010.

- [17] Bheda A, Gullapalli A, Caplow M, Pagano JS, Shackelford J (2010) Ubiquitin editing enzyme UCH L1 and microtubule dynamics: implication in mitosis. *Cell Cycle* **9**, 980-994.
- [18] Liu Z, Meray RK, Grammatopoulos TN, Fredenburg RA, Cookson MR, Liu Y, Logan T, Lansbury PT, Jr. (2009) Membrane-associated farnesylated UCH-L1 promotes alpha-synuclein neurotoxicity and is a therapeutic target for Parkinson's disease. *Proc Natl Acad Sci U S A* **106**, 4635-4640.
- [19] Wilkinson KD, Lee KM, Deshpande S, Duerksen-Hughes P, Boss JM, Pohl J (1989) The neuron-specific protein PGP 9.5 is a ubiquitin carboxyl-terminal hydrolase. *Science* **246**, 670-673.
- [20] Shirato I, Asanuma K, Takeda Y, Hayashi K, Tomino Y (2000) Protein gene product 9.5 is selectively localized in parietal epithelial cells of Bowman's capsule in the rat kidney. *J Am Soc Nephrol* **11**, 2381-2386.
- [21] Diomed-Camassei F, Rava L, Lerut E, Callea F, Van Damme B (2005) Protein gene product 9.5 and ubiquitin are expressed in metabolically active epithelial cells of normal and pathologic human kidney. *Nephrol Dial Transplant* **20**, 2714-2719.
- [22] Sekiguchi S, Kwon J, Yoshida E, Hamasaki H, Ichinose S, Hideshima M, Kuraoka M, Takahashi A, Ishii Y, Kyuwa S, Wada K, Yoshikawa Y (2006) Localization of ubiquitin C-terminal hydrolase L1 in mouse ova and its function in the plasma membrane to block polyspermy. *Am J Pathol* **169**, 1722-1729.
- [23] von Kopylow K, Kirchhoff C, Jezek D, Schulze W, Feig C, Primig M, Steinkraus V, Spiess AN (2010) Screening for biomarkers of spermatogonia within the human testis: a whole genome approach. *Hum Reprod* **25**, 1104-1112.
- [24] Luchansky SJ, Lansbury PT, Jr., Stein RL (2006) Substrate recognition and catalysis by UCH-L1. *Biochemistry* **45**, 14717-14725.
- [25] Setsue R, Wada K (2007) The functions of UCH-L1 and its relation to neurodegenerative diseases. *Neurochem Int* **51**, 105-111.
- [26] Liu Y, Fallon L, Lashuel HA, Liu Z, Lansbury PT, Jr. (2002) The UCH-L1 gene encodes two opposing enzymatic activities that affect alpha-synuclein degradation and Parkinson's disease susceptibility. *Cell* **111**, 209-218.
- [27] Yi YJ, Manandhar G, Sutovsky M, Li R, Jonakova V, Oko R, Park CS, Prather RS, Sutovsky P (2007) Ubiquitin C-terminal hydrolase-activity is involved in sperm acrosomal function and anti-polyspermy defense during porcine fertilization. *Biol Reprod* **77**, 780-793.
- [28] Kwon J, Kikuchi T, Setsue R, Ishii Y, Kyuwa S, Yoshikawa Y (2003) Characterization of the testis in congenitally ubiquitin carboxy-terminal hydrolase-1 (Uch-L1) defective (gad) mice. *Exp Anim* **52**, 1-9.
- [29] Chu KY, Li H, Wada K, Johnson JD (2012) Ubiquitin C-terminal hydrolase L1 is required for pancreatic beta cell survival and function in lipotoxic conditions. *Diabetologia* **55**, 128-140.
- [30] Hurst-Kennedy J, Chin LS, Li L (2012) Ubiquitin C-terminal hydrolase L1 in tumorigenesis. *Biochem Res Int* **2012**, 123706.
- [31] Hibi K, Westra WH, Borges M, Goodman S, Sidransky D, Jen J (1999) PGP9.5 as a candidate tumor marker for non-small-cell lung cancer. *Am J Pathol* **155**, 711-715.
- [32] Takano T, Miyauchi A, Matsuzuka F, Yoshida H, Nakata Y, Kuma K, Amino N (2004) PGP9.5 mRNA could contribute to the molecular-based diagnosis of medullary thyroid carcinoma. *Eur J Cancer* **40**, 614-618.
- [33] Tezel E, Hibi K, Nagasaka T, Nakao A (2000) PGP9.5 as a prognostic factor in pancreatic cancer. *Clin Cancer Res* **6**, 4764-4767.
- [34] Yanagisawa TY, Sasahara Y, Fujie H, Ohashi Y, Minegishi M, Itano M, Morita S, Tsuchiya S, Hayashi Y, Ohi R, Konno T (1998) Detection of the PGP9.5 and tyrosine hydroxylase mRNAs for minimal residual neuroblastoma cells in bone marrow and peripheral blood. *Tohoku J Exp Med* **184**, 229-240.

- [35] Jin C, Yu W, Lou X, Zhou F, Han X, Zhao N, Lin B (2013) UCHL1 Is a Putative Tumor Suppressor in Ovarian Cancer Cells and Contributes to Cisplatin Resistance. *J Cancer* **4**, 662-670.
- [36] Mitsui Y, Shiina H, Hiraki M, Arichi N, Hiraoka T, Sumura M, Honda S, Yasumoto H, Igawa M (2012) Tumor suppressor function of PGP9.5 is associated with epigenetic regulation in prostate cancer--novel predictor of biochemical recurrence after radical surgery. *Cancer Epidemiol Biomarkers Prev* **21**, 487-496.
- [37] Okochi-Takada E, Nakazawa K, Wakabayashi M, Mori A, Ichimura S, Yasugi T, Ushijima T (2006) Silencing of the UCHL1 gene in human colorectal and ovarian cancers. *Int J Cancer* **119**, 1338-1344.
- [38] Ummanni R, Jost E, Braig M, Lohmann F, Mundt F, Barrett C, Schlomm T, Sauter G, Senff T, Bokemeyer C, Sultmann H, Meyer-Schwesinger C, Brummendorf TH, Balabanov S (2011) Ubiquitin carboxyl-terminal hydrolase 1 (UCHL1) is a potential tumour suppressor in prostate cancer and is frequently silenced by promoter methylation. *Mol Cancer* **10**, 129.
- [39] Yu J, Tao Q, Cheung KF, Jin H, Poon FF, Wang X, Li H, Cheng YY, Rocken C, Ebert MP, Chan AT, Sung JJ (2008) Epigenetic identification of ubiquitin carboxyl-terminal hydrolase L1 as a functional tumor suppressor and biomarker for hepatocellular carcinoma and other digestive tumors. *Hepatology* **48**, 508-518.
- [40] Lien HC, Wang CC, Lin CH, Lu YS, Huang CS, Hsiao LP, Yao YT (2013) Differential expression of ubiquitin carboxy-terminal hydrolase L1 in breast carcinoma and its biological significance. *Hum Pathol* **44**, 1838-1848.
- [41] Yamazaki T, Hibi K, Takase T, Tezel E, Nakayama H, Kasai Y, Ito K, Akiyama S, Nagasaka T, Nakao A (2002) PGP9.5 as a marker for invasive colorectal cancer. *Clin Cancer Res* **8**, 192-195.
- [42] Ma Y, Zhao M, Zhong J, Shi L, Luo Q, Liu J, Wang J, Yuan X, Huang C (2010) Proteomic profiling of proteins associated with lymph node metastasis in colorectal cancer. *J Cell Biochem* **110**, 1512-1519.
- [43] Orr KS, Shi Z, Brown WM, O'Hagan KA, Lappin TR, Maxwell P, Percy MJ (2011) Potential prognostic marker ubiquitin carboxyl-terminal hydrolase-L1 does not predict patient survival in non-small cell lung carcinoma. *J Exp Clin Cancer Res* **30**, 79.
- [44] Lee YM, Lee JY, Kim MJ, Bae HI, Park JY, Kim SG, Kim DS (2006) Hypomethylation of the protein gene product 9.5 promoter region in gallbladder cancer and its relationship with clinicopathological features. *Cancer Sci* **97**, 1205-1210.
- [45] Howell VM, Gill A, Clarkson A, Nelson AE, Dunne R, Delbridge LW, Robinson BG, Teh BT, Gimm O, Marsh DJ (2009) Accuracy of combined protein gene product 9.5 and parafibromin markers for immunohistochemical diagnosis of parathyroid carcinoma. *J Clin Endocrinol Metab* **94**, 434-441.
- [46] Seliger B, Fedorushchenko A, Brenner W, Ackermann A, Atkins D, Hanash S, Lichtenfels R (2007) Ubiquitin COOH-terminal hydrolase 1: a biomarker of renal cell carcinoma associated with enhanced tumor cell proliferation and migration. *Clin Cancer Res* **13**, 27-37.
- [47] Fang Y, Fu D, Shen XZ (2010) The potential role of ubiquitin c-terminal hydrolases in oncogenesis. *Biochim Biophys Acta* **1806**, 1-6.
- [48] Jang MJ, Baek SH, Kim JH (2011) UCH-L1 promotes cancer metastasis in prostate cancer cells through EMT induction. *Cancer Lett* **302**, 128-135.
- [49] Borriello A, Bencivenga D, Criscuolo M, Caldarelli I, Cucciolla V, Tramontano A, Borgia A, Spina A, Oliva A, Naviglio S, Della Ragione F (2011) Targeting p27Kip1 protein: its relevance in the therapy of human cancer. *Expert Opin Ther Targets* **15**, 677-693.
- [50] Xiang T, Li L, Yin X, Yuan C, Tan C, Su X, Xiong L, Putti TC, Oberst M, Kelly K, Ren G, Tao Q (2012) The ubiquitin peptidase UCHL1 induces G0/G1 cell cycle arrest and apoptosis through stabilizing p53 and is frequently silenced in breast cancer. *PLoS One* **7**, e29783.

- [51] Li L, Tao Q, Jin H, van Hasselt A, Poon FF, Wang X, Zeng MS, Jia WH, Zeng YX, Chan AT, Cao Y (2010) The tumor suppressor UCHL1 forms a complex with p53/MDM2/ARF to promote p53 signaling and is frequently silenced in nasopharyngeal carcinoma. *Clin Cancer Res* **16**, 2949-2958.
- [52] Wang WJ, Li QQ, Xu JD, Cao XX, Li HX, Tang F, Chen Q, Yang JM, Xu ZD, Liu XP (2008) Over-expression of ubiquitin carboxy terminal hydrolase-L1 induces apoptosis in breast cancer cells. *Int J Oncol* **33**, 1037-1045.
- [53] Takami Y, Nakagami H, Morishita R, Katsuya T, Cui TX, Ichikawa T, Saito Y, Hayashi H, Kikuchi Y, Nishikawa T, Baba Y, Yasuda O, Rakugi H, Ogihara T, Kaneda Y (2007) Ubiquitin carboxyl-terminal hydrolase L1, a novel deubiquitinating enzyme in the vasculature, attenuates NF-kappaB activation. *Arterioscler Thromb Vasc Biol* **27**, 2184-2190.
- [54] Kim HJ, Kim YM, Lim S, Nam YK, Jeong J, Lee KJ (2009) Ubiquitin C-terminal hydrolase-L1 is a key regulator of tumor cell invasion and metastasis. *Oncogene* **28**, 117-127.
- [55] Hussain S, Foreman O, Perkins SL, Witzig TE, Miles RR, van Deursen J, Galardy PJ (2010) The de-ubiquitinase UCH-L1 is an oncogene that drives the development of lymphoma in vivo by deregulating PHLPP1 and Akt signaling. *Leukemia* **24**, 1641-1655.
- [56] Carnero A (2010) The PKB/AKT pathway in cancer. *Curr Pharm Des* **16**, 34-44.
- [57] Basseres E, Coppotelli G, Pfirrmann T, Andersen JB, Masucci M, Frisan T (2010) The ubiquitin C-terminal hydrolase UCH-L1 promotes bacterial invasion by altering the dynamics of the actin cytoskeleton. *Cell Microbiol* **12**, 1622-1633.
- [58] Zhu K, Kong X, Zhao D, Liang Z, Luo C (2014) c-MET kinase inhibitors: a patent review (2011 - 2013). *Expert Opin Ther Pat* **24**, 217-230.
- [59] Shapiro LH, Ashmun RA, Roberts WM, Look AT (1991) Separate promoters control transcription of the human aminopeptidase N gene in myeloid and intestinal epithelial cells. *J Biol Chem* **266**, 11999-12007.
- [60] Bhagwat SV, Lahdenranta J, Giordano R, Arap W, Pasqualini R, Shapiro LH (2001) CD13/APN is activated by angiogenic signals and is essential for capillary tube formation. *Blood* **97**, 652-659.
- [61] Olsen J, Classen-Linke I, Sjostrom H, Noren O (1995) Pseudopregnancy induces the expression of hepatocyte nuclear factor-1 beta and its target gene aminopeptidase N in rabbit endometrium via the epithelial promoter. *Biochem J* **312 (Pt 1)**, 31-37.
- [62] Olsen J, Kokholm K, Noren O, Sjostrom H (1997) Structure and expression of aminopeptidase N. *Adv Exp Med Biol* **421**, 47-57.
- [63] Olsen J, Kokholm K, Troelsen JT, Laustsen L (1997) An enhancer with cell-type dependent activity is located between the myeloid and epithelial aminopeptidase N (CD 13) promoters. *Biochem J* **322 (Pt 3)**, 899-908.
- [64] Olsen J, Laustsen L, Karnstrom U, Sjostrom H, Noren O (1991) Tissue-specific interactions between nuclear proteins and the aminopeptidase N promoter. *J Biol Chem* **266**, 18089-18096.
- [65] Hedge SP, Kumar A, Kurschner C, Shapiro LH (1998) c-Maf interacts with c-Myb to regulate transcription of an early myeloid gene during differentiation. *Mol Cell Biol* **18**, 2729-2737.
- [66] Shapiro LH (1995) Myb and Ets proteins cooperate to transactivate an early myeloid gene. *J Biol Chem* **270**, 8763-8771.
- [67] Yang C, Shapiro LH, Rivera M, Kumar A, Brindle PK (1998) A role for CREB binding protein and p300 transcriptional coactivators in Ets-1 transactivation functions. *Mol Cell Biol* **18**, 2218-2229.
- [68] Noren K, Hansen GH, Clausen H, Noren O, Sjostrom H, Vogel LK (1997) Defectively N-glycosylated and non-O-glycosylated aminopeptidase N (CD13) is normally expressed at the cell surface and has full enzymatic activity. *Exp Cell Res* **231**, 112-118.

- [69] Maroux S, Louvard D, Baratti J (1973) The aminopeptidase from hog intestinal brush border. *Biochim Biophys Acta* **321**, 282-295.
- [70] Sjostrom H, Noren O, Danielsen EM, Skovbjerg H (1983) Structure of microvillar enzymes in different phases of their life cycles. *Ciba Found Symp* **95**, 50-72.
- [71] Hussain MM, Trantum-Jensen J, Noren O, Sjostrom H, Christiansen K (1981) Reconstitution of purified amphiphilic pig intestinal microvillus aminopeptidase. Mode of membrane insertion and morphology. *Biochem J* **199**, 179-186.
- [72] Sjostrom H, Noren O, Olsen J (2000) Structure and function of aminopeptidase N. *Adv Exp Med Biol* **477**, 25-34.
- [73] Hooper NM, Hesp RJ, Tiekou S (1994) Metabolism of aspartame by human and pig intestinal microvillar peptidases. *Biochem J* **298 Pt 3**, 635-639.
- [74] Luciani N, Marie-Claire C, Ruffet E, Beaumont A, Roques BP, Fournie-Zaluski MC (1998) Characterization of Glu350 as a critical residue involved in the N-terminal amine binding site of aminopeptidase N (EC 3.4.11.2): insights into its mechanism of action. *Biochemistry* **37**, 686-692.
- [75] Wong AH, Zhou D, Rini JM (2012) The X-ray crystal structure of human aminopeptidase N reveals a novel dimer and the basis for peptide processing. *J Biol Chem* **287**, 36804-36813.
- [76] Hooper NM (1994) Families of zinc metalloproteases. *FEBS Lett* **354**, 1-6.
- [77] Kotlo K, Shukla S, Tawar U, Skidgel RA, Danziger RS (2007) Aminopeptidase N reduces basolateral Na⁺-K⁺-ATPase in proximal tubule cells. *Am J Physiol Renal Physiol* **293**, F1047-1053.
- [78] Danziger RS (2008) Aminopeptidase N in arterial hypertension. *Heart Fail Rev* **13**, 293-298.
- [79] Mina-Osorio P (2008) The moonlighting enzyme CD13: old and new functions to target. *Trends Mol Med* **14**, 361-371.
- [80] Mina-Osorio P, Winnicka B, O'Connor C, Grant CL, Vogel LK, Rodriguez-Pinto D, Holmes KV, Ortega E, Shapiro LH (2008) CD13 is a novel mediator of monocytic/endothelial cell adhesion. *J Leukoc Biol* **84**, 448-459.
- [81] Petrovic N, Schacke W, Gahagan JR, O'Connor CA, Winnicka B, Conway RE, Mina-Osorio P, Shapiro LH (2007) CD13/APN regulates endothelial invasion and filopodia formation. *Blood* **110**, 142-150.
- [82] Tani K, Ogushi F, Huang L, Kawano T, Tada H, Hariguchi N, Sone S (2000) CD13/aminopeptidase N, a novel chemoattractant for T lymphocytes in pulmonary sarcoidosis. *Am J Respir Crit Care Med* **161**, 1636-1642.
- [83] Jung K, Pergande M, Wischke UW (1984) Characterization of particulate and soluble variants of the brush-border enzymes alanine aminopeptidase, alkaline phosphatase and gamma-glutamyltransferase in human urine. *Biomed Biochim Acta* **43**, 1357-1364.
- [84] Lees T, Mantle D, Walker D, Jones P, Blake D (1991) Identification of aminopeptidases in synovial fluid from rheumatoid arthritis patients. *Biochem Soc Trans* **19**, 215S.
- [85] Favaloro EJ, Browning T, Facey D (1993) CD13 (GP150; aminopeptidase-N): predominant functional activity in blood is localized to plasma and is not cell-surface associated. *Exp Hematol* **21**, 1695-1701.
- [86] Lendeckel U, Kahne T, Riemann D, Neubert K, Arndt M, Reinhold D (2000) Review: the role of membrane peptidases in immune functions. *Adv Exp Med Biol* **477**, 1-24.
- [87] Ansorge S, Bank U, Heimburg A, Helmuth M, Koch G, Tadge J, Lendeckel U, Wolke C, Neubert K, Faust J, Fuchs P, Reinhold D, Thielitz A, Tager M (2009) Recent insights into the role of dipeptidyl aminopeptidase IV (DPIV) and aminopeptidase N (APN) families in immune functions. *Clin Chem Lab Med* **47**, 253-261.
- [88] Calloni R, Cordero EA, Henriques JA, Bonatto D (2013) Reviewing and updating the major molecular markers for stem cells. *Stem Cells Dev* **22**, 1455-1476.

- [89] Razak K, Newland AC (1992) The significance of aminopeptidases and haematopoietic cell differentiation. *Blood Rev* **6**, 243-250.
- [90] Mina-Osorio P, Shapiro LH, Ortega E (2006) CD13 in cell adhesion: aminopeptidase N (CD13) mediates homotypic aggregation of monocytic cells. *J Leukoc Biol* **79**, 719-730.
- [91] Proost P, Mortier A, Loos T, Vandercappellen J, Gouwy M, Ronsse I, Schutyser E, Put W, Parmentier M, Struyf S, Van Damme J (2007) Proteolytic processing of CXCL11 by CD13/aminopeptidase N impairs CXCR3 and CXCR7 binding and signaling and reduces lymphocyte and endothelial cell migration. *Blood* **110**, 37-44.
- [92] Larsen SL, Pedersen LO, Buus S, Stryhn A (1996) T cell responses affected by aminopeptidase N (CD13)-mediated trimming of major histocompatibility complex class II-bound peptides. *J Exp Med* **184**, 183-189.
- [93] Cowburn AS, Sobolewski A, Reed BJ, Deighton J, Murray J, Cadwallader KA, Bradley JR, Chilvers ER (2006) Aminopeptidase N (CD13) regulates tumor necrosis factor-alpha-induced apoptosis in human neutrophils. *J Biol Chem* **281**, 12458-12467.
- [94] Van Hal PT, Hopstaken-Broos JP, Wijkhuijs JM, Te Velde AA, Figdor CG, Hoogsteden HC (1992) Regulation of aminopeptidase-N (CD13) and Fc epsilon RIIB (CD23) expression by IL-4 depends on the stage of maturation of monocytes/macrophages. *J Immunol* **149**, 1395-1401.
- [95] de Waal Malefyt R, Figdor CG, Huijbens R, Mohan-Peterson S, Bennett B, Culpepper J, Dang W, Zurawski G, de Vries JE (1993) Effects of IL-13 on phenotype, cytokine production, and cytotoxic function of human monocytes. Comparison with IL-4 and modulation by IFN-gamma or IL-10. *J Immunol* **151**, 6370-6381.
- [96] Tangada SD, Peterson RD, Funkhouser JD (1995) Regulation of expression of aminopeptidase N in fetal rat lung by dexamethasone and epidermal growth factor. *Biochim Biophys Acta* **1268**, 191-199.
- [97] Fontijn D, Duyndam MC, van Berkel MP, Yuana Y, Shapiro LH, Pinedo HM, Broxterman HJ, Boven E (2006) CD13/Aminopeptidase N overexpression by basic fibroblast growth factor mediates enhanced invasiveness of 1F6 human melanoma cells. *Br J Cancer* **94**, 1627-1636.
- [98] Cohen A, Petsche D, Grunberger T, Freedman MH (1992) Interleukin 6 induces myeloid differentiation of a human biphenotypic leukemic cell line. *Leuk Res* **16**, 751-760.
- [99] Hatanaka Y, Ashida H, Hashizume K, Fukuda I, Sano T, Yamaguchi Y, Endo T, Tani Y, Suzukia K, Danno G (2002) Up-regulation of CD13/aminopeptidase N induced by phorbol ester is involved in redox regulation and tumor necrosis factor alpha production in HL-60 cells. *Inflammation* **26**, 175-181.
- [100] Kehlen A, Langner J, Riemann D (2000) Transforming growth factor-beta increases the expression of aminopeptidase N/CD13 mRNA and protein in monocytes and monocytic cell lines. *Adv Exp Med Biol* **477**, 49-56.
- [101] Kehlen A, Geisler M, Olsen J, Sablotzki A, Langner J, Riemann D (2004) IL-10 and TGF-beta differ in their regulation of aminopeptidase N/CD13 expression in monocytes. *Int J Mol Med* **13**, 877-882.
- [102] Kehlen A, Gohring B, Langner J, Riemann D (1998) Regulation of the expression of aminopeptidase A, aminopeptidase N/CD13 and dipeptidylpeptidase IV/CD26 in renal carcinoma cells and renal tubular epithelial cells by cytokines and cAMP-increasing mediators. *Clin Exp Immunol* **111**, 435-441.
- [103] Riemann D, Kehlen A, Langner J (1995) Stimulation of the expression and the enzyme activity of aminopeptidase N/CD13 and dipeptidylpeptidase IV/CD26 on human renal cell carcinoma cells and renal tubular epithelial cells by T cell-derived cytokines, such as IL-4 and IL-13. *Clin Exp Immunol* **100**, 277-283.
- [104] Kehlen A, Egbert I, Thiele K, Fischer K, Riemann D, Langner J (2001) Increased expression of interleukin-8 and aminopeptidase N by cell-cell contact: interleukin-8

- is resistant to degradation by aminopeptidase N/CD13. *Eur Cytokine Netw* **12**, 316-324.
- [105] Kehlen A, Olsen J, Langner J, Riemann D (2000) Increased lymphocytic aminopeptidase N/CD13 promoter activity after cell-cell contact. *J Cell Biochem* **80**, 115-123.
- [106] Riemann D, Kehlen A, Thiele K, Lohn M, Langner J (1997) Induction of aminopeptidase N/CD13 on human lymphocytes after adhesion to fibroblast-like synoviocytes, endothelial cells, epithelial cells, and monocytes/macrophages. *J Immunol* **158**, 3425-3432.
- [107] Riemann D, Kehlen A, Thiele K, Lohn M, Langner J (1997) Co-incubation of lymphocytes with fibroblast-like synoviocytes and other cell types can induce lymphocytic surface expression of aminopeptidase N/CD13. *Adv Exp Med Biol* **421**, 75-79.
- [108] Huschak G, Zur Nieden K, Stuttmann R, Riemann D (2003) Changes in monocytic expression of aminopeptidase N/CD13 after major trauma. *Clin Exp Immunol* **134**, 491-496.
- [109] Schroeter P, Sablotzki A, Riemann D (2007) CD13 and CD10 expression of granulocytes as markers for the functioning of the immune system: quantification of the expression of membrane molecules using 1:1 labeled monoclonal antibodies and flow cytometry. *Methods Mol Biol* **378**, 71-81.
- [110] Kolb AF, Hegyi A, Maile J, Heister A, Hagemann M, Siddell SG (1998) Molecular analysis of the coronavirus-receptor function of aminopeptidase N. *Adv Exp Med Biol* **440**, 61-67.
- [111] Kolb AF, Hegyi A, Siddell SG (1997) Identification of residues critical for the human coronavirus 229E receptor function of human aminopeptidase N. *J Gen Virol* **78 (Pt 11)**, 2795-2802.
- [112] Soderberg C, Giugni TD, Zaia JA, Larsson S, Wahlberg JM, Moller E (1993) CD13 (human aminopeptidase N) mediates human cytomegalovirus infection. *J Virol* **67**, 6576-6585.
- [113] Nomura R, Kiyota A, Suzaki E, Kataoka K, Ohe Y, Miyamoto K, Senda T, Fujimoto T (2004) Human coronavirus 229E binds to CD13 in rafts and enters the cell through caveolae. *J Virol* **78**, 8701-8708.
- [114] Hansen GH, Niels-Christiansen LL, Immerdal L, Hunziker W, Kenny AJ, Danielsen EM (1999) Transcytosis of immunoglobulin A in the mouse enterocyte occurs through glycolipid raft- and rab17-containing compartments. *Gastroenterology* **116**, 610-622.
- [115] Kramer W, Girbig F, Corsiero D, Pfenninger A, Frick W, Jahne G, Rhein M, Wendler W, Lottspeich F, Hochleitner EO, Orso E, Schmitz G (2005) Aminopeptidase N (CD13) is a molecular target of the cholesterol absorption inhibitor ezetimibe in the enterocyte brush border membrane. *J Biol Chem* **280**, 1306-1320.
- [116] Riemann D, Hansen GH, Niels-Christiansen L, Thorsen E, Immerdal L, Santos AN, Kehlen A, Langner J, Danielsen EM (2001) Caveolae/lipid rafts in fibroblast-like synoviocytes: ectopeptidase-rich membrane microdomains. *Biochem J* **354**, 47-55.
- [117] Navarrete Santos A, Roentsch J, Danielsen EM, Langner J, Riemann D (2000) Aminopeptidase N/CD13 is associated with raft membrane microdomains in monocytes. *Biochem Biophys Res Commun* **269**, 143-148.
- [118] Estey EH (2013) Acute myeloid leukemia: 2013 update on risk-stratification and management. *Am J Hematol* **88**, 318-327.
- [119] Riemann D, Kehlen A, Langner J (1999) CD13--not just a marker in leukemia typing. *Immunol Today* **20**, 83-88.
- [120] Imamura N, Kimura A (2000) Effect of ubenimex (Bestatin) on the cell growth and phenotype of HL-60 and HL-60R cell lines: up-and down-regulation of CD13/aminopeptidase N. *Leuk Lymphoma* **37**, 663-667.

- [121] Lohn M, Mueller C, Thiele K, Kahne T, Riemann D, Langner J (1997) Aminopeptidase N-mediated signal transduction and inhibition of proliferation of human myeloid cells. *Adv Exp Med Biol* **421**, 85-91.
- [122] Wex T, Lendeckel U, Reinhold D, Kahne T, Arndt M, Frank K, Ansorge S (1997) Antisense-mediated inhibition of aminopeptidase N (CD13) markedly decreases growth rates of hematopoietic tumour cells. *Adv Exp Med Biol* **421**, 67-73.
- [123] Alfalah M, Krahn MP, Wetzel G, von Horsten S, Wolke C, Hooper N, Kalinski T, Krueger S, Naim HY, Lendeckel U (2006) A mutation in aminopeptidase N (CD13) isolated from a patient suffering from leukemia leads to an arrest in the endoplasmic reticulum. *J Biol Chem* **281**, 11894-11900.
- [124] Dybkaer K, Kristensen JS, Pedersen FS (2001) Single site polymorphisms and alternative splicing of the human CD13 gene--different splicing frequencies among patients with acute myeloid leukaemia and healthy individuals. *Br J Haematol* **112**, 691-696.
- [125] Lendeckel U, Arndt M, Frank K, Wex T, Ansorge S (1999) Role of alanyl aminopeptidase in growth and function of human T cells (review). *Int J Mol Med* **4**, 17-27.
- [126] Ikeda N, Nakajima Y, Tokuhara T, Hattori N, Sho M, Kanehiro H, Miyake M (2003) Clinical significance of aminopeptidase N/CD13 expression in human pancreatic carcinoma. *Clin Cancer Res* **9**, 1503-1508.
- [127] Kehlen A, Lendeckel U, Dralle H, Langner J, Hoang-Vu C (2003) Biological significance of aminopeptidase N/CD13 in thyroid carcinomas. *Cancer Res* **63**, 8500-8506.
- [128] Perez I, Varona A, Blanco L, Gil J, Santaolalla F, Zabala A, Ibarguen AM, Irazusta J, Larrinaga G (2009) Increased APN/CD13 and acid aminopeptidase activities in head and neck squamous cell carcinoma. *Head Neck* **31**, 1335-1340.
- [129] Tokuhara T, Hattori N, Ishida H, Hirai T, Higashiyama M, Kodama K, Miyake M (2006) Clinical significance of aminopeptidase N in non-small cell lung cancer. *Clin Cancer Res* **12**, 3971-3978.
- [130] Hashida H, Takabayashi A, Kanai M, Adachi M, Kondo K, Kohno N, Yamaoka Y, Miyake M (2002) Aminopeptidase N is involved in cell motility and angiogenesis: its clinical significance in human colon cancer. *Gastroenterology* **122**, 376-386.
- [131] Murakami H, Yokoyama A, Kondo K, Nakanishi S, Kohno N, Miyake M (2005) Circulating aminopeptidase N/CD13 is an independent prognostic factor in patients with non-small cell lung cancer. *Clin Cancer Res* **11**, 8674-8679.
- [132] Sorensen KD, Abildgaard MO, Haldrup C, Ulhøi BP, Kristensen H, Strand S, Parker C, Hoyer S, Borre M, Orntoft TF (2013) Prognostic significance of aberrantly silenced ANPEP expression in prostate cancer. *Br J Cancer* **108**, 420-428.
- [133] Mawrin C, Wolke C, Haase D, Kruger S, Firsching R, Keilhoff G, Paulus W, Gutmann DH, Lal A, Lendeckel U (2010) Reduced activity of CD13/aminopeptidase N (APN) in aggressive meningiomas is associated with increased levels of SPARC. *Brain Pathol* **20**, 200-210.
- [134] Gohring B, Holzhausen HJ, Meye A, Heynemann H, Rebmann U, Langner J, Riemann D (1998) Endopeptidase 24.11/CD10 is down-regulated in renal cell cancer. *Int J Mol Med* **2**, 409-414.
- [135] Riemann D, Gohring B, Langner J (1994) Expression of aminopeptidase N/CD13 in tumour-infiltrating lymphocytes from human renal cell carcinoma. *Immunol Lett* **42**, 19-23.
- [136] Razvi MH, Peng D, Dar AA, Powell SM, Frierson HF, Jr., Moskaluk CA, Washington K, El-Rifai W (2007) Transcriptional oncogenomic hot spots in Barrett's adenocarcinomas: serial analysis of gene expression. *Genes Chromosomes Cancer* **46**, 914-928.
- [137] Kawamura J, Shimada Y, Kitaichi H, Komoto I, Hashimoto Y, Kaganoi J, Miyake M, Yamasaki S, Kondo K, Imamura M (2007) Clinicopathological significance of

- aminopeptidase N/CD13 expression in human gastric carcinoma. *Hepatogastroenterology* **54**, 36-40.
- [138] Zhu J, He J, Liu Y, Simeone DM, Lubman DM (2012) Identification of glycoprotein markers for pancreatic cancer CD24+CD44+ stem-like cells using nano-LC-MS/MS and tissue microarray. *J Proteome Res* **11**, 2272-2281.
- [139] Rocken C, Licht J, Roessner A, Carl-McGrath S (2005) Canalicular immunostaining of aminopeptidase N (CD13) as a diagnostic marker for hepatocellular carcinoma. *J Clin Pathol* **58**, 1069-1075.
- [140] Ranogajec I, Jakic-Razumovic J, Puzovic V, Gabrilovac J (2012) Prognostic value of matrix metalloproteinase-2 (MMP-2), matrix metalloproteinase-9 (MMP-9) and aminopeptidase N/CD13 in breast cancer patients. *Med Oncol* **29**, 561-569.
- [141] Bogenrieder T, Finstad CL, Freeman RH, Papandreou CN, Scher HI, Albino AP, Reuter VE, Nanus DM (1997) Expression and localization of aminopeptidase A, aminopeptidase N, and dipeptidyl peptidase IV in benign and malignant human prostate tissue. *Prostate* **33**, 225-232.
- [142] Fujii H, Nakajima M, Saiki I, Yoneda J, Azuma I, Tsuruo T (1995) Human melanoma invasion and metastasis enhancement by high expression of aminopeptidase N/CD13. *Clin Exp Metastasis* **13**, 337-344.
- [143] Ishii K, Usui S, Sugimura Y, Yoshida S, Hioki T, Tatematsu M, Yamamoto H, Hirano K (2001) Aminopeptidase N regulated by zinc in human prostate participates in tumor cell invasion. *Int J Cancer* **92**, 49-54.
- [144] Kido A, Krueger S, Haeckel C, Roessner A (2003) Inhibitory effect of antisense aminopeptidase N (APN/CD13) cDNA transfection on the invasive potential of osteosarcoma cells. *Clin Exp Metastasis* **20**, 585-592.
- [145] Menrad A, Speicher D, Wacker J, Herlyn M (1993) Biochemical and functional characterization of aminopeptidase N expressed by human melanoma cells. *Cancer Res* **53**, 1450-1455.
- [146] Saiki I, Fujii H, Yoneda J, Abe F, Nakajima M, Tsuruo T, Azuma I (1993) Role of aminopeptidase N (CD13) in tumor-cell invasion and extracellular matrix degradation. *Int J Cancer* **54**, 137-143.
- [147] van Hensbergen Y, Broxterman HJ, Rana S, van Diest PJ, Duyndam MC, Hoekman K, Pinedo HM, Boven E (2004) Reduced growth, increased vascular area, and reduced response to cisplatin in CD13-overexpressing human ovarian cancer xenografts. *Clin Cancer Res* **10**, 1180-1191.
- [148] Tsukamoto H, Shibata K, Kajiyama H, Terauchi M, Nawa A, Kikkawa F (2008) Aminopeptidase N (APN)/CD13 inhibitor, Ubenimex, enhances radiation sensitivity in human cervical cancer. *BMC Cancer* **8**, 74.
- [149] Seliger B, Dressler SP, Massa C, Recktenwald CV, Altenberend F, Bukur J, Marincola FM, Wang E, Stevanovic S, Lichtenfels R (2011) Identification and characterization of human leukocyte antigen class I ligands in renal cell carcinoma cells. *Proteomics* **11**, 2528-2541.
- [150] Bonazzi VF, Nancarrow DJ, Stark MS, Moser RJ, Boyle GM, Aoude LG, Schmidt C, Hayward NK (2011) Cross-platform array screening identifies COL1A2, THBS1, TNFRSF10D and UCHL1 as genes frequently silenced by methylation in melanoma. *PLoS One* **6**, e26121.
- [151] Brinkmann K, Zigrino P, Witt A, Schell M, Ackermann L, Broxtermann P, Schull S, Andree M, Coutelle O, Yazdanpanah B, Seeger JM, Klubertz D, Drebber U, Hacker UT, Kronke M, Mauch C, Hoppe T, Kashkar H (2013) Ubiquitin C-terminal hydrolase-L1 potentiates cancer chemosensitivity by stabilizing NOXA. *Cell Rep* **3**, 881-891.
- [152] Hoek K, Rimm DL, Williams KR, Zhao H, Ariyan S, Lin A, Kluger HM, Berger AJ, Cheng E, Trombetta ES, Wu T, Niinobe M, Yoshikawa K, Hannigan GE, Halaban R (2004) Expression profiling reveals novel pathways in the transformation of melanocytes to melanomas. *Cancer Res* **64**, 5270-5282.
- [153] Mandelker DL, Yamashita K, Tokumaru Y, Mimori K, Howard DL, Tanaka Y, Carvalho AL, Jiang WW, Park HL, Kim MS, Osada M, Mori M, Sidransky D (2005)

- PGP9.5 promoter methylation is an independent prognostic factor for esophageal squamous cell carcinoma. *Cancer Res* **65**, 4963-4968.
- [154] Mizukami H, Shirahata A, Goto T, Sakata M, Saito M, Ishibashi K, Kigawa G, Nemoto H, Sanada Y, Hibi K (2008) PGP9.5 methylation as a marker for metastatic colorectal cancer. *Anticancer Res* **28**, 2697-2700.
- [155] Larsen CN, Price JS, Wilkinson KD (1996) Substrate binding and catalysis by ubiquitin C-terminal hydrolases: identification of two active site residues. *Biochemistry* **35**, 6735-6744.
- [156] Osaka H, Wang YL, Takada K, Takizawa S, Setsue R, Li H, Sato Y, Nishikawa K, Sun YJ, Sakurai M, Harada T, Hara Y, Kimura I, Chiba S, Namikawa K, Kiyama H, Noda M, Aoki S, Wada K (2003) Ubiquitin carboxy-terminal hydrolase L1 binds to and stabilizes monoubiquitin in neuron. *Hum Mol Genet* **12**, 1945-1958.
- [157] Messick TE, Russell NS, Iwata AJ, Sarachan KL, Shiekhhattar R, Shanks JR, Reyes-Turcu FE, Wilkinson KD, Marmorstein R (2008) Structural basis for ubiquitin recognition by the Otu1 ovarian tumor domain protein. *J Biol Chem* **283**, 11038-11049.
- [158] Meier F, Schittek B, Busch S, Garbe C, Smalley K, Satyamoorthy K, Li G, Herlyn M (2005) The RAS/RAF/MEK/ERK and PI3K/AKT signaling pathways present molecular targets for the effective treatment of advanced melanoma. *Front Biosci* **10**, 2986-3001.
- [159] Ichikawa T, Li J, Dong X, Potts JD, Tang DQ, Li DS, Cui T (2010) Ubiquitin carboxyl terminal hydrolase L1 negatively regulates TNFalpha-mediated vascular smooth muscle cell proliferation via suppressing ERK activation. *Biochem Biophys Res Commun* **391**, 852-856.
- [160] Weber B, Schaper C, Wang Y, Scholz J, Bein B (2009) Interaction of the ubiquitin carboxyl terminal esterase L1 with alpha(2)-adrenergic receptors inhibits agonist-mediated p44/42 MAP kinase activation. *Cell Signal* **21**, 1513-1521.
- [161] Kabuta T, Mitsui T, Takahashi M, Fujiwara Y, Kabuta C, Konya C, Tsuchiya Y, Hatanaka Y, Uchida K, Hohjoh H, Wada K (2013) Ubiquitin C-terminal hydrolase L1 (UCH-L1) acts as a novel potentiator of cyclin-dependent kinases to enhance cell proliferation independently of its hydrolase activity. *J Biol Chem* **288**, 12615-12626.
- [162] Fang J, Nakamura H, Iyer AK (2007) Tumor-targeted induction of oxystress for cancer therapy. *J Drug Target* **15**, 475-486.
- [163] Sosa V, Moline T, Somoza R, Paciucci R, Kondoh H, ME LL (2013) Oxidative stress and cancer: an overview. *Ageing Res Rev* **12**, 376-390.
- [164] Hussain S, Feldman AL, Das C, Ziesmer SC, Ansell SM, Galardy PJ (2013) Ubiquitin hydrolase UCH-L1 destabilizes mTOR complex 1 by antagonizing DDB1-CUL4-mediated ubiquitination of raptor. *Mol Cell Biol* **33**, 1188-1197.
- [165] Bheda A, Shackelford J, Pagano JS (2009) Expression and functional studies of ubiquitin C-terminal hydrolase L1 regulated genes. *PLoS One* **4**, e6764.
- [166] Downward J (2004) PI 3-kinase, Akt and cell survival. *Semin Cell Dev Biol* **15**, 177-182.
- [167] Ummanni R, Mundt F, Pospisil H, Venz S, Scharf C, Baret C, Falth M, Kollermann J, Walther R, Schlomm T, Sauter G, Bokemeyer C, Sultmann H, Schuppert A, Brummendorf TH, Balabanov S (2011) Identification of clinically relevant protein targets in prostate cancer with 2D-DIGE coupled mass spectrometry and systems biology network platform. *PLoS One* **6**, e16833.
- [168] Leiblich A, Cross SS, Catto JW, Pesce G, Hamdy FC, Rehman I (2007) Human prostate cancer cells express neuroendocrine cell markers PGP 9.5 and chromogranin A. *Prostate* **67**, 1761-1769.
- [169] Muller PA, Vousden KH (2013) p53 mutations in cancer. *Nat Cell Biol* **15**, 2-8.
- [170] Bartek J, Iggo R, Gannon J, Lane DP (1990) Genetic and immunochemical analysis of mutant p53 in human breast cancer cell lines. *Oncogene* **5**, 893-899.

- [171] Respa A, Bukur J, Ferrone S, Pawelec G, Zhao Y, Wang E, Marincola FM, Seliger B (2011) Association of IFN-gamma signal transduction defects with impaired HLA class I antigen processing in melanoma cell lines. *Clin Cancer Res* **17**, 2668-2678.
- [172] Hodis E, Watson IR, Kryukov GV, Arold ST, Imielinski M, Theurillat JP, Nickerson E, Auclair D, Li L, Place C, Dicara D, Ramos AH, Lawrence MS, Cibulskis K, Sivachenko A, Voet D, Saksena G, Stransky N, Onofrio RC, Winckler W, Ardlie K, Wagle N, Wargo J, Chong K, Morton DL, Stenke-Hale K, Chen G, Noble M, Meyerson M, Ladbury JE, Davies MA, Gershenwald JE, Wagner SN, Hoon DS, Schadendorf D, Lander ES, Gabriel SB, Getz G, Garraway LA, Chin L (2012) A landscape of driver mutations in melanoma. *Cell* **150**, 251-263.
- [173] Griewank KG, Ugurel S, Schadendorf D, Paschen A (2013) New developments in biomarkers for melanoma. *Curr Opin Oncol* **25**, 145-151.
- [174] Surowiak P, Drag M, Materna V, Suchocki S, Grzywa R, Spaczynski M, Dietel M, Oleksyszyn J, Zabel M, Lage H (2006) Expression of aminopeptidase N/CD13 in human ovarian cancers. *Int J Gynecol Cancer* **16**, 1783-1788.
- [175] Bauvois B, Dauzone D (2006) Aminopeptidase-N/CD13 (EC 3.4.11.2) inhibitors: chemistry, biological evaluations, and therapeutic prospects. *Med Res Rev* **26**, 88-130.
- [176] Ichinose Y, Genka K, Koike T, Kato H, Watanabe Y, Mori T, Iioka S, Sakuma A, Ohta M (2003) Randomized double-blind placebo-controlled trial of bestatin in patients with resected stage I squamous-cell lung carcinoma. *J Natl Cancer Inst* **95**, 605-610.
- [177] Niimoto M, Hattori T (1991) Prospective randomized controlled study on bestatin in resectable gastric cancer. *Biomed Pharmacother* **45**, 121-124.
- [178] Pasqualini R, Koivunen E, Kain R, Lahdenranta J, Sakamoto M, Stryhn A, Ashmun RA, Shapiro LH, Arap W, Ruoslahti E (2000) Aminopeptidase N is a receptor for tumor-homing peptides and a target for inhibiting angiogenesis. *Cancer Res* **60**, 722-727.
- [179] Gregorc V, De Braud FG, De Pas TM, Scalamogna R, Citterio G, Milani A, Boselli S, Catania C, Donadoni G, Rossoni G, Ghio D, Spitaleri G, Ammannati C, Colombi S, Caligaris-Cappio F, Lambiase A, Bordignon C (2011) Phase I study of NGR-hTNF, a selective vascular targeting agent, in combination with cisplatin in refractory solid tumors. *Clin Cancer Res* **17**, 1964-1972.
- [180] Gregorc V, Zucali PA, Santoro A, Ceresoli GL, Citterio G, De Pas TM, Zilembo N, De Vincenzo F, Simonelli M, Rossoni G, Spreafico A, Grazia Vigano M, Fontana F, De Braud FG, Bajetta E, Caligaris-Cappio F, Bruzzi P, Lambiase A, Bordignon C (2010) Phase II study of asparagine-glycine-arginine-human tumor necrosis factor alpha, a selective vascular targeting agent, in previously treated patients with malignant pleural mesothelioma. *J Clin Oncol* **28**, 2604-2611.
- [181] Gregorc V, Santoro A, Bennicelli E, Punt CJ, Citterio G, Timmer-Bonte JN, Caligaris Cappio F, Lambiase A, Bordignon C, van Herpen CM (2009) Phase Ib study of NGR-hTNF, a selective vascular targeting agent, administered at low doses in combination with doxorubicin to patients with advanced solid tumours. *Br J Cancer* **101**, 219-224.
- [182] Kessler T, Schwoppe C, Liersch R, Schliemann C, Hintelmann H, Bieker R, Berdel WE, Mesters RM (2008) Generation of fusion proteins for selective occlusion of tumor vessels. *Curr Drug Discov Technol* **5**, 1-8.
- [183] Elder DE, Rodeck U, Thurin J, Cardillo F, Clark WH, Stewart R, Herlyn M (1989) Antigenic profile of tumor progression stages in human melanocytic nevi and melanomas. *Cancer Res* **49**, 5091-5096.
- [184] Stockwin LH, Blonder J, Bumke MA, Lucas DA, Chan KC, Conrads TP, Issaq HJ, Veenstra TD, Newton DL, Rybak SM (2006) Proteomic analysis of plasma membrane from hypoxia-adapted malignant melanoma. *J Proteome Res* **5**, 2996-3007.
- [185] Wang GL, Semenza GL (1993) Characterization of hypoxia-inducible factor 1 and regulation of DNA binding activity by hypoxia. *J Biol Chem* **268**, 21513-21518.

- [186] Aozuka Y, Koizumi K, Saitoh Y, Ueda Y, Sakurai H, Saiki I (2004) Anti-tumor angiogenesis effect of aminopeptidase inhibitor bestatin against B16-BL6 melanoma cells orthotopically implanted into syngeneic mice. *Cancer Lett* **216**, 35-42.
- [187] Saitoh Y, Koizumi K, Minami T, Sekine K, Sakurai H, Saiki I (2006) A derivative of aminopeptidase inhibitor (BE15) has a dual inhibitory effect of invasion and motility on tumor and endothelial cells. *Biol Pharm Bull* **29**, 709-712.
- [188] Laube F (2007) Immunoluminescent detection of intercellular adhesion molecule-1 and aminopeptidase N on human melanoma cells. *Anticancer Res* **27**, 2047-2052.
- [189] Inagaki Y, Tang W, Zhang L, Du G, Xu W, Kokudo N (2010) Novel aminopeptidase N (APN/CD13) inhibitor 24F can suppress invasion of hepatocellular carcinoma cells as well as angiogenesis. *Biosci Trends* **4**, 56-60.
- [190] Kido A, Krueger S, Haeckel C, Roessner A (1999) Possible contribution of aminopeptidase N (APN/CD13) to invasive potential enhanced by interleukin-6 and soluble interleukin-6 receptor in human osteosarcoma cell lines. *Clin Exp Metastasis* **17**, 857-863.
- [191] Winnepeninckx V, De Vos R, Stas M, van den Oord JJ (2003) New phenotypical and ultrastructural findings in spindle cell (desmoplastic/neurotropic) melanoma. *Appl Immunohistochem Mol Morphol* **11**, 319-325.
- [192] McGuinness C, Wesley UV (2008) Dipeptidyl peptidase IV (DPPIV), a candidate tumor suppressor gene in melanomas is silenced by promoter methylation. *Front Biosci* **13**, 2435-2443.
- [193] Li LC, Dahiya R (2002) MethPrimer: designing primers for methylation PCRs. *Bioinformatics* **18**, 1427-1431.
- [194] Seftor EA, Brown KM, Chin L, Kirschmann DA, Wheaton WW, Protopopov A, Feng B, Balagurunathan Y, Trent JM, Nickoloff BJ, Seftor RE, Hendrix MJ (2005) Epigenetic transdifferentiation of normal melanocytes by a metastatic melanoma microenvironment. *Cancer Res* **65**, 10164-10169.
- [195] Garcia-Manero G, Jabbour E, Borthakur G, Faderl S, Estrov Z, Yang H, Maddipoti S, Godley LA, Gabrail N, Berdeja JG, Nadeem A, Kassalow L, Kantarjian H (2013) Randomized open-label phase II study of decitabine in patients with low- or intermediate-risk myelodysplastic syndromes. *J Clin Oncol* **31**, 2548-2553.
- [196] Chu BF, Karpenko MJ, Liu Z, Aimiwu J, Villalona-Calero MA, Chan KK, Grever MR, Otterson GA (2013) Phase I study of 5-aza-2'-deoxycytidine in combination with valproic acid in non-small-cell lung cancer. *Cancer Chemother Pharmacol* **71**, 115-121.
- [197] Tawbi HA, Beumer JH, Tarhini AA, Moschos S, Buch SC, Egorin MJ, Lin Y, Christner S, Kirkwood JM (2013) Safety and efficacy of decitabine in combination with temozolomide in metastatic melanoma: a phase I/II study and pharmacokinetic analysis. *Ann Oncol* **24**, 1112-1119.
- [198] Sigalotti L, Fratta E, Coral S, Maio M (2013) Epigenetic drugs as immunomodulators for combination therapies in solid tumors. *Pharmacol Ther*.
- [199] Daskalakis M, Blagitko-Dorfs N, Hackanson B (2010) Decitabine. *Recent Results Cancer Res* **184**, 131-157.
- [200] Ateeq B, Unterberger A, Szyf M, Rabbani SA (2008) Pharmacological inhibition of DNA methylation induces proinvasive and prometastatic genes in vitro and in vivo. *Neoplasia* **10**, 266-278.
- [201] Marotti T, Balog T, Munic V, Sobocanec S, Abramic M (2000) The link between met-enkephalin-induced down-regulation of APN activity and the release of superoxide anion. *Neuropeptides* **34**, 121-128.
- [202] Gabrilovac J, Cupic B, Breljak D, Zekusic M, Boranic M (2004) Expression of CD13/aminopeptidase N and CD10/neutral endopeptidase on cultured human keratinocytes. *Immunol Lett* **91**, 39-47.
- [203] Umezawa H, Aoyagi T, Suda H, Hamada M, Takeuchi T (1976) Bestatin, an inhibitor of aminopeptidase B, produced by actinomycetes. *J Antibiot (Tokyo)* **29**, 97-99.

- [204] Muskardin DT, Voelkel NF, Fitzpatrick FA (1994) Modulation of pulmonary leukotriene formation and perfusion pressure by bestatin, an inhibitor of leukotriene A4 hydrolase. *Biochem Pharmacol* **48**, 131-137.
- [205] Sina A, Lord-Dufour S, Annabi B (2009) Cell-based evidence for aminopeptidase N/CD13 inhibitor actinonin targeting of MT1-MMP-mediated proMMP-2 activation. *Cancer Lett* **279**, 171-176.
- [206] Sekine K, Fujii H, Abe F (1999) Induction of apoptosis by bestatin (ubenimex) in human leukemic cell lines. *Leukemia* **13**, 729-734.
- [207] Grujic M, Renko M (2002) Aminopeptidase inhibitors bestatin and actinonin inhibit cell proliferation of myeloma cells predominantly by intracellular interactions. *Cancer Lett* **182**, 113-119.
- [208] Grujic M, Zavasnik-Bergant T, Pejler G, Renko M (2005) Actinonin induces apoptosis in U937 leukemia cells. *Cancer Lett* **223**, 211-218.
- [209] Kumano N, Sugawara S (1992) Ubenimex (Bestatin), an aminopeptidase inhibitor, modulates protein kinase C in K562 cells. *J Biol Regul Homeost Agents* **6**, 116-120.
- [210] Murata M, Kubota Y, Tanaka T, Iida-Tanaka K, Takahara J, Irino S (1994) Effect of ubenimex on the proliferation and differentiation of U937 human histiocytic lymphoma cells. *Leukemia* **8**, 2188-2193.
- [211] Piedfer M, Dauzonne D, Tang R, N'Guyen J, Billard C, Bauvois B (2011) Aminopeptidase-N/CD13 is a potential proapoptotic target in human myeloid tumor cells. *FASEB J* **25**, 2831-2842.
- [212] Santos AN, Langner J, Herrmann M, Riemann D (2000) Aminopeptidase N/CD13 is directly linked to signal transduction pathways in monocytes. *Cell Immunol* **201**, 22-32.
- [213] Laustsen PG, Vang S, Kristensen T (2001) Mutational analysis of the active site of human insulin-regulated aminopeptidase. *Eur J Biochem* **268**, 98-104.
- [214] Fukasawa K, Fukasawa KM, Iwamoto H, Hirose J, Harada M (1999) The HELLGH motif of rat liver dipeptidyl peptidase III is involved in zinc coordination and the catalytic activity of the enzyme. *Biochemistry* **38**, 8299-8303.
- [215] Chang YW, Chen SC, Cheng EC, Ko YP, Lin YC, Kao YR, Tsay YG, Yang PC, Wu CW, Roffler SR (2005) CD13 (aminopeptidase N) can associate with tumor-associated antigen L6 and enhance the motility of human lung cancer cells. *Int J Cancer* **116**, 243-252.
- [216] Miki T, Takegami Y, Okawa K, Muraguchi T, Noda M, Takahashi C (2007) The reversion-inducing cysteine-rich protein with Kazal motifs (RECK) interacts with membrane type 1 matrix metalloproteinase and CD13/aminopeptidase N and modulates their endocytic pathways. *J Biol Chem* **282**, 12341-12352.
- [217] Danielsen EM, van Deurs B (1997) Galectin-4 and small intestinal brush border enzymes form clusters. *Mol Biol Cell* **8**, 2241-2251.
- [218] Mina-Osorio P, Soto-Cruz I, Ortega E (2007) A role for galectin-3 in CD13-mediated homotypic aggregation of monocytes. *Biochem Biophys Res Commun* **353**, 605-610.
- [219] Baggiolini M (1998) Chemokines and leukocyte traffic. *Nature* **392**, 565-568.
- [220] Zlotnik A, Yoshie O (2000) Chemokines: a new classification system and their role in immunity. *Immunity* **12**, 121-127.
- [221] Domanska UM, Kruizinga RC, Nagengast WB, Timmer-Bosscha H, Huls G, de Vries EG, Walenkamp AM (2013) A review on CXCR4/CXCL12 axis in oncology: no place to hide. *Eur J Cancer* **49**, 219-230.
- [222] Ramsey DM, McAlpine SR (2013) Halting metastasis through CXCR4 inhibition. *Bioorg Med Chem Lett* **23**, 20-25.
- [223] Luster AD (1998) Chemokines--chemotactic cytokines that mediate inflammation. *N Engl J Med* **338**, 436-445.
- [224] Romagnani P, Lasagni L, Annunziato F, Serio M, Romagnani S (2004) CXC chemokines: the regulatory link between inflammation and angiogenesis. *Trends Immunol* **25**, 201-209.

- [225] Huss R, von Luttichau I, Lechner S, Notohamiprodjo M, Seliger C, Nelson P (2004) [Chemokine directed homing of transplanted adult stem cells in wound healing and tissue regeneration]. *Verh Dtsch Ges Pathol* **88**, 170-173.
- [226] Suarez-Alvarez B, Lopez-Vazquez A, Lopez-Larrea C (2012) Mobilization and homing of hematopoietic stem cells. *Adv Exp Med Biol* **741**, 152-170.
- [227] Scala S, Ottaiano A, Ascierto PA, Cavalli M, Simeone E, Giuliano P, Napolitano M, Franco R, Botti G, Castello G (2005) Expression of CXCR4 predicts poor prognosis in patients with malignant melanoma. *Clin Cancer Res* **11**, 1835-1841.
- [228] Taichman RS, Cooper C, Keller ET, Pienta KJ, Taichman NS, McCauley LK (2002) Use of the stromal cell-derived factor-1/CXCR4 pathway in prostate cancer metastasis to bone. *Cancer Res* **62**, 1832-1837.
- [229] Zagzag D, Krishnamachary B, Yee H, Okuyama H, Chiriboga L, Ali MA, Melamed J, Semenza GL (2005) Stromal cell-derived factor-1alpha and CXCR4 expression in hemangioblastoma and clear cell-renal cell carcinoma: von Hippel-Lindau loss-of-function induces expression of a ligand and its receptor. *Cancer Res* **65**, 6178-6188.
- [230] Furusato B, Mohamed A, Uhlen M, Rhim JS (2010) CXCR4 and cancer. *Pathol Int* **60**, 497-505.
- [231] Pan J, Mestas J, Burdick MD, Phillips RJ, Thomas GV, Reckamp K, Belperio JA, Strieter RM (2006) Stromal derived factor-1 (SDF-1/CXCL12) and CXCR4 in renal cell carcinoma metastasis. *Mol Cancer* **5**, 56.
- [232] Ramos EA, Grochoski M, Braun-Prado K, Seniski GG, Cavalli IJ, Ribeiro EM, Camargo AA, Costa FF, Klassen G (2011) Epigenetic changes of CXCR4 and its ligand CXCL12 as prognostic factors for sporadic breast cancer. *PLoS One* **6**, e29461.
- [233] Muller A, Homey B, Soto H, Ge N, Catron D, Buchanan ME, McClanahan T, Murphy E, Yuan W, Wagner SN, Barrera JL, Mohar A, Verastegui E, Zlotnik A (2001) Involvement of chemokine receptors in breast cancer metastasis. *Nature* **410**, 50-56.
- [234] Pople A, Durrant LG, Spendlove I, Rolland P, Scott IV, Deen S, Ramage JM (2012) The chemokine, CXCL12, is an independent predictor of poor survival in ovarian cancer. *Br J Cancer* **106**, 1306-1313.
- [235] Diodovich C, Malerba I, Ferrario D, Bowe G, Bianchi MG, Acquati F, Taramelli R, Parent-Massin D, Gribaldo L (2005) Gene and protein expressions in human cord blood cells after exposure to acrylonitrile. *J Biochem Mol Toxicol* **19**, 204-212.
- [236] Singh AK, Arya RK, Trivedi AK, Sanyal S, Baral R, Dormond O, Briscoe DM, Datta D (2013) Chemokine receptor trio: CXCR3, CXCR4 and CXCR7 crosstalk via CXCL11 and CXCL12. *Cytokine Growth Factor Rev* **24**, 41-49.
- [237] Xu Y, Wellner D, Scheinberg DA (1995) Substance P and bradykinin are natural inhibitors of CD13/aminopeptidase N. *Biochem Biophys Res Commun* **208**, 664-674.
- [238] Teicher BA, Fricker SP (2010) CXCL12 (SDF-1)/CXCR4 pathway in cancer. *Clin Cancer Res* **16**, 2927-2931.
- [239] Wu B, Chien EY, Mol CD, Fenalti G, Liu W, Katritch V, Abagyan R, Brooun A, Wells P, Bi FC, Hamel DJ, Kuhn P, Handel TM, Cherezov V, Stevens RC (2010) Structures of the CXCR4 chemokine GPCR with small-molecule and cyclic peptide antagonists. *Science* **330**, 1066-1071.
- [240] Tarasova NI, Stauber RH, Michejda CJ (1998) Spontaneous and ligand-induced trafficking of CXC-chemokine receptor 4. *J Biol Chem* **273**, 15883-15886.
- [241] Forster R, Kremmer E, Schubel A, Breitfeld D, Kleinschmidt A, Nerl C, Bernhardt G, Lipp M (1998) Intracellular and surface expression of the HIV-1 coreceptor CXCR4/fusin on various leukocyte subsets: rapid internalization and recycling upon activation. *J Immunol* **160**, 1522-1531.
- [242] Hu C, Yong X, Li C, Lu M, Liu D, Chen L, Hu J, Teng M, Zhang D, Fan Y, Liang G (2013) CXCL12/CXCR4 axis promotes mesenchymal stem cell mobilization to burn wounds and contributes to wound repair. *J Surg Res* **183**, 427-434.

- [243] van Malenstein H, Dekervel J, Verslype C, Van Cutsem E, Windmolders P, Nevens F, van Pelt J (2013) Long-term exposure to sorafenib of liver cancer cells induces resistance with epithelial-to-mesenchymal transition, increased invasion and risk of rebound growth. *Cancer Lett* **329**, 74-83.
- [244] Gao C, Wang AY (2009) Significance of increased apoptosis and Bax expression in human small intestinal adenocarcinoma. *J Histochem Cytochem* **57**, 1139-1148.
- [245] Lowe SW, Lin AW (2000) Apoptosis in cancer. *Carcinogenesis* **21**, 485-495.
- [246] Nguyen DH, Taub D (2002) CXCR4 function requires membrane cholesterol: implications for HIV infection. *J Immunol* **168**, 4121-4126.
- [247] Sbaa E, Dewever J, Martinive P, Bouzin C, Frerart F, Balligand JL, Dessy C, Feron O (2006) Caveolin plays a central role in endothelial progenitor cell mobilization and homing in SDF-1-driven postischemic vasculogenesis. *Circ Res* **98**, 1219-1227.
- [248] van Buul JD, Voermans C, van Gelderen J, Anthony EC, van der Schoot CE, Hordijk PL (2003) Leukocyte-endothelium interaction promotes SDF-1-dependent polarization of CXCR4. *J Biol Chem* **278**, 30302-30310.
- [249] Liu L, Xu HX, Wang WQ, Wu CT, Chen T, Qin Y, Liu C, Xu J, Long J, Zhang B, Xu YF, Ni QX, Li M, Yu XJ (2013) Cavin-1 is essential for the tumor-promoting effect of caveolin-1 and enhances its prognostic potency in pancreatic cancer. *Oncogene*.
- [250] Tourkina E, Richard M, Oates J, Hofbauer A, Bonner M, Goos P, Visconti R, Zhang J, Znoyko S, Hatfield CM, Silver RM, Hoffman S (2010) Caveolin-1 regulates leucocyte behaviour in fibrotic lung disease. *Ann Rheum Dis* **69**, 1220-1226.
- [251] Altenburg JD, Siddiqui RA (2009) Omega-3 polyunsaturated fatty acids down-modulate CXCR4 expression and function in MDA-MB-231 breast cancer cells. *Mol Cancer Res* **7**, 1013-1020.
- [252] Ho HT, Tsai IF, Wu CL, Lu YT (2014) Aminopeptidase N facilitates entry and intracellular survival of Mycobacterium tuberculosis in monocytes. *Respirology* **19**, 109-115.
- [253] Choi WT, Duggineni S, Xu Y, Huang Z, An J (2012) Drug discovery research targeting the CXC chemokine receptor 4 (CXCR4). *J Med Chem* **55**, 977-994.
- [254] Han F, Gu D, Chen Q, Zhu H (2009) Caveolin-1 acts as a tumor suppressor by down-regulating epidermal growth factor receptor-mitogen-activated protein kinase signaling pathway in pancreatic carcinoma cell lines. *Pancreas* **38**, 766-774.
- [255] Belanger MM, Roussel E, Couet J (2004) Caveolin-1 is down-regulated in human lung carcinoma and acts as a candidate tumor suppressor gene. *Chest* **125**, 106S.
- [256] Aldred MA, Ginn-Pease ME, Morrison CD, Popkie AP, Gimm O, Hoang-Vu C, Krause U, Dralle H, Jhiang SM, Plass C, Eng C (2003) Caveolin-1 and caveolin-2, together with three bone morphogenetic protein-related genes, may encode novel tumor suppressors down-regulated in sporadic follicular thyroid carcinogenesis. *Cancer Res* **63**, 2864-2871.
- [257] Wiechen K, Diatchenko L, Agoulnik A, Scharff KM, Schober H, Arlt K, Zhumabayeva B, Siebert PD, Dietel M, Schafer R, Sers C (2001) Caveolin-1 is down-regulated in human ovarian carcinoma and acts as a candidate tumor suppressor gene. *Am J Pathol* **159**, 1635-1643.
- [258] Pavlides S, Tsirigos A, Vera I, Flomenberg N, Frank PG, Casimiro MC, Wang C, Fortina P, Addya S, Pestell RG, Martinez-Outschoorn UE, Sotgia F, Lisanti MP (2010) Loss of stromal caveolin-1 leads to oxidative stress, mimics hypoxia and drives inflammation in the tumor microenvironment, conferring the "reverse Warburg effect": a transcriptional informatics analysis with validation. *Cell Cycle* **9**, 2201-2219.
- [259] Ando T, Ishiguro H, Kimura M, Mitsui A, Mori Y, Sugito N, Tomoda K, Mori R, Harada K, Katada T, Ogawa R, Fujii Y, Kuwabara Y (2007) The overexpression of caveolin-1 and caveolin-2 correlates with a poor prognosis and tumor progression in esophageal squamous cell carcinoma. *Oncol Rep* **18**, 601-609.

- [260] Qian N, Ueno T, Kawaguchi-Sakita N, Kawashima M, Yoshida N, Mikami Y, Wakasa T, Shintaku M, Tsuyuki S, Inamoto T, Toi M (2011) Prognostic significance of tumor/stromal caveolin-1 expression in breast cancer patients. *Cancer Sci* **102**, 1590-1596.
- [261] Tahir SA, Yang G, Goltsov AA, Watanabe M, Tabata K, Addai J, Fattah el MA, Kadmon D, Thompson TC (2008) Tumor cell-secreted caveolin-1 has proangiogenic activities in prostate cancer. *Cancer Res* **68**, 731-739.
- [262] Felicetti F, Parolini I, Bottero L, Fecchi K, Errico MC, Raggi C, Biffoni M, Spadaro F, Lisanti MP, Sargiacomo M, Care A (2009) Caveolin-1 tumor-promoting role in human melanoma. *Int J Cancer* **125**, 1514-1522.
- [263] MacIntyre EA, Roberts PJ, Jones M, Van der Schoot CE, Favalaro EJ, Tidman N, Linch DC (1989) Activation of human monocytes occurs on cross-linking monocytic antigens to an Fc receptor. *J Immunol* **142**, 2377-2383.
- [264] Mina-Osorio P, Ortega E (2005) Aminopeptidase N (CD13) functionally interacts with FcγR3 in human monocytes. *J Leukoc Biol* **77**, 1008-1017.
- [265] Orso E, Werner T, Wolf Z, Bandulik S, Kramer W, Schmitz G (2006) Ezetimib influences the expression of raft-associated antigens in human monocytes. *Cytometry A* **69**, 206-208.
- [266] Villasenor-Cardoso MI, Frausto-Del-Rio DA, Ortega E (2013) Aminopeptidase N (CD13) is involved in phagocytic processes in human dendritic cells and macrophages. *Biomed Res Int* **2013**, 562984.
- [267] Yang E, Shim JS, Woo HJ, Kim KW, Kwon HJ (2007) Aminopeptidase N/CD13 induces angiogenesis through interaction with a pro-angiogenic protein, galectin-3. *Biochem Biophys Res Commun* **363**, 336-341.
- [268] Gabrilovac J, Cupic B, Zivkovic E, Horvat L, Majhen D (2011) Expression, regulation and functional activities of aminopeptidase N (EC 3.4.11.2; APN; CD13) on murine macrophage J774 cell line. *Immunobiology* **216**, 132-144.
- [269] Navarrete Santos A, Langner J, Riemann D (2000) Enzymatic activity is not a precondition for the intracellular calcium increase mediated by mAbs specific for aminopeptidase N/CD13. *Adv Exp Med Biol* **477**, 43-47.
- [270] Subramani J, Ghosh M, Rahman MM, Caromile LA, Gerber C, Rezaul K, Han DK, Shapiro LH (2013) Tyrosine phosphorylation of CD13 regulates inflammatory cell-cell adhesion and monocyte trafficking. *J Immunol* **191**, 3905-3912.

9 Eigenständigkeitserklärung

Hiermit erkläre ich an Eides statt, dass ich die vorliegende Dissertation selbstständig und nur unter Verwendung der angegebenen Quellen und Hilfsmittel angefertigt habe. Wörtlich oder inhaltlich entnommene Literaturstellen sind als solche gekennzeichnet. Diese Arbeit wurde bisher weder an der Martin-Luther-Universität Halle-Wittenberg, noch an einer anderen Bildungseinrichtung zur Erlangung eines akademischen Grades eingereicht.

Halle (Saale), den...

Jens Wulfänger

10 Lebenslauf

Persönliche Daten

Name: Jens Wulfänger
Geburtsdatum: 19.03.1978
Geburtsort: Stendal
Staatsangehörigkeit: Deutsch
Familienstand: ledig

Akademischer Werdegang

ab 11/2013 Wissenschaftlicher Mitarbeiter am Institut für Physiologische Chemie der Martin-Luther-Universität Halle-Wittenberg unter Prof. Dr. Guido Posern

01/2004 – 05/2013 Doktorarbeit unter Anleitung von Prof. Dr. B. Seliger am Institut für Medizinische Immunologie der Martin-Luther-Universität Halle-Wittenberg mit dem Thema „Regulation und Funktion von Aminopeptidase N (APN)/ CD13 und Ubiquitin-Carboxy-terminale Hydrolase L1 in humanen Tumoren“

02/2002 – 12/2003 Wissenschaftlicher Mitarbeiter am Institut für Medizinische Immunologie der Martin-Luther-Universität Halle-Wittenberg unter Prof. Dr. Jürgen Langner

10/2001 – 01/2002 Wissenschaftlicher Mitarbeiter in der Firma ACGT ProGenomics AG Halle (Saale)

10/2000 – 09/2001 Diplomarbeit am Institut für Medizinische Immunologie in Halle-Wittenberg bei Prof. Dr. J. Langner mit dem Thema: „Untersuchungen zur Funktion der Cysteine am C-Terminus von Neprilysin“

10/1996 – 09/2001 Studium der Biochemie an der Martin-Luther-Universität Halle-Wittenberg
Abschluss: Diplom; Note: sehr gut

Schulischer Werdegang

09/1991 – 06/1996 Abitur am Rudolf-Hildebrand-Gymnasium in Stendal mit dem
Abschluss der Allgemeinen Hochschulreife; Note: Sehr gut

09/1984 – 07/1991 Erweiterte Oberschule „Adolph Diesterweg“ in Stendal

Halle (Saale), den...

Jens Wulfänger

11 Liste von Publikationen und Präsentationen

Publikationen

Wulfänger J, Biehl K, Tetzner A, Wild P, Ikenberg K, Meyer S, Seliger B (2013) Heterogeneous expression and functional relevance of the ubiquitin carboxyl-terminal hydrolase L1 in melanoma. *Int J Cancer*. 133(11):2522-32.

Recktenwald CV, Leisz S, Steven A, Mimura K, Müller A, **Wulfänger J**, Kiessling R, Seliger B. (2012) HER-2/neu-mediated down-regulation of biglycan associated with altered growth properties. *J Biol Chem*. 287:24320-9.

Wulfänger J, Schneider H, Ikenberg K, Wild P, Rodolfo M, Rivoltini L, Meyer S, Riemann D, Seliger B (2012) Promoter methylation of aminopeptidase N (APN)/ CD13 in malignant melanoma. *Carcinogenesis*. 33(4):781-90.

Seifert A, Klonisch T, **Wulfaenger J**, Haag F, Dralle H, Langner J, Hoang-Vu C, Kehlen A (2008) The cellular localization of autotaxin impacts on its biological functions in human thyroid carcinoma cells. *Oncol Rep*. 19:1485-91.

Wulfaenger J, Niedling S, Riemann D, Seliger B (2008) Aminopeptidase N (APN)/ CD13-dependent CXCR4 downregulation is associated with diminished cell migration, proliferation and invasion. *Mol Membr Biol*. 25(1):72-82.

Erhuma M, Köbel M, Mustafa T, **Wulfänger J**, Dralle H, Hoang-Vu C, Langner J, Seliger B, Kehlen A (2007) Expression of neutral endopeptidase (NEP/ CD10) on pancreatic tumor cell lines, pancreatitis and pancreatic tumor tissues. *Int J Cancer*. 120:2393-400.

Liebig B, Brabletz T, Staeger MS, **Wulfänger J**, Riemann D, Burdach S, Ballhausen WG (2005) Forced expression of deltaN-TCF-1B in colon cancer derived cell lines is accompanied by the induction of CEACAM5/6 and mesothelin. *Cancer Lett*. 223:159-67.

Riemann D, Tcherkes A, Hansen GH, **Wulfaenger J**, Blosz T, Danielsen EM (2005) Functional co-localization of monocytic aminopeptidase N/ CD13 with the Fc gamma receptors CD32 and CD64. *Biochem Biophys Res Commun*. 331(4):1408-12.

Navarrete Santos A, **Wulfänger J**, Helbing G, Blosz T, Langner J, Riemann D (2002) Two C-terminal cysteines are necessary for proper folding of the peptidase neprilysin/ CD10. *Biochem Biophys Res Commun*. 295:423-7.

Vorträge

Wulfänger J, Riemann D, Seliger B (2008) The role of aminopeptidase N (APN)/ CD13 in tumor biology and tumor immunology. Symposium „Tumor Immunology meets Oncology IV“, Halle (Saale).

Wulfänger J, Navarette-Santos A, Riemann D, Langner J (2002) The conserved C-terminal cysteines are necessary for the proper folding and membrane localisation of the raft-associated peptidase neprilysin/ CD10. 8th Spring Meeting of the German Society of Immunology, Halle (Saale).

Poster

Barthel D, **Wulfänger J**, Seliger B (2012) Characterization of differential gene expression of syndecan-2. Forschungstag 2012, Halle (Saale).

Schmidt S, Erb S, Burghoff S, Leisz S, **Wulfänger J**, Biehl K, Hoffmann K, Seliger B (2012) European Human Genetics Conference (ESHG), Nürnberg.

Wulfänger J, Schneider H, Riemann D, Seliger B (2009) Promoter methylation prevents APN-modulated migration of melanoma cells. 15th International AEK Cancer Congress, Berlin.

Puttkammer M, **Wulfänger J**, Hesse A, Seliger B (2009) Upregulation of ILBP in renal cell carcinoma. 15th International AEK Cancer Congress, Berlin.

Riemann D, **Wulfänger J**, Handke D, Zinkhan M, Schütte W, Seliger B (2006) Aminopeptidase N/ CD13-mediated enhancement of the MHC class I antigen surface expression in colon carcinoma cells. 16th European Congress of Immunology, Paris.

Wulfänger J, Niedling S, Riemann D, Seliger B (2005) Aminopeptidase N/ CD13 is involved in the expression of CXCR4 and in cell migration. 36th Annual Meeting of the DGfI German Society of Immunology, Kiel.

Tcherkes A, **Wulfänger J**, Blosz T, Pfeiffer A, Langner J, Riemann D (2004) FRET-based evidence of Aminopeptidase N/ CD13 and Fcγ RII/ CD32 co-localization in human monocytic cells. Eur J Cell Biol, 83 Suppl 54 p.36.

Blosz T, Kehlen A, **Wulfänger J**, Simm A, Sablotzki A, Navarrete Santos A, Langner J, Riemann D (2002) Signalling after ligation of aminopeptidase N/ CD13 augments

expression of monocytic manganese superoxide dismutase (MnSOD). Signal Transduction, 3-4 p.134.

Wulfänger J, Navarrete Santos A, Blosz T, Langner J, Riemann D (2002) The intracellular N-terminus of aminopeptidase N/ CD13 affects association with caveolae. GBM-Jahrestagung, Halle (Saale). [\[DOI:10.1240/sav_gbm_2002_h_000211\]](https://doi.org/10.1240/sav_gbm_2002_h_000211)

Wulfänger J, Navarrete Santos A, Blosz T, Langner J, Riemann D (2002) Aminopeptidase N/ CD13 is associated with Lubrol rafts. GBM-Jahrestagung, Halle (Saale). [\[DOI:10.1240/sav_gbm_2002_h_000213\]](https://doi.org/10.1240/sav_gbm_2002_h_000213)

Navarrete Santos A, **Wulfänger J**, Helbing G, Langer J, Riemann D (2001) The two conserved C-terminal cysteines are necessary for proper folding and membrane localization of the raft-associated peptidase neprilysin/ CD10. Immunobiology 204(1-2):8.

12 Danksagung

Jedem Einzelnen zu danken wäre eine Mammutaufgabe, die den Rahmen dieser Arbeit sprengen würde. Deswegen möchte ich zunächst die folgenden Worte an alle richten:

Danke ist eigentlich nur ein Wort. Doch am rechten Ort zur rechten Zeit aufrichtig fühlend ausgesprochen, kann es Vieles bewirken. Deswegen hier und jetzt...

Danke !!!

Um jedoch nicht ganz ohne Namen auszukommen, möchte ich mich zunächst bei Prof. Dr. Barbara Seliger für die sehr gute wissenschaftliche Betreuung, für ihr reges Interesse an den wissenschaftlichen Fragestellungen, sowie für die ständige und konstruktive Diskussionsbereitschaft zum Gelingen dieser Arbeit in all den Jahren bedanken. Bei Prof. Dr. Jürgen Langner möchte mich für die schnelle Integration in das Institut und die Bereitstellung der APN-Thematik sowie für jegliche Unterstützung bedanken. Prof. Dr. Sven-Erik Behrens danke ich für die freundliche Übernahme der Betreuung der Dissertation.

Liebe Dagmar Riemann. Ihnen gilt ein besonderes und großes Dankeschön. Sie waren von Anfang an bis zum heutigen Tag mein wissenschaftlicher Begleiter und Mentor. Sie haben mir den Rücken gestärkt, zur rechten Zeit die Wege aufgezeigt und wesentlich zum Gelingen dieser Arbeit beigetragen. Vielen Dank für Ihre Unterstützung. Mit ihnen teile ich sehr gern unser freundschaftliches „Sie“.

Ich möchte natürlich auch sehr gern meine Ausbilder/ Wegbereiter/ Kooperationspartner für all die Jahre danken. Ob Alexander Navarrete-Santos, Astrid Kehlen, Tanja Blosz und vielen mehr, ich danke für Eure Unterstützung. Weiterhin möchte ich an dieser Stelle, all die Personen danken, die ich ausbilden dürfte. Ihr habt mein Leben bereichert, mich geformt, mich motiviert, mich besser gemacht, mir ein paar Haare gekostet, aber auch sehr viel Spaß bereitet. Ein besonders freundschaftlicher Dank geht hiermit an Katrin, Susi, Heike, Liane, Maria, Juliane, Tim, Anja T. und Katha. Zusätzlich danke ich allen ehemaligen und aktuellen Mitarbeiter des Instituts für Medizinische Immunologie für die sehr schöne Arbeitsatmosphäre und die stetige Diskussionsbereitschaft.

Auch in den schwersten Stunden seid ihr immer da, motiviert mich mit Euren unterstützenden Worten und Taten. Neben meinen ehemaligen Betreuten und nun Freunden verdanke ich das Gelingen dieser Arbeit durch das Spenden an Kraft, von Freude und von spaßigen Momenten ebenso Christian, Thomas, Sven, Nancy, Björn, Diana, Anja M. und Sandra.

Natürlich muss ich an dieser Stelle mich besonders bei Ivonne und Mela bedanken, dass sie für viele Jahre an meiner Seite standen, mit mir durch dick und dünn gegangen sind. Danke Euch!!!

Ein letztes, aber dafür das größte Danke (Die anderen mögen es mir verzeihen!) gilt meiner Familie. Ohne Eure Unterstützung wäre ich nicht soweit gekommen. Ich herze Euch hiermit ganz liebevoll.